

Holothuria (Lessonothuria) coronata sp. nov. (Echinodermata, Holothuroidea), a new species of sea cucumber from Socorro Island, México

Brenda Anaid Yáñez Villanueva¹, Francisco Alonso Solís-Marín²,
Alfredo Laguarda-Figuera²

¹ Posgrado en Ciencias Biológicas, Universidad Nacional Autónoma de México, Mexico City, Mexico

² Colección Nacional de Equinodermos 'Dra. Ma. Elena Caso Muñoz', Laboratorio de Sistemática y Ecología de Equinodermos, Instituto de Ciencias del Mar y Limnología (ICML), Universidad Nacional Autónoma de México (UNAM), Mexico City, C.P. 04510, Mexico

Corresponding author: Francisco Alonso Solís-Marín (fasolis@cmarl.unam.mx)

Academic editor: D. Vanden Spiegel | Received 14 December 2021 | Accepted 14 February 2022 | Published 13 April 2022

<http://zoobank.org/45263338-A656-4F75-A83C-8AE409AF40DF>

Citation: Yáñez Villanueva BA, Solís-Marín FA, Laguarda-Figuera A (2022) *Holothuria (Lessonothuria) coronata* sp. nov. (Echinodermata, Holothuroidea), a new species of sea cucumber from Socorro Island, México. ZooKeys 1095: 1–12. <https://doi.org/10.3897/zookeys.1095.79375>

Abstract

Holothuria (Lessonothuria) coronata sp. nov. occurs in depths of 5–10 m off the Mexican Pacific coast at the Revillagigedo Archipelago. It is clearly distinguished from other species of the subgenus by the presence of tables with a circular disc and big peripheral holes, sometimes with a second series of peripheral ones, a disc with a spiny or smooth rim and a spire crossed by a single cross-beam, dorsal papillae, and ventral tube feet with curved supporting rods with a spiny edge.

Resumen

Holothuria (Lessonothuria) coronata sp. nov. habita a profundidades de 5–10 m frente a la costa del Pacífico mexicano en el archipiélago de Revillagigedo. Se distingue claramente de otras especies del subgénero por la presencia de tablas con disco circular y grandes orificios periféricos, a veces con una segunda serie de orificios periféricos, disco con borde espinoso o liso y espira con una sola viga transversal, papilas dorsales y pies ambulacrales ventrales con barrotos de soporte curvados, con borde espinoso.

Keywords

Holothuriidae, Revillagigedo Archipelago, morphology, ossicles, taxonomy

Palabras clave

Archipiélago Revillagigedo, espículas, Holothuriidae, morfología, Taxonomía

Introduction

The genus *Holothuria* Linnaeus, 1767 is the most diverse within the family Holothuriidae, with 163 of the 202 species in the family belonging to the genus (WoRMS 2021a, b, c, d, e). Currently, 18 subgenera are grouped in the genus *Holothuria* (WoRMS 2021c). In 1958, Deichmann erected the genus *Lessonothuria* and assigned *Holothuria pardalis* Selenka, 1867 as the type species. Contrary to Deichmann (1958), Rowe (1969) changed the category of *Lessonothuria* from genus to subgenus.

The ossicles of the species belonging to *Lessonothuria* consist of tables, regular to incomplete buttons and supporting rods that sometimes are modified into elongated buttons (Deichmann 1958). According to Rowe (1969), pseudo-buttons are abundant among the species of this subgenus. Species of this subgenus mostly inhabit shallow marine waters (Samyn 2003; Ahmed et al. 2020); nonetheless, *H. (L.) cavans* Massin & Tomascik, 1996 inhabits waters at low salinities in an anchialine lagoon (Massin and Tomascik 1996). Species grouped in this subgenus are mostly distributed in the Indian Ocean (Samyn et al. 2019; Ahmed et al. 2020).

Samyn et al. (2019) resurrected the species *H. (L.) lineata* Ludwig, 1875, which was considered as a synonym of *H. pardalis* Selenka, 1867. The authors also stated that pseudo-buttons are predominant in *H. insignis* Ludwig, 1875, while buttons are predominant in *H. lineata* Ludwig, 1875 and *H. pardalis* Selenka, 1867. Recently, Ahmed et al. (2020) formally resurrected *H. insignis* Ludwig, 1875, which was considered a synonym of *H. lineata* Ludwig, 1875 and *H. pardalis* Selenka, 1867.

Currently, only 11 species belong to the subgenus *Lessonothuria* Deichmann, 1958: *Holothuria (L.) cavans* Massin & Tomascik, 1996; *H. (L.) cumulus* Clark, 1921; *H. (L.) duoturricula* Cherbonnier, 1988; *H. (L.) glandifera* Cherbonnier, 1955; *H. (L.) immobilis* Semper, 1868; *H. (L.) insignis* Ludwig, 1875; *H. (L.) lineata* Ludwig, 1875; *H. (L.) multipilula* Liao, 1975; *H. (L.) pardalis* Selenka, 1867; *H. (L.) tuberculata* Thandar, 2007 and *H. (L.) verrucosa* Selenka, 1867 (WoRMS 2021c). However, Ahmed et al. (2020) concluded that some of these species probably do not belong to this subgenus.

The purpose of this paper is to describe a new species of *Holothuria (Lessonothuria)* from the eastern Pacific coast.

Materials and methods

Specimens were collected by snorkelling, relaxed in ~10% MgCl₂ solution, and preserved in 70% ethanol for morphological and ossicle examination. All measurements were obtained from fixed specimens. Ossicles were extracted from the body wall

(anterior, medium, and posterior regions), dorsal papillae, ventral tube feet, and tentacles. The tissue was dissolved in fresh household bleach (5–6.5%). After centrifugation at 1000 rpm for 10 min, bleach was pipetted off and the ossicles were rinsed and centrifuged with distilled water that was pipetted off afterwards. The same process was done with 70, 80, and 95% ethanol. Absolute ethanol was added to the ossicles, and a small aliquot was taken and placed to dry on a cylindrical double-coated conductive carbon tape stub. Then, it was sputter coated with gold 2.5 kV in the ionizer JEOL JFC-1100 for 3 min and photographed using a JEOL JSM-6360LV scanning electron microscope (SEM) at the ICML, UNAM. Specimens were deposited at the Colección Nacional de Equinodermos ‘Dra. Ma. Elena Caso Muñoz’, Instituto de Ciencias del Mar y Limnología, Universidad Nacional Autónoma de México, Mexico City (ICML-UNAM).

Taxonomy

Order Holothuriida Miller et al., 2017

Family Holothuriidae Burmeister, 1837

Genus *Holothuria* Linnaeus, 1767

Subgenus *Lessonothuria* Deichmann, 1958

Diagnosis (after Rowe 1969). Tentacles 17–30. Pedicels and papillae irregularly arranged ventrally and dorsally respectively, a ‘collar’ of papillae evident around the base of the tentacles, anal papillae usually apparent. Body wall soft, not very thick, usually 1 (1–3) mm, body almost cylindrical but with a more or less distinct, flattened sole. Size small to moderate, up to 150 mm long. Calcareous ring fairly stout, radial plates about twice as long as the interradial plates. Ossicles consisting of clumsy tables, the spire low to moderate and usually terminating in a ring or cluster of spines, disc well developed and spinose, rarely some tables with smooth-rimmed disc also present; rim often turned up to give a ‘cup and saucer’ appearance to the table in lateral view. Pseudo-buttons abundant, usually smooth, sometimes spinose, usually irregular in outline and often reduced to a single row of three or four holes. Occasionally, quite regular buttons are present, with three pairs of holes.

Type species. *Holothuria pardalis* Selenka, 1867 (original designation).

***Holothuria (Lessonothuria) coronata* sp. nov.**

<http://zoobank.org/0734862E-3F19-4790-AD3B-04440C36B869>

Figs 1–4

Type material. *Holotype* ICML-UNAM 18432, 49 mm total length (TL), 1 specimen, Bahía Vargas Lozano, Isla Socorro, Revillagigedo Archipelago, Pacific Ocean

18°43'89.3"N, 110°57'30.3"W, 1 m depth, 4 April 2014, coll. Estrada Galicia, D. & Isaac Novoa, Y. **Paratypes.** ICML-UNAM 18433, 48 mm TL, Bahía Vargas Lozano, Isla Socorro, Revillagigedo Archipelago, Pacific Ocean 18°43'89.3"N, 110°57'30.3"W, 0.5–8 m depth, 4 April 2014; coll. Estrada Galicia, D. & Isaac Novoa, Y.; ICML-UNAM 18434, 48 mm TL; 1 specimen, Bahía Vargas Lozano, Isla Socorro, Revillagigedo Archipelago, Pacific Ocean 18°43'29.14"N, 110°56'57.77"W, 5–10 m depth, 29 May 2010, coll. Estrada Galicia, D. & Isaac Novoa, Y.

Type locality. Bahía Vargas Lozano, Isla Socorro, Revillagigedo Archipelago, Pacific Ocean 18°43'29.14"N, 110°56'57"W.

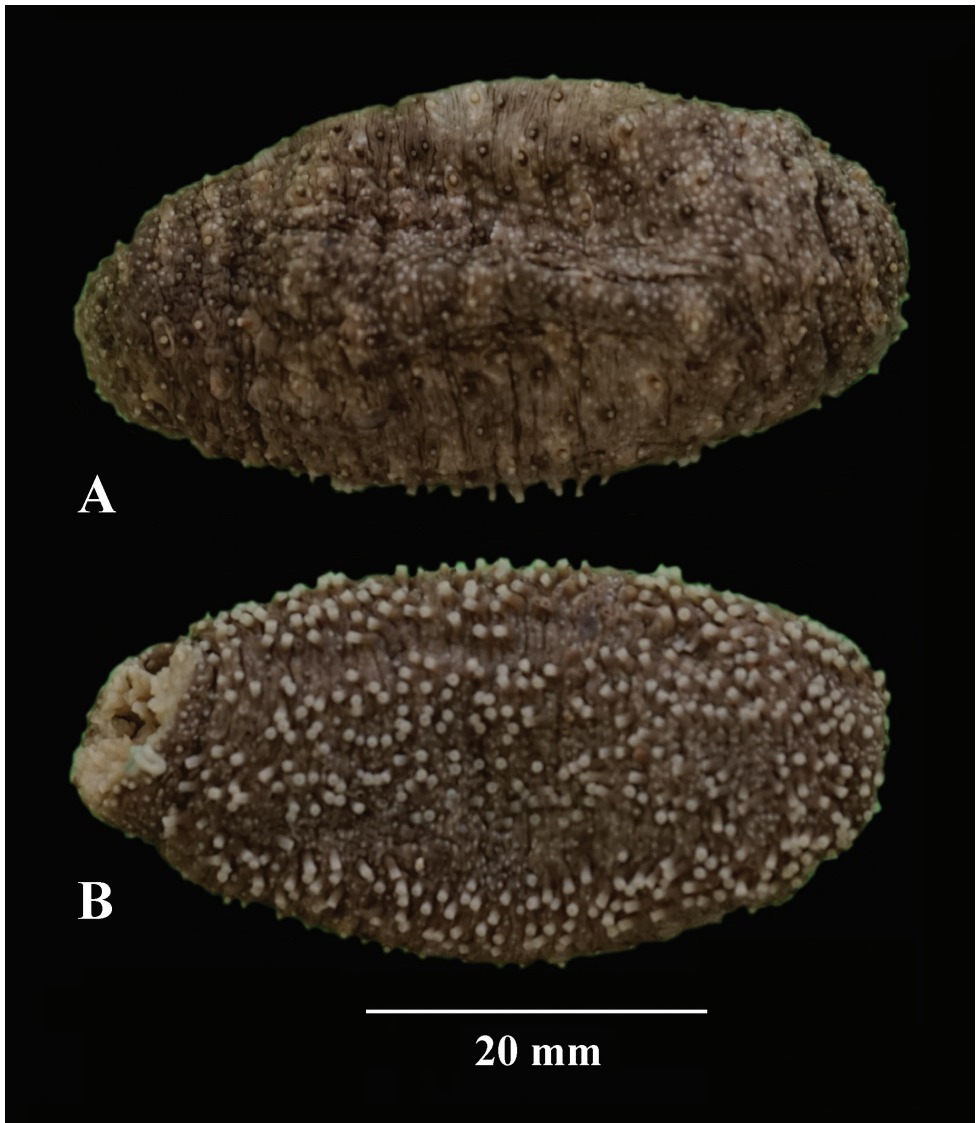


Figure 1. *Holothuria (Lessonothuria) coronata* sp. nov. Photos of preserved holotype, ICML-UNAM 18432 **A** dorsal view **B** ventral view.

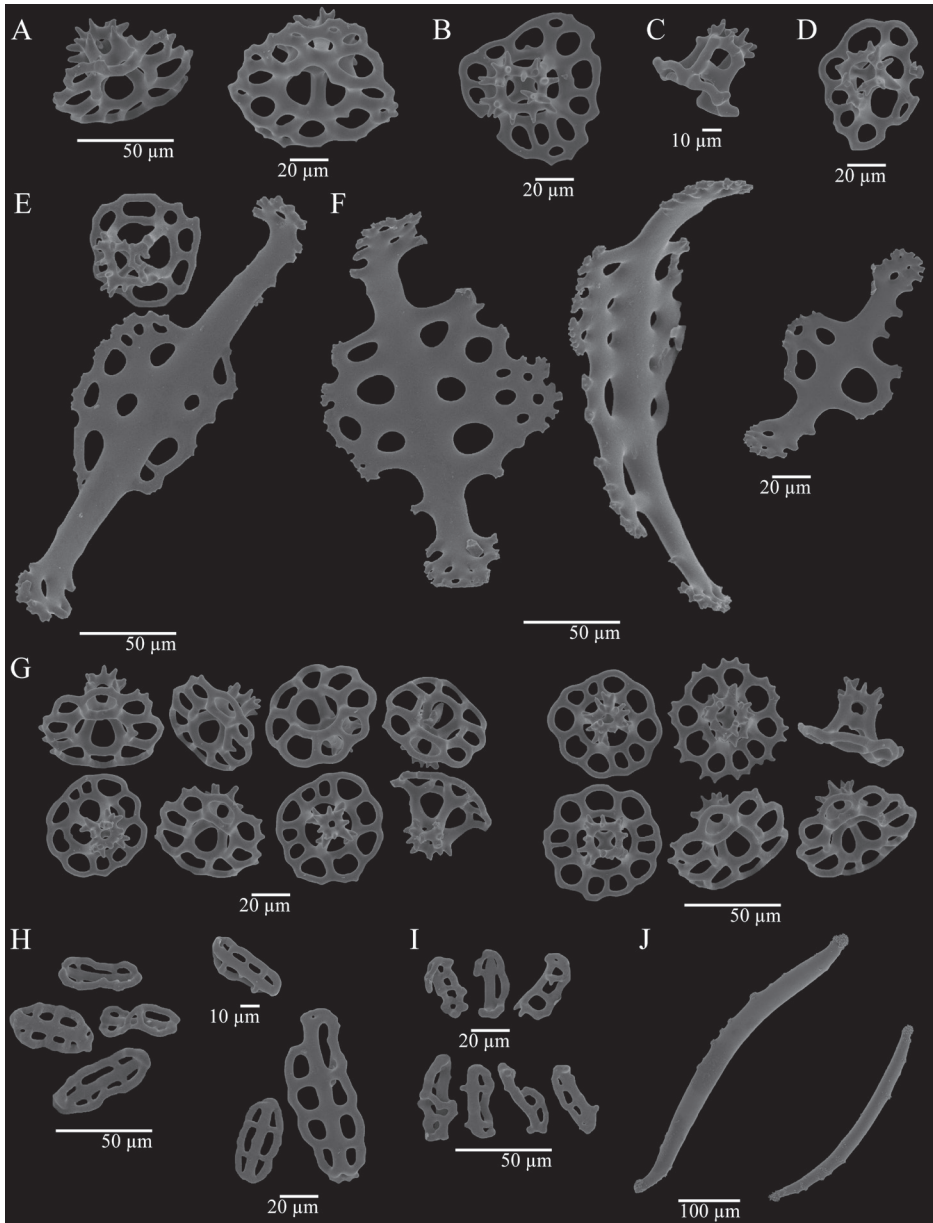


Figure 2. *Holothuria (Lessonothuria) coronata* sp. nov. Holotype, ICML-UNAM 18432. Ossicles of dorsal papillae (A–F) A tables B table with irregular disc C table with reduced disc D ‘rare table’ of the dorsal E supporting rod and table F supporting rods. Ossicles of dorsal body wall (G–I) G tables H pseudo-buttons I buttons. Ossicles of tentacles J rods.

Diagnosis. Small-sized holothurian (up to 49 mm), 20 peltate tentacles, no distinct collar; anal papillae present. Podia as conical papillae dorsally and tube feet ventrally. Body wall thin, leathery. Single Polian vesicle, free stone canal. Ossicles as tables, buttons, pseudo-buttons and supporting rods, tube feet with perforated plates. Table

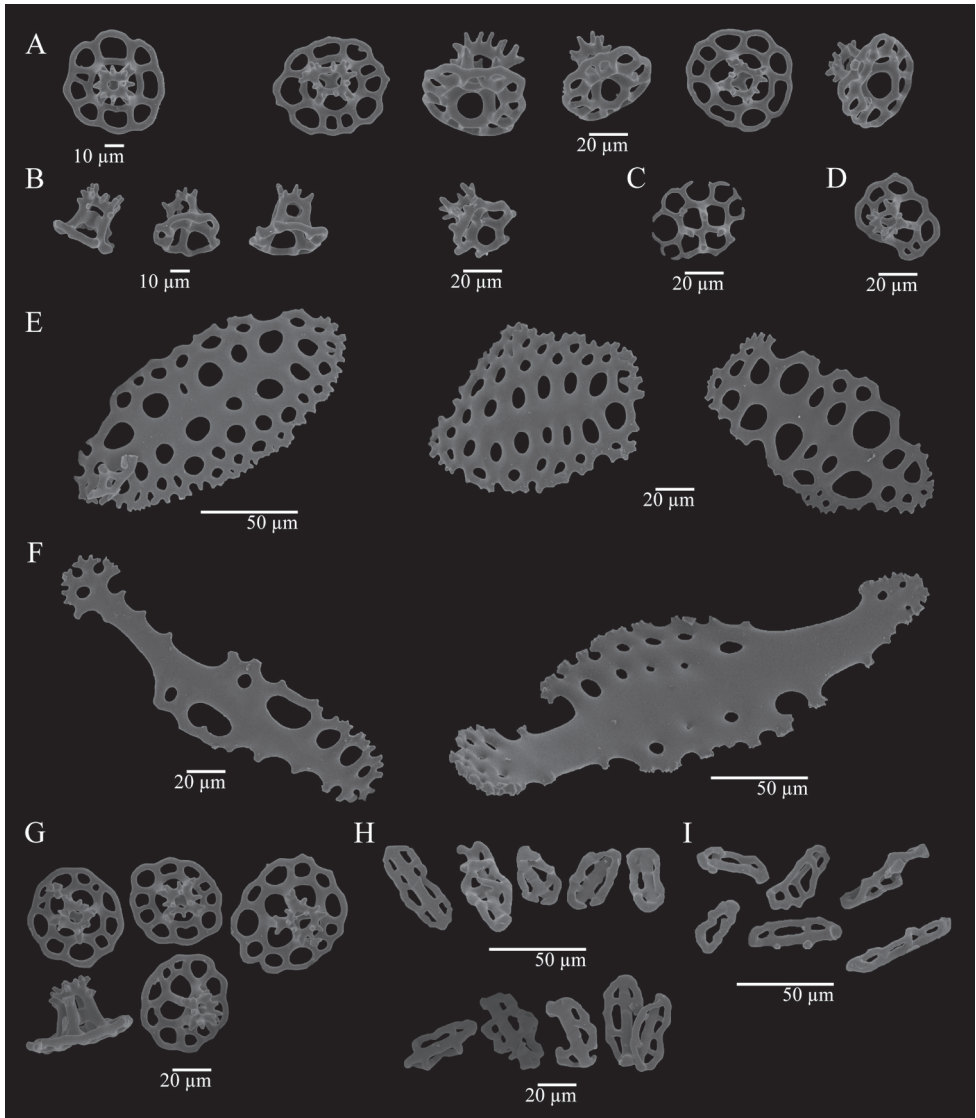


Figure 3. *Holothuria (Lessonothuria) coronata* sp. nov. Holotype, ICML-UNAM 18432. Ossicles of ventral tube feet (A–F) **A** tables **B** tables with reduced disc **C** table with reduced spire **D** ‘rare table’ **E** supporting rods **F** plates. Ossicles of ventral body wall (G–I) **G** tables **H** buttons **I** pseudo-buttons.

discs spinose to smooth with 6–13 marginal holes; spire of moderate height, one cross-beam, terminating in a crown with 14–20 teeth, such crown with a high shape diversity. Pseudo-buttons (25–50 μm long) mostly irregular, often twisted and/or knobbed, with two to five holes. Dorsal papillae and tube feet with curved supporting rods (180–240 μm), ends and central part are widened and perforated, the edge of the widened part slightly spinose. Tentacles with slightly curved rods, spiny ends, without perforations (300–600 μm).

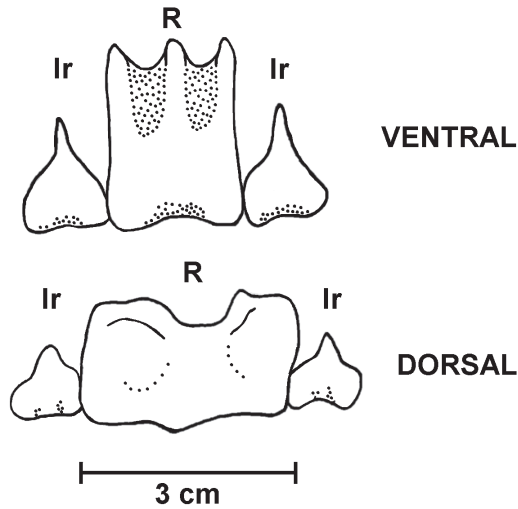


Figure 4. *Holothuria (Lessonothuria) coronata* sp. nov. Holotype, ICML-UNAM 18432. Calcareous ring. Single ventral and dorsal radials (R) and adjoining interradial plates (Ir).

Holotype description. Specimen preserved in alcohol with brownish body wall, the papillae, and ventral tube feet are white; 20 short beige tentacles. Ventral and dorsal body wall with minute white dots due to the presence of ossicle clusters. Anus surrounded by anal papillae. Calcareous ring stout (Fig. 4), interradial pieces with a median anterior projection; radial pieces with a median anterior notch and much wider than the interradial pieces; dorsal radial pieces are wider and stouter than the ventral ones. Polian vesicle 10 mm long. Free stone canal, 2 mm long. Single madreporite. Longitudinal muscles divided, 8–10 mm wide. Tentacular ampullae 5 mm long. Cuvierian organs present.

Ossicles. Dorsal papillae with three types of tables, supporting rods, and a reduced terminal plate. The first type of table possesses circular disc (Fig. 2A), sometimes irregular (Fig. 2B), diameter of 50–70 μm , the rim is either smooth or spinous and turned up; four big central holes and 6–13 peripheral holes, sometimes a second series of smaller peripheral holes is present. Spire is low to medium and consists of four pillars, spiny crown with a central hole; single cross-beam. The second type of table (Fig. 2C) has a reduced disc with irregular rim, four central holes, and usually lacking peripheral holes, but some tables bear up to three peripheral holes. Spire is medium size (35–45 μm) and consists of four pillars, spiny crown with a central hole; single cross-beam. The third type of table (Fig. 2D) has reduced disc and smooth rim, four big central holes. Zero to seven peripheral holes, spire of four pillars; spiny crown. Curved supporting rods (140–240 μm) (Fig. 2E, F), the ends and the central part are widened and perforated; spiny edge. Reduced terminal plate, 50–60 μm wide. Anal papillae with three types of tables and supporting rods, these four types of ossicles are identical to those present in the dorsal papillae. Dorsal body wall with tables, buttons, and pseudo-buttons. Tables with circular disc (45–60 μm wide) (Fig. 2G), irregular rim, spinous or smooth; four central holes and eight to eleven peripheral holes, some tables present a second series

of smaller peripheral holes. Spire low to medium sized consisting of four pillars, spiny crown with one central hole; single cross-beam. Some tables with button-shape and four big holes. Sometimes up to three peripheral holes are present, spire of four pillars, spiny crown. Irregular buttons (35–70 μm long) (Fig. 2H) with smooth edge, three to four pairs of holes. Pseudo-buttons (25–40 μm long) (Fig. 2I) with smooth and irregular edge, two to five holes. Ventral tube feet with three types of tables, plates, supporting rods, and terminal plate. The first type of table with circular disc (Fig. 3A), sometimes irregular (35–55 μm wide), and its rim is also irregular, whether spinose or smooth; four central holes and six to twelve peripheral holes. Spire low to medium with four pillars, spiny crown with central hole; single cross-beam. The second type of table bearing a reduced disc (30–40 μm wide) (Fig. 3B), four central holes and usually lacking peripheral holes, but rarely up to three peripheral holes are present. Medium size spire consisting of four pillars, spiny crown with central hole; single cross-beam. Tables rarely with a reduced spire (Fig. 3C). The third type are button-shaped tables (Fig. 3D) with spire of four pillars, spiny crown, disc with smooth rim and four big central holes. Perforated plates (Fig. 3E) with spiny irregular edge, 80–135 μm long. Curved supporting rods (130–230 μm) (Fig. 3F), the extremes and the central part are widened and perforated, irregular edge, sometimes with few spines. The terminal plates are bigger than the terminal plates from dorsal papillae. Ventral body wall with tables, buttons, and pseudo-buttons. Tables with circular disc (40–50 μm wide) (Fig. 3G) perforated by four central holes and eight to twelve peripheral holes. Spire low to medium with four pillars and spiny crown with central hole; single cross-beam. Button-shaped tables present, but scarcely. Disc with four big central holes and smooth rim, spire of four pillars, spiny crown. Buttons (40–50 μm length) (Fig. 3H) are irregular with three pairs of holes and smooth edge. Pseudo-buttons (Fig. 3I) with smooth edge and two to five holes (35–50 μm). Tentacles with slightly curved rods (Fig. 2J), both ends are spiny, without perforations (300–600 μm); some small rods are triradiated. Ossicles are not present in the longitudinal muscles, respiratory trees nor cloaca.

Etymology. The specific name refers to the crown of the table spires at the dorsal papillae, dorsal and ventral body wall, and ventral tube feet; such crowns exhibit a high shape diversity.

Ecology. *Holothuria* (*L.*) *coronata* sp. nov. occurs at 0.5–10 m depth, hidden under rocks in a well-aerated environment. It is a burrowing, deposit feeding holothurian.

Geographical distribution. Only known from Isla Socorro, Revillagigedo Archipelago, Pacific Ocean.

Discussion

The number of tentacles and the presence of tables and buttons are characteristic of the subgenus *Lessonothuria* Deichmann, 1958. *Holothuria* (*L.*) *coronata* sp. nov. was grouped within this subgenus because of the presence of ossicles such as pseudo-buttons and tables with a disc whose rim is turned up (Rowe 1969).

Holothuria (L.) *coronata* sp. nov. is closely related to *H.* (L.) *glandifera*. The disc of the tables is spiny or smooth in both species, and Cherbonnier (1955) reported the presence of rudimentary tables in *H.* (L.) *glandifera*; such tables are similar to the tables with a reduced disc present in *H.* (L.) *coronata* sp. nov. According to Cherbonnier (1955), the body wall of *H.* (L.) *glandifera* also presents 'rare tables' that are similar to buttons; this kind of table is present in the ventral and dorsal body wall and ventral tube feet of *H.* (L.) *coronata* sp. nov. In addition, both species present some knobbed buttons (Cherbonnier 1955). Nonetheless, Cherbonnier (1955) did not mention the presence of a second series of peripheral holes on the disc of the tables of *H.* (L.) *glandifera*, a character which is present in some tables of *H.* (L.) *coronata* sp. nov., *H.* (L.) *cumulus*, *H.* (L.) *duoturricula* and *H.* (L.) *multipilula* (Clark 1921; Cherbonnier 1955, 1988; Liao 1975). Unlike *H.* (L.) *glandifera*, the tables of *H.* (L.) *coronata* sp. nov. bear a single cross-beam (Clark 1921; Cherbonnier 1955). The buttons of *H.* (L.) *coronata* sp. nov. are more irregular than those present in *H.* (L.) *glandifera*. The supporting rods (90–230 µm long) of the ventral ambulacral feet of *H.* (L.) *glandifera* don't seem to be curved, their ends are perforated, and their edge is smooth; however, *H.* (L.) *coronata* sp. nov. presents longer and more complex supporting rods (130–230 µm long), curved, with a spiny edge, the ends and the central part are widened and perforated. The ventral tube feet of *H.* (L.) *coronata* sp. nov. and *H.* (L.) *glandifera* are supported by plates, while the plates of the ventral tube feet of *H.* (L.) *coronata* sp. nov. are wider and their edge is spinier (Cherbonnier 1955).

Holothuria (L.) *coronata* sp. nov. is also closely related to *H.* (L.) *pardalis*, but the tube feet supporting rods in *H.* (L.) *pardalis* are simpler than those in *H.* (L.) *coronata* sp. nov. and the table discs in *H.* (L.) *pardalis* have a spiny rim and are reduced, in addition to the fact that the spire is poorly developed, while in *H.* (L.) *coronata* sp. nov. the disc is generally well developed and the peripheral holes of the first series are large, the rim is smooth or spiny, but not as spiny as that of *H.* (L.) *pardalis* Selenka, 1867.

One species, *Holothuria* (L.) *pardalis*, has been reported inhabiting the Mexican Pacific. It is widely distributed, having been reported inhabiting the Indian Ocean and Western Pacific Ocean (Deichmann 1958; Samyn et al. 2019; Ahmed et al. 2020). Cherbonnier (1951) reported the presence of *H.* (L.) *pardalis* in the Gulf of California, Mexico. Seven years later, Deichmann (1958) reported *H.* (L.) *pardalis* inhabiting Tenacatita, Jalisco, Mexico and concluded that this species is not a permanent element of the fauna of the Mexican Pacific. She reviewed several specimens from different localities of the Central Eastern Pacific and reported ossicle variation among those specimens: 'in some individuals the inner layer of buttons almost entirely composed of regular six-holed buttons, in others all deformed, twisted, incomplete or with few knobs on the surface'. Unfortunately, Deichmann (1958) did not give the information about where the illustrated material was collected, leaving the previous explanation without support.

Cherbonnier (1951) described minute white dots on the body wall of *H.* (L.) *pardalis* formed by clusters of ossicles, this character is also present in *H.* (L.) *coronata* sp. nov. According to the keys and the descriptions of Samyn et al. (2019) and Ahmed et

al. (2020), we conclude that the ossicle illustrations provided by Cherbonnier (1951) truly belong to *H. pardalis* Selenka, 1867, due to the presence of peripheral holes in the majority of tables, the rods of the tentacles lacking holes, and the rods of the tube feet being curved. However, after reviewing the specimens of the subgenus *Lessonothuria* deposited in Colección Nacional de Equinodermos ‘Dra. Ma. Elena Caso Muñoz’, ICML, UNAM, we conclude that the statements of Deichmann (1958) are correct: *H. (L.) pardalis* does not naturally occur in the Mexican Pacific. The specimen reported by Solís-Marín et al. (2009) does not belong to *H. pardalis* but rather, *H. (Vaneyothuria) zacae* Deichmann, 1937. In conclusion, *H. (L.) coronata* sp. nov. is the second species of subgenus *Lessonothuria* that is distributed in the Mexican Pacific.

Holothuria (L.) coronata sp. nov. is clearly distinguished from other species of the subgenus by the presence of tables with a circular disc and big peripheral holes, sometimes with a second series of peripheral ones, disc with a spiny or smooth rim and a spire crossed by a single cross-beam, dorsal papillae and ventral tube feet with curved supporting rods with spiny edge, tentacles with non-perforated rods, all these characters have been used to differentiate species of the subgenus by various authors (Massin and Tomascik 1996; Ahmed et al. 2020).

Acknowledgements

We thank M.Sc. Laura Elena Gómez Lizárraga (ICML, UNAM) for taking the SEM micrographs that illustrate this work. To Alicia Durán González (ICML, UNAM) for her technical support. Carlos Conejeros (Posgrado en Ciencias del Mar, UNAM) prepared figure 1; Ma. Esther Diupotex (ICML, UNAM) prepared figures 2 and 4. To Yuri Yerye Isaac Novoa and Diana E. Estrada Galicia for collecting the specimens. To Didier Vanden Spiegel and Rafael B. de Moura for valuable suggestions and comments that improved this manuscript. Also would like to thank M. G. Lovegrove and Andrea Caballero for their valuable comments on the manuscript’s English and scientific content. BAYV thanks Maximilian Martin for his support and Posgrado en Ciencias Biológicas, UNAM, and finally to CONACYT for the funding provided.

References

- Ahmed Q, Thandar A, Mohammad Ali Q (2020) *Holothuria (Lessonothuria) insignis* Ludwig, 1875 (formally resurrected from synonymy of *H. pardalis* Selenka, 1867) and *Holothuria (Lessonothuria) lineata* Ludwig, 1875—new additions to the sea cucumber fauna of Pakistan, with a key to the subgenus *Lessonothuria* Deichmann (Echinodermata: Holothuroidea). *Zootaxa* 4767(2): 307–318. <https://doi.org/10.11646/zootaxa.4767.2.6>
- Burmeister H (1837) *Handbuch der Naturgeschichte. Zum Gebrauch bei Vorlesungen. Zweite Abtheilung: Zoologie*, 858 pp. <https://doi.org/10.5962/bhl.title.100177>

- Cherbonnier G (1951) Holothuries de l'Institut Royal des Sciences Naturelles de Belgique, Mémoire de l'Institut Royal des Sciences Naturelles de Belgique, Mémoire 2^{ème} série 41: 1–65.
- Cherbonnier G (1955) Holothuries récoltées en Océan française par G. Ranson en 1952. 4^e note. Bulletin Muséum National Histoire Naturelle Paris. 2 série. 27(4): 319–323.
- Cherbonnier G (1988) Echinodermes: Holothurides. Faune de Madagascar 70: 1–292.
- Clark HL (1921) The echinoderm fauna of Torres Strait: its composition and its origin. Department of Marine Biology of the Carnegie Institute 10: 1–223. <https://doi.org/10.5962/bhl.title.14613>
- Deichmann E (1937) The Templeton Crocker Expedition. IX. Holothurians from the Gulf of California, the West Coast of Lower California and Clarion Island. Zoologica (New York) 22(10): 161–176. <https://doi.org/10.5962/p.184685>
- Deichmann E (1958) The Holothuroidea collected by the Velero III and IV during the years 1932 to 1954. Part II Aspidochirotida. The University of Southern California Publications. Allan Hancock Pacific Expeditions 11(2): 253–349.
- Liao Y (1975) The echinoderms of Xisha islands. 1. Holothuroidea, Guangdong Province, China. Studia mar. sin. No. 10: 199–230.
- Linnaeus C (1767) Systema naturae per regna tria naturae: secundum classes, ordines, genera, species, cum characteribus, differentiis, synonymis, locis. (Ed.) 12. 1., Regnum Animale. 1 & 2. Holmiae [Stockholm], Laurentii Salvii, 1–532 [1766], 533–1327 [1767].
- Ludwig HL (1875) Beiträge zur Kenntniss der Holothurien. Arbeiten aus dem zoologisch-zootomischen Institut Würzburg 2: 77–118.
- Massin C, Tomascik T (1996) Two new holothurians (Echinodermata: Holothuroidea) from an anchialine lagoon of an uplifted atoll, Kakaban Island, East Kalimantan, Indonesia. The Raffles Bulletin of Zoology 44(1): 157–172.
- Miller AK, Kerr AM, Paulay G, Reich M, Wilson G, Carvajal JI, Rouse GW (2017) Molecular phylogeny of extant Holothuroidea (Echinodermata). Molecular Phylogenetics and Evolution 111: 110–131. <https://doi.org/10.1016/j.ympev.2017.02.014>
- Rowe FWE (1969) A review of the family Holothuriidae (Holothuroidea: Aspidochirotida). Bulletin of The British Museum (Natural History). Zoology (Jena, Germany) 18(4): 119–170. <https://doi.org/10.5962/bhl.part.18419>
- Samyn Y (2003) Shallow-water Holothuroidea (Echinodermata) from Kenya and Pemba Island, Tanzania. Studies in afrotropical zoology 292: 1–158.
- Samyn Y, Massin C, Vandenspiegel D (2019) The sea cucumber *Holothuria lineata* Ludwig, 1875 (Holothuroidea, Aspidochirotida, Holothuriidae) re-described from the newly found type. ZooKeys 836: 81–91. <https://doi.org/10.3897/zookeys.836.29932>
- Selenka E (1867) Beiträge zur Anatomie und Systematik der Holothurien. Zeitschrift für Wissenschaftliche Zoologie 17(2): 291–374.
- Semper C (1867–1868) Holothurien. In: Semper C (Ed.) Reisen im Archipel der Philippinen. Zweiter Theil. Wissenschaftliche Resultate. Erster Band. Leipzig: W. Engelmann, [iv +] 288 pp. <https://doi.org/10.5962/bhl.title.11687>
- Solís-Marín FA, Arriaga-Ochoa J, Laguarda-Figueras A, Frontana-Uribe S, Durán-González A (2009) Holoturoideos (Echinodermata: Holothuroidea) del Golfo de California.

CONABIO, Instituto de Ciencias del Mar y Limnología, Universidad Nacional Autónoma de México, 164 pp.

- Thandar AS (2007) Additions to the aspidochirotid, molpadid and apodid holothuroids (Echinodermata: Holothuroidea) from the east coast of southern Africa, with descriptions of new species. *Zootaxa* 1414(1): 1–62. <https://doi.org/10.11646/zootaxa.1414.1.1>
- WoRMS (2021a) *Actinopyga* Bronn, 1860. <http://www.marinespecies.org/aphia.php?p=taxdetails&cid=205662> [Accessed on 2021-10-12]
- WoRMS (2021b) *Bohadschia* Jaeger, 1833. <http://www.marinespecies.org/aphia.php?p=taxdetails&cid=204900> [Accessed on 2021-10-12]
- WoRMS (2021c) *Holothuria* Linnaeus, 1767. <http://www.marinespecies.org/aphia.php?p=taxdetails&cid=123456> [Accessed on 2021-10-12]
- WoRMS (2021d) *Labiododemas* Selenka, 1867. <http://www.marinespecies.org/aphia.php?p=taxdetails&cid=203875> [Accessed on 2021-10-12]
- WoRMS (2021e) *Pearsonothuria* Levin in Levin, Kalinin & Stonik, 1984. <http://www.marinespecies.org/aphia.php?p=taxdetails&cid=204297> [Accessed on 2021-10-12]

Four new *Parasterope* (Ostracoda, Myodocopina) from the Northwest Pacific and their phylogeny based on 16S rRNA

Huyen T. M. Pham^{1*}, Ivana Karanovic^{1,2*}

1 Department of Life Science, Research Institute for Convergence of Basic Science, College of Natural Sciences, Hanyang University, Seoul, 04763, Republic of Korea **2** Institute for Marine and Antarctic Studies, University of Tasmania, Private Bag 49, 7001, Hobart, Tasmania, Australia

Corresponding author: Huyen T. M. Pham (minhhuyen.ks.nb@gmail.com)

Academic editor: Saskia Brix | Received 14 November 2021 | Accepted 14 February 2022 | Published 13 April 2022

<http://zoobank.org/94B1536F-F07C-4595-BE95-A795A861D9E9>

Citation: Pham HTM, Karanovic I (2022) Four new *Parasterope* (Ostracoda, Myodocopina) from the Northwest Pacific and their phylogeny based on 16S rRNA. ZooKeys 1095: 13–42. <https://doi.org/10.3897/zookeys.1095.77996>

Abstract

Parasterope Kornicker, 1975 is a marine ostracod genus with 49 species described so far, which makes it the most diverse representative of the subfamily Cylindroleberidinae, as well as the entire family Cylindroleberididae. Despite its global distribution no species are reported from South Korea. Three new species collected from the Korean coast of the Sea of Japan (*Parasterope busanensis* **sp. nov.**, *P. singula* **sp. nov.**, and *P. sohi* **sp. nov.**), and one from the Japanese coast of the Pacific Ocean (*P. sagami* **sp. nov.**) are described. A taxonomic key to all named species from East Asia is provided. A phylogenetic tree is reconstructed based on partial 16S rRNA sequences of the four new species and other Cylindroleberidinae available from GenBank. Monophyly of *Parasterope* is supported by high posterior probabilities, but the phylogenetic analyses also indicate that some of the GenBank data attributed to this genus are probably misidentifications. A map of distribution and a checklist of all described *Parasterope* species are also provided.

Keywords

Crustacea, East Asia, marine benthos, new species, taxonomic key

* These authors contributed equally to this work.

Introduction

Cylindroleberididae is one of the largest myodocopid families with remarkable morphological diversity. It accounts for 225 species classified in 33 genera and the following four subfamilies: Cylindroleberidinae, Cyclasteropinae, Asteropteroinae, and Macroasteropteroinae. The primary defining feature of the family is the presence of seven or eight leaf-like pairs of gills at the posterior end of the body, the presence of a “baleen-comb” on the maxilla and the fifth limb, a mandible with a sword-shaped coxal endite, and a hatchet shaped sixth limb (Müller 1906; Poulsen 1965). The family has a worldwide marine distribution and can be found from shallow waters to depths of more than 4570 m (Kornicker 1975). The most speciose of all cylindroleberid genera is *Parasterope* Kornicker, 1975 (of the subfamily Cylindroleberidinae) with 47 species and subspecies currently listed on the World Ostracod Database (Brandão et al. 2022), although six of the listed species are considered synonyms. *Parasterope* representatives have the following combination of characters: first antenna has 0+6 (proximal+distal filament configuration) sensory bristles and the d-bristle is minute or absent; mandible has an e-bristle; and the posterior infold has no ridges between list and the edge of the valve (Poulsen 1965; Kornicker 1975). Species can be found in shallow waters, such as sandy mud flats near mangrove area (i.e., *P. zamboangae* Kornicker, 1970), to abyssal depths of 4303 m (i.e., *P. styx* Kornicker, 1975). The genus has a global distribution (Fig. 1). Of all species recognized so far, only six have been recorded from East Asia: three from Japan (*P. jenseni* Poulsen, 1965; *P. obesa* Poulsen, 1965; and *P. hirutai* Chavtur, 1983), two from the Philippines (*P. zamboangae* Kornicker, 1970 and *P. mckenziei* Kornicker, 1970), and

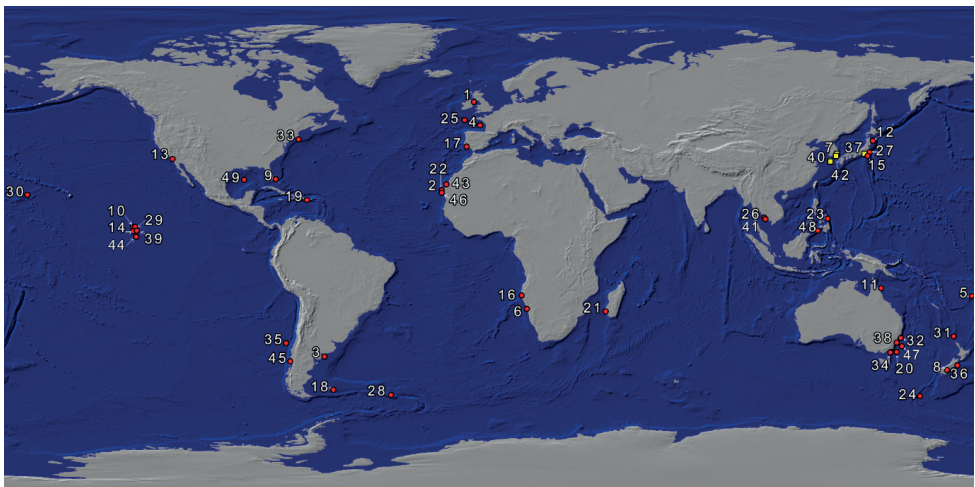


Figure 1. Geographic distribution of *Parasterope* Kornicker, 1975 based on the species’ type localities: red circle indicates previously known species; yellow square indicates species from this study. All the numbers follow the order of species on the checklist (Suppl. material 1).

one from Thailand (*P. nana* Poulsen, 1965) (Chavtur 1983; Poulsen 1965; Kornicker 1970).

The cylindroleberid fauna of East Asia is generally poorly known and mostly consists of species records without many details on their morphology. For example, a systematic study of the Korean ostracods as indicators of water pollution lists nine Cylindroleberidae, all left in the open nomenclature (Lee et al. 2000). Similarly, Tanaka and Ohtsuka (2015) reported eight cylindroleberids from Japan, belonging to six genera, of which only three were named: *Cyclasterope* cf. *hilgendorfi* (Müller, 1890), *Leuroleberis surugaensis* Hiruta, 1982, and *Tetraleberis* cf. *brevis* (Müller, 1890). Most recently, Pham et al. (2021) published the first taxonomic record of the entire family from Korea and described five species, of which one was proposed as a member of a new genus, *Toyoshioleberis* Pham, Jöst & Karanovic, 2021, one was a new record of *Xenoleberis yamadai* (Hiruta, 1979) from Korea, and another two were new to science, *X. parvus* Pham, Jöst & Karanovic, 2021 and *X. tanakai* Pham, Jöst & Karanovic, 2021.

In the present paper, we describe four new species belonging to *Parasterope* that have been collected from seas around Korea and Japan. To facilitate their further identification, we provide a taxonomic key to all East Asian species. In addition, partial 16S rRNA sequences of all new species and partial 18S rRNA sequences of only three new species were successfully amplified. Currently, there are two 16S rRNA sequences, five 18S rRNA sequences, and eleven 28S rRNA sequences available on GenBank (Benson et al. 2015) attributed to *Parasterope*. They belong to three named species and two in the open nomenclature. These GenBank sequences were used in previous studies that aimed to resolve the relationships between Cylindroleberididae and other myodocopid families (Yamaguchi and Endo 2003; Oakley 2005; Syme and Oakley 2012), but the phylogenetic relationship between *Parasterope* species has never been specifically mentioned. In general, phylogenetic relationships between the four cylindroleberid subfamilies is still not resolved despite many attempts to do so by using morphology only (Kornicker 1981), or a combination of morphological and molecular data (Syme 2007; Syme and Oakley 2012). The most recent phylogenetic tree constructed based on a concatenated data set with a combination of 16S, 18S, and 28S markers (Pham et al. 2021) provided little resolution to the problem of polyphyletic nature of the subfamily Cyclasteropinae. In addition, many of the genera on all phylogenetic trees reconstructed so far seem to be paraphyletic or polyphyletic. Resolving intragenic relationship could be a step towards understanding phylogeny on the higher systematic levels. Here we use newly obtained 16S rRNA sequences in combination with those already available on GenBank to reconstruct phylogenetic relationship between *Parasterope* species and the position of the genus within the subfamily Cylindroleberidane. The marker 16S is proven to be suitable for evolutionary studies at lower taxonomic levels for many animal groups (Bridge et al. 1995; Collins 2000; Collins et al. 2006; Govindarajan et al. 2006), including ostracods (see Pham et al. 2020). We also provide a list of all known *Parasterope* species with currently recognized synonyms (Suppl. material 1).

Materials and methods

Samples from Japan were collected from Sagami Bay during the 6th JAMBIO (Japanese Association for Marine Biology) project, on 13 February 2015 with a dredge from shallow waters (130–241 m) (Nakano et al. 2015). Samples were fixed in 99% ethanol on site and fractioned with 500 µm and 300 µm sieves. From the sea around the two Korean Islands, Maemul and Chuja, samples were collected with a dredge net from a boat. Collecting methods were described in Karanovic and Soh (2015). Ostracods were also collected from Minrack harbor (Busan), by diving at 30 m, by members of MABIK (Marine Biodiversity Institute of Korea). Specimens were dissected and soft parts mounted on slides in CMC-10 Mounting Media (Masters Company, Inc.), while carapaces were kept on the SEM stubs. All drawings were prepared using a drawing tube attached to the Olympus BX51 microscope. For observations under the scanning electron microscope (SEM) carapaces were coated with platinum. SEM photographs were taken at Eulji University (Korea) with the Hitachi S-4700 electron microscope. All specimens are deposited in the invertebrate collection of the National Institute of the Biological Resources (NIBR) in South Korea. The distribution map has been created with the Map Creator Private version 2.0.

The extraction followed the HotSHOT method described in Williams et al. (1992). All PCR reactions were carried out in 25 µl volume containing: 5 µl of diluted DNA template, 1 µl of each forward and reverse primer, 15 µl ultra-distilled water and 5 µl AccuPower[®] PCR Premix (Bioneer Inc.). Fragments of 16S were amplified using the specific primer pairs 16S MYOF1: CCGGTTTGAAGCTCAGATCAC; 16S MYOF2: TCAAATCATGTTGARATTWAATGG; 16S MYOR1: GTYTTTTAATTGGRGACTGG; 16S MYOR2: TAAACGGCTGCGGTATYYTG. The primer pairs of *Cylind_18S_F* (5'-GGGAGCATTTATTAGACCAAACC-3') and *Cylind_18S_R* (5'-TTCCCGTGTTGAGTCAAATTAAGCC-3') were used for the amplification of the 18S rRNA gene fragment. All PCR reactions run in a TaKaRa PCR Thermal Cycler Dice, using 3.5 µl DNA template, 17 µl ultra-distilled water, 5 µl AccuPower[®] PCR Premix (Bioneer Inc., Korea), and 1 µl of forward and backward primer each. PCR setting consisted of initial denaturation at 94 °C for 5 min, 35 cycles of denaturation for 30 s at 94 °C, annealing for 30 s at 48 °C for 16S/ 1 min at 50 °C for 18S, extension at 72 °C for 10 min before decreasing to 4 °C at the end. PCR products were electrophoresed (for 20 min at 100 V) on 1% agarose gels (0.5X TAE buffer dyed with GelRed[®] Nucleic Acid Gel Stain) to determine the presence of target DNA bands. PCR products were purified for sequencing by ethanol precipitation and neutralized by Sodium acetate (pH 5.5). Sequencing reactions were run for both strands to confirm sequence reliability using the Sanger method for dideoxy sequencing (Bionics Inc., Seoul, Korea). All 16S rRNA and 18S rRNA sequences have been deposited in GenBank (Table 1).

Forward and Reverse strands were visually compared and checked for signal quality and low-resolution sites using FinchTV (version 1.4.0) (Geospiza, Inc., Seattle, WA, USA; <http://www.geospiza.com>). The strands were aligned with MAFFT v.7.127b (Katoh et al. 2019) using the EINS-i algorithm. All sequences used in the phyloge-

netic analysis are in the Table 1. The best fit evolutionary model was used based on the Akaike Information Criterion (AIC) as implemented in ModelFinder (Kalyaana-moorthy et al. 2017). Bayesian Inference, implemented in BEAST v2.6.4 (Bouckaert et al. 2014), was used to estimate phylogenetic relationships. Settings included the best fit evolutionary model with four gamma categories, a strict molecular clock, gamma shape alpha 0.645, and 0.3583 in proportion of invariable site. The analysis run for 10,000,000 generations, sampling every 1,000 generations. Software Tracer (Rambaut et al. 2018) was used to visualize results of the BEAST analyses and FigTree v1.4.3 (Rambaut 2010) for tree visualization. Molecular pairwise distances were calculated as uncorrected p-distances (Kimura 1981) and intrageneric distances were calculated as within group mean in MEGA 7 (Kumar et al. 2016).

Table 1. List of 16S sequences used for phylogenetic analysis. ¹ Syme and Oakley (2012); ² Wakayama and Abe (2006); ³ Pham et al. (2021); ⁴ Oakley and Cunningham (2002); numbers in bold indicate sequences from this study.

Genus	Species	GenBank number	
		16S	18S
<i>Bathyleberis</i>	<i>B. oculata</i>	EU587251 ¹	EU591814 ¹
	<i>C. marranyin</i>		EU587243 ¹
<i>Cylindroleberis</i>	<i>Cylindroleberis</i> J57069	EU587253 ¹	EU587244 ¹
	<i>Cylindroleberis</i> NW-2004	AY624729 ²	
UnID	Cylindroleberididae J57076	EU587257 ¹	
<i>Parasterope</i>	<i>P. busanensis</i> sp. nov. 24_6	OK048681	OK048719
	<i>P. busanensis</i> sp. nov. 24_7	OK048682	OK048720
	<i>P. gamurru</i> J53224	EU587255 ¹	EU591819 ¹
	<i>P. pollex</i>		AF363309 ⁴
	<i>P. sagami</i> sp. nov. 26_9	OK048683	OK048721
	<i>P. sagami</i> sp. nov. 27_0	OK048684	OK048722
	<i>P. singula</i> sp. nov. 1_1	OK048686	OK048723
	<i>P. singula</i> sp. nov. 1_2	OK048687	
	<i>P. sohi</i> sp. nov.	OK048685	
	<i>P. styx</i>		EU587236 ¹
	<i>Parasterope</i> J57072*		EU587247 ¹
<i>Parasterope</i> NW-2004	AY624728 ²		
<i>Postasterope</i>	<i>P. barensi</i> J57079	EU587258 ¹	EU587248 ¹
	<i>P. corrugata</i>	EU587259 ¹	EU591816 ¹
<i>Synasterope</i>	<i>Synasterope</i> J57066	EU587252 ¹	EU587250 ¹
	<i>Synasterope</i> J57067		EU591815 ¹
<i>Toyoshioleberis</i>	<i>T. magnabucca</i>	MW534153 ³	MZ092883 ³
<i>Xenoleberis</i>	<i>X. parvus</i>	MW534150 ³	
	<i>X. pacifica</i> 38	MW534151 ³	MZ092881 ³
	<i>X. pacifica</i> 39	MW534152 ³	MZ092882 ³
	<i>X. pacifica</i> 275	MW534140 ³	MZ092883 ³
	<i>X. tanakai</i> 266	MW534141 ³	
	<i>X. tanakai</i> 284	MW534142 ³	MZ092884 ³
	<i>X. yamadai</i> 272	MW534143 ³	MZ092879 ³
	<i>X. yamadai</i> 273	MW534144 ³	MZ092880 ³
	<i>X. yamadai</i> 14	MW534145 ³	MZ092878 ³
	<i>X. yamadai</i> 30	MW534147 ³	

Abbreviations used in text and figures

A1	first antenna;	Md	mandibula;
A2	second antenna;	Mxl	maxillula;
F	Furca;	NIBR	National Institute of Biodiversity Research;
L5	fifth limb;	SEM	scanning electron microscope.
L6	sixth limb;		
L7	seventh limb;		

Results

Systematics

Phylum Arthropoda Latreille, 1829
Subphylum Crustacea Brünnich, 1772
Class Ostracoda Latreille, 1802
Subclass Myodocopa Sars, 1866
Order Myodocopida Sars, 1866
Family Cylindroleberididae Müller, 1906
Genus *Parasterope* Kornicker, 1994

Key to *Parasterope* from East and Southeast Asia

- | | | |
|---|---|-------------------------|
| 1 | Mandible, dorsal margin of basale with mid-bristle..... | 2 |
| – | Mandible, dorsal margin of basale without mid-bristle | 3 |
| 2 | 6 th limb, ventral and postero-ventral margin without plumose bristles | |
| | <i>P. nana</i> Poulsen, 1965 | |
| – | 6 th limb, ventral margin of end-joint with 11 or 12 plumose bristles..... | |
| | <i>P. zamboangae</i> Kornicker, 1970 | |
| 3 | Adult female Md with 3 long terminal setae next to exopodite..... | |
| | <i>P. sagami</i> sp. nov. | |
| – | Adult female Md with 2 long terminal setae next to exopodite | 4 |
| 4 | 7 th limb with 4 bristles (2 on each side) on the terminal segment | |
| | <i>P. singula</i> sp. nov. | |
| – | 7 th limb with 6 bristles (3 on each side) on the terminal segment | 5 |
| 5 | Mandibular basale with 6 spinous end bristles | <i>P. sobi</i> sp. nov. |
| – | Mandibular basale with 3 or 4 spinous end bristles | 6 |
| 6 | Mandibular basale spinous and with cluster of spines near middle | |
| | <i>P. mckenziei</i> Kornicker, 1970 | |
| – | Mandibular basale with no hair on broad surface..... | 7 |
| 7 | First antenna 8 th joint with small spine-like d-bristle..... | |
| | <i>P. hirutai</i> Chavtur, 1983 | |
| – | First antenna 8 th joint without d-bristle | 8 |

- 8 An open row of ~ 7–15 long medial bristles between the posterior ridge and the shell margin *P. obesa* Poulsen, 1965
- No bristles or only short, scattered bristles between the posterior ridge and the shell margin 9
- 9 2nd joint of first antenna without lateral bristle; second antenna protopodite with a row of spines on the ventral margin..... *P. jenseni* Poulsen, 1965
- 2nd joint of first antenna with lateral bristle; second antenna protopodite without spine on the ventral margin
..... *P. busanensis* sp. nov.

***Parasterope busanensis* sp. nov.**

<http://zoobank.org/E03199FB-A217-4451-B924-45A64817C83B>

Figs 2–4

Specimens examined. *Holotype* female dissected on one slide, shells on SEM stub (NIBR IV 0000879898_1). *Paratypes*: three males and one female dissected on one slide, shells on SEM stub (NIBR IV 0000879898_2;3;4 &5). All from the type locality: South Korea, Busan, Min-rack harbor (35°09'11.9"N, 129°07'38.4"E), collected by the Marine Biodiversity Institute of Korea (MABIK) on 11 April 2019.

Etymology. This species is named in reference to the type locality. It is used as an adjective for a place, with the Latin suffix *-ensis*.

Diagnosis. Surface of the shell mostly smooth. Posterior infold of the carapace with a broad shelf. Dorsal margin rounded in both female and male. Posterior end clearly wider than anterior. Lateral eye well developed with black pigmented ommatidia. A1 8-segmented without d-bristle on the 8th joint. Uropodal lamellae with nine claws.

Description. Female. Shell (Fig. 2a–f) Carapace oval, broadening at posterior, greatest height near middle, carapace length 1.25 mm, height 0.94 mm. Nine small horn-like spines near dorsal margin. Posterior infold between broad list and valve margin without setae.

A1 (Fig. 3a). 1st joint: with no hair on broad surface; longer than 2nd joint. 2nd joint: one spinous dorsal seta, one short lateral bristle, and three proximal dorsal spines. 3rd joint: seven setae (one short ventral and six dorsal). 4th joint: three bristles (one long dorsal and two short ventral bristles) and two small ventral spines at mid length. 5th joint: sensory bristle with six filaments without short proximal terminal. 6th joint: one medial seta, attached to bottom of 7th joint boundary. 7th joint: a-bristle claw-like, bare; b-seta with marginal filaments; c-seta with marginal filaments. 8th joint: d-bristle absent; e-bristle with blunt tip; f- and g-bristles with marginal filaments.

Bellonci organ (Fig. 3b). Elongate with rounded tip, constriction at mid-point.

Eyes. Lateral eye with many ommatidia obscured by black pigment; 13 ommatidia visible. Medial eye rounded and unpigmented.

A2. Protopodite: rounded without medial bristle. Endopodite (Fig. 3c): 2-jointed with long terminal bristle. Exopodite: 9-jointed; bristle of 2nd segment with spinules along ventral margin and spines along dorsal margin reaching 8th joint; 3rd–8th joints with natatory

hairs and spines along proximal part of ventral margin. 9th article: four bristles (two long natatory and two short bristles). Articles 1–8 with minute spines at inner terminal corner.

Md (Fig. 3d). Coxale endite ventral branch with spines forming four oblique rows. Basale endite with four spinous end bristles, three triaenid bristles with three or four pairs spines excluding terminal pair. Basale dorsal margin with two long terminal setae, without mid-bristle. Exopodite with hirsute tip and two small subterminal setae, exopodite almost same length as dorsal margin of first endopodite article. Endopodite: 1st joint: ventral margin with three bristles (one broken with short spines, one long with long marginal spines, and one shorter without spine or hair); 2nd joint: ventral margin: with three terminal bristles; dorsal margin: with stout a-, b-, c-, and d-bristles and one short bristle proximal to a-bristle; one long e-bristle and three medial bristles forming an oblique row between b- and c-bristles and adjacent to b-bristle; four medial bristles forming an oblique row adjacent to c-bristle; and one short bristle adjacent to d-bristle; f-bristle between c- and d-bristles, long, bare; g-bristle longer than f-bristle. End segment with a strong dorsal claw-like bristle without marginal spines, three juxtaposed stout bristles of equal length, and two thin bristles.

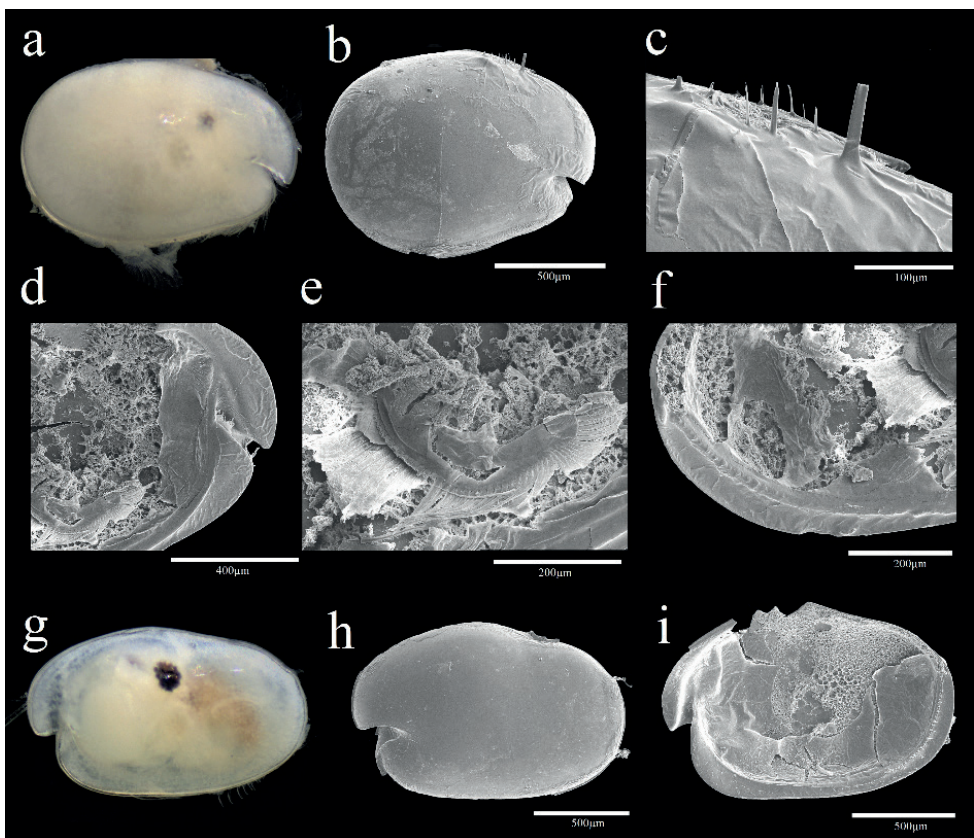


Figure 2. Light microscopy and scanning electron microscopy images of *Parasterope busanensis* sp. nov. **a–f** holotype female adult: **a** External view **b** Lateral view from left valve **c** Spines on dorsal margin **d** Internal view of anterior part **e** L5 ventral section **f** Internal view of posterior part **g, h** paratype male adult: **g** External view **h** Lateral view from right valve **i** Internal view of left valve.

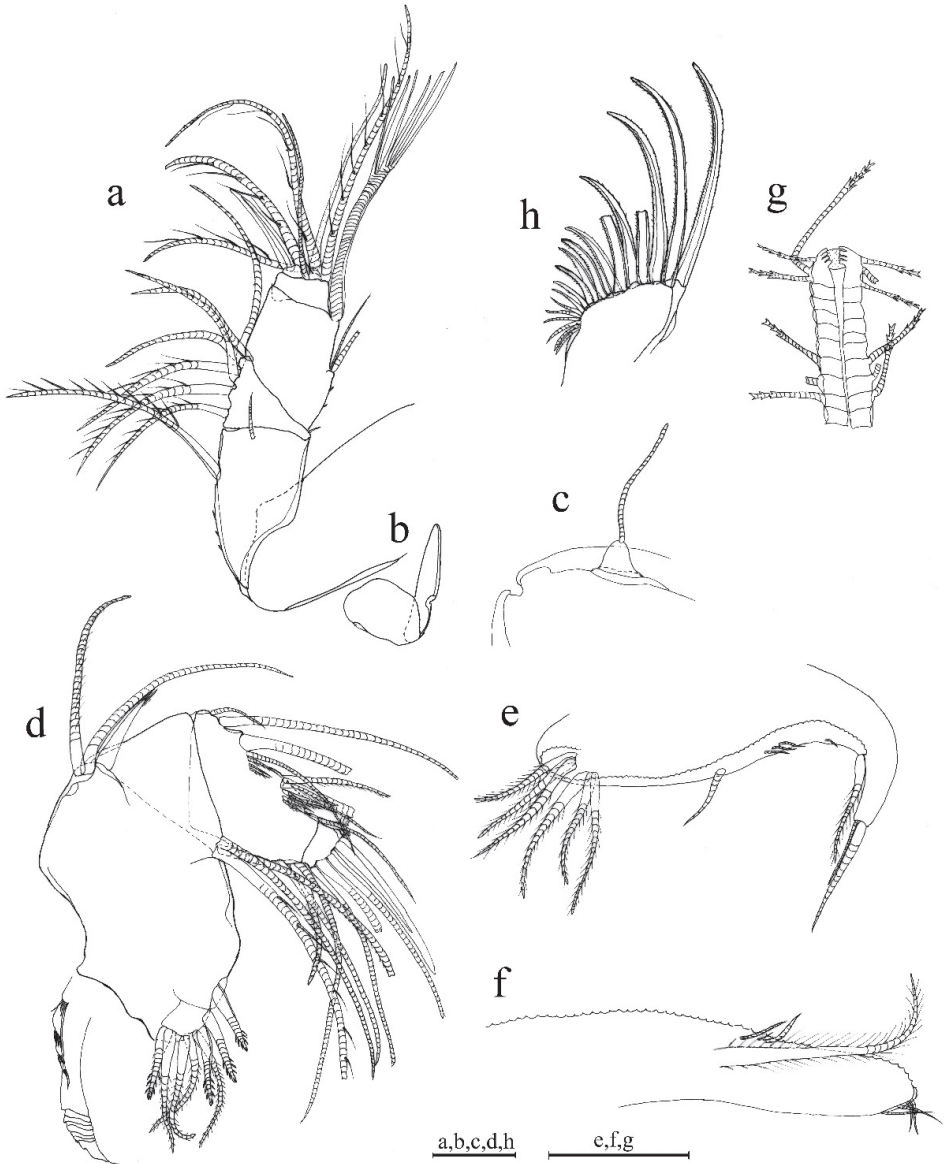


Figure 3. *Parasterope busanensis* sp. nov. holotype female adult: **a** A1 **b** Bellonci organ **c** A2 **d** Md **e** Mxl **f** L5 **g** L7 **h** F. Scale bar: 0.1 mm.

Mxl (Fig. 3e). Endite I with three bristles. Endite II with three bristles. Basale: one bare proximal ventral bristle at the middle and four short distal ventral bristles. Endopodite: 1st article absent α -seta and one hairy β -seta; 2nd article with two terminal bristles.

L5 (Fig. 3f). Ventral section with fan of long setae. Comb: spinous exopodite bristle over past distal end of comb, two short bristles (ventral to base of exopodite bristle)

with bases almost on ventral edge of comb, four bristles just proximal at the ventral edge of comb, without bristle to base of exopodite bristle.

L6. Unknown

L7 (Fig. 3g). Each limb with 12 bristles. Six proximal and six distal bristles (three on each side).

F (Fig. 3h). Each lamella with six claws and three posterior claws bristle-like. A total of nine claws and bristles.

Male. All features are comparable to adult female; important differences are listed below.

Shell (Fig. 2g–i). Carapace more elongate than that of female and with more open incisure, hairs forming vertical row near posterior end, carapace length 1.36 mm, height at middle 0.9 mm.

A1 (Fig. 4a). Sensory seta with robust stem and many filaments. 7th and 8th joints with very long c- and f- setae (long as carapace length) each with numerous of marginal filaments. 2nd and 4th joints without dorsal margin spines.

A2 (Fig. 4b). Endopodite with 3-jointed, article two with two lateral setae, article three recurved with 1 proximal seta.

Md (Fig. 4c). Basale dorsal margin with one seta at mid-length. Endopodite: two relatively long bristles proximal to a-bristle.

Eyes (Fig. 4d). Lateral eye with more than 17 ommatidia. Medial eye rounded and unpigmented.

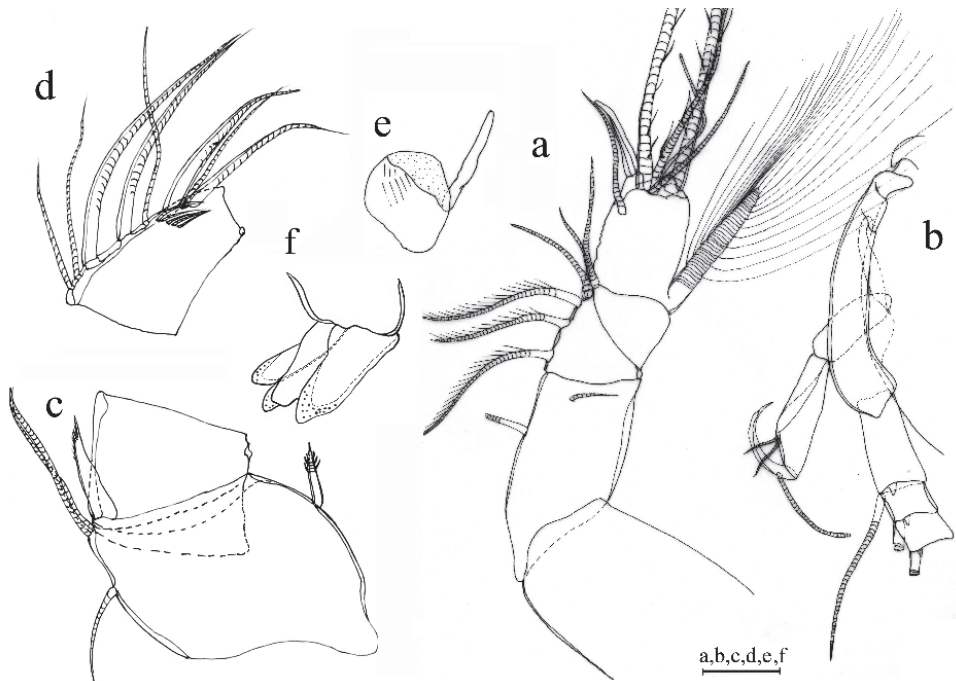


Figure 4. *Parasterope busanensis* sp. nov. paratype male adult: **a** A1 **b** A2 **c** Md **d** Bellonci organ. Scale bar: 0.1 mm.

Reproductive organs (Fig. 4f). Copulatory limbs are coalesced proximally, in generally, shorter than the furca lamella. The lobe is distally subdivided into three small lobes.

Remarks. The new species is closely related to *P. iota* Kornicker, Harrison-Nelson & Coles, 2007, described from Kapua Channel (Waikiki, Hawaii). The first joint of the A1 of *P. busanensis* is without hair on the broad surface, present in *P. iota*. In addition, the 3rd–8th joints of *P. iota* each have fairly stout proximal ventral spines, absent in *P. busanensis*. The distal margin of the Mx1 of *P. busanensis* bears four bristles compared to two in *P. iota*, and three bristles (one minute) near the ventral margin rather than five in *P. iota*. The new species shares many characters with *P. gamurru* Syme & Poore, 2006 described from Queensland, Australia (Syme and Poore 2006a), but lacks the nodes on the dorsal margin of the 5th joint on the A1, which is a prominent character of *P. gamurru*. The new species also bears two oblique rows of cleaning setae on the medial side of the Md 2nd joint, compared to only one in *P. gamurru*. The endite II of *P. busanensis* differs from that of *P. pacifica* Kornicker and Harrison-Nelson, 2005 from Johnston Atoll (Kornicker and Harrison-Nelson 2005) in having three rather than four bristles. The 3rd joint of the Md in *P. theta* Kornicker, Harrison-Nelson & Coles, 2007 from Waikiki, Hawaii (Kornicker et al. 2007). The same character is present in *P. sigma* Kornicker, Harrison-Nelson & Coles, 2007 from Kāneohe Bay, Hawaii (Kornicker et al. 2007), and *P. zeta* Kornicker, 1986 from the Gulf of Mexico (Kornicker 1986).

The sexual dimorphism found in the new species, the morphology of the dorsal mid-bristle on the basale of Md, and the number of bristles proximal to the a-bristle on the endopodite of the Md, have never been described in *Parasterope*.

GenBank numbers 16S: OK048681, OK048682; 18S: OK048719, OK048720.

***Parasterope sagami* sp. nov.**

<http://zoobank.org/5404E848-CCDC-4025-8E9F-B3725DCADD8A>

Figs 5–7

Specimens examined. **Holotype** female dissected on one slide, shells on SEM stub (NIBR IV0000890541). **Paratypes:** one male and one female dissected on separate slides, shells on SEM stub (NIBR IV0000890542). All from the type locality: Japan, Kanagawa, Sagami Bay (35°09.420'N, 139°36.556'E), 5 m, collected during 6th JAMBIO project on 13 February 2015.

Etymology. The species name was chosen after the Sagami Bay, from where the species was collected. It is an adjective agreeing with female gender of the genus.

Diagnosis. Surface of the shell completely smooth. Posterior infold of the carapace with a broad shelf. Dorsal margin rounded in female and almost perpendicular in male. Lateral eye well developed with black pigmented ommatidia, smaller in female than in male. A1 8-segmented without d-bristle on the 8th joint. Uropodal lamellae with eight claws.

Description. Female. Shell (Fig. 5a–c). Carapace oval, broadening at posterior, greatest height near middle, carapace length 1.21 mm, height 0.83 mm. Carapace smooth and without ornamentation.

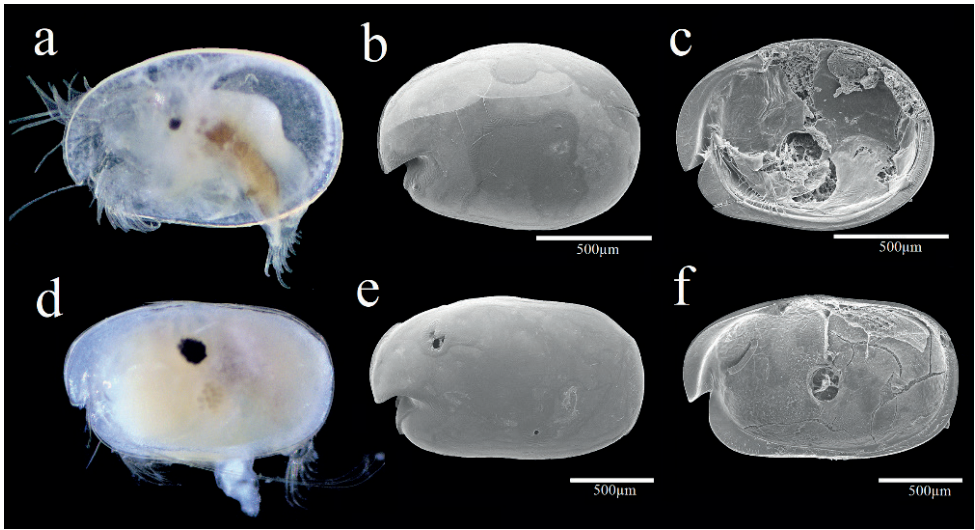


Figure 5. Light microscopy and scanning electron microscopy images of *Parasterope sagami* sp. nov. **a–c** holotype female adult: **a** External view **b** Lateral view from right valve **c** Internal view from left valve. **d–f** paratype male adult: **d** External view **e** Lateral view from right valve **f** Internal view of left valve.

A1 (Fig. 6a). 1st joint: with no hair on broad surface. 2nd joint: one spinous dorsal seta, no lateral bristle, and two dorsal spines on each side of dorsal margin. 3rd joint: seven setae: one short ventral and six dorsal. 4th joint: three setae (one long dorsal bristle and two short ventral bristle) and two small ventral spines. 5th joint: sensory bristle with six filaments without short proximal terminal. 6th joint: unidentified. 7th joint: a-bristle claw-like, bare; b-seta with marginal filaments; c-seta with marginal filaments. 8th joint: d-bristle absent; e-bristle bare, with blunt tip; f- bristle with marginal filaments; g-bristle with three filaments without proximal and marginal filament.

Bellonci orange (Fig. 7a). Elongate with rounded tip, unclear constriction.

Eyes (Fig. 7a). Lateral eye with 12 ommatidia obscured by black pigment; Medial eye rounded and pigmented.

A2 (Fig. 6b). Protopodite: rounded without medial bristle. Endopodite: 3-jointed with long terminal bristle near junction between 2nd and 3rd join. Exopodite: 9-jointed; bristle of 2nd segment along ventral margin and spines along dorsal margin reaching 8th joint; 3rd–8th joints with natatory hairs and spines along proximal part of ventral margin. 9th article: four bristles (two long natatory and two short bristles). 1st–8th with minute spines at inner terminal corner.

Md (Fig. 6c). Coxale endite: unable to determine. Basale endite with four spinous end bristles, three triaenid bristles with three pairs spines excluding terminal pair. Basale dorsal margin with three long terminal setae, without mid-bristle. Exopodite with hirsute tip and two small subterminal setae, exopodite length $\sim \frac{3}{4}$ of dorsal margin of first endopodite article. Endopodite: 1st joint: ventral margin with three bristles (one

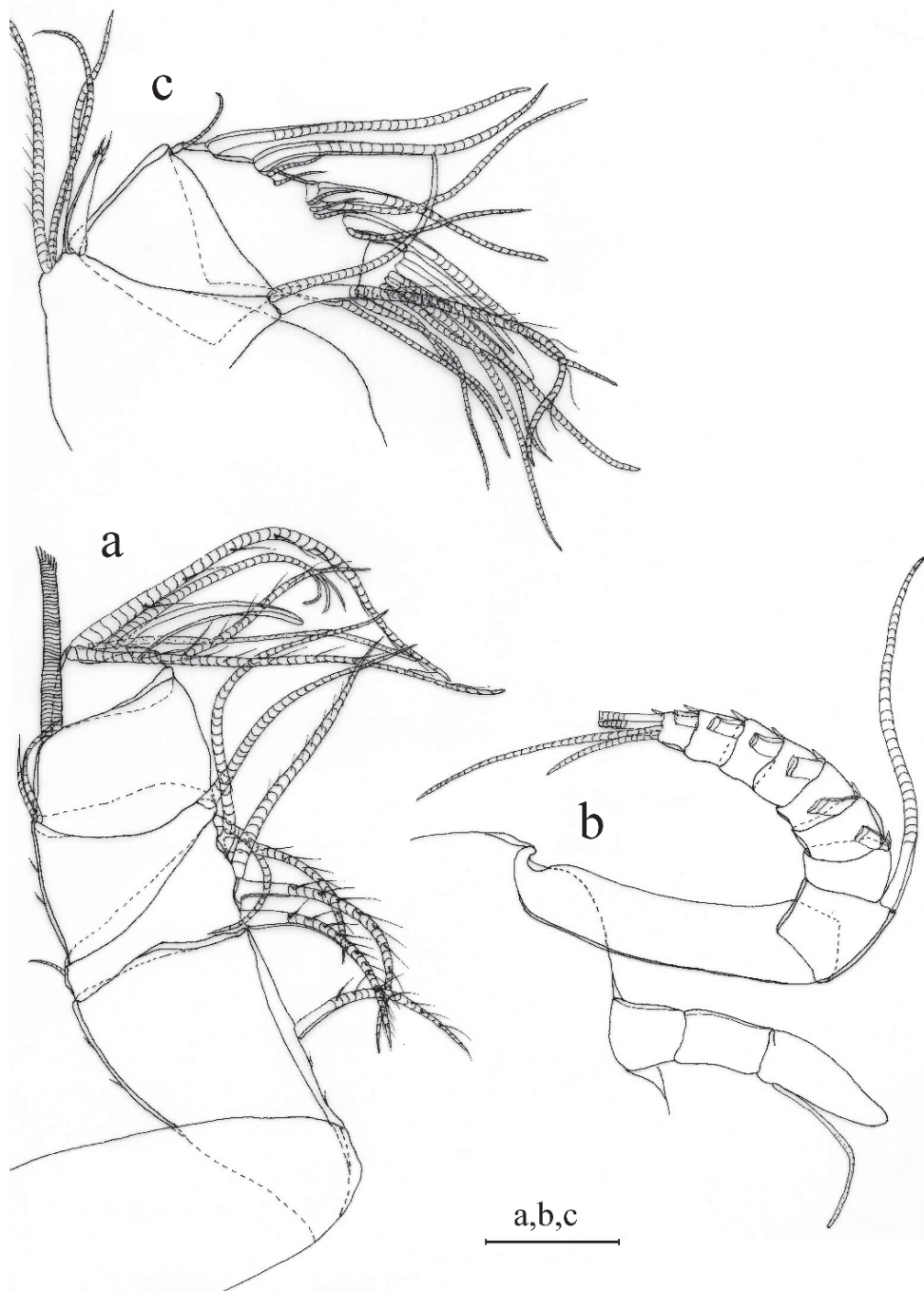


Figure 6. *Parasterope sagami* sp. nov. holotype female adult: **a** A1 **b** A2 **c** Md. Scale bar: 0.1 mm.

missing, one long with long marginal spines, and one shorter without spine or hair); 2nd joint: ventral margin: with three terminal bristles; dorsal margin: with stout a-, b-, c-, and d-bristles and one short bristle proximal to a-bristle; e-bristle missing, two medial bristles adjacent to b-bristle; three medial bristles forming an oblique row adjacent to c-bristle; f-bristle between c- and d-bristle, long, bare; g-bristle shorter than f-bristle. End segment with a strong dorsal claw-like bristle without marginal spines, three juxtaposed stout bristles of equal length.

Mxl (Fig. 7e). Endite I with three bristles. Endite II with four bristles. Basale: one dorsal medial distal bristle, two ventral medial proximal bristles. Endopodite: 1st with one short α -seta and one hairy β -seta; 2nd article with two terminal bristles.

L5 (Fig. 7f). Ventral section with fan of long setae. Comb: spinous exopodite bristle over past distal end of comb, one bristle just proximal at the ventral edge of comb.

L6 (Fig. 7g). Anterior margin with one endite bristle. Ventral margin with two spinous anterior bristles separated by space from 13 bristles. Anterior, ventral, and posterior margins, and medial surfaces hirsute. Lateral flap spinous but without bristles.

L7 (Fig. 7h). Each limb with 12 bristles. Six proximal and six distal bristles (three on each side).

F (Fig. 7i). Each lamella with five claws and three posterior claws bristle-like. A total of eight claws and bristles.

Male. All features comparable to adult female; important differences are:

Shell (Fig. 5d–f). Carapace more elongate than that of female and, carapace length 1.65 mm, height at middle 1.02 mm.

A1 (Fig. 7b). Sensory seta with robust stem and many filaments. 7th and 8th joints with very long c- and f-setae (long as carapace length) each with numerous of marginal filaments. 2nd joint with lateral bristle. 2nd and 4th joints without dorsal margin spines.

Eyes. Lateral eye with 18 ommatidia obscured by black pigment.

A2 (Fig. 7c). Endopodite with three articles, article two with two lateral setae, article three recurved with one small proximal seta.

Md (Fig. 7d). Basale dorsal margin with two long terminal setae. Endopodite: 2nd joint: dorsal margin: with stout a-, b-bristles, c- and d-claws bristle-like, and two short bristles proximal to a-bristle; e-bristle present on male. Two oblique rows between b- and c-bristles (a row adjacent to b-bristle with four bristles, a row adjacent to c-claw bristle-like with six bristles).

Reproductive organs. Unknown.

Remarks. *Parasterope sagami* differs from all other *Parasterope* representatives by the combination of the following characters:

Female. Dorsal margin of the Md basale has three long terminal setae next to the exopodite, and it has no mid-bristle. In addition, the A1 g-bristle has a peculiar shape, and there is no lateral bristle on the A1 2nd joint;

Male. The presence of the c- and d-claws bristle-like on the Md endopodite 2nd joint in the adult males is unique for the new species.



Figure 7. *Parasterope sagami* sp. nov. holotype male adult: **a** Bellonci organ **e** Mxl **f** L5 **g** L6 **h** L7 **i** F. Paratype male adult: **b** A1 **c** A2 endopodite **d** Md. Scale bar: 0.1 mm.

In addition to the above characters, *P. sagami* differs from *P. busanensis* and the morphology of the endite II of Mxl. Namely, the endite carries three rather than four bristles. Also, the short α -seta on the Mxl exopodite is absent in *P. busanensis*.

Parasterope jenseni was also described from Sagami Sea, Japan (Poulsen 1965) and it also has no lateral bristle on the A1 2nd joint. It differs from *P. sagami* by having small lateral eyes with ~ 10 ommatidia; a long stem of the sensory bristle (~ 4 × the length of the 6th joint); and the presence of spines on the ventral margin of the protopodite of A2 (Poulsen 1965).

Parasterope obesa Poulsen, 1965 from Misaki, Japan has a lateral bristle on the 2nd joint of A1 which is absent in the two above species; 4th joint of the A1 is without lateral spines on the ventral margin otherwise present in the new species; and there are more than ten bristles on the ventral edge of the comb.

GenBank numbers 16S: OK048683, OK048684; 18S: OK048721, OK048722.

***Parasterope singula* sp. nov.**

<http://zoobank.org/4C34D735-E105-40E7-83A4-67BA3BD2C9EF>

Figs 8, 9

Specimens examined. *Holotype* female dissected on one slide, shells on SEM stub (NIBR IV 0000887835). *Paratypes*: two females dissected on one slide each, shells on SEM stub (NIBR IV 0000879835_2&3). The sample was collected from the type locality: South Korea, Chuja Island by Ho Young Soh on 29 November 2012.

Etymology. The name is a Latin noun, *singula*, because only a female has been collected. The name is in nominative, feminine singular, agreeing in gender with the genus.

Diagnosis. Surface of the shell completely smooth. Anterior end with a deep incisure and posterior infold of the carapace with a broad shelf. Posterior end wider than anterior. Dorsal margin rounded. Lateral eye well developed with black pigmented ommatidia. Uropodal lamellae with nine claws.

Description. Female. Shell (Fig. 8). Carapace oval, broadening at posterior, greatest height near middle, carapace length 1.25 mm, height 0.9 mm. Carapace smooth and without ornamentation.

A1 (Fig. 8a). 1st joint: with no hair on broad surface. 2nd joint: one spinous dorsal seta, one short lateral bristle, and small proximal dorsal spines. 3rd joint: seven setae (one short ventral and six dorsal). 4th joint: three bristles (one long dorsal bristle and two short ventral bristles). 5th joint: sensory bristle with six filaments without short proximal terminal. 6th joint: one medial seta, attached to bottom of 7th joint boundary. 7th joint: a-bristle claw-like, bare; b-seta with marginal filaments; c-seta with marginal filaments. 8th joint: d-bristle absent; e-bristle bare with blunt tip; f- and g-bristles with marginal filaments.

Bellonci orange (Fig. 9b). Elongate with rounded tip with unclear constriction.

Eyes. Lateral eye with 18 ommatidia.

A2 (Fig. 9c, d). Protopodite: rounded without medial bristle. Endopodite (Fig. 9c): not strongly jointed, with long terminal bristle. Exopodite (Fig. 9d): 9-jointed; bristle

of 2nd segment along ventral margin and spines along dorsal margin reaching 8th joint; 3rd–8th joints with natatory hairs and spines along proximal part of ventral margin. 9th article: four bristles (two long natatory and two short bristles). 4th–8th joints with minute spines at inner terminal corner.

Md (Fig. 9e–g). Coxale endite (Fig. 9e) same as that on *P. busanensis*. Basale (Fig. 9f): Basale endite with three spinous end bristles, four triaenid bristles with three spines excluding terminal pair, and two equal-length bare bristles. Basale dorsal margin with two long terminal setae, without mid-bristle; five rows of small spines on the broad surface near dorsal margin. Exopodite with hirsute tip and two small subterminal setae, exopodite almost same length as dorsal margin of first endopodite article. Endopodite (Fig. 9g): 1st joint: ventral margin with three bristles (two long with long marginal spines, and one shorter without spine or hair); 2nd joint: ventral margin: with three terminal bristles; dorsal margin: with stout a-, b-, c-, and d-bristles and without bristle proximal to a-bristle; one long e-bristle between b- and c-bristles; four medial bristles forming an oblique row adjacent to c-bristle; f-bristle between c- and d-bristles, long, bare; g-bristle longer than f-bristle. 3rd segment with a strong dorsal claw-like bristle without marginal spines, three juxtaposed stout bristles of equal length, and two thin bristles.

Mxl. Endite I with three bristles. Endite II with three bristles. Basale: one dorsal medial distal bristle, two ventral medial proximal bristles. Endopodite: 1st with one short α -seta and one hairy β -seta; 2nd article with two terminal bristles.

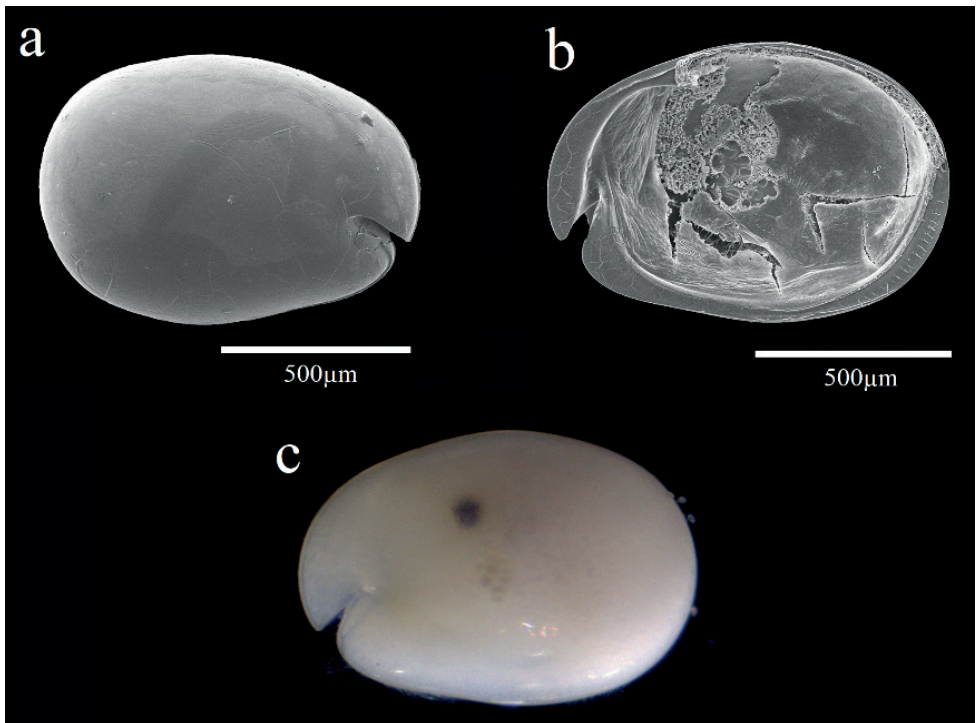


Figure 8. Light microscopy and scanning electron microscopy images of *Parasterope singula* sp. nov. holo-type female adult: **a** Lateral view from left valve **b** Internal view from left valve **c** External view.

L5 (Fig. 9h). Ventral section with fan of long setae. Comb with spinous exopodal bristle just reaching past distal end of comb, one short slender bristle just ventral to base of stout bristle, one bristle near exopodal bristle stem, and four lateral bristles set back from edge at comb mid length.

L6 (Fig. 9i). Unidentified number of endite bristle on the anterior margin. Lateral flap with hairs but no bristles. Anterior tip of skirt with two small bristles. Ventral and postero-ventral margin with 17 plumose bristles (one missing).

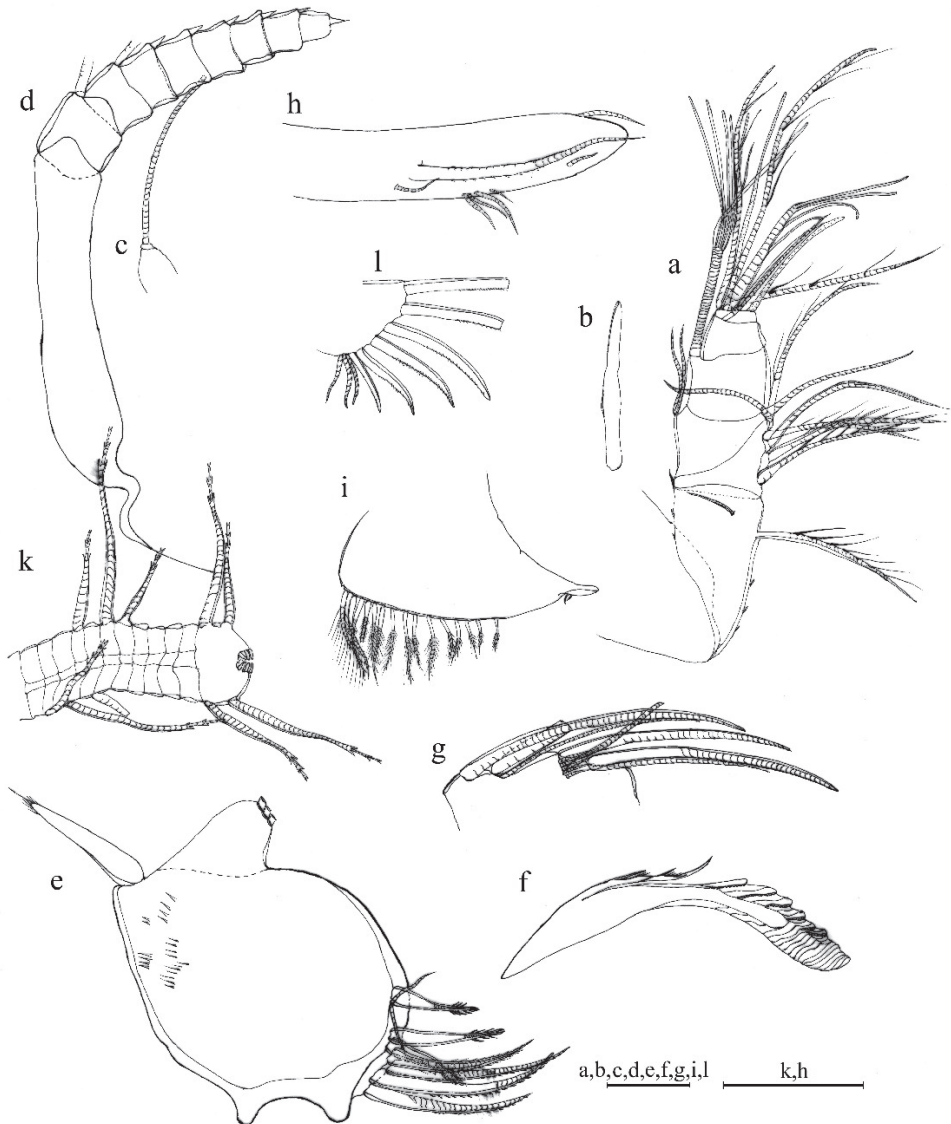


Figure 9. *Parasterope singula* sp. nov. holotype female adult: **a** A1 **b** bellonci organ **c** A2 endopodite **d** A2 exopodite **e** Md basale and coxale endite **f** Md basale endite **g** Md endopodite **h** L5 **i** L6 **k** L7 **l** F. Scale bar: 0.1 mm.

L7 (Fig. 9k). Each limb with ten bristles. Four proximal and six distal bristles.

F (Fig. 9l). Each lamella with six claws plus three posterior claws bristle-like. A total of nine claws and bristles.

Male. Not collected.

Remarks. The presence of rows of small spines on the broad surface near the dorsal margin of the Md basale is a unique feature of *Parasterope singula*. Additionally, the number of bristles on the L7 (ten bristles: four on the terminal segment (two on each side), six on the proximal segments (three on each side) is less than in all other *Parasterope* representatives. The new species is similar to *P. mckenziei*, described from Samar Province, Philippines (McKenzie, 1970) but differs in the following characters: the Md endopodite is without a proximal bristle next to the a-bristle, a character not known in any other *Parasterope*, and the number of claws on UL (nine vs. seven).

The 2nd joint of the Md endopodite in *P. singula* carries one oblique row of cleaning setae, also recorded in *P. antyx* Kornicker, 1989 from Bay of Biscay (Kornicker, 1989), *P. gamma* Kornicker, Harrison-Nelson & Coles, 2007 from Hawaiian Islands (Kornicker et al. 2007), *P. hulingsi* Baker, 1978 from California (Baker 1978), *P. jenseni* from Sagami Sea, Japan (Poulsen 1965), *P. lagunicola* Hartmann, 1984 from French Polynesia (Hartmann 1984), *P. mckenziei* from the Philippines (Kornicker 1970), *P. muelleri* Skogsberg, 1920 from England (Poulsen 1965), *P. proluxa* Kornicker, 1975 from Australia (Kornicker 1975), *P. sequex* Kornicker & Poore, 1996 from Australia (Kornicker and Poore 1996), *P. styx* from Chile (Kornicker 1975), and *P. theta* from Waikiki (Kornicker et al. 2007). The three other new species, *P. busanensis*, *P. sagami*, and *P. sohi* also have two oblique rows. The exopodite of the A2 in *P. singula* and *P. sohi* carries minute spines at inner terminal corner on the 5th–8th joints, while these spines are present from the 1st–8th joints in *P. busanensis* and *P. sagami*.

GenBank numbers 16S: OK048686, OK048687; 18S OK048723.

***Parasterope sohi* sp. nov.**

<http://zoobank.org/94451EAB-B789-4279-9CB7-585F59753729>

Figs 10, 11

Specimens examined. *Holotype* female dissected on one slide, shells on SEM stub (NIBR IV 0000887834). The sample was collected from the type locality: South Korea, Maemul Island, 34°32'00.4"N, 128°43'54.4"E, by Ho Young Soh on 25th July 2011.

Etymology. The species named after Prof. Ho-young Soh (Faculty of Marine Technology, Chonam National University, Jeonnam, Korea), whom we are greatly indebted to for collecting and providing samples for this publication.

Diagnosis. Carapace elongated. Surface of the shell completely smooth. Posterior end with a short, rounded incisure, while the anterior has relatively deep incisure. Dorsal and ventral margins rounded. Posterior end wider than anterior. Lateral eye well developed with black pigmented ommatidia.

Description. Female. Shell (Fig. 10). Carapace oval, broadening at posterior, greatest height near middle, carapace length 1.48 mm, height 0.98 mm. Carapace smooth and without ornamentation.

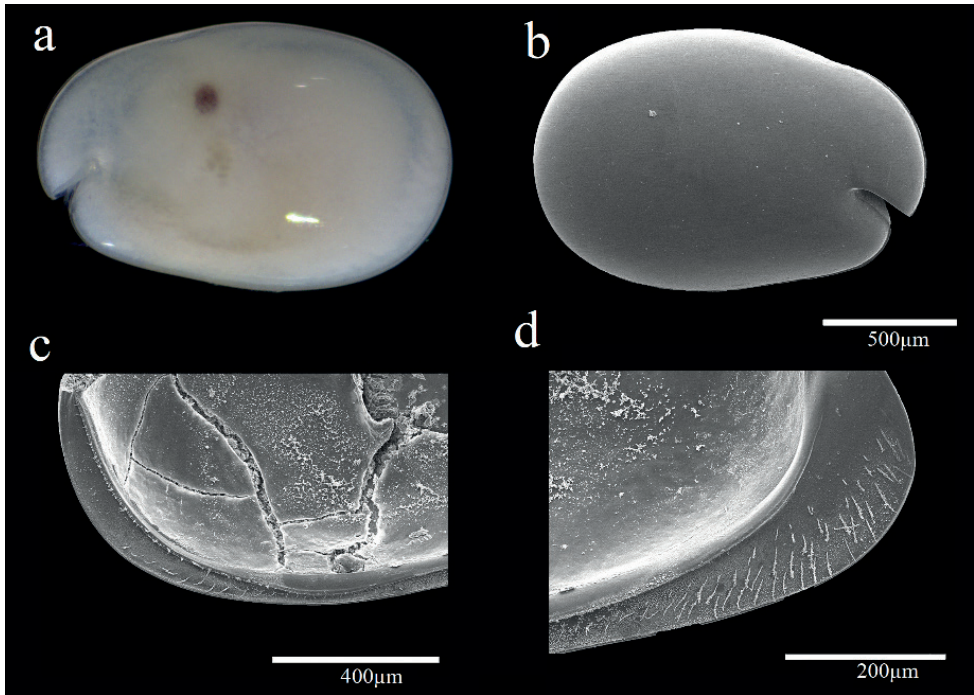


Figure 10. Light microscopy and scanning electron microscopy images of *Parasterope sobi* sp. nov. holo-type female adult: **a** External view **b** Lateral view from left valve **c** Anterior of left valve from inside showing bristles of infold.

A1 (Fig. 11a). 1st joint: with no hair on broad surface and longer than 2nd joint. 2nd joint without spines along dorsal or ventral margin, one spinous dorsal seta, one short lateral bristle. 3rd joint: seven setae (one short ventral and six dorsal). 4th joint: three bristles (one long dorsal and two short ventral bristles). 5th joint: sensory bristle with six filaments without short proximal terminal. 6th joint: one medial seta, attached to bottom of 7th joint boundary. 7th joint: a-bristle claw-like, bare; b-seta with marginal filaments; c-seta with marginal filaments. 8th joint: d-bristle absent; e-bristle bare, with blunt tip; f- and g-bristles with marginal filaments.

Bellonci orange (Fig. 11b). Elongate with rounded tip with unclear constriction.

Eyes. Lateral eye with 15 ommatidia.

A2 (Fig. 11c, d). Protopodite: rounded. Endopodite (Fig. 11c): 2-jointed, with long terminal bristle, ~ 1/3 of stem length. Exopodite (Fig. 11d): 9-jointed; bristle of 2nd segment along ventral margin and spines along dorsal margin reaching 8th joint; 3th–8th joints with natatory hairs and spines along proximal part of ventral margin. 9th article: four bristles (two long natatory and two short bristles). 5th–8th joints with minute spines at inner terminal corner.

Md (Fig. 11e, f). Coxale endite same as that on *P. busanensis* and *P. singula*. Basal endite (Fig. 11e) with six spinous end bristles and one triaenid bristle with three spines excluding terminal pair. Basale dorsal margin with two long terminal setae, without

mid-bristle. Exopodite with spine-like tip and small subterminal setae, exopodite just reaching past end of dorsal margin of the 1st endopodite article. Endopodite (Fig. 11f): 1st joint: ventral margin with three long bristles with long marginal spines; 2nd joint: ventral margin: with three terminal bristles; dorsal margin: with stout a-, b-, c-, and d-bristles and with one short bristle proximal to a-bristle (missing on drawing line figure); one long e-bristle between b- and c-bristles; four medial cleaning bristles forming an oblique adjacent to b-bristle; five medial bristles forming an oblique row adjacent to c-bristle; f-bristle between c- and d-bristles, long, bare; g-bristle longer than f-bristle. 3rd segment with a strong dorsal claw-like bristle without marginal spines, three juxtaposed stout bristles of equal length, and two thin bristles.

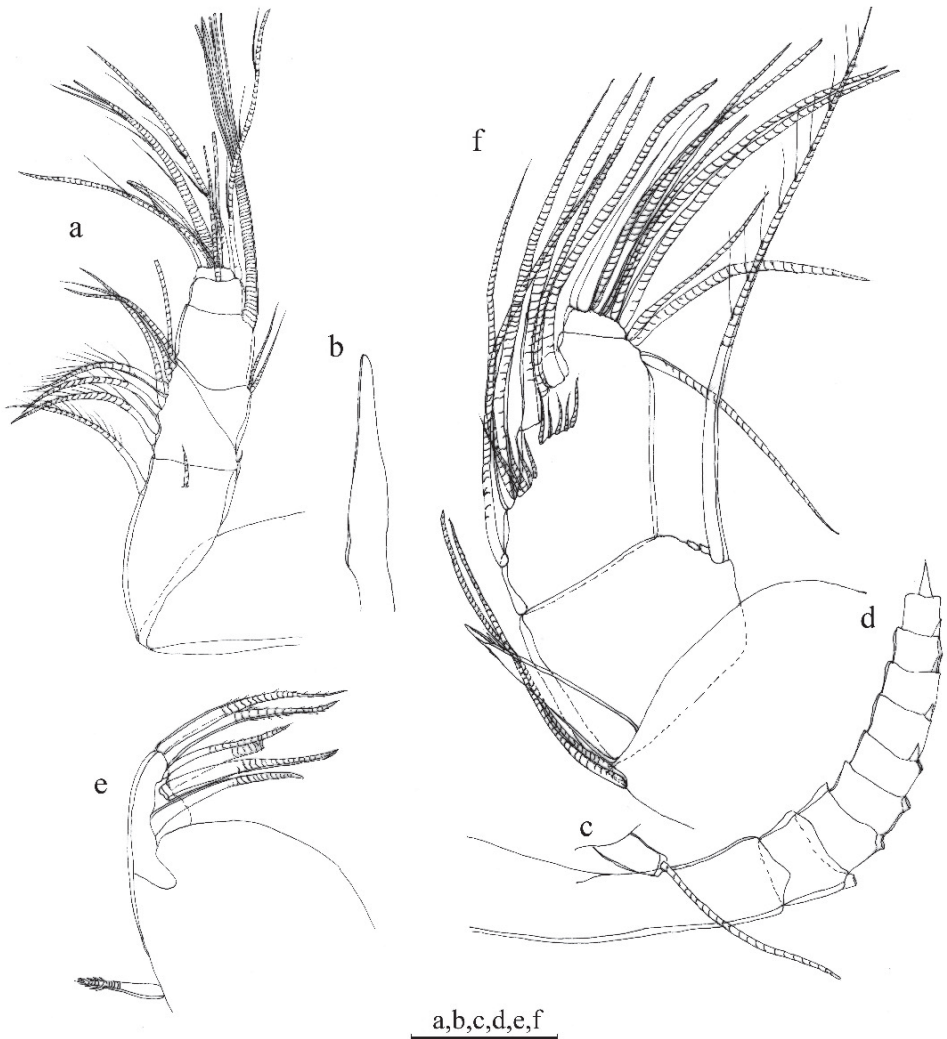


Figure 11. *Parasterope sobi* sp. nov. holotype female adult: **a** A1 **b** bellonci organ **c** A2 endopodite **d** A2 exopodite **e** Md basale endite **f** Md endopodite. Scale bar: 0.1 mm.

Mxl. Endite unknown. Basale: one dorsal medial distal bristle. Endopodite: 1st with one short α -seta and one hairy β -seta; 2nd article with two terminal bristles.

L5. Unknown.

L6. Unknown.

L7. Unknown.

F. Unknown.

Male. Not collected.

Remarks. The new species *Parasterope sobi* sp. nov. is poorly known because of the missing L5, L6, L7, and furca but we propose a new name because of the presence of the combination of the following characters: A1 sensory bristle carry 0+6 filaments; exopodite of Md is unusually long; and the Md endopodite has the e-bristle. In majority of *Parasterope* described so far, the mandible exopodite is at most longer than ½ length of the dorsal margin of the 1st endopodite joint; in *P. sobi* the exopodite length is greater than the length of the dorsal margin of the 1st endopodite joint. Other species with such a long exopodite include *P. lagunicola* from French Polynesia (Hartmann 1984), *P. omega* Kornicker, Harrison-Nelson & Coles, 2007 from Hawaiian Islands (Kornicker, Harrison-Nelson and Coles 2007), and *P. sohni* Kornicker & Caraion, 1974 from West Africa (Kornicker and Caraion 1974). However, the first two species have small proximal spines on A1, absent in *P. sobi*. The last species has a mid-bristle on the dorsal margin of the basale, absent in *P. sobi*. Also, *P. sobi* differs from another *Parasterope* species by having six spinous end bristles and one triaenid bristle on the endite of the Md basale. All other *Parasterope* species are armed with at least four triaenid bristles.

GenBank number 16S: OK048685. 18S could not be obtained.

A checklist of species of *Parasterope*

A checklist of species the 49 named *Parasterope*, including four new species described in this study, is presented in Suppl. material 1. This is an updated species checklist published by Syme and Poore (2006b), and at the World Ostracoda Database (Brandão et al. 2022).

Results of molecular analysis

The final alignment of the 16S data set consisted of 33 sequences 445 base pairs long, of which 210 were constant sites (= 47.191% of all sites), 210 were invariant (= 47.191% of all sites), 207 were parsimony informative, and 275 were distinct site patterns. The substitution model TPM2+F+I+G4 was found to be the best fit evolutionary model. Effective sample size for all the continuous parameters (posterior, prior, tree likelihood, tree height, Yule model, and birthrate) estimated by Tracer analysis was far above a recommended number (200). Phylogram is presented on the Fig. 12. The results of pairwise distance analysis between species

used in this study are shown in Suppl. material 2: Table S1. The interspecies pairwise distances between 16S rRNA sequences belonging to *Parasterope* ranged between 22% (between *Parasterope* sp. NW-2004 and *P. sohi*) and 45% (between *P. sohi* and *P. busanensis*). The pairwise distance between *Parasterope* and the other *Cylindroleberidinae* groups varied between 0% (with *Cylindroleberis*) and 59% (with *X. yamadai*). Distances between genera (Suppl. material 3: Table S2) varied from 32.7% (between *Cylindroleberis* and *Bathyleberis*) to 53.3% (between *Postasterope* and *Parasterope*). Of all genera included in the analyses, *Parasterope* had the highest values of intrageneric distances of 32.2%. We failed to amplify 18S sequence of *P. sohi*, however, distance between 18S of other *Parasterope*, as well as distance between *Cylindroleberidinae* genera, for which data are available, are presented in the Suppl. material 4: Table S3. Distances between genera were less than 4% (in the range between 0.3% and 3.7%). Similar values were calculated for the intrageneric distances (from 1.0% to 4.0%). Interspecies pairwise distances between 18S sequence are shown in the Suppl. material 5: Table S4. The highest value was 4% between *Cylindroleberis* sp. J57069 and *C. marranyin*.

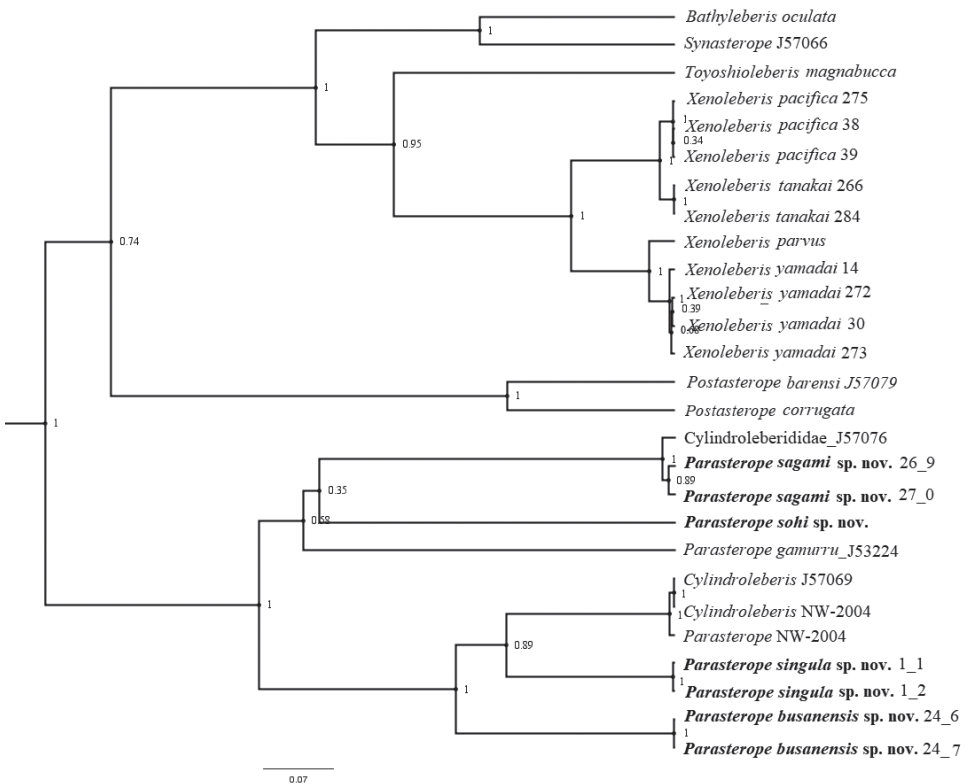


Figure 12. Bayesian inference cladogram of the *Cylindroleberidinae* subfamily based on 16S rRNA sequences. Numbers at nodes represent posterior probability.

The resulting phylogenetic tree based on the newly obtained sequences and those belonging to the subfamily Cylindroleberidinae reconstructed based on the 16S alignment (Fig. 12) suggests that *Parasterope* is not a monophyletic taxon, as it clusters with several *Cylindroleberis* sequences, downloaded from GenBank. *Parasterope* sequences, *Cylindroleberis* sequences, and one unidentified sequence from GenBank form a clade separate from the rest of the included genera. Two of the species described from Korea, *P. busanensis* and *P. singula* form a monophyletic unit together with two undescribed *Cylindroleberis* and one *Parasterope* species downloaded from GenBank. This branch received a high posterior probability support of 1. The Japanese species, *P. sagami* clusters with one GenBank sequences attributed to an unidentified Cylindroleberididae taxon, and the branch has a high posterior probability support. The third Korean species, *P. sohi* clustered with *P. gamurru* and the new Japanese species, but this branch did not receive a high posterior probability support.

Discussion

The unusual clustering of *Parasterope* and several unidentified Cylindroleberididae and *Cylindroleberis* on the phylogenetic tree, assigned to other genera, should be considered as misidentification and/or contaminations, and not an indication of polyphyletic nature of *Parasterope*. This can be supported by the results from previous, more complex, phylogenetic analyses of the entire family Cylindroleberididae (Syme and Oakley 2012; Pham et al. 2021) where the same GenBank sequences have been used, but they did not cluster with *Parasterope* sequences.

Due to a very limited number of available sequences attributed to the subfamily Cylindroleberidinae (27 in total) our phylogenetic tree included only 18 species belonging to seven genera. This can be considered a very poor sample, since the subfamily contains ~ 200 species belonging to 23 genera (see Pham et al. 2021; Brandão et al. 2022). Therefore, the interpretation of our results is very limited. However, it should be noted that only two out of three newly described Korean species form a monophyletic unit, while the third species, *P. busanensis* clusters with the Japanese species *P. sagami*, albeit with almost no support.

The results of pairwise distance analysis show a fast evolutionary rate of 16S rRNA, in contrary to 18S rRNA. Calculated pairwise distances between 18S sequences were very similar to those of other for Cylindroleberidae, Cypridinidae, and Philomedidae published by Pham et al. (2020). These results indicate that 18S gene marker does not provide enough resolution for the reconstruction of phylogenetic relationships below the subfamily level. The pairwise distance values of this genetic marker between genera in the subfamily Cylindroleberidinae mainly ranges from 1 to 2%, and even < 1% in the case of *Synasterope* and *Postasterope* (0.2%), indicating that 18S is ineffective genetic tools to construct a phylogenetic tree at a lower taxonomic level (below family) of this target taxa. From these results and those published in previous work (Pham et al. 2020; Pham et al. 2021), we recommend using a combination of fast-evolving gene markers (COI, 16S) and highly-conservative gene markers (18S and 28S) for

constructing a phylogenetic tree for the Myodocopida group rather than analysis based on a single marker.

In the Syme and Oakley (2012) study where molecular and morphological data for the entire family Cylindroleberididae were combined to study phylogenetic relationships, *Parasterope* was polyphyletic. This may be due to the fact that molecular data set was smaller than morphological data set for all included genera. Nevertheless, it is very likely that the new genetic data will change current view on the phylogeny of this diverse genus, and its position within the subfamily.

In terms of biodiversity, our results are important as they provide new data for the marine fauna of Korea and Japan. They also point out that samples taken from areas where human impact on ecosystems is high due to dense population and industrial development can yield new species, and enrich our knowledge on the biodiversity of the planet.

Acknowledgements

We would like thank Dr. Hayato Tanaka (Tokyo Sea Life Park) and the crews of TR/V Toyoshio-maru and R/V Rinkai-maru for providing the Japanese specimens, Prof. Ho-young Soh (Faculty of Marine Technology, Chonam National University, Jeonnam, Korea), Dr. Hyunsu Yoo (Marine Environmental Research and Information Laboratory (MERIL), and the Marine Biodiversity Institute of Korea (MABIK) for providing additional Korean specimens. This study was funded by the Basic Science Research Program through NRF funded by the Ministry of Education (grant number: 2020R1A6A1A06046827), and the National Institute of Biological Resources (NIBR), funded by the Ministry of Environment (MOE) of the Republic of Korea (grant number: NIBR202102203).

References

- Baker JH (1978) Two new species of *Parasterope* (Myodocopina, Ostracoda) from southern California. *Crustaceana* 35(2): 139–151. <https://doi.org/10.1163/156854078X00042>
- Benson DA, Clark K, Karsch-Mizrachi I, Lipman DJ, Ostell J, Sayers EW (2015) GenBank. *Nucleic Acids Research* 43(D1): D30–D35. <https://doi.org/10.1093/nar/gku1216> [accessed 21 August 2021]
- Bouckaert R, Heled J, Kühnert D, Vaughan T, Wu CH, Xie D, Suchard MA, Rambaut A, Drummond AJ (2014) BEAST 2: A Software Platform for Bayesian Evolutionary Analysis. *PLoS Computational Biology* 10(4): e1003537. <https://doi.org/10.1371/journal.pcbi.1003537>
- Brandão SN, Antonietto LS, Karanovic I (2022) World Ostracoda Database. <https://www.marinespecies.org/ostracoda> [accessed 3 February 2022]
- Bridge D, Cunningham CW, DeSalle R, Buss LW (1995) Class-level relationships in the Phylum Cnidaria: Molecular and morphological evidence. *Molecular Biology and Evolution* 12: 679–689. <https://doi.org/10.1093/oxfordjournals.molbev.a040246>
- Chavtur VG (1983) Ostrakody Myodocopina, Cladocopina umerennykh I kholodnykh vod Severnogo polusharila. [Ostracodes (Myodocopina, Cladocopina) of Temperate and Cold

- Waters of the Northern Hemisphere.]. Academy of Sciences of the USSR, Far-Eastern Science Center, Institute of Marine Biology, 132 pp.
- Collins AG (2000) Towards understanding the phylogenetic history of Hydrozoa: Hypothesis testing with 18S gene sequence data. *Scientia Marina* 64(S1): 5–22. <https://doi.org/10.3989/scimar.2000.64s15>
- Collins AG, Schuchert P, Marques AC, Jankowski T, Medina M, Schierwater B (2006) Medusozoan phylogeny and character evolution clarified by new large and small subunit rDNA data and an assessment of the utility of phylogenetic mixture models. *Systematic Biology* 55(1): 97–115. <https://doi.org/10.1080/10635150500433615>
- Govindarajan AF, Boero F, Halanych KM (2006) Phylogenetic analysis with multiple markers indicates repeated loss of the adult medusa stage in Campanulariidae (Hydrozoa, Cnidaria). *Molecular Phylogenetics and Evolution* 38(3): 820–834. <https://doi.org/10.1016/j.ympev.2005.11.012>
- Hartmann G (1984) Zur Kenntnis der Ostracoden der polynesischen Inseln Huahiné (Gesellschaftsinseln) und Rangiroa (Tuamotu-Inseln). Mit Bemerkungen zur Verbreitung und Ausbreitung litoraler Ostracoden und einer Übersicht über die bislang auf den pazifischen Inseln gefunden. *Mitteilungen aus dem Hamburgischen Zoologischen Museum und Institut* 81: 117–169.
- Kalyaanamoorthy S, Minh BQ, Wong TKF, Haeseler A, Jermiin LS (2017) ModelFinder: Fast model selection for accurate phylogenetic estimates. *Nature Methods* 14(6): 587–589. <https://doi.org/10.1038/nmeth.4285>
- Karanovic I, Soh HY (2015) Five Sarsiellidae ostracods (Crustacea: Myodocopida) from the South Coast of Korea (East China Sea). *Zootaxa* 3947(4): 451–488. <https://doi.org/10.11646/zootaxa.3947.4.1>
- Katoh K, Rozewicki J, Yamada KD (2019) MAFFT online service: Multiple sequence alignment, interactive sequence choice and visualization. *Briefings in Bioinformatics* 20(4): 1160–1166. <https://doi.org/10.1093/bib/bbx108>
- Kimura M (1981) Estimation of evolutionary distances between homologous nucleotide sequences. *Proceedings of the National Academy of Sciences of the United States of America* 78(1): 454–458. <https://doi.org/10.1073/pnas.78.1.454>
- Kornicker LS (1970) Myodocopid Ostracoda (Cypridinacea) from the Philippine Islands. *Smithsonian Contributions to Zoology* 39: 1–32. <https://doi.org/10.5479/si.00810282.39>
- Kornicker LS (1975) Antarctic Ostracoda (Myodocopina), Part 2. *Smithsonian Contributions to Zoology* 163: 375–720. <https://doi.org/10.5479/si.00810282.163>
- Kornicker LS (1981) Revision, distribution, ecology, and ontogeny of the Ostracode subfamily Cyclasteropinae (Myodocopina: Cylindroleberididae). *Smithsonian Contributions to Zoology* 319: 1–541. <https://doi.org/10.5479/si.00810282.319>
- Kornicker LS (1986) Cylindroleberididae of the Western North Atlantic and the Northern Gulf of Mexico, and Zoogeography of the Myodocopina (Ostracoda). *Smithsonian Contributions to Zoology* 425: 1–139. <https://doi.org/10.5479/si.00810282.425>
- Kornicker LS (1989) Bathyal and Abyssal Myodocopid Ostracoda of the Bay of Biscay and Vicinity. *Smithsonian Contributions to Zoology* 467: 1–134. <https://doi.org/10.5479/si.00810282.467>

- Kornicker LS, Caraion FE (1974) West African Myodocopid Ostracoda (Cylindroleberididae). *Smithsonian Contributions to Zoology* 179: 1–88.
- Kornicker LS, Harrison-Nelson E (2005) Ostracoda from Johnston Atoll, Pacific Ocean, and proposal of a new tribe, Bruuniellini (Myodocopina: Cylindroleberididae). *Pacific Science* 59(3): 323–362. <https://doi.org/10.1353/psc.2005.0038>
- Kornicker LS, Poore GC (1996) Ostracoda (Myodocopina) of the SE Australian Continental Slope: Part 3. *Smithsonian Contributions to Zoology* 573: 1–186. <https://doi.org/10.5479/si.00810282.573>
- Kornicker LS, Harrison-Nelson E, Coles SL (2007) Ostracoda (Myodocopina) from O‘ahu and French Frigate Shoals, Hawaiian Islands. *Bishop Museum bulletin in Zoology* 8: 1–128.
- Kumar S, Stecher G, Tamura K (2016) MEGA7: Molecular Evolutionary Genetics Analysis Version 7.0 for Bigger Datasets. *Molecular Biology and Evolution* 33(7): 1870–1874. <https://doi.org/10.1093/molbev/msw054>
- Lee EH, Huh M, Schornikov EI (2000) Ostracod fauna from the East Sea coast of Korea and their distribution— Preliminary study on ostracods as indicators of water pollution. *Journal of the Geological Society of Korea* 36: 435–472.
- Müller GW (1890) Neue Cypridiniden. *Zoologische Jahrbucher* 5: 211–252. https://doi.org/10.1007/978-3-662-36389-8_6
- Müller GW (1906) Die Ostracoda der Siboga Expedition. *Siboga-Expedition* 30: 1–40.
- Nakano H, Kakui K, Kajihara H, Shimomura M, Jimi N, Tomioka S, Tanaka H, Yamasaki H, Tanaka M, Izumi T, Okanishi M, Yamada Y, Shinagawa H, Sato T, Tsuchiya Y, Omori A, Sekifuji M, Kohtsuka H (2015) JAMBIO Coastal Organism Joint Surveys reveals undiscovered biodiversity around Sagami Bay. *Regional Studies in Marine Science* 2: 77–81. <https://doi.org/10.1016/j.rsma.2015.05.003>
- Oakley TH (2005) Myodocopa (Crustacea: Ostracoda) as models for evolutionary studies of light and vision: Multiple origins of bioluminescence and extreme sexual dimorphism. *Hydrobiologia* 538(1–3): 179–192. <https://doi.org/10.1007/s10750-004-4961-5>
- Oakley TH, Cunningham CW (2002) Molecular phylogenetic evidence for the independent evolutionary origin of an arthropod compound eye. *Proceedings of the National Academy of Sciences of the United States of America* 99(3): 1426–1430. <https://doi.org/10.1073/pnas.032483599>
- Pham TMH, Tanaka H, Karanovic I (2020) Molecular and morphological diversity of *Heterodesmus* Brady and its phylogenetic position within Cypridinidae (Ostracoda). *Zoological Science* 37(3): 240–254. <https://doi.org/10.2108/zs190118>
- Pham TMH, Jöst AB, Karanovic I (2021) Phylogenetic position of *Xenoleberis* Kornicker within Cylindroleberidinae (Ostracoda: Myodocopa) with descriptions of three new species and one new genus from the Northwest Pacific Ocean. *Marine Biodiversity* 51(86): 1–22. <https://doi.org/10.1007/s12526-021-01223-7>
- Poulsen EM (1965) Ostracoda - Myodocopa, Part II: Cypridiniformes - Rutidermatidae, Sarsiellidae and Asteropidae. *Dana Report Carlsberg Foundation* (65): 1–484.
- Rambaut A (2010) FigTree v1.3.1. Institute of Evolutionary Biology, University of Edinburgh, Edinburgh. <http://tree.bio.ed.ac.uk/software/figtree/>

- Rambaut A, Drummond AJ, Xie D, Baele G, Suchard MA (2018) Posterior summarization in Bayesian phylogenetics using Tracer 1.7. *Systematic Biology* 67(5): 901–904. <https://doi.org/10.1093/sysbio/syy032>
- Skogsberg T (1920) Studies on marine ostracods. Part 1. (Cypridinids, Halocyprids and Polycopids). *Zoologiska bidrag fran Uppsala, Supplement 1*: 1–784. <https://doi.org/10.5962/bhl.title.10427>
- Syme AE (2007) A Systematic Revision of the *Cylindroleberididae* (Crustacea: Ostracoda: Myodocopa). Unpublished PhD thesis, Zoology Department, the University of Melbourne.
- Syme AE, Oakley TH (2012) Dispersal between shallow and abyssal seas and evolutionary loss and regain of compound eyes in *Cylindroleberidid* ostracods: Conflicting conclusions from different comparative methods. *Systematic Biology* 61(2): 314–336. <https://doi.org/10.1093/sysbio/syr085>
- Syme AE, Poore GCB (2006a) Three new ostracod species from coastal Australian waters (Crustacea: Ostracoda: Myodocopa: *Cylindroleberididae*). *Zootaxa* 1305(1): 51–67. <https://doi.org/10.11646/zootaxa.1305.1.5>
- Syme AE, Poore GCB (2006b) A checklist of species of *Cylindroleberididae* (Crustacea: Ostracoda). *Museum Victoria Science Report* 9: 1–20. <https://doi.org/10.24199/j.mvsr.2006.09>
- Tanaka H, Ohtsuka S (2015) An illustrated guide to the genera of Myodocopida (Ostracoda: Crustacea) collected from western Japan during the cruise of TRV Toyoshiomaru. *Bulletin of the Hiroshima University Museum* 7: 75–87. [in Japanese]
- Wakayama N, Abe K (2006) The evolutionary pathway of light emission in myodocopid Ostracoda. *Biological Journal of the Linnean Society* 87: 449–455. <https://doi.org/10.1111/j.1095-8312.2006.00589.x>
- Williams BD, Schrank B, Huynh C, Shownkeen R, Waterston RH (1992) A genetic mapping system in *Caenorhabditis elegans* based on polymorphic sequence-tagged sites. *Genetics* 131(3): 609–624. <https://doi.org/10.1093/genetics/131.3.609>
- Yamaguchi S, Endo K (2003) Molecular phylogeny of Ostracoda (Crustacea) inferred from 18S ribosomal DNA sequences: Implication for its origin and diversification. *Marine Biology* 143(1): 23–38. <https://doi.org/10.1007/s00227-003-1062-3>

Supplementary material I

A checklist species of *Parasterope* Kornicker, 1975

Authors: Huyen T. M. Pham, Ivana Karanovic

Data type: Checklist

Explanation note: A checklist of species of *Parasterope* Kornicker, 1975.

Copyright notice: This dataset is made available under the Open Database License (<http://opendatacommons.org/licenses/odbl/1.0/>). The Open Database License (ODbL) is a license agreement intended to allow users to freely share, modify, and use this Dataset while maintaining this same freedom for others, provided that the original source and author(s) are credited.

Link: <https://doi.org/10.3897/zookeys.1095.77996.suppl1>

Supplementary material 2

Table S1

Authors: Huyen T. M. Pham, Ivana Karanovic

Data type: gene distances

Explanation note: Pairwise p-distances among 16S sequences of species presented in Fig. 12.

Copyright notice: This dataset is made available under the Open Database License (<http://opendatacommons.org/licenses/odbl/1.0/>). The Open Database License (ODbL) is a license agreement intended to allow users to freely share, modify, and use this Dataset while maintaining this same freedom for others, provided that the original source and author(s) are credited.

Link: <https://doi.org/10.3897/zookeys.1095.77996.suppl2>

Supplementary material 3

Table S2

Authors: Huyen T. M. Pham, Ivana Karanovic

Data type: gene distances

Explanation note: Between group means distance of 16S sequences from *Cylindroleberidinae* genera. IG: intrageneric.

Copyright notice: This dataset is made available under the Open Database License (<http://opendatacommons.org/licenses/odbl/1.0/>). The Open Database License (ODbL) is a license agreement intended to allow users to freely share, modify, and use this Dataset while maintaining this same freedom for others, provided that the original source and author(s) are credited.

Link: <https://doi.org/10.3897/zookeys.1095.77996.suppl3>

Supplementary material 4

Table S3

Authors: Huyen T. M. Pham, Ivana Karanovic

Data type: gene distances

Explanation note: Between group means distance of 18S sequences from *Cylindroleberidinae* genera. IG: intrageneric.

Copyright notice: This dataset is made available under the Open Database License (<http://opendatacommons.org/licenses/odbl/1.0/>). The Open Database License (ODbL) is a license agreement intended to allow users to freely share, modify, and use this Dataset while maintaining this same freedom for others, provided that the original source and author(s) are credited.

Link: <https://doi.org/10.3897/zookeys.1095.77996.suppl4>

Supplementary material 5

Table S4

Authors: Huyen T. M. Pham, Ivana Karanovic

Data type: gene distances

Explanation note: Pairwise p-distances among 18S sequences of species presented in Table 1.

Copyright notice: This dataset is made available under the Open Database License (<http://opendatacommons.org/licenses/odbl/1.0/>). The Open Database License (ODbL) is a license agreement intended to allow users to freely share, modify, and use this Dataset while maintaining this same freedom for others, provided that the original source and author(s) are credited.

Link: <https://doi.org/10.3897/zookeys.1095.77996.suppl5>

Crab spiders (Araneae, Thomisidae) of Jinggang Mountain National Nature Reserve, Jiangxi Province, China

Ke-Ke Liu^{1,4}, Yuan-hao Ying¹, Alexander A. Fomichev^{2,3}, Dan-chen Zhao¹,
Wen-hui Li¹, Yong-hong Xiao¹, Xiang Xu⁵

1 College of Life Science, Jinggangshan University, Ji'an 343009, Jiangxi, China **2** Altai State University, Lenina Pr., 61, Barnaul, RF-656049, Russia **3** Tomsk State University, Lenina Pr., 36, Tomsk, RF-634050, Russia **4** Key Laboratory of Agricultural Environmental Pollution Prevention and Control in Red Soil Hilly Region of Jiangxi Province, Jinggangshan University, Ji'an, 343009, Jiangxi, China **5** College of Life Science, Hunan Normal University, Changsha 410081, Hunan, China

Corresponding authors: Yong-hong Xiao (yonghongxiao01@126.com), Xiang Xu (xux@hunnu.edu.cn)

Academic editor: Yuri Marusik | Received 10 August 2021 | Accepted 14 March 2022 | Published 13 April 2022

<http://zoobank.org/AD2E6055-9E6D-434D-8758-3D108C6A187C>

Citation: Liu K-K, Ying Y-h, Fomichev AA, Zhao D-c, Li W-h, Xiao Y-h, Xu X (2022) Crab spiders (Araneae, Thomisidae) of Jinggang Mountain National Nature Reserve, Jiangxi Province, China. ZooKeys 1095: 43–74. <https://doi.org/10.3897/zookeys.1095.72829>

Abstract

A list of 34 thomisid species belonging to 21 genera collected in Jiangxi Province of China is provided. Five new species are described: *Angaeus xieluae* Liu, **sp. nov.** (♂♀), *Lysiteles subspirellus* Liu, **sp. nov.** (♀), *Oxytate mucunica* Liu, **sp. nov.** (♀), *Pharta lingxiufengica* Liu, **sp. nov.** (♀), *Stephanopis xiangzhouica* Liu, **sp. nov.** (♀). A new combination is proposed: *Ebelingia forcipata* (Song & Zhu, 1993) **comb. nov.** (ex. *Ebrechtella* Dahl, 1907). Previously unknown females of *E. forcipata* (Song & Zhu, 1993), *Oxytate bicornis* Liu, Liu & Xu, 2017, and *Xysticus lesserti* Schenkel, 1963 are described for the first time. *Stephanopis* O Pickard-Cambridge, 1869, a genus previously known from Australasia and South America, is recorded from the Asian mainland for the first time.

Keywords

Aranei, biodiversity, distribution, East Asia, new record, new species, taxonomy

Introduction

Thomisidae Sundevall, 1833, commonly known as crab spiders, is the seventh largest spider family with a global distribution, comprising 2154 extant species belonging to 171 genera (WSC 2022). More than half of the Thomisidae species are known from a single sex: 752 of these were described from females and 337 from males (WSC 2022). More than fifty species were described from juveniles (WSC 2022).

The family has never been globally revised, but regional revisions have been made in, e.g., Canada (Dondale and Redner 1978), Japan (Ono 2009), and China (Song et al. 1999), etc. In the past ten years, many efforts were made to review or re-assign species described or recorded from China. Although there are several recent publications dealing with revisions, re-assignments of species, and descriptions of unknown sexes of Chinese crab spiders, there are still many species requiring study.

Thomisids in China are relatively well studied due to the revisions by Song et al. (1999) and Tang and Li (2010a, b). Currently, 306 species belonging to 51 genera are known from this country (Li 2020; WSC 2022). Level of knowledge is uneven in different provinces. Numbers of species known per province varies from north (Heilongjiang, $n = 10$) to south (Hainan, $n = 47$). One of the poorly studied provinces is Jiangxi, with only eight known species (Li and Lin 2016). To fill this gap, we studied material collected from the Jinggang Mountain National Nature Reserve in Jiangxi Province of China.

The aims of the present paper are (1) to report findings of 34 species belonging to 21 genera, (2) to provide detailed descriptions of five new species, (3) to provide descriptions of previously unknown females of three species, (4) to propose a new combination, and (5) to provide the first record of the genus *Stephanopsis* from Asian mainland.

Materials and methods

More than 300 adult specimens belonging to 34 species from 21 genera were collected from Jinggang Reserve. Specimens were examined using a Zeiss Stereo Discovery V12 stereomicroscope with a Zoom Microscope System. Both male palps and female copulatory organs were detached and examined in 75% ethanol, using a Zeiss Axio Scope A1 compound microscope with a KUY NICE CCD. For SEM photographs, specimens were dried under natural conditions and photographed with a ZEISS EVO LS15 scanning electron microscope. The epigynes were cleared in pancreatin. Specimens including detached male palps and epigynes were stored in 80% ethanol after examination. All the specimens treated in this work are deposited in the Animal Specimen Museum, Life Science of College, Jinggangshan University (ASM-JGSU).

Measurements were taken with the AxioVision software (SE64 Rel. 4.8.3) and are given in millimetres. Terminology of the male and female copulatory organs follows

Benjamin (2011), Ramírez (2014), and Machado et al. (2019). Promarginal and retro-marginal teeth on the chelicerae are given as the first, second, third, etc., and measured from the base of the fang to the distal groove.

Leg measurements are given as total length (femur, patella, tibia, metatarsus, tarsus). The abbreviations used in the text are:

Eyes

ALE	anterior lateral eye;	PLE	posterior lateral eye;
AME	anterior median eye;	PME	posterior median eye.
MOA	median ocular area;		

Leg segments

Fe	femur;	Pt	Patella;	Ti	tibia.
Mt	metatarsus;	Ta	tarsus;		

Spination

d	dorsal;	r	retrolateral;
p	prolateral;	v	ventral.

Male palp

Mac	macroseta;	RTA	retrolateral tibial apophysis;
BTA	basal tegular apophysis;	RTP	ridge-shaped tegular process;
C	conductor;	SD	sperm duct;
E	embolus;	T	tegulum;
Eb	base of the embolus;	TR	tegular ridge;
Gr	embolic groove;	Tt	tutaculum;
MA	median apophysis;	VTA	ventral tibial apophysis.

Epigyne

AH	anterior hood;	P	lateral pocket;
At	atrium;	Se	septum;
CD	copulatory duct;	SP	spermatheca;
CO	copulatory openings;	SS	septal stem;
ET	epigynal teeth;	TrR	transverse ridge of copulatory opening.
FD	fertilisation duct;		
GA	glandular appendage;		
MS	membranous sac;		

Taxonomic survey

Family Thomisidae Sundevall, 1833

The known crab spider fauna of Jiangxi Province is complemented by 31 additional species belonging to 15 genera and now numbers 38 species in 21 genera. The full list of thomisid spiders recorded in this province is presented in Table 1, which follows the taxonomic accounts.

Genus *Angaeus* Thorell, 1881

Comments. This genus includes 11 species, mainly distributed in tropical Asia (India, Malaysia (Borneo), Myanmar, Vietnam, Singapore, and Indonesia) (WSC 2022). More than half of these species are recorded from China and have been revised by Benjamin (2013). It is worth mentioning that the female of the type species, *Angaeus pudicus* Thorell, 1881, remains unknown.

Angaeus xieluae Liu, sp. nov.

<http://zoobank.org/EADDA1BA-DD6D-4A83-9945-50116A0A90BD>

Figs 1–3

Material examined. Holotype: ♂, CHINA: Jiangxi Province, Ji'an City, Jinggangshan County Level City, Jinggang Mountain National Nature Reserve, Eling Town, Tangnan Village, 26°43'8.4"N, 114°7'51.6"E, 289 m, 3.X.2015, K. Liu et al. leg. **Paratypes:** 1 ♀, Longshi Town, Huishi Park, 26°42'32.4"N, 113°56'49.2"E, 242 m, 2.V.2015, K. Liu et al. leg.; 1 ♂, Eling Town, Shenyuan Village, 26°43'26.4"N, 114°7'44.4"E, 277 m, 28.V.2015, K. Liu et al. leg.; 1 ♂, Huangao Town, Zhongqiuba, 4.IV.2015, K. Liu et al. leg.

Etymology. The specific name is a matronym in honour of Miss Xie Lu from the College of Life Science, Jinggangshan University, who helped us in Longshi Town, where the paratype of the new species was collected.

Diagnosis. The male of the new species resembles those of *A. rhombifer* Thorell, 1890, widely distributed in South-East Asia, in having embolus (*E*) with widened tip and retrolateral tibial apophysis (*RTA*) as long as tibia but can be distinguished from it by having embolus with bill-shaped tip and widened base and the median apophysis (*MA*) shifted retrolaterally (vs. embolus with narrow base and the median apophysis starting from the centre of the tegulum) (cf. Figs 1D, 2B, C and Benjamin 2013: fig. 2A). The female of *A. xieluae* sp. nov. also resembles that of *A. rhombifer* in having elongated comma-shaped spermathecae (*SP*) but can be separated from the latter by reduced septal stem (*SS*) and arcuate anterior hood (*AH*) spaced from spermathecae (vs. well-developed septal stem and horizontal anterior hood adjoining to spermathecae) (cf. Fig. 3C, D and Benjamin 2013: fig. 2D, E).

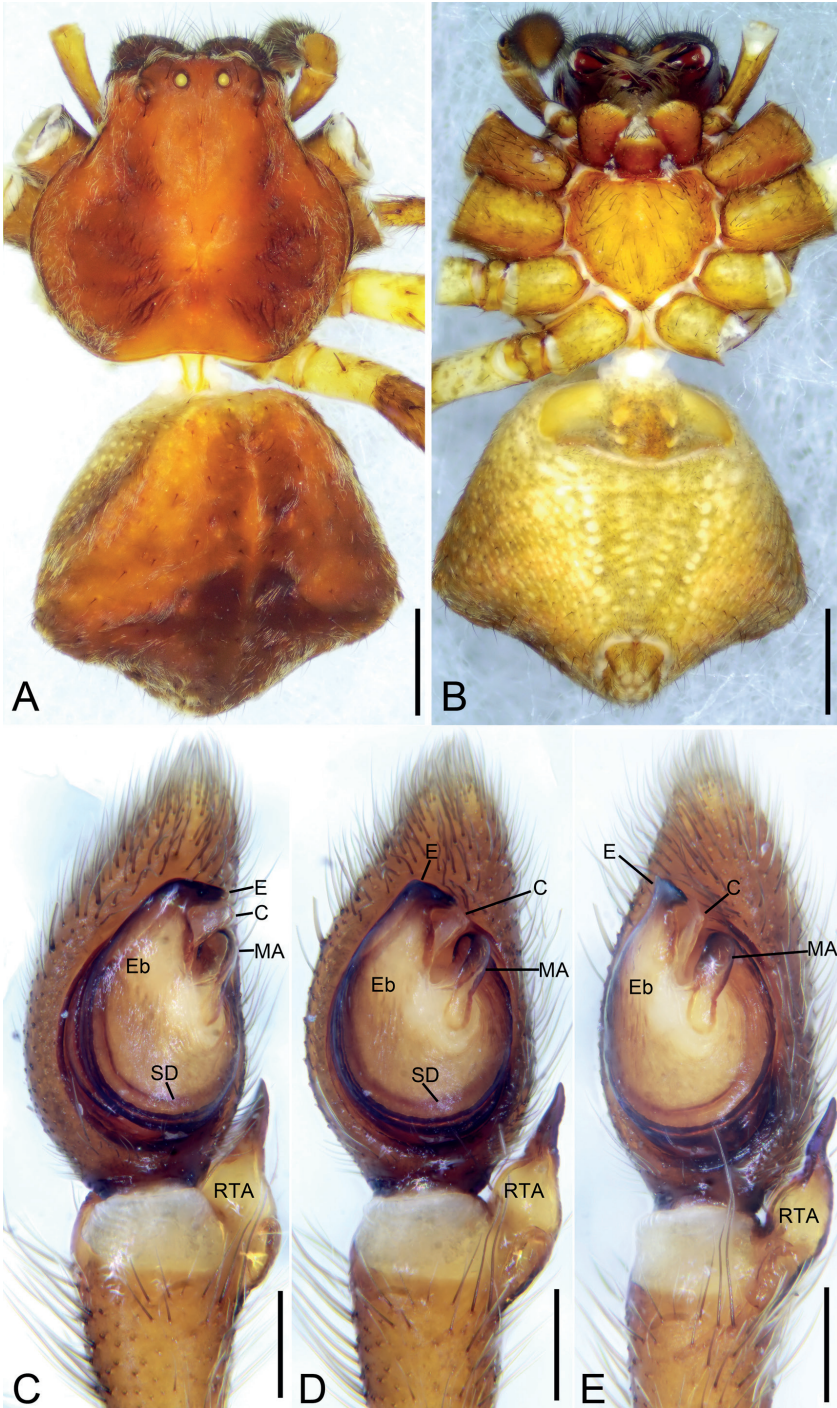


Figure 1. *Angaeus xieluae* sp. nov., male holotype. **A** habitus, dorsal view **B** same, ventral view **C** palp, prolateral view **D** same, ventral view **E** same, retrolateral view. Abbreviations: C – conductor, E – embolus, Eb – base of the embolus, MA – median apophysis, RTA – retrolateral tibial apophysis, SD – sperm duct. Scale bars: 0.5 mm (**A, B**), 0.1 mm (**C-E**).

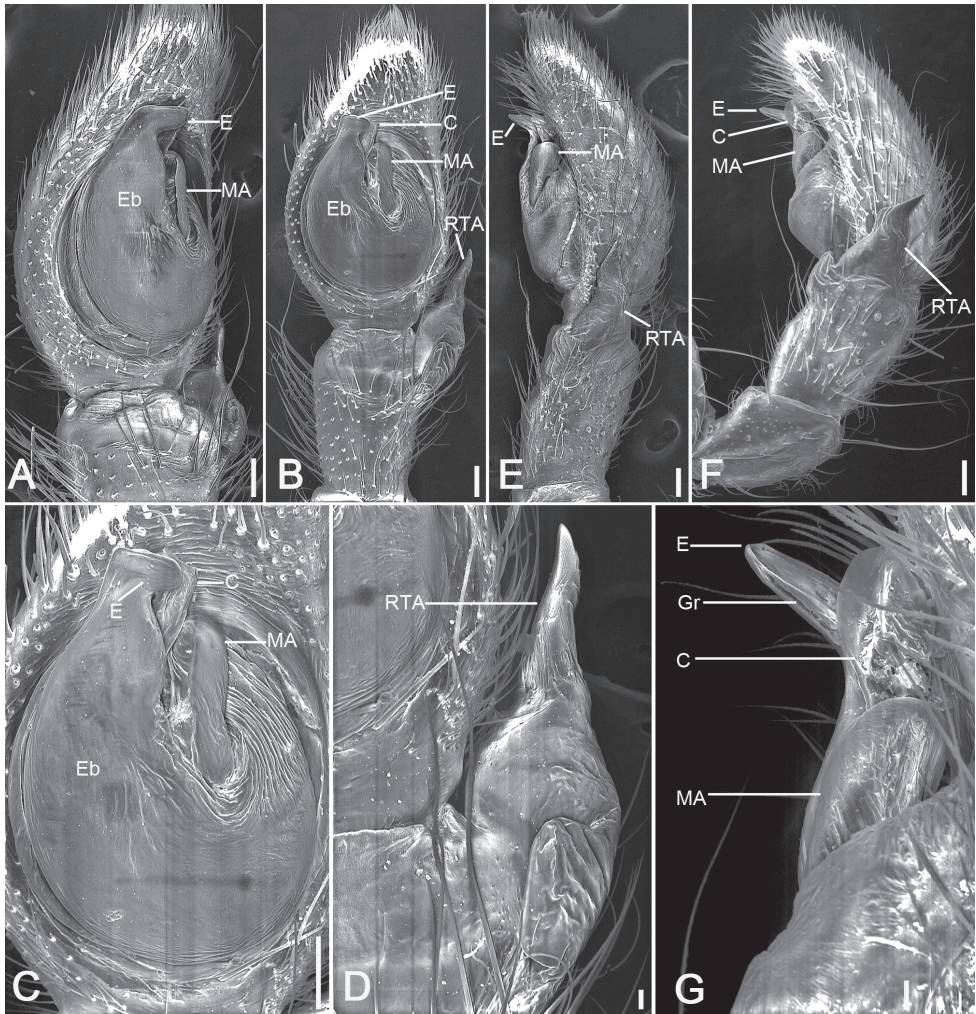


Figure 2. SEM micrographs of *Angaeus xieluae* sp. nov. male palp (holotype). **A** prolatero-ventral view **B** ventral view **C** same, details of bulb **D** same, details of retrolateral tibial apophysis **E** retrolateral view **F** retrolateral view, slightly dorsal **G** same, details of embolus. Abbreviations: C – conductor, E – embolus, Eb – base of the embolus, Gr – groove, MA – median apophysis, RTA – retrolateral tibial apophysis. Scale bars: 0.1 mm (**A–C, E, F**), 20 μ m (**D, G**).

Description. Male (holotype). Habitus as in Fig. 1A, B. Total length 6.22. Carapace: 2.70 long, 3.11 wide, anteriorly narrowed to 1.6, with abundant fluffy setae. Eye sizes and interdistances: AME 0.09, ALE 0.22, PME 0.11, PLE 0.19, AME–AME 0.16, AME–ALE 0.14, PME–PME 0.28, PME–PLE 0.28, AME–PME 0.29, AME–PLE 0.54, ALE–ALE 0.64, PLE–PLE 1.0, ALE–PLE 0.26; MOA 0.45 long, front width 0.33, back width 0.51. Sternum (Fig. 1B) oval, with notch anteromedially. Abdomen (Fig. 1A, B): 3.58 long, 3.67 wide. Leg measurements: I 13.33 (4.22, 1.58,

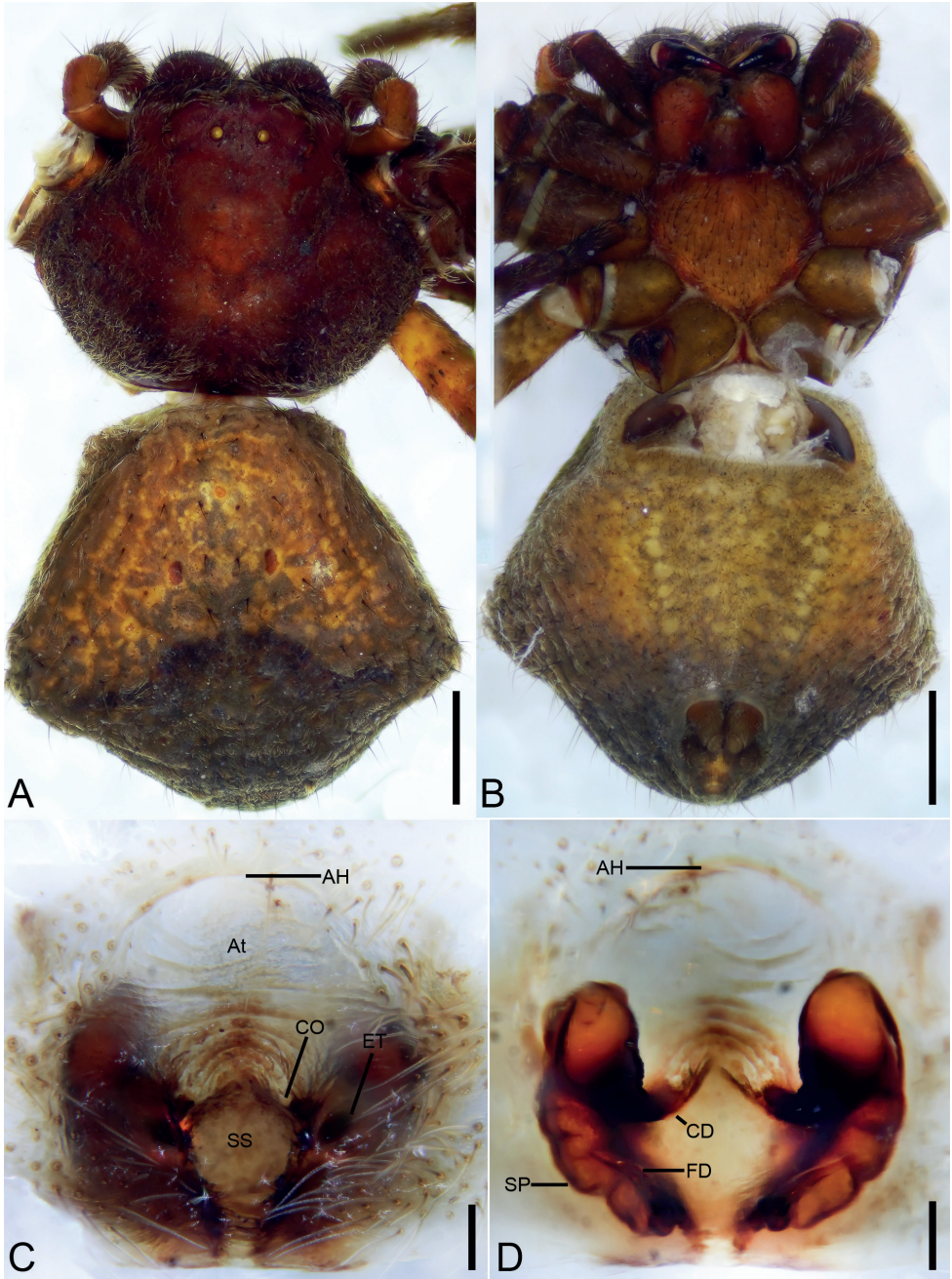


Figure 3. *Angaeus xieluae* sp. nov., female paratype. **A** habitus, dorsal view **B** same, ventral view **C** epigyne, ventral view **D** same, dorsal view. Abbreviations: AH – anterior hood, At – atrium, CD – copulatory duct, CO – copulatory opening, ET – epigynal teeth, FD – fertilisation duct, SP – spermatheca, SS – septal stem. Scale bars: 0.5 mm (**A**, **B**), 0.1 mm (**C**, **D**).

3.88, 2.44, 1.21); II 13.56 (4.34, 1.59, 4.11, 2.38, 1.14); III 5.99 (1.86, 0.83, 1.48, 1.06, 0.76); IV 6.82 (2.15, 0.94, 1.57, 1.43, 0.73). Leg spination: I Fe: d4, p5, r4; Ti: p2, r2, v8; Mt: p2, r2, v6; II Fe: d10; Ti: p2, r2, v7; Mt: p3, r3, v4; III Fe: d2, p2, r2; Ti: p2, r1, v2; Mt: d2, v4; IV: Fe: d2; Ti: p2, r1, v2; Mt: d2, v2.

Colouration. Carapace reddish brown. Chelicerae dark brown. Endites and labium reddish brown. Sternum yellow. Legs yellow brown, with several dark spots near bases of setae; legs III and IV paler, with pale and dark colours. Abdomen reddish brown, medially with arch-shaped dark mark.

Palp (Figs 1C–E, 2). Femur 2 × longer than patella. Patella slightly shorter than tibia. Retrolateral tibial apophysis (*RTA*) large, as long as tibia, with thick and swollen base and ventral tibial apophysis, apex of *RTA* gradually pointed, directed dorsally. Cymbium drop-shaped, 2 × longer than wide. Tegulum oval, median apophysis (*MA*) spoon-shaped, extending from subcentre to 1 o'clock position, with a small hook-like apex. Sperm duct (*SD*) U-shaped, gradually tapering, arising at 1 o'clock position. Conductor (*C*) partly hidden by embolus, located close to the apex of median apophysis. Base of the embolus (*Eb*) ~ 3 × wider than the median apophysis. Embolus with clear sperm groove (*Gr*).

Female. Habitus as in Fig. 3A, B. Total length 8.07. Carapace: 3.56 long, 3.51 wide, anteriorly narrowed to 0.6 × of its maximum width. Eye sizes and interdistances: AME 0.08, ALE 0.19, PME 0.11, PLE 0.18, AME–AME 0.25, AME–ALE 0.15, PME–PME 0.29, PME–PLE 0.30, AME–PME 0.34, AME–PLE 0.52, ALE–ALE 0.71, PLE–PLE 1.00, ALE–PLE 0.23. MOA 0.56 long, front width 0.39, back width 0.52. Abdomen (Fig. 3A, B): 4.51 long, 4.16 wide, with abundant depressed patches. Leg measurements: I 11.99 (3.70, 1.42, 3.53, 2.20, 1.14); II 11.95 (3.78, 1.48, 3.44, 2.20, 1.05); III 5.81 (1.87, 0.78, 1.36, 1.10, 0.7); IV 6.74 (2.16, 0.86, 1.63, 1.34, 0.75). Leg spination: I Fe: d6, p1; Ti: p2, r2, v8; Mt: p3, r3, v4; II Fe: d6; Ti: p1, v2; Mt: p3, r3, v4; III Fe: d2; Ti: p1, v2; Mt: d2, p1, v4; IV: Fe: d2; Ti: p1, r1, v2; Mt: d2, p1, r1, v2.

Colouration as in Fig. 3A, B. Carapace reddish brown. Chelicerae dark brown. Endites and labium reddish brown. Sternum reddish brown. Legs yellow brown, with several dark spots near bases of setae; legs III and IV paler, with pale and dark colours. Abdomen yellow brown, subposteriorly with arch-shaped dark mark.

Epigyne (Fig. 3C, D). Anterior hood (*AH*) arcuate. Atrium (*At*) oval, 1.5 × wider than long, with several transverse wrinkles. Copulatory openings (*CO*) clearly visible, located within posteromedian part of the atrium. Epigynal teeth (*ET*) robust and blunt, inclined posteriorly. Septal stem (*SS*) round and convex. Spermathecae (*SP*) 2.5 × longer than wide, with several distinct constrictions, separated in the anterior part by 1.5 × their width and closely spaced in the posterior part. Copulatory ducts (*CD*) shorter than the spermathecae width. Fertilisation ducts (*FD*) nearly as long as 1/2 spermathecal length.

Distribution. Known only from the type locality in Jiangxi Province of China (Fig. 17).

Genus *Ebelingia* Lehtinen, 2004

Comments. This genus includes only two species, both from East Asia (WSC 2022).

Ebelingia forcipata (Song & Zhu, 1993), **comb. nov.**

Figs 4–6

Misumenops forcipatus Song & Zhu, in Song, Zhu & Li, 1993: 879, fig. 50A–C (♂);

Song and Zhu 1997: 139, fig. 99A–C (♂); Song et al. 1999: 482, fig. 279H (♂).

Ebrechtella forcipata: Lehtinen 2004: 165.

Material examined. CHINA: Jiangxi Province, Ji'an City, Jinggangshan County Level City, Jinggang Mountain National Nature Reserve: 1 ♂: Luofu Town, Changguling Forest Farm, 26°38'28"N, 114°14'6"E, 583 m, 5.X.2014, K. Liu et al. leg.; 1 ♀, Luofu Town, Pingtuo Village, Changguling Forest Farm, road side, 26°39'18"N, 114°14'2.4"E, 438 m, 5.X.2014, K. Liu et al. leg.; 2 ♂, Ciping Town, Xingzhou Village, Baimukeng, 26°31'4.8"N, 114°11'9.6"E, 669 m, 3.X.2014, K. Liu et al. leg.; 1 ♀, Ciping Town, Xiazhuang Village, Zhushachong Forest Farm, 26°33'7.2"N, 114°11'27.6"E, 683 m, 4.X.2014, K. Liu et al. leg.; 2 ♀, Luofu Town, Pingtuo Village, Tea forest, 26°38'14.4"N, 114°13'48"E, 419 m, 5.X.2014, K. Liu et al. leg.; 1 ♀, Huang'ao Town, Shantang Group, 26°28'22.8"N, 114°13'55.2"E, 315 m, 5.X.2015, K. Liu et al. leg.

Diagnosis. The species differs from both congeners by the retrolateral tibial apophysis (*RTA*) with two equally long and thick branches (vs. dorsal branch much thinner and shorter than the ventral) (cf. Figs 4E, 5B, C, E, F; Song and Zhu 1997: fig. 100F; and Logunov 1992: fig. 9) in male and by thick and swollen copulatory ducts (*CD*) (vs. tube-shaped) (cf. Fig. 6D; Song and Zhu 1997: fig. 100D; and Kim and Gwon 2001: fig. 34) in female.

Description. Male. Habitus as in Fig. 4A, B. Total length 2.60. Carapace: 1.35 long, 1.50 wide, with dense setae dorsally. Eye sizes and interdistances: AME 0.07, ALE 0.11, PME 0.06, PLE 0.08, AME–AME 0.16, AME–ALE 0.16, PME–PME 0.27, PME–PLE 0.21, AME–PME 0.13, AME–PLE 0.37, ALE–ALE 0.61, PLE–PLE 0.75, ALE–PLE 0.15. MOA 0.24 long, front width 0.29, back width 0.40. Sternum (Fig. 4B) slightly wider than long, anteromedial margin procurved, lateral margins serrulate, posterior end blunt. Abdomen (Fig. 4A, B): 3.58 long, 3.67 wide, with dense setae dorsally. Leg measurements: I 7.28 (2.25, 0.83, 1.82, 1.58, 0.80); II 6.63 (2.11, 0.80, 1.75, 1.18, 0.79); III 2.83 (0.87, 0.44, 0.69, 0.50, 0.33); IV 2.80 (0.87, 0.38, 0.71, 0.51, 0.33). Leg spination: I Fe: d3, p4, r2; Pa: p1, r1; Ti: d2, r3, v6; Mt: p4, r4, v4; II Fe: d4, p1; Pa: p1, r1; Ti: d2, p3, r3, v4; Mt: p4, r4, v4; III Fe: d3, p1; Pa: d1; Ti: d2, p1, r1, v2; Mt: p2, r2, v2; IV: Fe: d3, p1; Pa: d2, p1, r1; Ti: d2, p2, r1, v1; Mt: p2, r1.



Figure 4. *Ebelingia forcipata* (Song & Zhu, 1993), male. **A** habitus, dorsal view **B** same, ventral view **C** palp, prolateral view **D** same, ventral view **E** same, retrolateral view. Abbreviations: E – embolus, RTA – retrolateral tibial apophysis, SD – sperm duct, TR – tegular ridge, VTA – ventral tibial apophysis. Scale bars: 0.5 mm (**A, B**), 0.1 mm (**C–E**).

Colouration (Fig. 4A, B). Carapace reddish brown, medially with yellowish band. Chelicerae, endites, and labium reddish yellow. Sternum and legs yellow. Abdomen yellow, posteriorly with two pairs of irregular yellow brown stripes, posterior one larger, with several white spots.

Palp (Figs 4C–E, 5). Femur 2 × longer than patella. Patella shorter than tibia. Retrolateral tibial apophysis (*RTA*) large, almost as long as tibia, with a broad base and

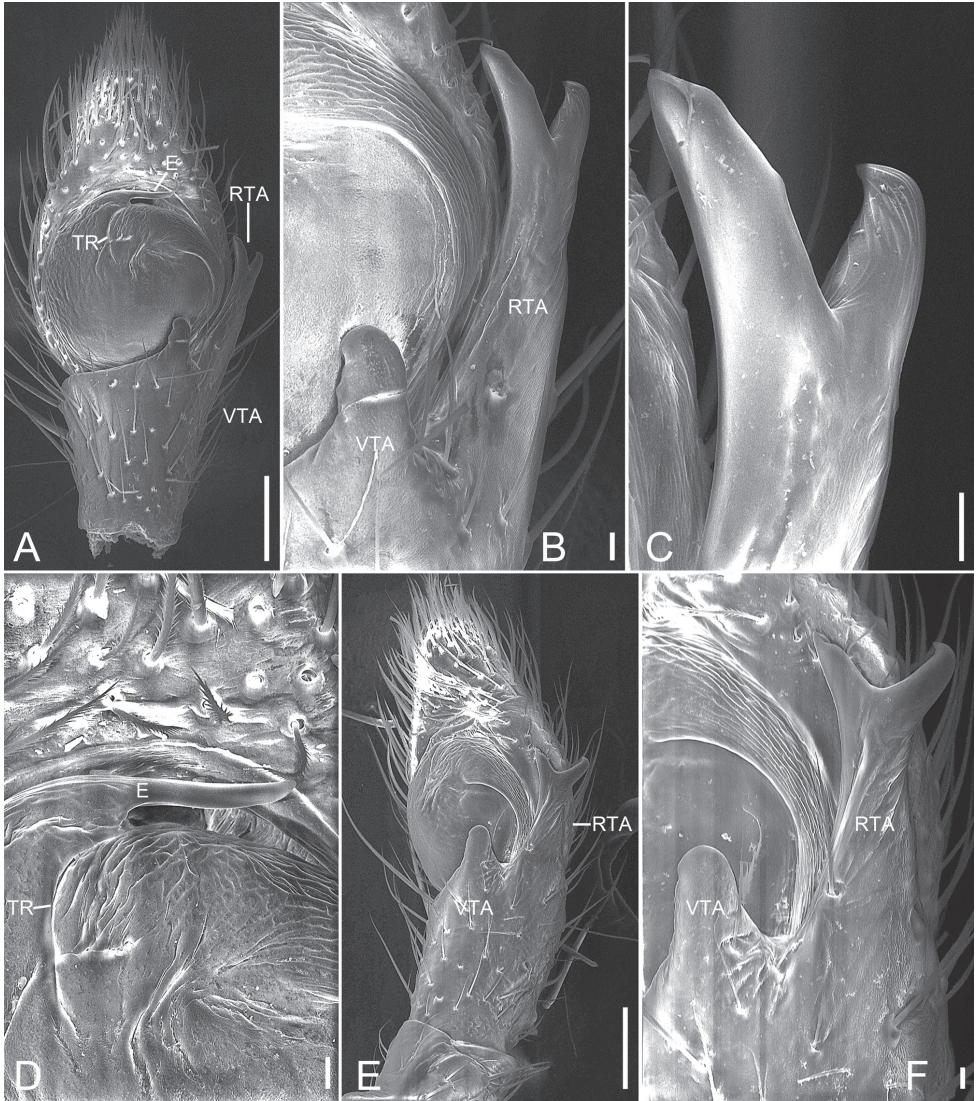


Figure 5. SEM micrographs of *Ebelingia forcipata* (Song & Zhu, 1993) comb. nov., male palp. **A** ventral view **B** same, details of tibial apophysis **C** same, details of retrolateral tibial apophysis **D** same, details of embolus **E** retrolateral view **F** same, details of tibial apophyses. Abbreviations: E – embolus, RTA – retrolateral tibial apophysis, TR – tegular ridge, VTA – ventral tibial apophysis. Scale bars: 0.1 mm (**A, E**), 10 μ m (**B, C, D, F**).

apex split into two branches. Ventral tibial apophysis (*VTA*) short and blunt. Cymbium oval, length/width ratio 1.7. Tegulum almost round, with tegular ridge (*TR*) at the 12 o'clock position. Sperm duct (*SD*) wide, encircles almost the whole tegulum. Embolus (*E*) short, originating from ~ 11 o'clock position, free part at 12 o'clock, free part as long as ventral branch of RTA.

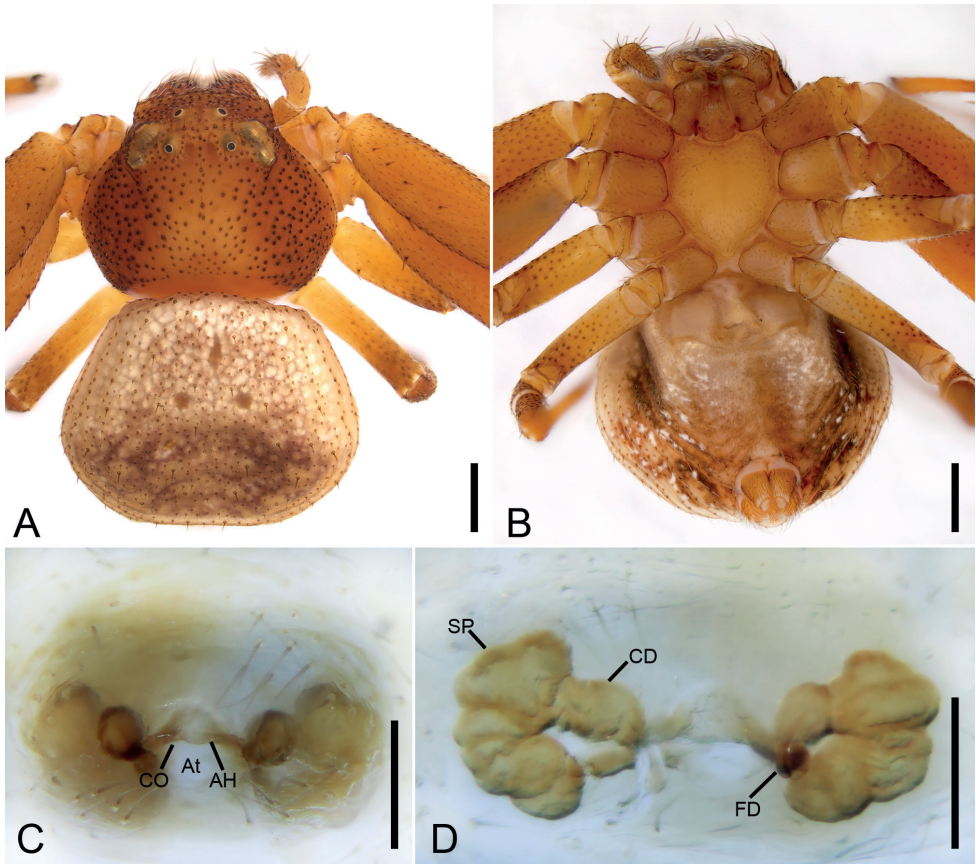


Figure 6. *Ebelingia forcipata* (Song & Zhu, 1993), female. **A** habitus, dorsal view **B** same, ventral view **C** epigyne, ventral view **D** same, dorsal view. Abbreviations: AH – anterior hood, At – atrium, CD – copulatory duct, CO – copulatory opening, FD – fertilisation duct, SP – spermatheca. Scale bars: 0.5 mm (**A, B**), 0.1 mm (**C, D**).

Female. Habitus as in Fig. 6A, B. As in male, except as noted. Total length 3.69. Carapace: 1.65 long, 1.77 wide. Eye sizes and interdistances: AME 0.07, ALE 0.1, PME 0.05, PLE 0.10, AME–AME 0.2, AME–ALE 0.2, PME–PME 0.36, PME–PLE 0.25, AME–PME 0.23, AME–PLE 0.44, ALE–ALE 0.72, PLE–PLE 0.92, ALE–PLE 0.19. MOA 0.34 long, front width 0.32, back width 0.48. Abdomen (Fig. 6A, B): 2.05 long, 2.19 wide, with abundant depressed patches. Leg measurements: I 6.17 (1.99, 0.89, 1.44, 1.15, 0.7); II 6.21 (2.08, 0.9, 1.37, 1.15, 0.71); III 2.95 (0.95, 0.57, 0.64, 0.46, 0.33); IV 3.07 (1.08, 0.41, 0.72, 0.46, 0.40). Leg spination: I missing; II Fe: d1; Ti: d2, r1, v4; Mt: p3, r3, v10; III Fe: d1; Pa: d2; Ti: d2; Mt: d1; IV: Fe: d3; Ti: d1; Mt: p2.

Colouration (Fig. 6A, B). Carapace reddish brown, medially with yellowish band. Chelicerae, endites and labium reddish yellow. Sternum and legs yellow. Abdomen, with numerous guanine spots, subposteriorly with two mottled stripes on the dorsal side, venter with few white spots.

Epigyne (Fig. 6C, D), width/length ratio ~ 2.6. Atrium (*At*) small, 3 × shorter than epigynal plate, located posteriorly from bell-shaped anterior hood (*AH*). Anterior hood located in centre. Copulatory openings (*CO*) located at posterolateral part of anterior hood. Spermathecae (*SP*) C-shaped, with several clearly visible constrictions, separated by more than width of anterior hood. Copulatory ducts (*CD*) broad, slightly longer than wide. Fertilisation ducts (*FD*) short, directed anteriorly.

Distribution. China: Jiangxi and Fujian Provinces (Song et al. 1993; present data).

Note. The left leg I was lost when we reviewed the holotype after photography.

Comments. This species clearly belongs to *Ebelingia* due to the markedly bifurcated retrolateral tibial apophysis, short embolus, broad anterior hood, and kidney-shaped spermathecae.

Genus *Lysiteles* Simon, 1895

Comments. This genus includes 60 species, mainly distributed in eastern Asia. Half of them are recorded from China, but there are still 13 species known only from females in China, and three from males. Most of them (ten species) are recorded from Yunnan Province. No species were recorded from Jiangxi Province.

Lysiteles subspirellus Liu, sp. nov.

<http://zoobank.org/F49B4189-C5CC-48D4-AB90-B141DAF7745D>

Fig. 7

Material examined. Holotype: ♀, CHINA, Jiangxi Province, Ji'an City, Jinggangshan County Level City, Jinggang Mountain National Nature Reserve, Ciping Town, Dajing Village, Jingzhu Mountain, 26°30'10.8"N, 114°5'16.8"E, 1085 m, 20.XII.2015, K. Liu et al. leg. **Paratype:** 1 ♀, same data as for holotype, 26°29'42"N, 114°4'44.4"E, 1158 m, 13.VIII.2016, K. Liu et al. leg.

Etymology. The specific name is derived from that of a similar species, *L. spirellus* Tang, Yin, Peng, Ubick & Griswold, 2008; adjective.

Diagnosis. The new species is similar to *L. auriculatus* Tang, Yin, Peng, Ubick & Griswold, 2008 and *L. spirellus* Tang, Yin, Peng, Ubick & Griswold, 2008 in having coiling spermathecae (*SP*), but differs from them by the carapace lacking pale median band (vs. present), abdomen with three pairs of large, touching, dark brown markings (Fig. 7A) (vs. relatively narrowed and widely separated markings). The new species can be distinguished from *L. auriculatus* by copulatory ducts (*CD*) located at posteromedian part of epigyne (vs. located anteriorly) (cf. Fig. 7C and Tang et al. 2008: fig. 2b, d). Finally, *L. subspirellus* sp. nov. differs from *L. spirellus* by spermathecae forming a tight coil (vs. loose coil) (cf. Fig. 7D and Tang et al. 2008: fig. 16d, f).

Description. Habitus as in Fig. 7A, B. Total length 3.64. Carapace: 1.60 long, 1.49 wide, with several long setae around eye area and sublateral part of carapace. Eye

sizes and interdistances: AME 0.12, ALE 0.19, PME 0.08, PLE 0.15, AME–AME 0.17, AME–ALE 0.17, PME–PME 0.30, PME–PLE 0.3, AME–PME 0.22, AME–PLE 0.17, ALE–ALE 0.71, PLE–PLE 0.87, ALE–PLE 0.26. MOA 0.37 long, front width 0.37, back width 0.47. Chelicerae with two promarginal (proximal larger, distal very small, nearly $1/3 \times$ size of proximal one) and one (very small) retromarginal tooth. Sternum (Fig. 7B) longer than wide, anteromedial margin procurved, lateral margins serrulate, intercoxal triangles long, almost joining carapace, posterior end arch-shaped. Abdomen (Fig. 7A, B): 2.10 long, 1.81 wide, with abundant slender setae dorsally. Leg measurements: I 5.34 (1.62, 0.60, 1.35, 1.14, 0.63); II 5.52 (1.67, 0.67, 1.52, 1.02, 0.64); III 3.71 (1.18, 0.44, 0.97, 0.64, 0.48); IV 3.63 (1.19, 0.38, 0.88, 0.76, 0.42). Leg spination: I Fe: d2, p4; Pa: d1; Ti: d2, p4, r3, v4; Mt: p3, r3, v6; II Fe: d3, p1; Pa: d2, p1, r1; Ti: d1, p3, r2, v3; Mt: p3, r3, v4; III Fe: d3; Pa: d1; Ti: d2, p2, r1, v1; Mt: p2, r2, v1; IV: Fe: d2; Pa: d2; Ti: d3, p2, r2, v1; Mt: d2, p1, r1, v1.

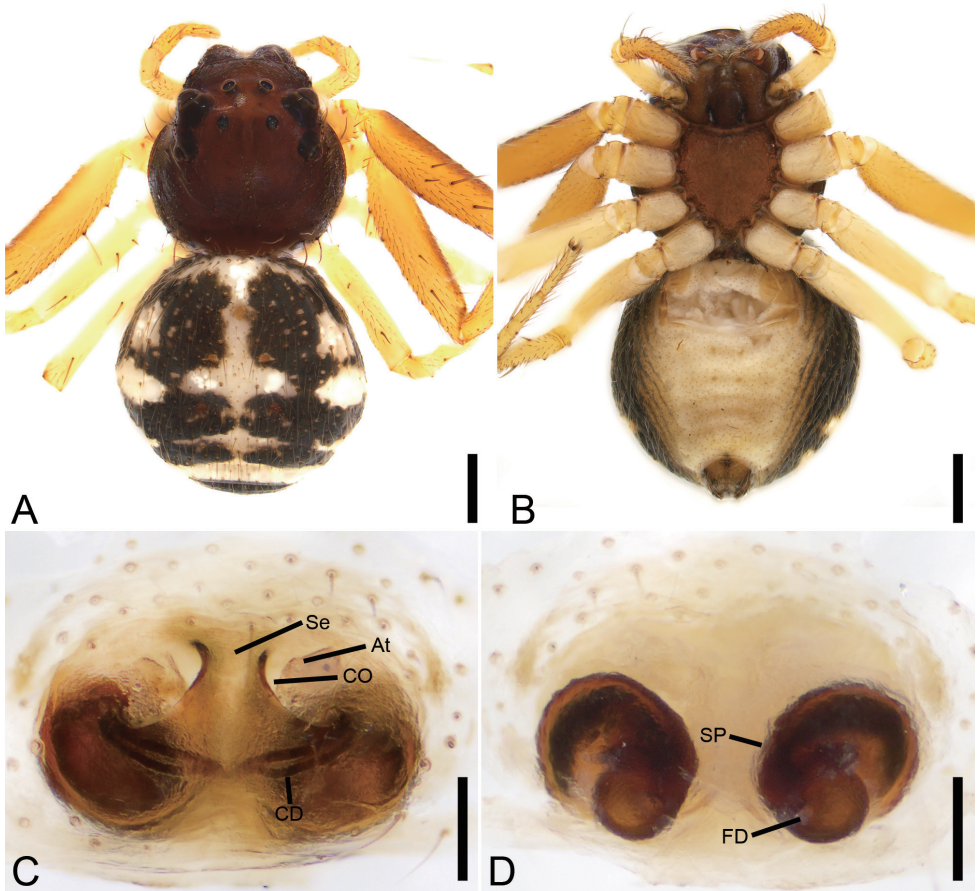


Figure 7. *Lysiteles subspirellus* sp. nov., female. **A** habitus, dorsal view **B** same, ventral view **C** epigyne, ventral view **D** same, dorsal view. Abbreviations: At – atrium, CD – copulatory duct, CO – copulatory opening, FD – fertilisation duct, Se – septum, SP – spermatheca. Scale bars: 0.5 mm (**A, B**), 0.1 mm (**C, D**).

Colouration (Fig. 7A, B). Carapace reddish brown. Chelicerae, endites, and sternum reddish brown. Labium dark reddish brown. Abdomen pale white, with three pairs of large dark brown stripes, anterior one irregular, others transverse, medially with paired white guanine spots, posteriorly with a semi-oval dark brown stripe; venter with two rows of yellow spots medially.

Epigyne (Fig. 7C, D). Epigyne $1.8 \times$ wider than long. Anteromedian part with septum (*Se*) dividing atrium (*At*) into two oval parts. Copulatory openings (*CO*) located at posterior part of the fovea. Copulatory ducts (*CD*) almost straight, same length as spermathecal width. Spermathecae (*SP*) anticlockwise coiled, forming one full turn. Fertilisation duct (*FD*) shorter than spermathecal wide, directed anteriorly.

Male. unknown.

Comments. At present, *L. digitatus* Zhang, Zhu & Tso, 2006, *L. distortus* Tang, Yin, Peng, Ubick & Griswold, 2008, and *L. torsivus* Zhang, Zhu & Tso, 2006 are known only from the males in mainland China; therefore, the new species may be conspecific with one of these three species.

Distribution. Known only from the type locality in Jiangxi Province of China (Fig. 17).

Genus *Oxytate* L. Koch, 1878

Comments. This genus includes 28 species distributed mainly in Asia and Africa. Half of them have been recorded from China, mainly in Yunnan and Guangxi provinces (Li and Lin 2016), but two species are known only from females and three from males.

Oxytate bicornis Liu, Liu & Xu, 2017

Figs 8, 9

Oxytate bicornis Liu, Liu & Xu, 2017: 194, figs 1A–D, 2A–C (♂).

Material examined. CHINA: *holotype* ♂, Jiangxi Province, Ji'an City, Jinggangshan County Level City, Jinggang Mountain National Nature Reserve, Ciping Town, Dajing village, 26.566°N, 114.125°E, 922 m, 13.VII.2014, K. Liu et al. leg.; 2 ♀, other data as in holotype; 1 ♀, Longshi Town, Yuankou Village, 26°41'31.2"N, 113°57'10.8"E, 265 m, 1.V.2015, K. Liu et al. leg.; 1 ♀, Huang'ao Town, Shantang Group, 26°28'26.4"N, 114°13'58.8"E, 306 m, 5.IV.2015, K. Liu et al. leg.

Diagnosis. Female of this species similar to that of *O. bhutanica* Ono, 2001 and *O. mucunica* sp. nov. in having vulva with M-shaped pattern formed by copulatory ducts (*CD*) and spermathecae (*SP*), but differs from both species by the copulatory openings (*CO*) oriented outwards (vs. inwards or anteriorly) and copulatory ducts (*CD*) $2 \times$ thinner than spermathecae (*SP*) (vs. equal in size) (cf. Fig. 8C, D vs. Fig. 10C, D and Ono 2001: figs 4, 5). Male of *O. bicornis* resembles those of *O. bhutanica* in having spine-like embolus (*E*) and moderately long retrolateral tibial apophysis (*RTA*),

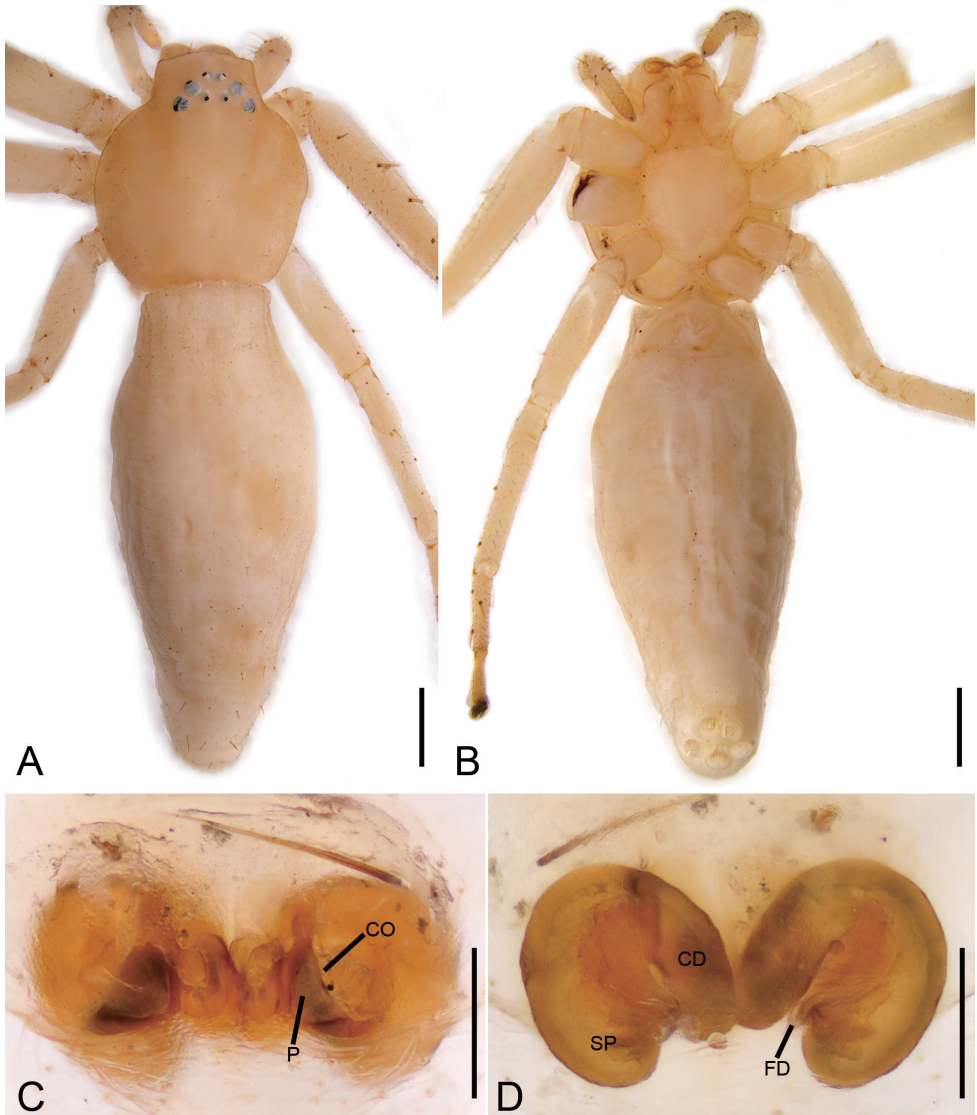


Figure 8. *Oxytate bicornis* Liu, Liu & Xu, 2017, female. **A** habitus, dorsal view **B** same, ventral view **C** epigyne, ventral view **D** same, dorsal view. Abbreviations: CD – copulatory duct, CO – copulatory opening, FD – fertilisation duct, P – pocket, SP – spermatheca. Scale bars: 0.5 mm (**A, B**), 0.1 mm (**C, D**).

reaching to the middle of the cymbium but can be distinguished by the bifurcated retrolateral tibial apophysis (vs. horn-like) (cf. Fig. 9B–D and Ono 2001: figs 2, 3).

Description. Female. Habitus as in Fig. 8A, B. Total length 5.77. Carapace: 2.09 long, 2.02 wide. Eye sizes and interdistances: AME 0.08, ALE 0.11, PME 0.08, PLE 0.1, AME–AME 0.22, AME–ALE 0.16, PME–PME 0.22, PME–PLE 0.38, AME–PME 0.29, AME–PLE 0.58, ALE–ALE 0.66, PLE–PLE 1.08, ALE–PLE 0.31. MOA 0.42 long, front width 0.36, back width 0.38. Endites more than 2 × longer than wide. Sternum as in Fig. 8B with arch-shaped posterior end. Abdomen (Fig. 8A, B): 3.92

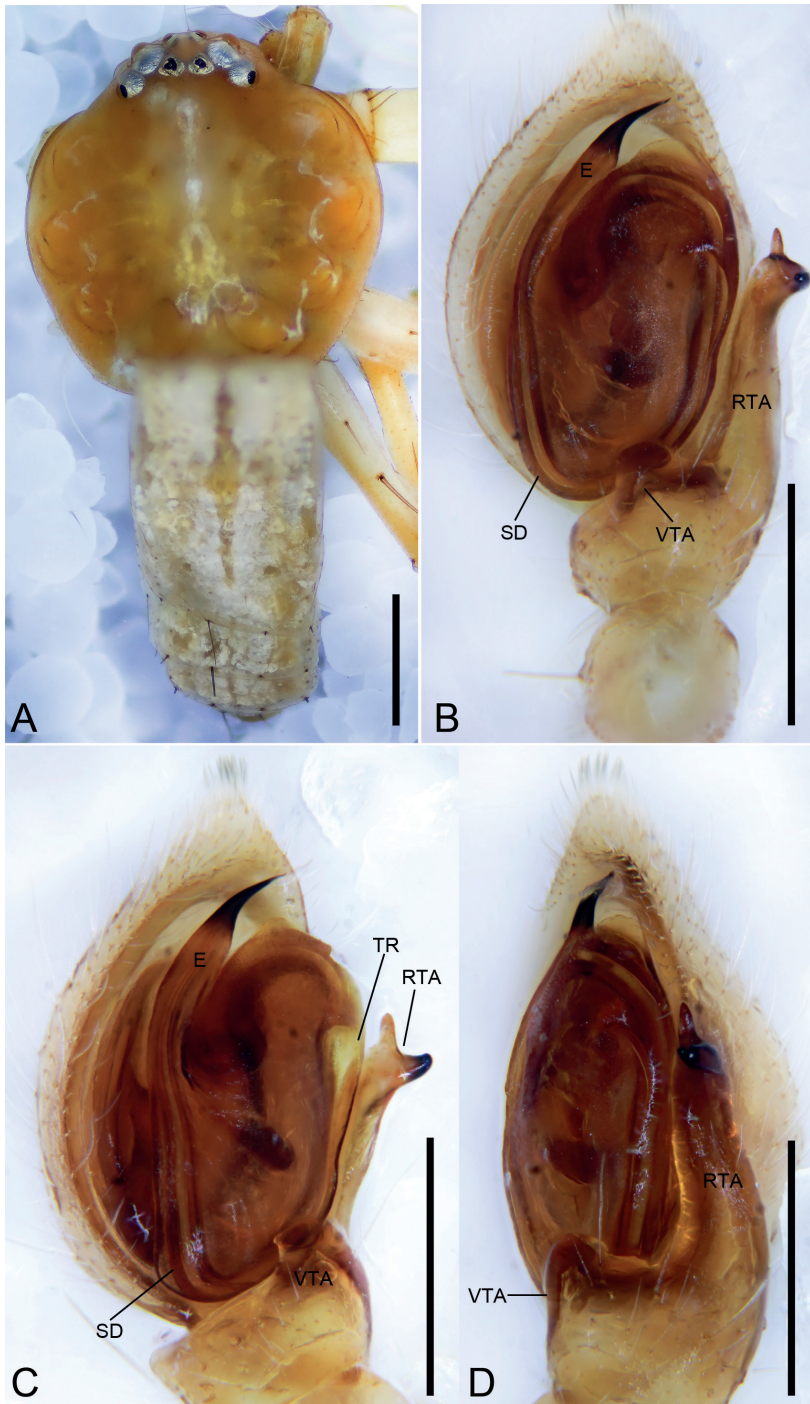


Figure 9. *Oxytate bicornis* Liu, Liu & Xu, 2017, male. **A** habitus, dorsal view **B** palp, ventral view **C** same, prolateral view **D** same, retrolateral view. Abbreviations: E – embolus, RTA – retrolateral tibial apophysis, SD – sperm duct, TR – tegular ridge, VTA – ventral tibial apophysis. Scale bars: 1 mm (**A**), 0.5 mm (**B–D**).

long, 1.11 wide, with regular transverse rows of strong spines on posterior part. Leg measurements: I 7.98 (2.45, 1.15, 2.15, 1.58, 0.65); II 7.79 (2.41, 1.10, 2.06, 1.50, 0.72); III 4.65 (1.39, 0.68, 1.27, 0.84, 0.47); IV 4.95 (1.76, 0.50, 1.25, 0.97, 0.47). Leg spination: I Fe: d4, p4, r1; Pa: d2, p1, r1; Ti: d2, p3, r3, v8; Mt: p2, r2, v6; II Fe: d4, p1, r1; Pa: d2, p1, r1; Ti: d3, p3, r3, v6; Mt: p2, r2, v6; III Fe: d2, p1; Pa: d2, p1; Ti: d1, p2, r1, v2; Met: p2, r2, v2; IV: Fe: d2; Pa: d2, p1, r1; Ti: d3, p2; Mt: p2.

Colouration. Carapace, chelicerae, endites, sternum, legs, and abdomen yellowish.

Epigyne (Fig. 8C, D). Epigyne 2 × wider than long. Copulatory openings (*CO*) hidden by lateral pockets (*P*). Spermathecae (*SP*) kidney-shaped, 2 × longer than wide. Copulatory ducts (*CD*) shorter than spermathecae, slightly curved, aggregative form V-shaped figure. Fertilisation ducts (*FD*) small, poorly visible and directed laterally.

Male (Fig. 9): See Liu et al. (2017: 194).

Comments. Some females were collected in the type locality and others raised from juveniles. Newly collected females have general appearance and leg spination similar to the holotype male. Based on this, we consider them conspecific. This judgment will be confirmed or rejected in future when both sexes are collected together, simultaneously.

Distribution. Known only from Jiangxi Province, China (Fig. 17).

Oxytate mucunica Liu, sp. nov.

<http://zoobank.org/55A995BC-01C4-4586-B645-67A517D3D9CE>

Fig. 10

Material examined. Holotype: ♀, CHINA, Jiangxi Province, Ji'an City, Jinggangshan City, Jinggang Mountain National Nature Reserve, Mucun Town, Guibian Village, 26°38'32.11"N, 113°53'51.99"E, 322 m, 31.VII.2019, K. Liu et al. leg.

Etymology. The specific name is derived from the type locality, Mucun Town.

Diagnosis. Female of the new species is similar to those of *O. bhutanica* Ono, 2001 and *O. bicornis* in having vulva with M-shaped pattern formed by copulatory ducts (*CD*) and spermathecae (*SP*), but differ from both species by the copulatory openings oriented anteriorly (vs. outwards or inwards) (cf. Fig. 10C vs. Fig. 9C and Ono 2001: fig. 4). Additionally, *O. mucunica* sp. nov. differs from *O. bicornis* by the copulatory ducts being as wide as spermathecae (vs. copulatory ducts 2 × thinner) (cf. Fig. 10D and Fig. 8D).

Description. Habitus as in Fig. 10A, B. Total length 11.74. Carapace: 3.67 long, 3.33 wide. Eye sizes and interdistances: AME 0.08, ALE 0.14, PME 0.09, PLE 0.11, AME–AME 0.14, AME–ALE 0.07, PME–PME 0.08, PME–PLE 0.20, AME–PME 0.14, AME–PLE 0.39, ALE–ALE 0.39 PLE–PLE 0.77, ALE–PLE 0.05. MOA 0.52 long, front width 0.38, back width 0.43. Endites more than 2 × longer than wide, sub-trapezoidal. Abdomen (Fig. 10A, B): 8.42 long, 2.68 wide, with abundant white guanine spots dorsally and regular transverse rows of strong spines on posterior part. Leg measurements: I 8.56 (2.69, 0.99, 2.36, 1.65, 0.87); II 8.06 (2.50, 0.97, 2.24, 1.62, 0.73); III 4.77 (1.41, 0.60, 1.34, 0.90, 0.52); IV 4.88 (1.75, 0.54, 1.20, 0.93, 0.46). Leg spination: I Fe: d4 p4, r1; Pa: d2, p1, r1; Ti: d2, p3, r3, v8; Mt: p2, r2, v6;

II Fe: d4, p1, r1; Pa: d2, p1, r1; Ti: d3, p3, r3, v6; Mt: p2, r2, v6; III Fe: d2, p1; Pa: d2, p1; Ti: d3, r2, v2; Mt: p2, r2, v2; IV: Fe: d2; Pa: d2, p1, r1; Ti: d2, p2; Mt: p2.

Colouration (Fig. 10A, B). Carapace, chelicerae, endites, sternum, legs, and abdomen yellowish.

Epigyne (Fig. 10C, D). Epigyne 1.5 × wider than long. Pockets absent. Copulatory openings (CO) large, as long as wide, with weakly sclerotised margins. Spermatheca (SP) cylindrical, smoothly merging into copulatory ducts. Copulatory ducts (CD) very wide, touching each other almost the entire length. Fertilisation ducts (FD) short, directed laterally.

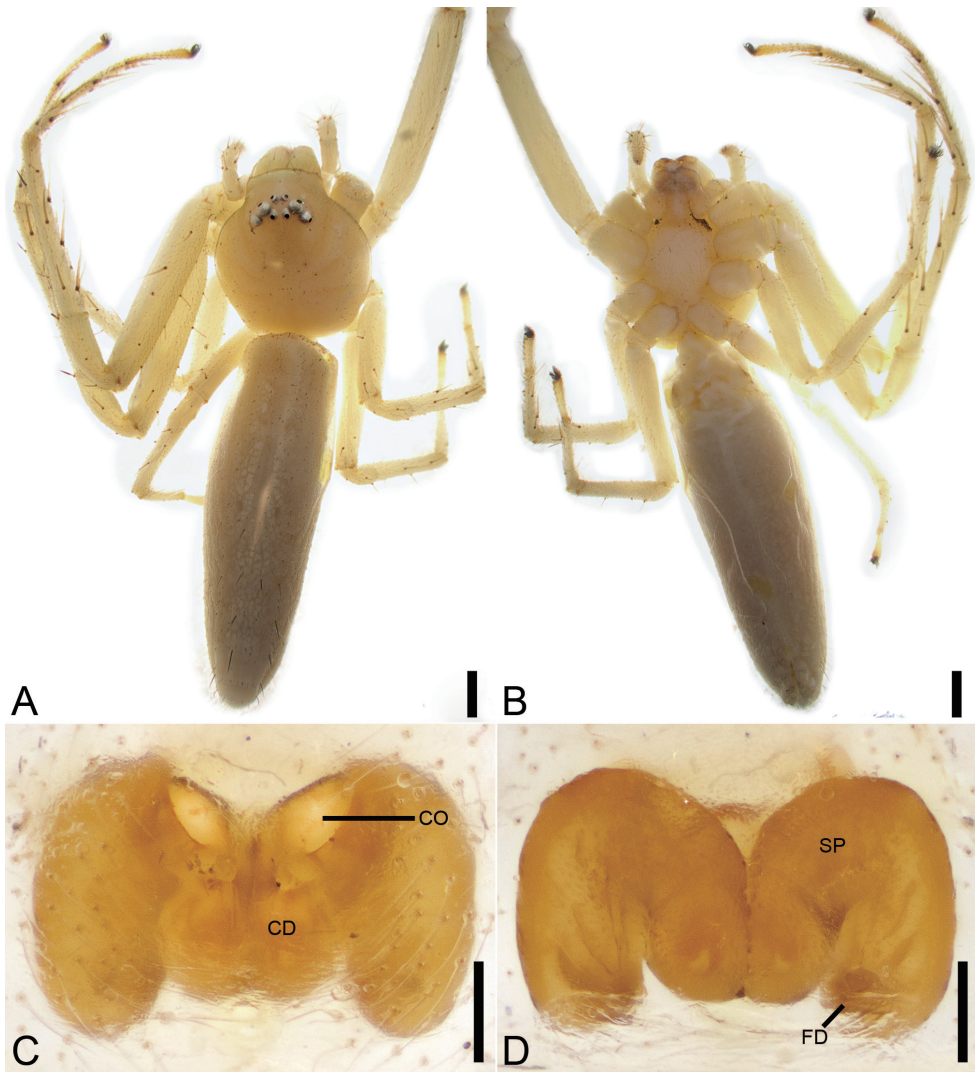


Figure 10. *Oxytate mucunica* sp. nov., female. **A** habitus, dorsal view **B** same, ventral view **C** epigyne, ventral view **D** same, dorsal view. Abbreviations: CD – copulatory duct, CO – copulatory opening, FD – fertilisation duct, SP – spermatheca. Scale bars: 0.5 mm (**A**, **B**), 0.1 mm (**C**, **D**).

Male. Unknown.

Notes. While many juveniles were collected and reared in the lab, only one female reached maturity.

Comments. The new species could potentially be a synonym of one of the species known only from males and occurring in China: *O. clavulata* Tang, Yin & Peng, 2008 (Yunnan) or *O. placentiformis* Wang, Chen & Zhang, 2012 (Guangxi).

Distribution. Known only from the type locality in Jiangxi Province of China (Fig. 17).

Genus *Pharta* Thorell, 1891

Comments. This genus includes nine species, the majority of which are distributed in Southeast Asia (WSC 2022). Four species are known to occur in China, all in Yunnan and Guizhou provinces (Li and Lin 2016). Among them, only *P. tengchong* (Tang, Griswold & Yin, 2009) is known from the female.

Pharta lingxiufengica Liu, sp. nov.

<http://zoobank.org/E2EB3363-9EEC-4BD7-82C4-65340A5F9CA3>

Fig. 11

Material examined. Holotype: ♀, CHINA, Jiangxi Province, Ji'an City, Jinggangshan County Level City, Jinggang Mountain National Nature Reserve, Ciping Town, Dajing Village, Lingxiufeng Scenic Spot, 26°34'16.72"N, 114°07'00.56"E, 971 m, 1.X.2018, K. Liu et al. leg.

Etymology. The specific name is derived from the type locality, Lingxiufeng Scenic Spot; adjective.

Diagnosis. The female of *P. lingxiufengica* is similar to that of *P. tangi* Wang, Mi & Peng, 2016 in having well-developed transverse ridge of copulatory openings (*TrR*) (= atrial intermediate margin of Wang et al. 2016) and invisible copulatory openings (*CO*). The new species can be easily differentiated from *P. tangi* by the convex transverse ridge of copulatory openings (vs. concave) (cf. Fig. 11C and Wang et al. 2016: fig. 2C).

Description. Habitus as in Fig. 11A, B. Total length 3.08. Carapace: 3.67 long, 3.33 wide. Eye sizes and interdistances: AME 0.05, ALE 0.15, PME 0.10, PLE 0.14, AME–AME 0.07, AME–ALE 0.04, PME–PME 0.12, PME–PLE 0.13, AME–PME 0.22, AME–PLE 0.31, ALE–ALE 0.25, PLE–PLE 0.57, ALE–PLE 0.14. MOA 0.35 long, front width 0.18, back width 0.32. Chelicerae with three promarginal (proximal largest, distal smallest) and three retromarginal (middle and distal with a same base, distal largest, middle smallest) teeth. Endites slightly longer than wide, anterior part broad. Labium slightly wider than long. Sternum (Fig. 11B) with numerous setae, anteromedially procurved, with subtriangular posterior end. Abdomen (Fig. 11A, B): 1.69 long, 1.63 wide, with sparse, erected setae. Leg measurements: I 4.28 (1.35, 0.51, 1.22, 0.87, 0.33); II 4.09 (1.23, 0.48, 1.18, 0.80, 0.40); III 2.31 (0.73, 0.36, 0.59,

0.38, 0.25); IV 2.71 (0.93, 0.33, 0.64, 0.55, 0.26). Leg spination: I Fe: d4, p2; Pa: d2; Ti: d2, v10; Mt: v8; II Fe: d1; Pa: d2; Ti: d2, v10; Mt: v8; III Fe: d3; Pa: d1; Ti: d2, p2, v2; Mt: d2, v2; IV: Fe: d1; Pa: d1, r1; Ti: d3, p1, r1; Mt: d2.

Colouration (Fig. 11A, B). Carapace yellow-brown, medially with single broad, dark brown, mottled band. Legs yellow, basis of macrosetae on legs appearing as darkish brown dots. Chelicerae, endites, sternum, legs, and abdomen reddish yellow. Abdomen with sparse white guanine spots, medially with clear inverted T-shaped dark brown marking; macrosetal bases reddish brown; venter with pairs of longitudinal, short, guanine stripes.

Epigyne (Fig. 11C, D). Epigyne oval, 1.5 × wider than long, lacking hood. Copulatory openings (CO) invisible, hidden by transverse ridge of copulatory openings

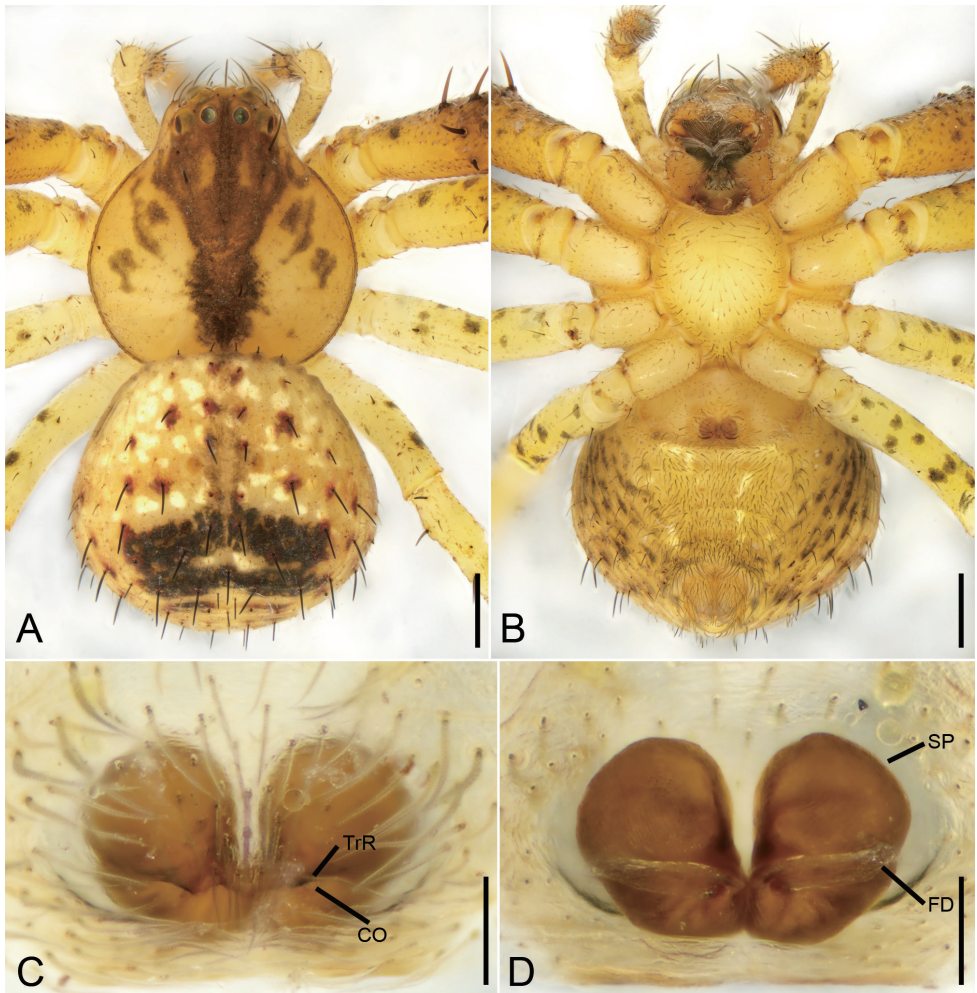


Figure 11. *Pharta lingxiufengica* sp. nov., female holotype. **A** habitus, dorsal view **B** same, ventral view **C** epigyne, ventral view **D** same, dorsal view. Abbreviations: CO – copulatory opening, FD – fertilisation duct, SP – spermatheca, TrR – transverse ridge of copulatory openings. Scale bars: 0.5 mm (**A, B**), 0.1 mm (**C, D**).

(*TrR*). Copulatory ducts (*CD*) not visible, possibly absent. Spermathecae (*SP*) oval, $\sim 1.4 \times$ longer than wide, anterior part of spermathecae slightly separated, posterior parts touching. Fertilisation ducts (*FD*) as long as width of spermatheca, directed laterally.

Male. unknown.

Comments. There is only one species in the region known from the male only, *P. koponeni* Benjamin, 2014 (Thailand); however, it is unlikely to be conspecific with our female because of differences in colouration, and the long distance between type localities.

Distribution. Known only from the type locality in Jiangxi Province of China (Fig. 17).

Genus *Stephanopis* O. Pickard-Cambridge, 1869

Comments. This genus includes 23 species (WSC 2022). Most of them are distributed in South America, Oceania, Australia, and Papua New Guinea (WSC 2022). The recent phylogenetic analyses based on a matrix of 117 morphological characters scored for 77 terminal taxa have revealed a large variation in morphology among *Stephanopis* species (Machado and Teixeira 2021); these taxonomic revisions have greatly contributed to a better understanding of the group. Here we report the first species from the Asian continent as well as from the entire Oriental zoogeographical realm.

Stephanopis xiangzhouica Liu, sp. nov.

<http://zoobank.org/65E3AE25-DFA8-4629-9E0E-1EABD1AB4716>

Figs 12, 13

Material examined. Holotype: ♀, CHINA, Jiangxi Province, Ji'an City, Jinggangshan County Level City, Jinggang Mountain National Nature Reserve, Luofu Town, Xiangzhou Village, Fengshuping Group, 26°36'10.8"N, 114°15'28.8"E, 412 m, 5.VIII.2015, leg. K. Liu et al. leg.

Etymology. The specific name refers to the type locality, Xiangzhou Village.

Diagnosis. The new species is similar to *S. nigra* O. Pickard-Cambridge, 1869 by having slit-like copulatory openings (*CO*), but differs by lacking lateral sclerotised margins of copulatory openings (vs. lateral margins sclerotised), touching membranous sacs (vs. separated) and slightly separated spermathecae (vs. touching) (cf. Fig. 13 and Machado et al. 2019: fig. 37C, D).

Description. Female. Habitus as in Fig. 12A, B. Total length 5.48. Carapace: 2.78 long, 2.96 wide, covered with numerous strong, short, radially diverging setae and dense short plumose setae, with three rows of short strong setae along midline. Eye sizes and interdistances (Fig. 12C): AME 0.04, ALE 0.07, PME 0.05, PLE 0.06, AME–AME 0.07, AME–ALE 0.04, PME–PME 0.12, PME–PLE 0.13, AME–PME 0.22, AME–PLE 0.31, ALE–ALE 0.25, PLE–PLE 0.57, ALE–PLE 0.14. MOA 0.26 long, front width 0.13, back width 0.24. Chelicerae (Fig. D) with three promarginal (middle largest, distal and proximal smaller) and two retromarginal (proximal large,

distal very small) teeth, and numerous macrosetae anteriorly. Endites $2 \times$ longer than wide, ectal part without distinct constriction. Labium wider than long. Sternum (Fig. 12B) oval with short dense macrosetae. Abdomen (Fig. 12A, B, G): 2.79 long, 2.94

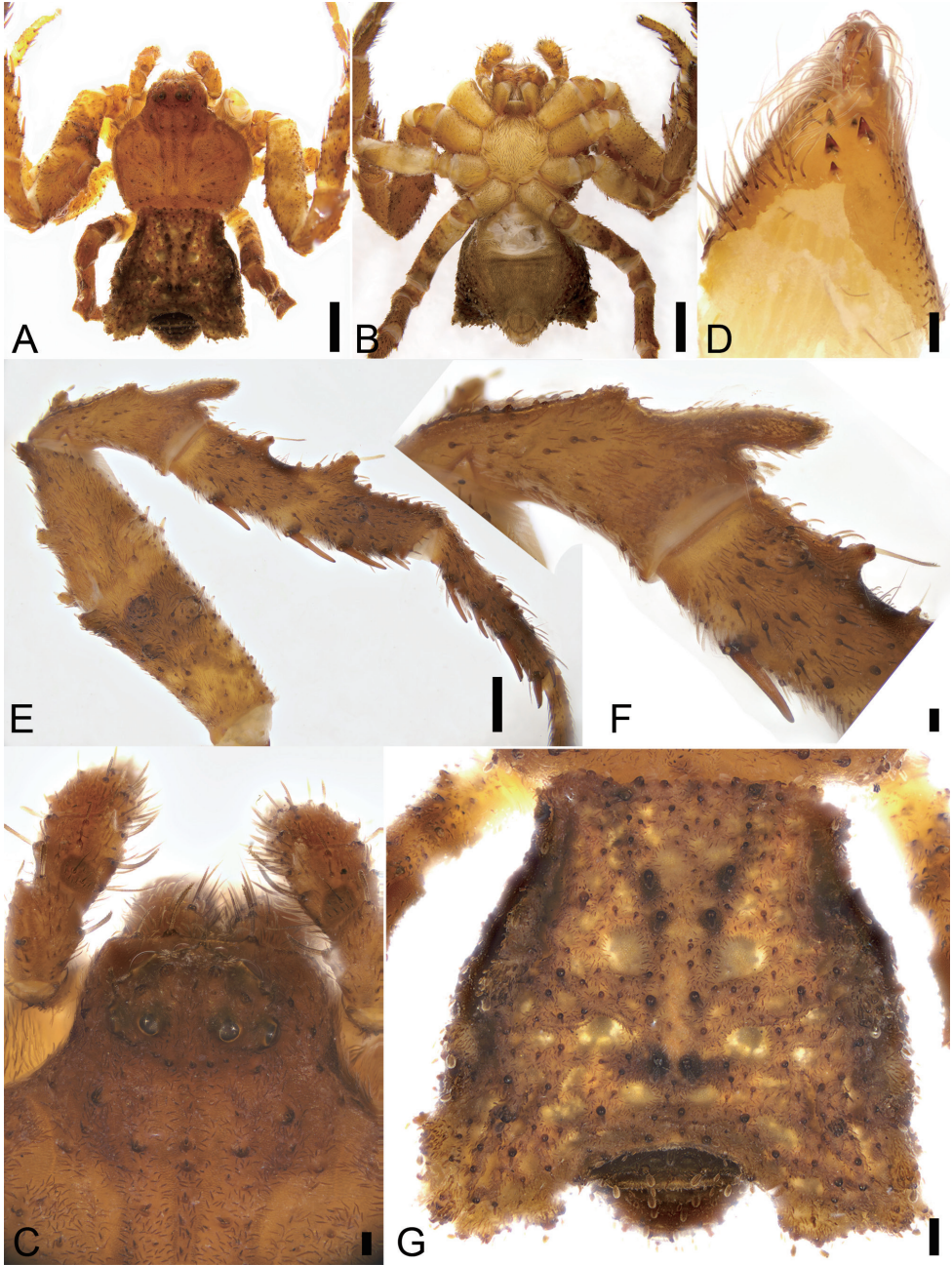


Figure 12. *Stephanopsis xiangzhouica* sp. nov., female holotype. **A** habitus, dorsal view **B** same, ventral view **C** cephalic part, dorsal view **D** left chelicera, mesal view **E** left leg I, prolateral view **F** patella I, prolateral view **G** abdomen, dorsal view. Scale bars: 1 mm (**A**, **B**), 0.1 mm (**C**, **D**, **F**), 0.5 mm (**E**, **G**).

wide, pentagonal with pair of latero-posterior horns; dorsum covered with sparse brown clavate and small dense plumose setae. Leg measurements: I 5.52 (1.78, 0.82, 1.31, 1.14, 0.47); II 4.80 (1.74, 0.73, 1.08, 0.86, 0.39); III 3.18 (0.95, 0.50, 0.80, 0.51, 0.42); IV 3.30 (1.24, 0.46, 0.74, 0.50, 0.36). Femora, patellae, and tibiae of legs I and II with dorsal outgrowths, especially long in distal parts of patellae. Spination: I Fe: d1, p4, v4; Pa: d3; Ti: d2, v8; Mt: r1, v8; II Fe: d3, v4; Pa: d2; Ti: d2, v8; Mt: v6; IV: Ti: d1, r1.

Colouration as in Fig. 12. Carapace, chelicerae, endites, and labium reddish brown. Sternum yellow. Palpal tibia with one clear round dark brown patch. Legs yellow to dark brown, with numerous dark brown patches on femora and tibiae. Abdomen reddish brown, dorsally with numerous pale brown dots, without setae on those dots.

Epigyne (Fig. 13). Epigynal plate sub-trapezoidal, 1.3 × wider than long. Copulatory openings (CO) oriented horizontally separated by nearly 1/3 of their width. Membranous sacs (MS) transparent, located anteriorly, covering 2/3 of epigynal plate, touching each other. Glandular appendages of membranous sac (GA) spherical, short, as long as 1/3–1/2 width of spermatheca (SP). Spermathecae oval, slightly separated by 1/3 of its width. Fertilisation ducts (FD) gramineous leaf-shaped, as long as spermathecae, directed laterally.

Male. unknown.

Distribution. Known only from the type locality in Jiangxi Province of China (Fig. 17).

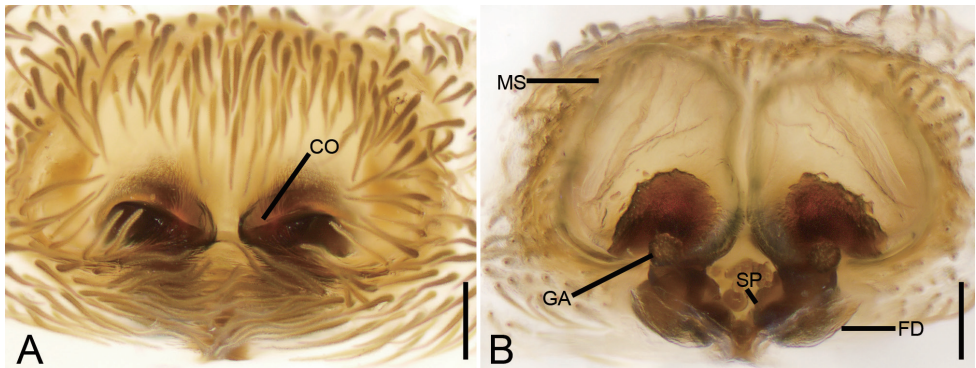


Figure 13. *Stephanopsis xiangzhouica* sp. nov., female epigyne, holotype. **A** ventral view **B** dorsal view. Abbreviations: CO – copulatory opening, FD – fertilisation duct, GA – glandular appendage, MS – membranous sac, SP – spermatheca. Scale bars: 0.1 mm.

Genus *Xysticus* C. L. Koch, 1835

Comments. *Xysticus* is one of the most diverse genera in Thomisidae with 293 named species (WSC 2022). Fifty-nine species are known from China. Of these, 19 are known only from females, and five from males. Most species are distributed in northern China and only one species, *Xysticus lesserti* Schenkel, 1963, is known from Guizhou Province (Li and Lin 2016).

Xysticus lesserti Schenkel, 1963

Figs 14–16

Xysticus lesserti Schenkel, 1963: 219, fig. 124a–c (♂); Marusik and Omelko 2014: 280, figs 15–17, 24 (♂).

Material examined. CHINA, Jiangxi Province: 1 ♀, Ji'an City, Jinggangshan County Level City, Jinggang Mountain National Nature Reserve, Ciping Town, Xiazhuang Village, Zhushachong Forest Farm, 26°33'3.6"N, 114°11'20.4"E, 630 m, 4.X.2014, K. Liu et al. leg.; 1 ♀, Ciping Town, Tongmuling, 26°37'12"N, 114°11'45.6"E, 780 m, 2.VIII.2014, Ke-ke Liu et al. leg.; 1 ♀, Ciping Town, Xiaojing Village, 26°35'20.4"N, 114°8'13.2"E, 913 m, 2.VIII.2014, K. Liu et al. leg.; 1 ♀, Ciping Town, Dajing Village, General of forest, 26.566°N, 114.125°E, 922 m, 13.VII.2014, K. Liu et al. leg.; 1 ♂, 1 ♀, Ciping Town, Dajing Village, 26°33'21.70"N, 114°07'20.08"E, 906 m, 31.VII.2019, K. Liu et al. leg.; 1 ♀, Dongshang Town, Ji-angshan Village, Qilichuan, 26°46'18.91"N, 113°51'55.59"E, 666 m, 30.VII.2019, other data as previous; 1 ♀, 26°46'23.73"N, 113°52'02.83"E, 665 m, K. Liu et al. leg.; 2 ♂, Longshi Town, Bashang Village, 26°39'58.29"N, 114°04'35.34"E, 491 m, 29.VII.2019, K. Liu et al. leg.; 1 ♀, Suichuan County, Gaoping Town, Gaoping Bus Station, 26°02'49.6"N, 114°07'2.8"E, 482 m, 1.VIII.2019, K. Liu et al. leg.; 1 ♀, Ciping Town, Wuzhifeng Scenic Spot, 26°32'48.23"N, 114°09'10.61"E, 811 m, 2.X.2018, K. Liu et al. leg.

Comments. The female of this species has remained undescribed till now and the male was confused with *X. kurilenis* Strand, 1907 in the past until Marusik and Omelko (2014) revealed some differences between these two species based on comparisons of the holotype of *X. lesserti* and specimens of *X. kurilenis* from the Kuril Islands. Several specimens of both sexes of *X. lesserti* were collected in the Jinggang Mountain National Nature Reserve including one pair which was in copula. Thus, collected females are considered by us as belonging to this species.

Diagnosis. The female of this species is similar to that of *X. kurilenis* in having two large oval atria (*At*) divided by septum (*Se*). Female of *X. lesserti* can be differentiated from those of sibling species by touching atria (vs. not touching) (cf. Fig. 14C and Kim and Lee 2012: fig. 21–4H). The male of *X. lesserti* is also very similar to those of *X. kurilenis*, but can be distinguished by the median apophysis (*MA*) reaching the sub-apex of the basal regular apophysis (*BTA*) in ventral view (vs. not reaching the sub-apex of the conductor) (cf. Fig. 15D and Marusik and Omelko 2014: fig. 18).

Description. Female. Habitus as in Fig. 14A, B. Total length 4.23. Carapace: 1.82 long, 1.81 wide. Eye sizes and interdistances: AME 0.12, ALE 0.24, PME 0.12, PLE 0.24, AME–AME 0.48, AME–ALE 0.28, PME–PME 0.51, PME–PLE 0.56, AME–PME 0.39, AME–PLE 0.87, ALE–ALE 1.25, PLE–PLE 1.82, ALE–PLE 0.39. MOA 0.62 long, front width 0.71, back width 0.77. Chelicerae toothless. Abdomen (Fig. 12A, B): 2.05 long, 2.19 wide, with numerous depressed patches. Leg measurements: I 5.39 (1.71, 0.81, 1.28, 1.05, 0.54); II 5.59 (1.70, 0.87, 1.30, 1.12, 0.6); III 3.36 (1.18, 0.44, 0.79, 0.55, 0.40); IV 4.03 (1.17, 0.60, 0.95, 0.75, 0.56). Leg spination:

I Fe: d1, p4; Ti: p3, v11; Mt: p3, r2, v11; II Fe: d1; Ti: p3, r1, v10; Mt: p3, r2, v10; III Fe: d1; Ti: p2, v5; Mt: p2, r1, v4; IV: Fe: d1; Pa: d2; Ti: d1, p2, v2; Mt: p2, r1, v3.

Colouration (Fig. 14A, B). Carapace reddish brown with dark mottling, medially with broad pale yellow stripe extending from PME to posterior edge. Chelicerae, endites, and labium reddish yellow. Sternum yellow, with numerous dark brown spots. Legs: I and II darker than III and IV; femora I–IV dorsally with reddish brown stripes, other segments yellowish to dark brown, with dark brown spots. Abdomen with grey oval patten, sub-medially with two indistinct transverse whitish stripes.

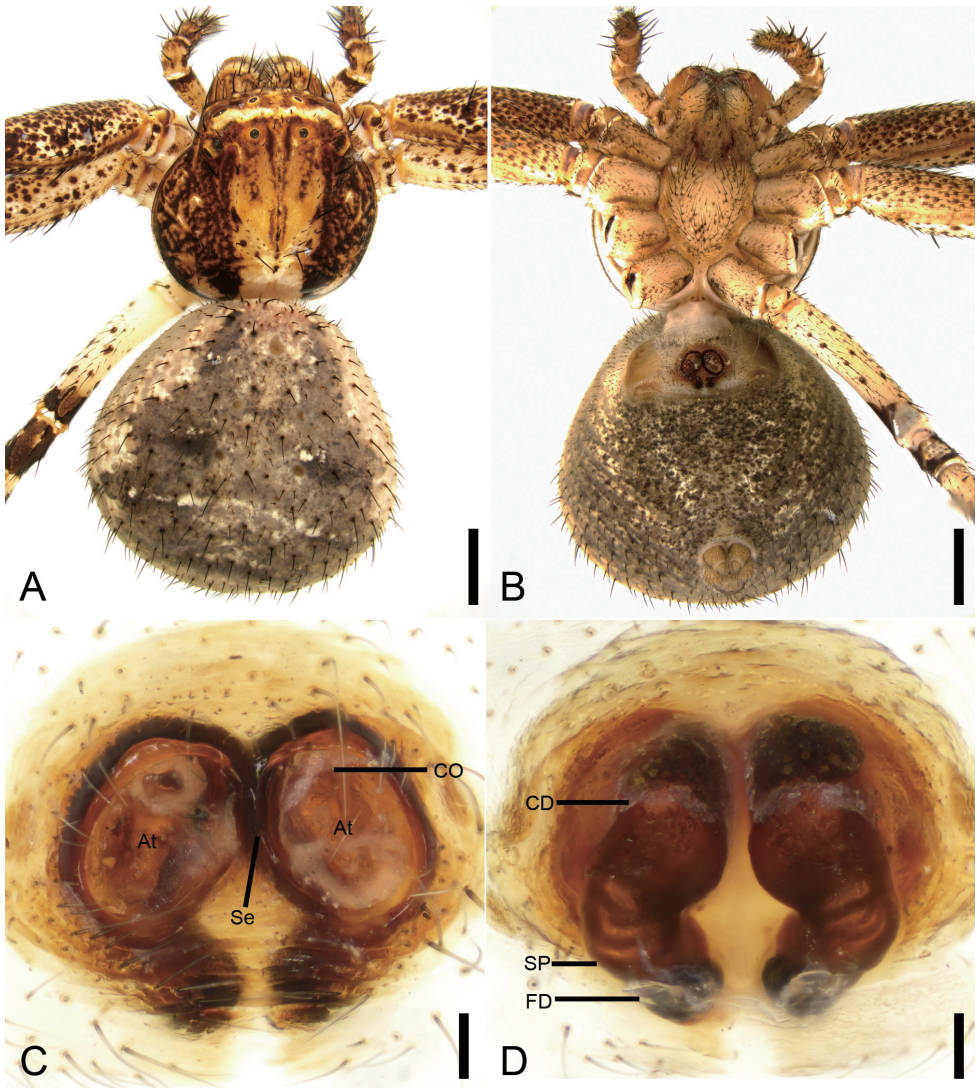


Figure 14. *Xysticus lesserti* Schenkel, 1963, female. **A** habitus, dorsal view **B** same, ventral view **C** epigyne, ventral view **D** same, dorsal view. Abbreviations: At – atrium, CD – copulatory duct, CO – copulatory opening, FD – fertilisation duct, Se –septum, SP – spermatheca. Scale bars: 1 mm (**A, B**), 0.1 mm (**C, D**).

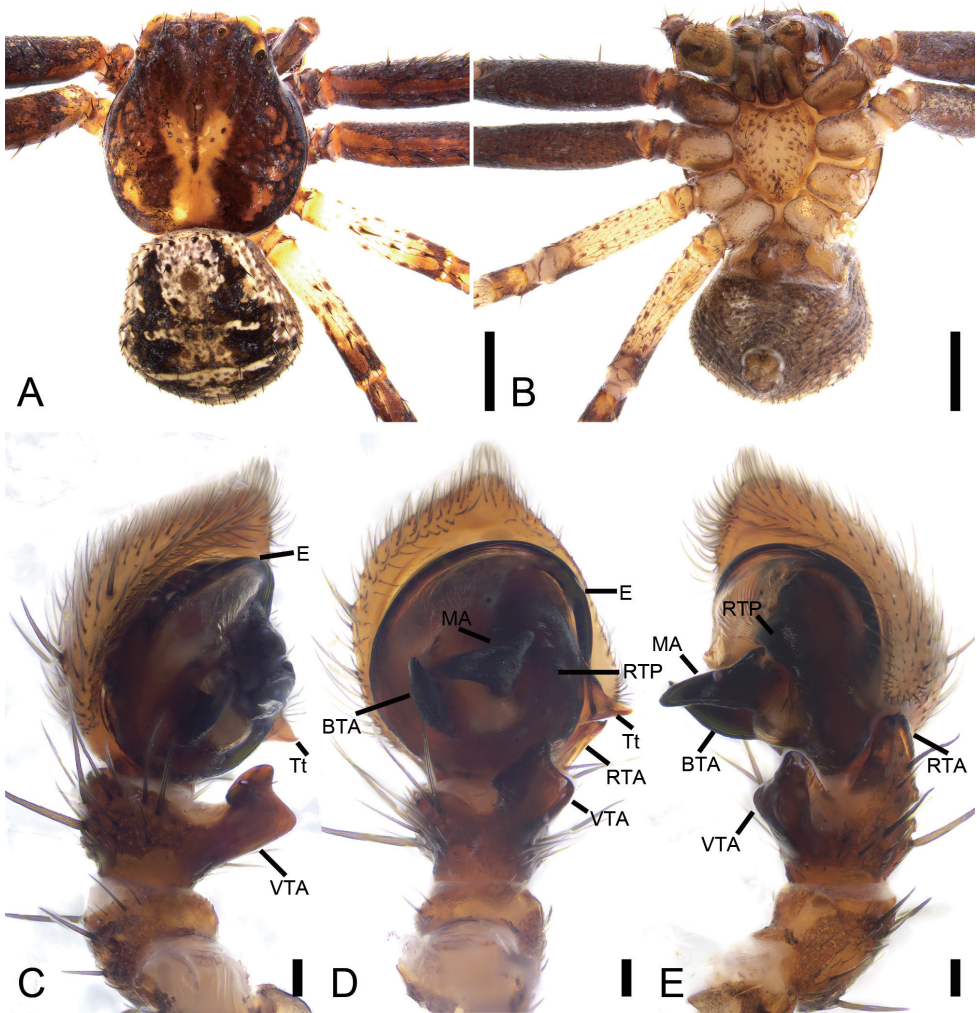


Figure 15. *Xysticus lesserti* Schenkel, 1963, male. **A** habitus, dorsal view **B** same, ventral view **C** palp, prolateral view **D** same, ventral view **E** same, retrolateral view. Abbreviations: BTA – basal tegular apophysis, E – embolus, MA – median apophysis, RTA – retrolateral tibial apophysis, RTP – ridge-shaped regular process, Tt – tutaculum, VTA – ventral tibial apophysis. Scale bars: 1 mm (**A, B**), 0.1 mm (**C–E**).

Epigyne (Fig. 14C, D). Epigyne approximately as long as wide. Anteriorly with two atria (*At*) separated by the septum (*Se*). Copulatory openings (*CO*) located in the anterior part of atria, hidden by sclerotised anterior margins of atria. Spermathecae (*SP*) kidney-shaped, with several constrictions. Fertilisation duct (*FD*) short, as long as width of the spermatheca in its posterior part, directed laterally.

Male. Habitus as in Fig. 15A, B. As in female, except as noted. Total length 3.07. Carapace: 1.80 long, 1.56 wide, with a few strong setae around eye area. Eye sizes and interdistances: AME 0.12, ALE 0.27, PME 0.13, PLE 0.22, AME–AME 0.36, AME–ALE 0.22, PME–PME 0.39, PME–PLE 0.46, AME–PME 0.29, AME–PLE 0.71, ALE–ALE 0.99, PLE–PLE 1.30, ALE–PLE 0.35. MOA 0.51 long, front width

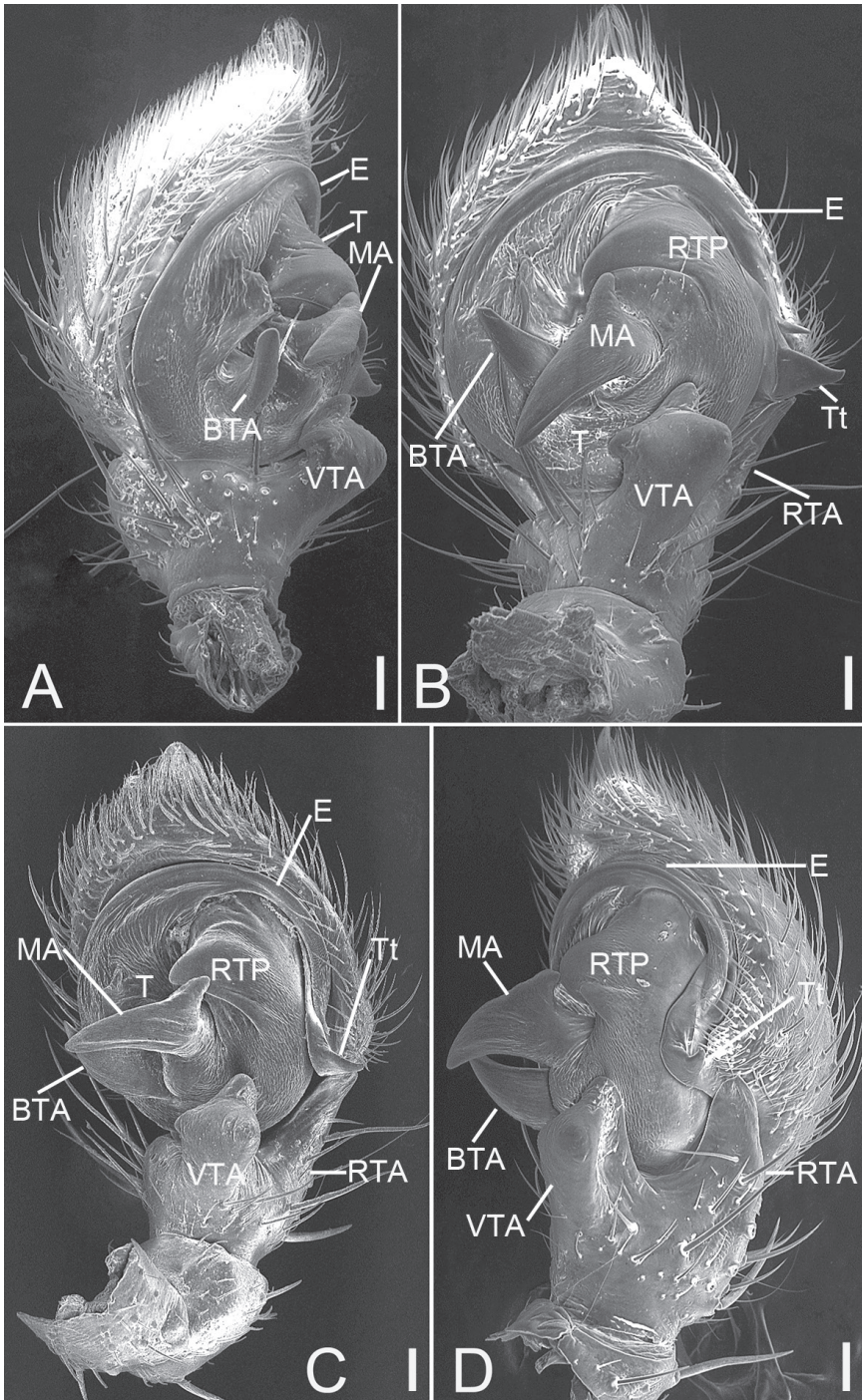


Figure 16. SEM micrographs of *Xysticus lesserti* Schenkel, 1963, male palp. **A** prolateral view **B** ventral view **C** ventral view, slightly retrolateral **D** retrolateral view. Abbreviations: BTA – basal tegular apophysis, E – embolus, MA – median apophysis, RTA – retrolateral tibial apophysis, RTP – ridge-shaped tegular process, T – tegulum, Tt – tutaculum, VTA – ventral tibial apophysis. Scale bars: 0.1 mm.

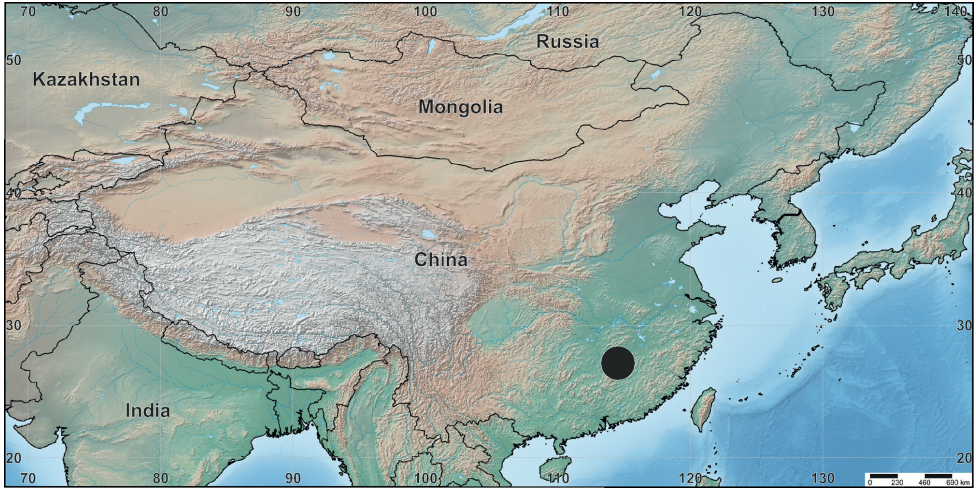


Figure 17. The location of the Jinggang Mountain National Nature Reserve in China indicated by a large black dot.

Table 1. List of Thomisidae species recorded in Jinggang Mountain National Nature Reserve. Genera recorded for the first time are marked with an asterisk (*).

Genus	Species	No. of ♂♂	No. of ♀♀	Total
<i>Alcimochthes</i> Simon, 1885 *	<i>A. limbatus</i> Simon, 1885	2	7	9
<i>Angaeus</i> Thorell, 1881 *	<i>A. liangweii</i> (Tang & Li, 2010)	0	4	4
	<i>A. xieluae</i> sp. nov.	2	1	3
<i>Borboropactus</i> Simon, 1884 *	<i>B. jiangyong</i> Yin et al., 2004	1	3	4
<i>Diaea</i> Thorell, 1869 *	<i>D. subdola</i> O. P.-Cambridge, 1885	8	2	10
<i>Ebelingia</i> Lehtinen, 2004*	<i>E. forcipata</i> (Song & Zhu, 1993) comb. nov.	3	5	8
<i>Ebrechtella</i> Dahl, 1907 *	<i>E. pseudovatia</i> (Schenkel, 1936)	1	2	3
	<i>E. tricuspadata</i> (Fabricius, 1775)	4	1	5
	<i>E. gongi</i> (Song & Kim, 1992)	2	5	7
<i>Epidius</i> Thorell, 1877 *	<i>I. tangi</i> Jin & Zhang, 2012	2	0	2
<i>Indoxysticus</i> Benjamin & Jaleel, 2010 *				
<i>Lysiteles</i> Simon, 1895 *	<i>L. minusculus</i> Song & Chai, 1990	1	0	1
	<i>L. silvanus</i> Ono, 1980	10	55	65
	<i>L. subspirellus</i> sp. nov.	0	2	2
<i>Misumenops</i> F. O. P.-Cambridge, 1900 *	<i>M. hunanensis</i> Yin, Peng & Kim, 2000	1	2	3
<i>Monaes</i> Thorell, 1869	<i>M. aciculus</i> (Simon, 1903)	2	1	3
<i>Oxyate</i> L. Koch, 1878	<i>O. bicornis</i> Liu, Liu & Xu, 2017	1	2	3
	<i>O. forcipatus</i> Zhang & Yin, 1998	1	0	1
	<i>O. mucunica</i> sp. nov.	0	1	1
	<i>O. striatipes</i> L. Koch, 1878	4	0	4
	<i>O. nipponica</i> Ono, 1985	1	0	1
<i>Ozyptila</i> Simon, 1864 *				
<i>Pharta</i> Thorell, 1891 *	<i>P. brevipalpus</i> (Simon, 1903)	23	19	42
	<i>P. lingxiufengica</i> sp. nov.	0	1	1
	<i>S. hupingensis</i> Tang, Yin & Peng, 2004	0	1	1
<i>Smodicinodes</i> Ono, 1993 *	<i>S. xiangzhouica</i> sp. nov.	0	1	1
<i>Stephanopsis</i> O. Pickard-Cambridge, 1869 *				
<i>Strigopus</i> Simon, 1885 *	<i>S. guizhouensis</i> Song, 1990	1	2	3
<i>Synema</i> Simon, 1864	<i>S. zonatum</i> Tang & Song, 1988	0	1	1
<i>Thomisus</i> Walckenaer, 1805 *	<i>T. labefactus</i> Karsch, 1881	36	8	44
<i>Tmarus</i> Simon, 1875 *	<i>T. circinalis</i> Song & Chai, 1990	0	1	1
	<i>T. longqicus</i> Song & Zhu, 1993	3	4	7
	<i>X. croceus</i> Fox, 1937	26	8	34
<i>Xysticus</i> C. L. Koch, 1835	<i>X. hedini</i> Schenkel, 1936	2	0	2
	<i>X. kansuensis</i> (Tang, Song & Zhu, 1995)	0	2	2
	<i>X. kurilensis</i> Strand, 1907	5	5	10
	<i>X. lesserti</i> Schenkel, 1963	3	9	12

0.58, back width 0.69. Abdomen (Fig. 15A, B): 1.40 long, 1.43 wide, with abundant strong setae dorsally. Leg measurements: I 5.56 (1.66, 0.79, 1.13, 1.30, 0.68); II 5.36 (1.62, 0.70, 1.22, 1.20, 0.62); III 3.36 (1.18, 0.44, 0.79, 0.55, 0.40); IV 3.83 (1.17, 0.42, 0.94, 0.79, 0.51). Leg spination: I Fe: d5, p3; Pa: v1; Ti: p3, r3, v10; Mt: p3, r2, v8; II Fe: d5, p3; Pa: v1; Ti: p3, r3, v10; Mt: p3, r2, v10; III Fe: d4; Pa: d2, v1; Ti: d2, p2, r2, v6; Mt: p3, r3, v4; IV: Fe: d4; Pa: d2, r1; Ti: d2, p2, r2, v6; Mt: p3, r3, v4.

Palp (Figs 15C–E, 16). Tibia with two apophysis: the retrolateral one (*RTA*) triangular, shorter than tibia, the ventral one (*VTA*) square, longer than tibia. Cymbium irregularly oval, length/width ratio ~ 1.2. Tutaculum (*Tt*) triangular, forming a canal. Median apophysis (*MA*), strongly sclerotised, wing-shaped, its apex reaching the sub-apex of basal regular apophysis (*BTA*). Basal regular apophysis broad and stocky. Tegulum with a ridge-shaped retrolateral process (*RTP*). Base of the embolus (*E*) gradually separating from the tegulum, slightly tapering during its median portion, apex embedded in tutaculum.

Distribution. China: Jiangxi (Fig. 17) and Guizhou Provinces (Schenkel 1963); Russia: Sakhalin Is., Kurile Isles (Marusik and Omelko 2014); Korea and Japan (Song and Zhu 1997).

Acknowledgements

We thank Zhan-Feng Wang, Zhi-Wu Chen, Ze-Yuan Meng, Xiao-Ping Huang, Peichong Gong, Yu-Bao Tang, Wen-Jun Xie, Sha Wu, Guang-feng Li, Ce Xu, Shi-Cong He, Yi-Fan Zhao, Huo-kai Wang (all from Jingtangshan University), and Wen Sun (Jingtangshan Economic and Trade School) for their assistance during the fieldwork. We also thank Dr. Suresh P. Benjamin and Christoph Muster for improving earlier drafts of this manuscript. We are grateful to the reviewers especially Dr. David Court and the subject editor Dr. Yuri Marusik for providing significant comments, and Dr Nathalie Yonow and Victor Fet for improving the English of the manuscript. The work of all authors except Alexander A. Fomichev was supported by the Natural Science Foundation of China (32000301, 32160243, 32070429) and PhD Research Startup Foundation of Jingtangshan University (JZB2010).

References

- Benjamin SP (2011) Phylogenetics and comparative morphology of crab spiders (Araneae: Dionycha, Thomisidae). *Zootaxa* 3080(1): 1–108. <https://doi.org/10.11646/zootaxa.3080.1.1>
- Benjamin SP (2013) On the crab spider genus *Angaeus* Thorell, 1881 and its junior synonym *Paraborboropactus* Tang and Li, 2009 (Araneae: Thomisidae). *Zootaxa* 3635(1): 71–80. <https://doi.org/10.11646/zootaxa.3635.1.7>

- Dondale CD, Redner JH (1978) The insects and arachnids of Canada, Part 5. The crab spiders of Canada and Alaska, Araneae: Philodromidae and Thomisidae. Research Branch Agriculture Canada Publication 1663: 1–255.
- Kim JP, Gwon SP (2001) A revisional study of the spider family Thomisidae Sundevall, 1833 (Arachnida: Araneae) from Korea. Korean Arachnology 17(1): 13–78.
- Kim ST, Lee SY (2012) Arthropoda: Arachnida: Araneae: Thomisidae. Thomisid spiders. Invertebrate Fauna of Korea 21(9): 1–88.
- Li S (2020) Spider taxonomy for an advanced China. Zoological Systematics 45(2): 73–77.
- Li SQ, Lin YC (2016) Species Catalogue of China. Vol. 2. Animals. Invertebrates (1). Arachnida: Araneae. Science Press, Beijing, 549 pp.
- Liu K, Liu J, Xu X (2017) Two new species of the genus *Oxytate* from China (Araneae: Thomisidae). Zootaxa 4320(1): 193–200. <https://doi.org/10.11646/zootaxa.4320.1.12>
- Logunov DV (1992) On the spider fauna of the Bolshekhkhehtsyrski State Reserv (Khabarovsk Province). I. Families Araneidae, Lycosidae, Philodromidae, Tetragnathidae and Thomisidae. Sibirskij Biologicheskij Zhurnal 4: 56–68.
- Machado M, Teixeira RA (2021) Phylogenetic relationships in Stephanopinae: systematics of *Stephanopsis* and *Sidymella* based on morphological characters (Araneae: Thomisidae). Organisms, Diversity & Evolution 21(2): 281–313. <https://doi.org/10.1007/s13127-020-00472-x>
- Machado M, Teixeira RA, Milledge GA (2019) On the Australian bark crab spider genus *Stephanopsis*: taxonomic review and description of seven new species (Araneae: Thomisidae: Stephanopinae). Records of the Australian Museum 71(6): 217–276. <https://doi.org/10.3853/j.2201-4349.71.2019.1698>
- Marusik YM, Omelko MM (2014) Reconsideration of *Xysticus* species described by Ehrenfried Schenkel from Mongolia and China in 1963 (Araneae: Thomisidae). Zootaxa 3861(3): 275–289. <https://doi.org/10.11646/zootaxa.3861.3.5>
- Ono H (2001) Crab spiders of the family Thomisidae from the Kingdom of Bhutan (Arachnida, Araneae). Entomologica Basiliensis 23: 203–236.
- Ono H (2009) The spiders of Japan with keys to the families and genera and illustrations of the species. Tokai University Press, Kanagawa, 739 pp.
- Ramírez MJ (2014) The morphology and phylogeny of dionychan spiders (Araneae: Araneomorphae). Bulletin of the American Museum of Natural History 390: 1–374. <https://doi.org/10.1206/821.1>
- Schenkel E (1963) Ostasiatische Spinnen aus dem Muséum d'Histoire naturelle de Paris. Mémoires du Muséum National d'Histoire Naturelle de Paris (A, Zool.) 25: 1–481.
- Song DX, Zhu MS (1997) *Fauna Sinica: Arachnida: Araneae: Thomisidae, Philodromidae*. Science Press, Beijing, 259 pp.
- Song DX, Zhu MS, Li SQ (1993) Arachnida: Araneae. In: Huang CM (Ed.) Animals of Longqi Mountai. China Forestry Publishing House, Beijing, 852–890.
- Song DX, Zhu MS, Chen J (1999) The spiders of China. Hebei Science and Technology Publishing House, Shijiazhuang, 640 pp.
- Tang G, Li SQ (2010a) Crab spiders from Hainan Island, China (Araneae, Thomisidae). Zootaxa 2369(1): 1–68. <https://doi.org/10.11646/zootaxa.2369.1.1>

- Tang G, Li SQ (2010b) Crab spiders from Xishuangbanna, Yunnan Province, China (Araneae, Thomisidae). *Zootaxa* 2703(1): 1–105. <https://doi.org/10.11646/zootaxa.2703.1.1>
- Tang G, Yin CM, Peng XJ, Ubick D, Griswold C (2008) The crab spiders of the genus *Lysiteles* from Yunnan Province, China (Araneae: Thomisidae). *Zootaxa* 1742(1): 1–41. <https://doi.org/10.11646/zootaxa.1742.1.1>
- Wang C, Mi XQ, Peng XJ (2016) A new species of *Pharta* Thorell, 1891 (Araneae: Thomisidae) from China. *Oriental Insects* 50(3): 129–134. <https://doi.org/10.1080/00305316.2016.1197163>
- World Spider Catalog (2022) World Spider Catalog. Natural History Museum Bern. Version 22.5. <https://wsc.nmbe.ch/> [accessed 2 January 2022]

A new species of *Trisiniotus* Jeannel from Mao-shan, East China (Coleoptera, Staphylinidae, Pselaphinae)

Ting Feng¹, Zi-Wei Yin²

1 Shanghai Zoological Park, 2381 Hongqiao Road, Changning District, Shanghai 200335, China **2** Laboratory of Systematic Entomology, College of Life Sciences, Shanghai Normal University, 100 Guilin Road, Xuhui District, Shanghai 200234, China

Corresponding author: Zi-Wei Yin (pselaphinae@gmail.com)

Academic editor: Adam Brunke | Received 24 January 2022 | Accepted 9 March 2022 | Published 13 April 2022

<http://zoobank.org/E9BD2122-A304-4E1D-AB16-E887DBE7BB31>

Citation: Feng T, Yin Z-W (2022) A new species of *Trisiniotus* Jeannel from Mao-shan, East China (Coleoptera, Staphylinidae, Pselaphinae). ZooKeys 1095: 75–81. <https://doi.org/10.3897/zookeys.1095.81076>

Abstract

The genus *Trisiniotus* Jeannel of the pselaphine tribe Batrisini comprises two species distributed in North India and southern Myanmar. Here, a third species, *T. taoismus* Feng & Yin **sp. nov.**, is described from Mao-shan, Jiangsu Province, East China. The new species can be readily distinguished from both congeners by the unmodified male antennae.

Keywords

China, Jiangsu, new species, taxonomy, *Trisiniotus*

Introduction

In his review of the pselaphine fauna of North India, Jeannel (1960) established a number of batrisine genera that, from a modern point of view, lack adequate justification. The genus *Trisiniotus* Jeannel certainly falls into this category. No specific comments were provided on generic characteristics, nor was the genus compared to potentially related genera. In the key to genera (Jeannel 1960: 409), *Trisiniotus* was coupled with *Batristhenes* Jeannel by the shared absence of a median longitudinal sulcus on the

pronotum, and separated from the latter by the modified antennae and different shapes of the head and aedeagus. The absence (or loss) of a median sulcus on the pronotum appears to be homoplastic in a number of Asian batrisine genera, as pointed out by Nomura (1991: 11), and the presence of antennal modifications is a common state in numerous batrisine groups. Both characters can hardly be considered as bearing any systematic significance above the species level. The constricted basal capsule of the aedeagus of *Trisiniotus* may indicate, to a certain degree, close relationships with the Japanese species of *Batriscenaulax* Jeannel and *Physomerinus* Jeannel, which have the same type of the aedeagus and are separated from each other mainly by different locations of the male sexual characters (Jeannel 1958). The type species of *Trisiniotus*, *T. nodicornis* Jeannel, was reported from Dehradun in Uttarakhand, India and remained the sole member of the genus until Nomura and Aung (2020, 2021) recently identified *Batrisus nitidulus* Motschulsky (type locality: “Ind. or.”) among material from southern Myanmar, and transferred the species to *Trisiniotus*. A third, distinct but unnamed species that has an enlarged antennomere 9 and a medially sulcate pronotum was reported by Nomura et al. (2013) from Kaeng Krachan National Park, southern Thailand. Putting aside the uncertain generic placement of *Trisiniotus*, both named species are easily recognizable by the swollen antennomere 10 in the male.

In August 2020, we organized a collecting trip to Mao-shan Scenic Area, Jiangsu Province in the hope of finding additional material of a distinctive clavigerite beetle (described as *Archiclaviger gaofani* Yin, Hlaváč & Cuccodoro in Yin et al. 2020) collected in the city of Changzhou and sent to the junior author shortly before the trip. We failed to find this beetle, probably owing to it being the wrong season. Nevertheless, a small series of pselaphines were collected by sifting the leaf litter layer in forests along the Mao-shan Mountain range. Among this material we recognized a distinct species of Batrisini, which is evidently related to the two *Trisiniotus* species from India and Myanmar based on the shape of the pronotum and aedeagus. As no attempt is made here to clarify the relationships of *Trisiniotus* with potentially related groups, we simply describe the new species and place it as a member of *Trisiniotus*.

Material and methods

The type material of the new species described in this paper is deposited in the Insect Collection of Shanghai Normal University, Shanghai (SNUC). The label data of the material are quoted verbatim.

Dissected parts were mounted in Euparal on plastic slides pinned with the specimen. The habitus image of the beetle was taken using a Canon 5D Mark III camera with Canon MP-E 65 mm f/2.8 1–5 × Macro Lens, with a Canon MT-24EX Macro Twin Lite Flash as the light source. Images of the morphological details were produced using a Canon G9 camera mounted to an Olympus CX31 microscope under reflected or transmitted light. Zerene Stacker (version 1.04) was used for image stacking. All images were modified and grouped into plates using Adobe Photoshop CC 2020.

Measurements were taken as follows: total body length was measured from the anterior margin of the clypeus to the apex of the abdomen; head length was measured from the anterior margin of the clypeus to the head base, excluding the occipital constriction; head width was measured across the eyes; the length of the pronotum was measured along the midline; the width of the pronotum is its maximum width; the length of the elytra was measured along the suture; the width of the elytra was measured as the maximum width across both elytra; the length of the abdomen is the length of the dorsally exposed part of the abdomen along its midline; the width of the abdomen is its maximum width. Abdominal tergites and sternites are numbered following Chandler (2001), in Arabic (starting from the first visible segment) and Roman (reflecting true morphological position) numerals, e.g., tergite 1 (IV), or sternite 1 (III). Paired structures in the description of the new species are treated as singular.

Taxonomy

Trisiniotus taoismus Feng & Yin, sp. nov.

<http://zoobank.org/C2995259-9A1F-42FF-B22D-A0169BB25162>

Chinese common name: 道隱沟蚁甲

Figs 1, 2

Type material (15 exx.). *Holotype*: CHINA: ♂, 'China: Jiangsu, Jurong City, Mao Shan, 31°47'41.99"N, 119°18'43.38"E, leaf litter, sifted, 140 m, 24.viii.2020, Ting Feng leg., 江苏句容市茅山风景区' (SNUC). *Paratypes*: CHINA: 6 ♂♂, 3 ♀♀, same data as that of holotype; 1 ♂♂, 2 ♀♀, 'China: Jiangsu, Jurong City, Yaji-shan, 31°39'24.06"N, 119°17'253.71"E, leaf litter, sifted, 100 m, 23.viii.2020, Zi-Wei Yin leg., 江苏句容市丫髻山脚; 2 ♀♀, China: Jiangsu, Jurong City, nr. Wawu-shan, 31°39'6.28"N, 119°16'20.99"E, leaf litter, sifted, 100 m, 22.viii.2020, Ting Feng leg., 江苏句容市瓦屋山上杆湖农庄 (all SNUC).

Diagnosis. Male. Body length approximately 1.9 mm. Head sub-rectangular at base; vertex with large and setose foveae, with transverse sulcus at anterior portion; antenna elongate; antennomeres more or less elongate, lacking modifications. Pronotum lacking a median longitudinal sulcus. Discal stria of elytron long, extending posteriorly to approximately apical 3/4 of elytral length. Mesotibia with small apical spine. Metaventrite with setose admesal longitudinal ridges. Tergite 1 (IV) predominantly large, dorsally longer than 2–4 (V–VII) combined, lacking modifications. Aedeagus strongly asymmetrical; median lobe with restricted basal capsule and triangular foramen, ventral stalk erect, narrowing towards apex in lateral view; dorsal lobe narrowed at base, broadened towards apex. **Female.** Body length approximately 1.8 mm, legs and metaventrite lacking modifications, genitalia as in Fig. 1F.

Description. Male. Body (Fig. 1A) length 1.88–1.92 mm; color reddish-brown, tarsi and mouthparts lighter. Dorsal surface of body covered with short pubescence.

Head (Fig. 1B) roundly triangular, sub-rectangular at base, much wider than long, length 0.37–0.39 mm, width across eyes 0.44 mm; vertex finely punctate, with large,

setose vertexal foveae (dorsal tentorial pits), with transverse sulcus at apical portion of vertex, mediobasal carina thin and faint; antennal tubercles weakly raised; frons slightly impressed medially, confluent with clypeus; clypeus smooth, its anterior margin carinate and moderately raised; ocular-mandibular carina complete, distinct, carina branched below eye, extended ventrally and then anteriorly to posteroventral articulation of mandible. Venter with single, small gular fovea (posterior tentorial pit), with distinct median carina extending from fovea anteriorly to mouthparts. Eyes greatly prominent, each composed of approximately 35 large ommatidia. Antenna moderately elongate, length 0.94–0.97 mm, simple, club loosely formed by moderately enlarged apical three antennomeres; antennomere 1 thick, subcylindrical, 2–7 each elongate, 8 shortest, 9 much longer and broader than 8, 10 as long as and slightly wider than 9, 11 longest, shorter than 9 and 10 combined, sub-conical.

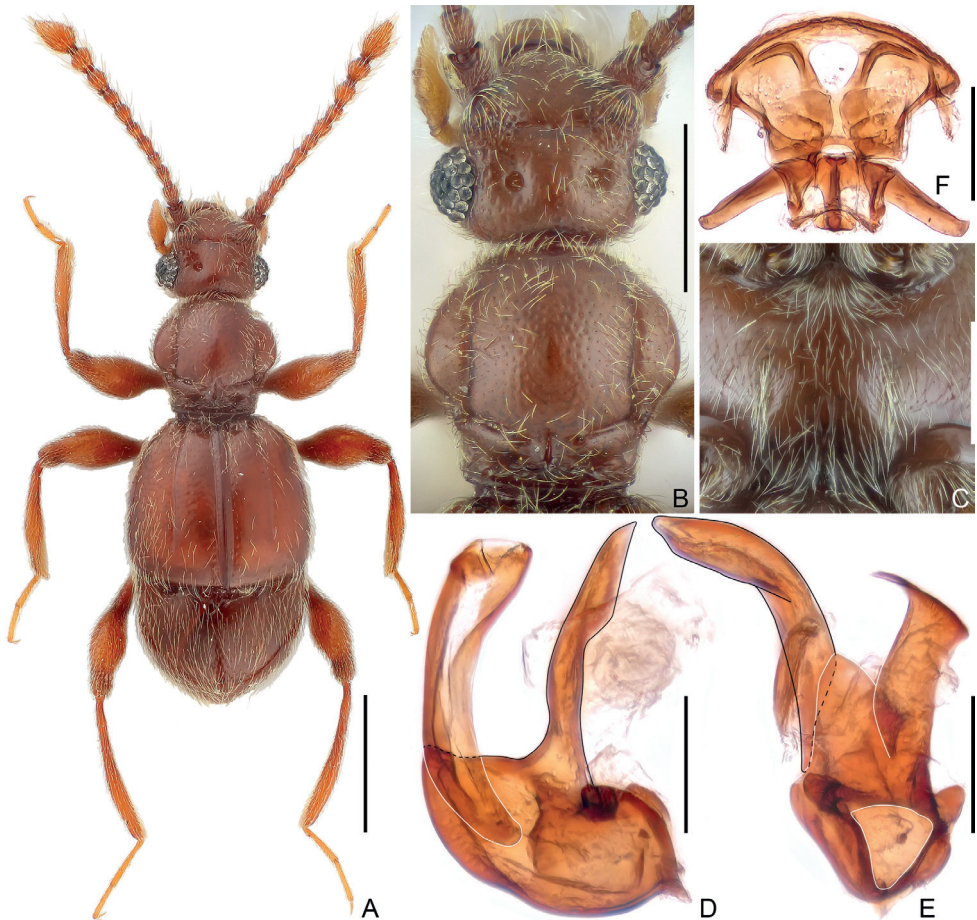


Figure 1. Morphological characters of *Trisiniotus taoismus* sp. nov. **A** dorsal habitus **B** head dorsum and pronotum **C** central part of metaventrite **D, E** aedeagus, lateral (**D**) and ventral (**E**) **F** female genitalia. Scale bars: 0.5 mm (**A**); 0.3 mm (**B**); 0.2 mm (**D–F**).



Figure 2. Distribution (A, B) and habitat (C, D) of *Trisiniotus*. A distribution of *T. taoismus* sp. nov. (circle), *T. nitidulus* (triangle), and *T. nodicornis* (square) B distribution of *T. taoismus* sp. nov. in the Mao-shan mountains C environment of Mao-shan D habitat of *T. taoismus* sp. nov.

Pronotum (Fig. 1B) approximately as long as broad, length 0.45–0.46 mm, width 0.46–0.47 mm, widest at middle; sides rounded; disc slightly convex, finely punctate, median longitudinal sulcus absent, semi-circular lateral sulci extending from dorsal surface laterally and posteriorly and then fused with lateral ends of antebasal sulcus; lacking median antebasal fovea, with short mediobasal impression, antebasal tubercles small, lateral antebasal foveae connected by transverse antebasal sulcus; outer and inner pairs of basolateral foveae distinct. Prosternum with anterior part as long as coxal part, with small lateral procoxal foveae; hypomerar ridge short, present only at base, with a lateral antebasal hypomerar impression; margin of coxal cavity weakly carinate.

Elytra much wider than long, length 0.62–0.63 mm, width 0.69–0.70 mm; each elytron with two large, asetose basal foveae, lacking a subbasal fovea; discal stria long, carinate, extending from outer basal fovea to approximately apical 3/4 of elytral length; humerus rounded, weakly prominent, subhumeral fovea absent, with sulcate marginal stria from below middle to posterior margin of elytron. Metathoracic wings fully developed.

Mesoventrite short, demarcated from metaventrite by ridged anterior edges of impressed areas where lateral mesocoxal foveae situated at mesal ends of impressions, with pair of thin admesal carinae; setose median mesoventral foveae widely separated, lateral

mesoventral foveae large and setose, broadly forked internally; intercoxal process short. Metaventrite (Fig. 1C) broadly impressed at middle, with setose admesal longitudinal ridges; with large, setose lateral mesocoxal foveae and a pair of smaller, setose lateral metaventral foveae, posterior margin broadly emarginate, with narrow split at middle.

Legs moderately elongate; mesotibia with small spine at apex.

Abdomen compressed, widest at lateral margins of tergite 1 (IV), length 0.47–0.50 mm, width 0.64–0.68 mm. Tergite 1 (IV) in dorsal view longer than 2–4 (V–VII) combined, lacking basal sulcus, with one pair of basolateral foveae and a short discal carina; tergites 2–4 each with one pair of small basolateral foveae, 4 as long as 2 and 3 combined along middle, 5 (VIII) semicircular, posterior margin roundly emarginate at middle. Sternite 2 (IV) with mediobasal and two basolateral foveae, with a pair of short lateral carinae; midlength of sternite 2 as long as 3–5 (V–VII) combined, 3–5 each short at middle, lacking fovea, 6 (VIII) transverse, posterior margin emarginate at middle, 7 (IX) membranous or absent.

Aedeagus (Fig. 1D, E) 0.30 mm long, strongly asymmetrical; median lobe with constricted basal capsule and small, roundly triangular foramen, ventral stalk erect, in lateral view broadest anterior to middle and then narrowing towards apex; dorsal lobe approximately as long as ventral stalk, narrowed at base and broadening towards apex; parameres reduced to single broad membranous structure.

Female. Similar to male in external morphology; antenna shorter; each compound eye composed of approximately 30 ommatidia; elytra constricted at bases, humerus not prominent; metathoracic wings absent; mesotibia lacking apical spine, metaventrite lacking admesal ridges. Measurements (as for male): body length 1.79–1.83 mm; length/width of head 0.37/0.42–0.43 mm, pronotum 0.41–0.43/0.45 mm, elytra 0.56–0.57/0.69 mm; abdomen 0.52–0.53/0.65 mm; length of antenna 0.85–0.87 mm; maximum width of genitalia (Fig. 1F) 0.23 mm.

Comparative notes. *Trisiniotus taoismus* sp. nov. shares with its two congeners the lack of a median longitudinal sulcus on the pronotum, as well as a similar aedeagus. This species can be readily separated by the simple male antennomere 10, which is swollen in both species from India and Myanmar.

Distribution. East China: Jiangsu (Fig. 2A, B).

Bionomics. All individuals were collected by sifting the leaf litter layer in broad-leaved forests (Fig. 2C, D).

Etymology. The specific epithet reflects that Mao-shan is a Taoist sacred mountain in eastern China.

Acknowledgements

We are grateful to the Administrative Committee of Mao-shan Scenic Area for permitting our field samplings. Shûhei Nomura (National Museum of Nature and Science, Tsukuba, Japan) provided helpful discussion of *Trisiniotus*. Ivan Löbl (Muséum d'histoire naturelle, Genève, Switzerland) and Peter Hlaváč (National Museum, Praha, Czech Republic) criti-

cally read the manuscript and provided helpful comments. Adam J. Brunke (Agriculture and Agri-Food Canada, Canadian National Collection of Insects, Arachnids and Nematodes, Ottawa, Canada) helped to improve the English narrative. The present study was supported by the National Natural Science Foundation of China (no. 31872965), and the Science and Technology Commission of Shanghai Municipality (no. 19QA1406600) granted to ZWY.

References

- Chandler DS (2001) Biology, morphology, and systematics of the antlike litter beetles of Australia (Coleoptera: Staphylinidae: Pselaphinae). *Memoirs on Entomology International* 15: 1–560.
- Jeannel R (1958) Révision des Pselaphides du Japon. *Mémoires du Muséum National d'Histoire Naturelle (A: Zoologie)* 18(1): 1–138.
- Jeannel R (1960) Sur les Pselaphides (Coleoptera) de l'Inde septentrionale. *Bulletin of the British Museum (Natural History). Entomology* 9: 403–456. <https://doi.org/10.5962/bhl.part.27559>
- Nomura S (1991) Systematic study on the genus *Batrisoplisus* and its allied genera from Japan (Coleoptera, Pselaphidae). *Esakia* 30: 1–462. <https://doi.org/10.5109/2550>
- Nomura S, Aung MM (2020) Inventory studies on the subfamily Pselaphinae (Coleoptera, Staphylinidae) of Myanmar part 2: A list of collected species in Tanintharyi Region in January 2017. *Bulletin of the National Museum of Nature and Science, Series A, Zoology* 46(4): 203–213.
- Nomura S, Aung MM (2021) Inventory studies on the subfamily Pselaphinae (Coleoptera, Staphylinidae) of Myanmar part 3: A list of collected species in Tanintharyi Region in November 2018. *Bulletin of the National Museum of Nature and Science, Series A, Zoology* 47(1): 19–29.
- Nomura S, Sakchoowong W, Maruyama M (2013) Further study on the pselaphine fauna (Insecta, Coleoptera, Staphylinidae) of the Kaeng Krachan National Park, West Thailand in 2010–2012. *Bulletin of the National Museum of Nature and Science. Series A, Zoology* 39(2): 73–92.
- Yin Z-W, Hlaváč P, Cuccodoro G (2020) The first record of *Archiclaviger* in continental Asia, with description of a new species from China (Coleoptera: Staphylinidae: Pselaphinae). *Acta Entomologica Musei Nationalis Pragae* 60(2): 537–544. <https://doi.org/10.37520/aemnp.2020.036>

A new species of medicinal leech in the genus *Hirudo* Linnaeus, 1758 (Hirudiniformes, Hirudinidae) from Tianjin City, China

Hao Wang^{1*}, Fan-Ming Meng^{2*}, Si-Jie Jin¹,
Jiang-Wei Gao¹, Xiang-Rong Tong¹, Zi-Chao Liu¹

1 Engineering Research Center for Exploitation & Utilization of Leech Resources in Universities of Yunnan Province, School of Agriculture & Life Sciences, Kunming University, Kunming 650214, China **2** Department of Parasitology, Xiangya School of Medicine, Central South University, Changsha 430001, China

Corresponding author: Zi-Chao Liu (abclzc@aliyun.com)

Academic editor: Fredric Govedich | Received 7 September 2021 | Accepted 24 March 2022 | Published 13 April 2022

<http://zoobank.org/61624862-0A7B-41B4-8E5D-D20A5F5A338F>

Citation: Wang H, Meng F-M, Jin S-J, Gao J-W, Tong X-R, Liu Z-C (2022) A new species of medicinal leech in the genus *Hirudo* Linnaeus, 1758 (Hirudiniformes, Hirudinidae) from Tianjin City, China. ZooKeys 1095: 83–96. <https://doi.org/10.3897/zookeys.1095.74071>

Abstract

Medicinal leeches in the genus *Hirudo* have been utilized for therapeutic procedures for thousands of years. To date, six known species of *Hirudo* are widely distributed in different regions of the Eurasian continent. In this study, a new medicinal leech species *Hirudo tianjinensis* Liu, **sp. nov.** is described based upon specimens collected from Tianjin City, China. The new species can be distinguished from its congeners by a combination of characters: blackish green dorsum with five continuous yellow longitudinal stripes; six sensillae on dorsal annulus a2 of segments VIII–XXV; greyish green ventrum with irregular bilateral dark brown spots; dorsum and abdomen separated by a pair of pale yellow stripes; front half atrium wrapped by white prostate; apparent albumen gland; epididymis massive in relation to ejaculatory bulb. The phylogenetic tree based upon COI implies a sister relationship to *H. nipponia* Whitman, 1886. A key to the known species is provided.

Keywords

Blood-feeding leech, COI, molecular phylogeny, new species, taxonomy

* These authors contributed equally to this article.

Introduction

Leeches are carnivorous, hermaphroditic, and wormlike invertebrates with a sucker at each end of their bodies, belonging to the class Hirudinea of phylum Annelida. Approximately 650–680 leech species belonging to four subclasses, five orders, 13 families, and 149 genera have been nominated worldwide (Sawyer 1986; Sket and Trontelj 2008), of which 116 species are distributed in China. Natural habitats are predominantly fresh water and occasionally grassland, soil, or ocean water.

“Medicinal leech” is a common name referring to a group of aquatic blood-feeding ectoparasitic leech species traditionally employed for treating such a large variety of human diseases as amenorrhea, osteoarthritis, trauma, and blood stasis syndrome (Sig et al. 2017; Wang, et al. 2018). In the modern era, it also serves as important model systems for understanding the structure, function, development, regeneration, and repair of nervous systems (Herlin et al. 2017; Liu, et al. 2018). Most medicinal leech species belong to genus *Hirudo* of family Hirudinidae of which the most widely used are *H. medicinalis* Linnaeus, 1758 and *H. nipponia* Whitman, 1886 with wide distributions in the European Palearctic and Sino-Japanese regions, respectively. In addition, a few species belonging to genus *Poecilobdella* of family Hirudinidae e.g., *P. manillensis* (Lesson, 1842) and genus *Whitmania* of family Haemopidae e.g., *W. pigra* (Whitman, 1884) are also used as medicine in some East and Southeast Asian countries. The salient characteristics of *Hirudo* are as follows: the vagina bears a small caecum; there is no vaginal duct present; there are no/few salivary papillae; and there is no furrow on upper lip (Sawyer 1986). To date, six species of this genus have been described: *H. nipponia*, *H. medicinalis*, *H. verbena* Cerena, 1820, *H. orientalis* Utevsky, 2005, *H. troctina* Johnson, 1816, and *H. sulukii* Shain, 2016 (Utevsky and Trontelj 2005; Sağlam et al. 2016). Among these, *H. nipponia* is distributed in eastern Russia, China, Japan, and Mongolia while the other five species are endemic in Europe, North Africa, and western Asia.

As a well-known medicinal leech species, *H. nipponia* has been reported in China for many decades (Gee and Wu 1926). It is widely distributed in most areas of China except for Xinjiang and Tibet Autonomous Regions (Yang 1996). Reputed as an important traditional Chinese medicine, it has been recorded in Chinese Pharmacopoeia for the treatments of blood stasis, amenorrhea, edema, apoplexy, hemiplegia, and trauma (Committee 2020). In ancient folklore, medicinal leech therapy had been also widely applied for varicosity and arthrolithiasis by sucking blood from diseased sites using this leech species.

Located in North China, Tianjin City is one of the four major municipalities directly under the central Chinese government. It is one of the major areas producing medicinal leeches such as *H. nipponia* and *W. pigra* (Whitman, 1884) in China. In a recent collection, a total of 30 medicinal leech specimens differed significantly in morphology from the other *Hirudo* species collected from Tianjin City. These specimens represent a new species of *Hirudo*.

Materials and methods

Specimen sampling and morphological observation

On 19 August 2020, a total of 30 specimens described herein was captured in Caobai River, Haogezhuang Town, Baodi District, Tianjin City, China (39°36'40"N, 117°23'13"E). After relaxing in 15% ethanol, leeches were fixed with 95% ethanol for preservation, measurement, dissection, and molecular analysis. All type specimens (one holotype and 16 paratypes) were measured with a digital caliper with an accuracy of 0.1 mm. Six specimens were used for anatomical observation. The female and male reproductive systems were observed after dissecting along dorsal midline and fixing with insect needles on a wax tray. Jaws and teeth inside the anterior sucker were observed after cutting along the ventral midline of the anterior sucker. Morphological traits of the holotype specimen were observed and photographed by a stereomicroscopy with digital camera. To determine the taxonomy, seven specimens of the new species, two specimens of its sister species *H. nipponia* from Tianjin City (39°28'04"N, 117°28'48"E), and one specimen of the outgroup species *Haemadipsa yanyuanensis* Liu et Song, 1977 from Yunnan Province (26°02'35"N, 102°49'34"E) were utilized for molecular studies (Fig. 1). Voucher specimens were deposited at the Engineering Research Center for Exploitation & Utilization of Leech Resources in Universities of Yunnan Province, School of Agriculture & Life Sciences, Kunming University, Kunming.

DNA extraction, PCR, and DNA sequencing

Caudal suckers were removed with a scalpel and immediately ground to powder in liquid nitrogen. The objective of selecting caudal sucker tissue was to avoid contamination from the gut contents of DNA from unknown host blood and various microorganisms. According to the manufacturer's instructions, genomic DNA was extracted with Universal DNA kit (Mei5bio, China).

Mitochondrial cytochrome c oxidase subunit I (COI) fragments were amplified by polymerase chain reaction (PCR) with primers LCO 1490 and HCO 2198 (Folmer et al. 1994). PCR program was as follows: 2 min at 94 °C followed by 30 cycles of 30 s at 92 °C, 45s at 55 °C, 60 s at 72 °C, and a final extension step of 10 min at 72 °C. All PCR products were purified by elution from 1% agarose gel and then submitted to Qingke Biotech for bi-directional sequencing on an Applied Biosystems DNA sequencer (ABI 3730XL, USA).

Phylogenetic analyses

Prior to further analysis, DNA sequences generated here were deposited into the database of GenBank with the following accession numbers: MZ820656–MZ820659 for *H. tianjinensis*; MZ820661 and MZ820662 for its sister species *H. nipponia*;

MZ820660 for *Haemadipsa yanyuanensis* as outgroup. In addition, three sequences of *Whitmania* were also included here for its close relationship with *Hirudo*, which were reported in previous studies (Phillips and Siddall 2009; Nikitina et al. 2016). A total of 29 *Hirudo* COI sequences from GenBank were also downloaded for phylogenetic analysis (Table 1).

Table 1. Locality with geographic coordinates and GenBank accession numbers of specimens for phylogenetic analysis.

Species	Voucher ID	Locality	Coordinates	GenBank Acc. No.	References
<i>H. tianjinensis</i>	20200251	Tianjin, CN	39°36'40"N, 117°23'13"E	MZ820656	This study
	20200254				
	20200256				
	20200252	Tianjin, CN	39°36'40"N, 117°23'13"E	MZ820657	This study
	20200253				
<i>H. nipponia</i>	20200255	Tianjin, CN	39°36'40"N, 117°23'13"E	MZ820658	This study
	20200257	Tianjin, CN	39°36'40"N, 117°23'13"E	MZ820659	This study
	20200301	Tianjin, CN	39°28'04"N, 117°28'48"E	MZ820661	This study
<i>H. nipponia</i>	20200302	Tianjin, CN	39°28'04"N, 117°28'48"E	MZ820662	This study
		KR		AY763153	(Trontelj and Utevsky 2005)
		KR		AY425450	(Borda and Siddall 2004)
		KR		GQ368749	(Phillips and Siddall 2009)
		Halle, DE		AY763148	(Trontelj and Utevsky 2005)
<i>H. medicinalis</i>	SMNH111543	Gasavartar, SE	57°40'52"N, 18°35'35"E	HQ333519	(Kvist et al. 2010)
	HR20	Hrast, SI		EF446712	(Siddall et al. 2007)
		FR		EU100093	(Borda et al. 2008)
<i>H. orientalis</i>	COIH03	Saratov, RU	51°91'03"N, 47°34'90"E	KU672396	(Nikitina et al. 2016)
		Urmia, IR	37°32'51.09"N, 56°22'56.72"E	KY989464	(Darabi-Darestani et al. 2018)
		Agdam, AZ		AY763154	(Trontelj and Utevsky 2005)
		Samarkand, UZ		EF405599	(Utevsky et al. 2007)
		AZ		GQ368750	(Phillips and Siddall 2009)
<i>H. verbana</i>		Stavropol, RU	49°01'09"N, 43°48'21"E	KU672397	(Nikitina et al. 2016)
	HV3	Bursa, TR	40°10'23"N, 28°37'26"E	KU216244	(Saglam et al. 2016)
	HV19	Samsun, TR	41°34'48"N, 36°04'31"E	KT692947	(Saglam et al. 2016)
	H2P	Galicia, ES		MT797290	(Arias et al. 2021)
	17(1)	Kherson, UA		JN104644	(Trontelj and Utevsky 2012)
	13(1)	Izmir, TR		JN083804	(Trontelj and Utevsky 2012)
		Giessen, DE		EF125043	(Kutschera et al. 2007)
		Ohrid, MK		AY763150	(Trontelj and Utevsky 2005)
	KA46	Povir, SI		EF446701	(Siddall et al. 2007)
	<i>H. troctina</i>		Marrakech, MA		AY763155
HT56		Lebna Dam, TN		JQ364946	(Trontelj and Utevsky 2012)
H28b		AZ		GQ368751	(Phillips and Siddall 2009)
<i>H. sulukii</i>	HS1	Adiyaman, TR	37°59'35"N, 38°48'52"E	KU216239	(Saglam et al. 2016)
	HS2	Adiyaman, TR	37°59'35"N, 38°48'52"E	KU216240	(Saglam et al. 2016)
	HS5	Gaziantep, TR	37°18'12"N, 37°14'53"E	KU216241	(Saglam et al. 2016)
	HS6	Batman, TR	37°51'46"N, 41°01'00"E	KU216242	(Saglam et al. 2016)
	HS7	Batman, TR	37°51'46"N, 41°01'00"E	KU216243	(Saglam et al. 2016)
<i>W. acranulata</i>			NC023928		
<i>W. pigra</i>			MN729556		
<i>W. laevis</i>		Shaanxi, CN	32°43"N, 108°46"E	KM655839	(Ye et al. 2015)
<i>Haemadipsa yanyuanensis</i>	20200351	Yunnan, CN	26°02'35"N, 102°49'34"E	MZ820660	This study

*ISO country codes: AZ, Azerbaijan; CN, China; DE, Germany; ES, Spain; FR, France; IR, Iran; KR, Korea; MA, Morocco; MK, Former Yugoslav Republic of Macedonia; RU, Russia; SE, Sweden; SI, Slovenia; TN, Tunisia; TR, Turkey; UA, Ukraine, and UZ, Uzbekistan.

Sequences were aligned and edited using ClustalW implemented in MEGA7 (Kumar et al. 2016). The dataset of COI gene was used for phylogenetic tree construction using Maximum-Likelihood (ML) and Bayesian-Inference (BI) approaches with *Haemadipsa yanyuanensis* as the outgroup. ML analysis was conducted using 1000 ML bootstrap replications. BI analysis was performed in program MrBayes 3.2.6 with Markov chain Monte Carlo analysis (MCMC) in two parallel runs and with four chains each (Ronquist et al. 2012). Chain length was set as 1,500,000 generations and sampled every 1000 generations during calculations. Genetic divergences based upon the COI sequences were calculated for depicting evolutionary divergence between *Hirudo* species using uncorrected p-distances as implemented in MEGA 7 (Kumar et al. 2016).

Results

Taxonomy

Family Hirudinidae Whitman, 1886

Genus *Hirudo* Linnaeus, 1758

Hirudo tianjinensis Liu, sp. nov.

<http://zoobank.org/Fdf1eb12-A436-4e50-B15e-Dc0324773443>

Material examined. Holotype. 20200231; Engineering Research Center for Exploitation & Utilization of Leech Resources in Universities of Yunnan Province, School of Agriculture & Life Sciences, Kunming University, Kunming; Body length 31.2 mm, maximal body width 3.6 mm, width of anterior sucker 1.8 mm, width of posterior sucker 3.3 mm; Caobai River, Haogezhuang Town, Baodi District, Tianjin City, China; 39°36'40"N, 117°23'13"E, 5 m; collected by Zichao Liu, 19 Aug. 2020 (Figs 1, 2, 3). **Paratypes.** 16 ex.; collected information same as holotype; 20200232–20200247, Engineering Research Center for Exploitation & Utilization of Leech Resources in Universities of Yunnan Province, School of Agriculture & Life Sciences, Kunming University, Kunming.

Diagnosis. *Hirudo tianjinensis* can be distinguished from its congeners by the following combination of characters: blackish green dorsum with five continuous yellow longitudinal stripes; six sensillae on dorsal annulus a2 of segments VIII–XXV making dorsal golden midline notched, and two lateral blackish green dorsal line rosary; greyish green ventrum with irregular dark brown spots bilaterally; dorsum and abdomen separated by a pair of pale yellow stripes; front half of atrium wrapped by white prostate; apparent albumen gland; epididymis massive in relation to ejaculatory bulb.

Description. Blood-feeding aquatic leech, medium body size, length 34.8 ± 3.5 mm ($n = 17$), maximum body width 3.7 ± 0.4 mm, width of anterior sucker 1.8 ± 0.2 mm, width of caudal sucker 3.6 ± 0.4 mm. Caudal sucker diameter slightly narrower than maximal body breadth.

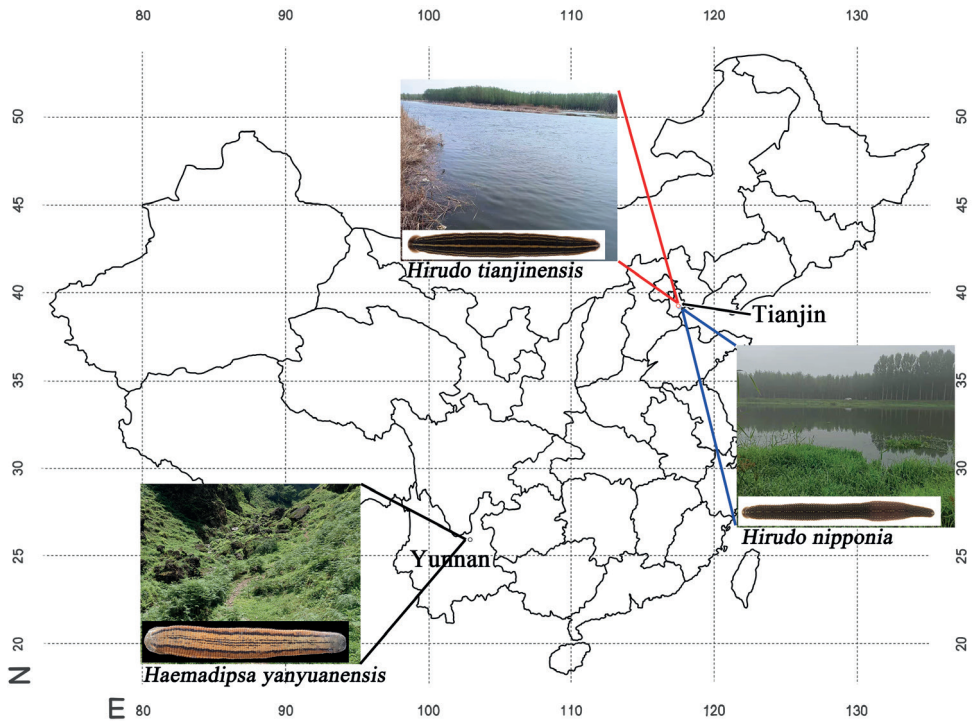


Figure 1. Map of geographic collecting locations for three species of Chinese leeches. *H. tianjinensis* and *H. nipponia* were collected in adjacent areas of Tianjin City, and *Haemadipsa yanyuanensis* was collected in Yunnan Province.

In relaxed state, dorsum and abdomen flat and willow-leaf like. Blackish green dorsum with five continuous yellow stripes. Dorsal midline widest, extending from the first to the last somite. Yellow stripes separate dorsum into six blackish green longitudinal stripes of which the middle two are the widest and the lateral four are narrower. Six sensillae on middle a2 of segments VIII–XXV making middle golden stripe notched and two lateral blackish green stripes rosary. Venter greyish green with irregular dark brown spots bilaterally edged by a pair of pale yellow stripes. No visible sensillae in abdomen. Caudal sucker reddish brown, with dark dorsum and pale-colored abdomen.

Complete somite five-annulate, numbers of annuli per somite: I–III: one, IV–V: two, VI–VII: three, VIII: four, IX–XXIII: five (b1, b2, a2, b5, b6), XXIV: four, XXV: three, XXVI–XXVII: two, in total: 27 somites and 103 annuli.

Wide mouth in white anterior sucker. Jaws trignathous, one in the middle and one on each side, 55–67 horny teeth in each jaw. Five pairs of eyes almost circular or irregular shaped on annulus 2, 3, 4, 6, and 9. Fifth pair of eyes smallest and sometimes difficult to observe. Two nephridiopores in submarginal annulus b2 of each complete somite. Gonopores situated in furrow between annuli, separated by five annuli, male pore in furrow XI b5/b6 (annulus 31/32), female pore in furrow XII b5/b6 (annulus 35/36). Anus in middle dorsum between the last two annuli.

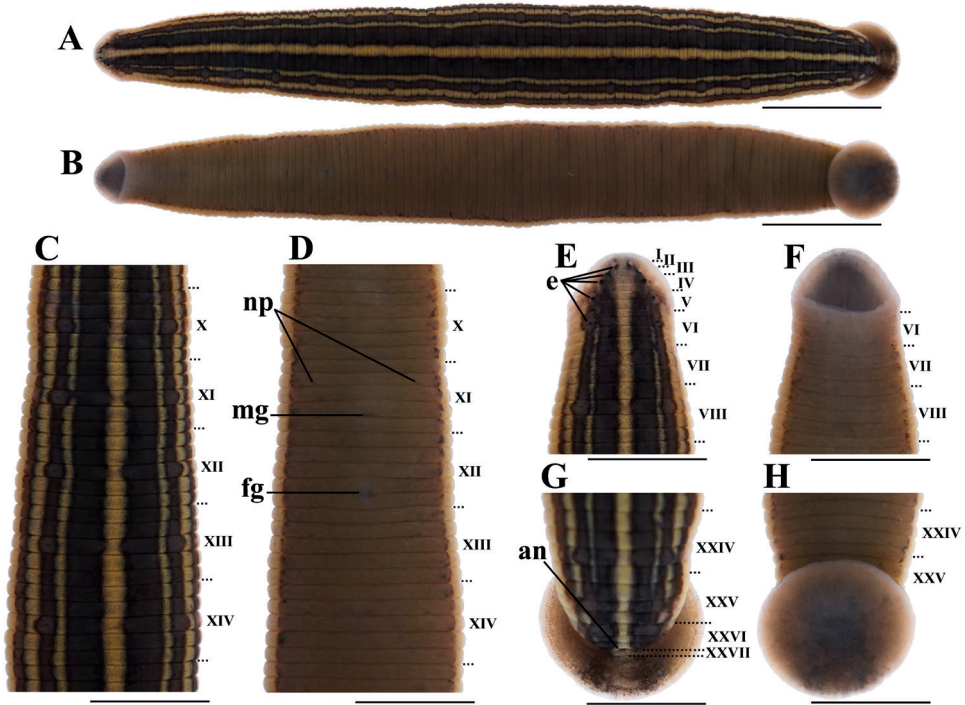


Figure 2. External morphology of *H. tianjinensis* holotype **A** dorsal and **B** ventral view of whole body **C** dorsal and **D** ventral view of somites X–XIV **E** dorsal and **F** ventral view of somites I–VIII **G** dorsal and **H** ventral view of somites XXIV–XXVII and caudal sucker. Abbreviations: an, anus; e, eye; fg, female gomopore; mg, male gomopore; np, nephridiopores. Scale bars: 5 mm (**A**, **B**), 2.5 mm (**C–H**).

Male reproductive system: pyriform atrium large, located at venter of ganglion in segment XI; prostate white and developed, covering front half of atrium, strikingly different from its sister species *H. nipponia* whose prostate is almost invisible; penis sheath with a duct bent anteriorly in segment XI; epididymis massive in relation to ejaculatory bulb, tightly packed masses of ducting standing upright on either atrial side; ejaculatory bulb tapering sharply and connected to dorsal epididymis; testisacs ovoid, 11 pairs, in segments XIII–XXIII.

Female reproductive system: composed usually of one vagina, two ovisacs, and a curved duct in segments XII–XIII; vagina long, upright, and ellipsoidal with apparent albumen gland on middle surface, no vaginal duct; ovisacs ovoid, smaller than testisacs, connected to vagina via a curved common oviduct.

Remarks. This species is frequently confused with *H. nipponia* due to their morphological similarities and overlapping distributions. Local villagers often mistook it for *H. nipponia* for therapeutic usage. However, they can be distinguished using a series of morphological characteristics such as color pattern, number of sensillae, and reproductive system morphology (Table 2).

Etymology. The specific name *tianjinensis* is derived from Tianjin City, a municipality directly under the central government in China, where type specimens were collected.

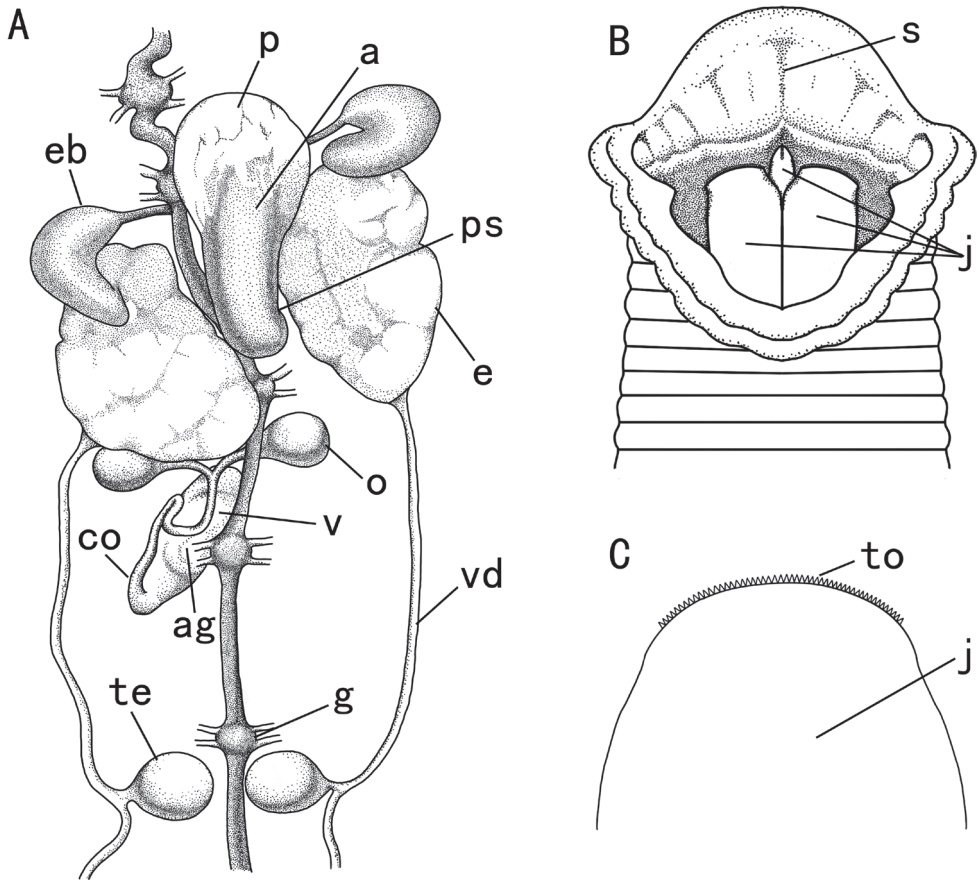


Figure 3. Internal characters of *H. tianjinensis* **A** dorsal view of reproductive system **B** ventral view of dissected anterior sucker **C** ventral view of jaw. Abbreviations: a, atrium; ag, albumen gland; co, common oviduct; e, epididymis; eb, ejaculatory bulb; g, ganglion; j, jaw; o, ovisac; p, prostate; ps, penis sheath; s, sulcus; te, testis; to, tooth; v, vagina; vd, vas deferens.

Table 2. Morphological comparison between *H. tianjinensis* and *H. nipponia*.

Traits	<i>H. tianjinensis</i>	<i>H. nipponia</i>
Sensillae	six sensillae in dorsum, absent in abdomen	six sensillae both in dorsum and abdomen
Stripes on dorsal surface	five yellow continuous longitudinal stripes	five yellow dotted longitudinal stripes, yellow spots on a2 weak or absent
Prostate	developed, wrapping front-half of atrium	absent
Ejaculatory bulb	tapering sharply	tapering gradually

Distribution. *Hirudo tianjinensis* was collected from Caobai River, Haogezhuang Town, Baodi District, Tianjin City, China, which flows into Bohai Sea. Water was moderately polluted. Aquatic plants and irregular pumice stones were abundant along the riverbed. This species normally hid under pumice stones. Whenever people and animals pass by, it quickly adsorbs on their ankles for sucking blood.

Molecular phylogeny and genetic divergence

Phylogenetic analysis was performed based upon available COI sequences of *Hirudo* from NCBI. Generally, sequences of each species were all well clustered. The results of ML and BI trees were largely similar to each other with the exception of *H. sulukii*. The newly reported species *H. tianjinensis* was clustered with *H. nipponia* and species of *Whitmania* and formed a single branch separated from the other species. This result was consistent with previous phylogenetic analysis on *Hirudo* and revealed the *Hirudo* a paraphyletic group (Fig. 4) (see also Phillips and Siddall 2009; Ye et al. 2015; Nikitina et al. 2016).

The average genetic divergence based upon uncorrected p-distances was also performed. In general, the distance of intra-species was < 1.5% except for sequences of *H. verbana* (range 0.2% to 6.4%). The intraspecific distance of the new species *H. tianjinensis* ranged from 0.2% to 0.9%. And the interspecific distance between *H. tianjinensis* and *H. nipponia* was 16.7% (Table 3).

Table 3. Interspecific genetic divergence between seven *Hirudo* species and intraspecific difference within each species based upon analyses of their COI sequences (uncorrected p-distance: %±SD).

Species	Intraspecific range & SD		Interspecific mean ±SD				
<i>H. tianjinensis</i>	0.2–0.9±0.2						
<i>H. nipponia</i>	0–0.6±0.4	16.7±0.2					
<i>H. medicinalis</i>	0–0.6±0.2	18.1±0.2	19.3±0.2				
<i>H. orientalis</i>	0–0.2±0.1	16.5±0.1	20.7±0.0	8±0.2			
<i>H. verbana</i>	0.2–6.4±2	19.3±0.6	19.3±0.5	9.3±0.5	8.7±0.4		
<i>H. troctina</i>	0–0.9±0.5	17.7±0.2	18.5±0.1	8.9±0.1	8.7±0.1	9.5±0.5	
<i>H. sulukii</i>	0–1.5±0.6	17.2±0.2	19.6±0.5	9.6±0.4	10.6±0.3	11.3±0.4	11.3±0.3

A key to the seven species of *Hirudo*

- 1 Dorsum with five longitudinal yellow or greenish yellow stripes 2
- Dorsum with two or four reddish or orange stripes 3
- 2 Dorsum with five continuous yellow or greenish yellow stripes; prostate apparent ***H. tianjinensis* sp. nov.**
- Dorsum with five yellow dotted stripes; prostate absent ***H. nipponia***
- 3 Epidimymis massive in relation to ejaculatory bulb 4
- Epidimymis small/medium-sized in relation to ejaculatory bulb 6
- 4 Vagina terminally folded ***H. medicinalis***
- Vagina long and upright 5
- 5 Dorsum green, two orange paramedian stripes thin; venter black, irregularly arranged and sized black markings ***H. troctina***
- Dorsum olive green, two orange paramedian stripes thick; venter pale greenish, and covered with small number of irregular black markings... ***H. sulukii***
- 6 Dorsum with broad, pale orange diffuse paramedian stripes; vagina sharply folded; epidimymis small, not much larger than ejaculatory bulb ... ***H. verbana***
- Dorsum with thin, deep orange colored paramedian stripes; vagina evenly curved; epidimymis medium-sized, somewhat larger than ejaculatory bulb.....
..... ***H. orientalis***

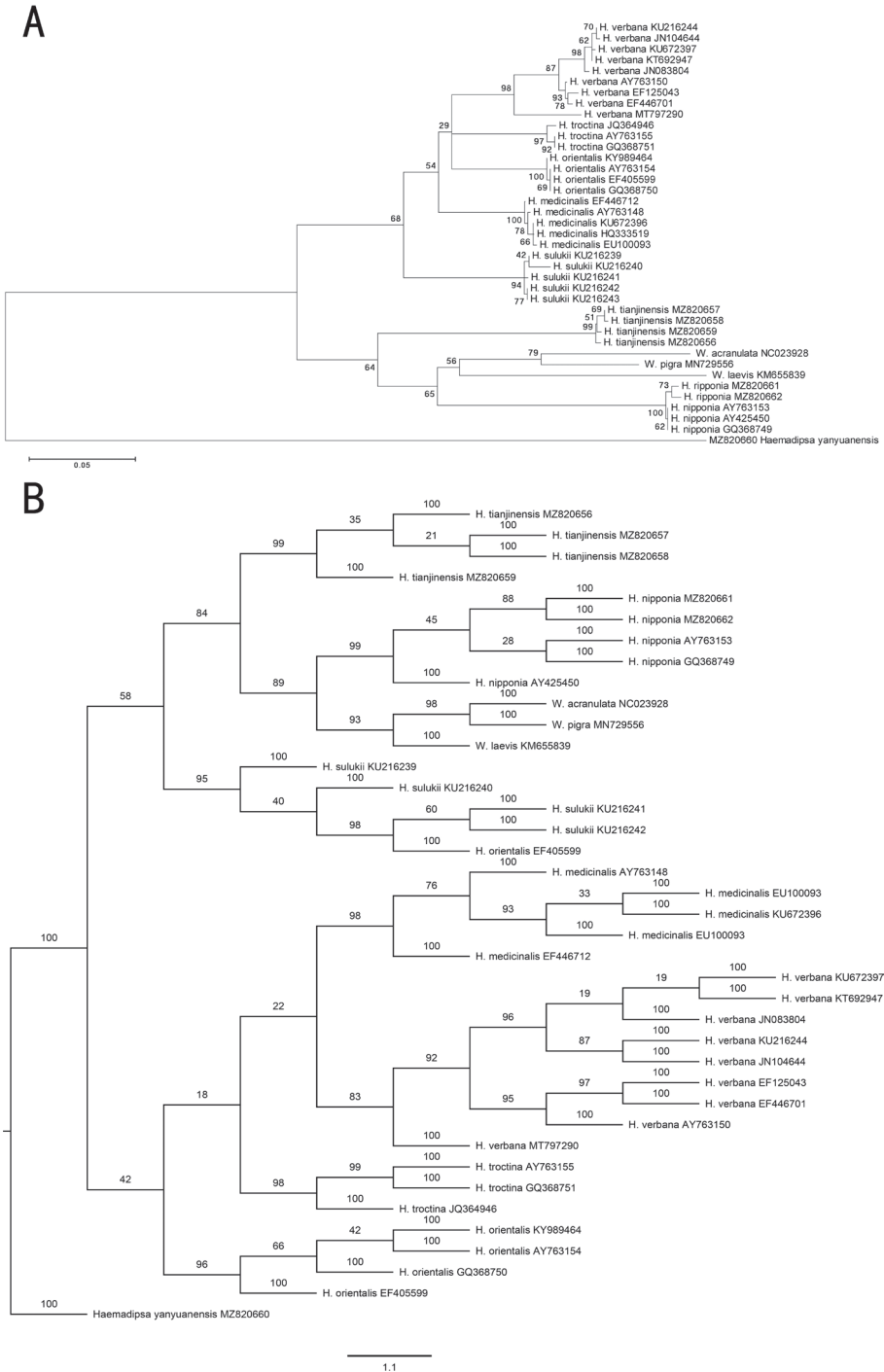


Figure 4. Phylogenetic analysis of *H. tianjinensis* with other species of *Hirudo* **A** maximum-likelihood tree was constructed using MEGA 7 with 1000 ML bootstrap replications **B** bayesian inference tree was constructed using MrBayes with four Markov chains. Chain length was set as 1,500,000 generations and sampled every 1000 generations.

Discussion

Six species of *Hirudo* have been identified globally. Except *H. nipponia*, the other five species are distributed in Europe and the Middle East, usually referred to as the European leeches. Their diagnostic features and species differences were described in detail (Utevsky and Trontelj 2005; Saglam 2019). The results of molecular taxonomy showed that they are closely correlated. *Hirudo nipponia* is easily distinguished from the remaining five species in morphology, because the former is obviously smaller and has five longitudinal stripes in dorsum. *Hirudo nipponia* is mainly distributed in East Asia, including Japan, Mongolia, the Russian Far East, and most of China.

Hirudo tianjinensis has been collected from Tianjin City, a northern Chinese metropolis. It belongs to *Hirudo* based upon a series of morphological characteristics (Sawyer 1986). The detailed morphological comparison between *H. tianjinensis* and *H. nipponia* were obtained by combining specimen observation and previous descriptions (Whitman 1886; Lai and Chen 2010). *Hirudo tianjinensis* is similar to *H. nipponia* in morphology but with some distinct differences in color pattern and reproductive system morphology (Table 2). When they were cultured together, *H. tianjinensis* often sucked on the blood of *H. nipponia* while the latter never sucked that of the former. The results of molecular taxonomy showed that *H. tianjinensis* is a sister species to *H. nipponia*. In geographical distribution, *H. tianjinensis* and *H. nipponia* partially overlap. *Hirudo nipponia* is found in the whole distribution area of *H. tianjinensis*, indicating that there is probably a common origin between the two species.

Although most medical leeches can bite people, causing continuous bleeding, inflammation, itching, and even bacterial infection, the major reason for attracting people's attention lies in their important medical values. In China, medicinal application of leeches was first recorded in Shennong's Herbal Classic 2,000 years ago. In the modern era, Chinese Pharmacopoeia recommends three leech species, *H. nipponia*, *W. pigra*, and *W. acranulata* (Whitman, 1886) for treating arthritis, stroke, myocardial infarction, and amenorrhea (Committee 2020). *Hirudo nipponia* is the most widely utilized medicinal leech species with the strongest antithrombin activity compared with the other two medicinal leech species listed in Chinese Pharmacopoeia. Nearly 2,000 tons of leeches are freeze-dried for medicinal uses with an annual value of 1.4 billion US dollars. Due to the importance in medicine, wild-type *H. nipponia* have been overly harvested, and thus become somewhat endangered. For the purposes of sustainable utilization of medical leech resources and species protection, it is imperative to study the medical leech.

The medical leech has important clinical applications since it contains many of bioactive components with the functions of anticoagulant, thrombolytic, matrix degradation analgesic, and anti-inflammatory, such as hirudin, antistasin, and hyaluronidase (Sig et al. 2017; Kwak et al. 2019; Muller et al. 2020). More than 20 molecules and their mechanistic modes have been identified, and more unique active ingredients of leeches await discovery.

Although the medical leech has important medical value, its taxonomic research is rather behind. Traditional practitioners tend to refer to *H. nipponia* and *H. tianjinensis*

as the linear and dotted leeches respectively in Tianjin City. In this work, *H. tianjinensis* is formally named as a new species and its medical value needs to be further studied in the future.

Acknowledgments

This work was supported by the grants from National Natural Science Foundation of China (31360516), Joint Special Project of Universities in Yunnan Province (2017FH001-004), Yunnan Provincial Training Program of Youth Leaders in Academic & Technical Reserve Talent (2018HB101), and Yunnan Provincial Ten Thousand People Plan.

References

- Arias A, Surugiu V, Carballeira R, Popa OP, Popa LO, Utevsky S (2021) Unravelling the extent of diversity within the Iberian medicinal leeches (Hirudinea: Hirudo) using molecules and morphology. *Biology (Basel)* 10(4): e315. <https://doi.org/10.3390/biology10040315>
- Borda E, Siddall ME (2004) Arhynchobdellida (Annelida: Oligochaeta: Hirudinida): phylogenetic relationships and evolution. *Molecular Phylogenetics and Evolution* 30(1): 213–225. <https://doi.org/10.1016/j.ympev.2003.09.002>
- Borda E, Ocegüera-Figueroa A, Siddall ME (2008) On the classification, evolution and biogeography of terrestrial haemadipsoid leeches (Hirudinida: Arhynchobdellida: Hirudiniformes). *Molecular Phylogenetics and Evolution* 46(1): 142–154. <https://doi.org/10.1016/j.ympev.2007.09.006>
- Committee NP (2020) Pharmacopoeia of the People's Republic of China. Medicine Science and Technology Press, Beijing, 85–86.
- Darabi-Darestani K, Sari A, Sarafrazi A, Utevsky S (2018) Entrapped by the uneven central and Middle Eastern terrains: Genetic status of populations of *Hirudo orientalis* (Annelida, Clitellata, Hirudinida) with a phylogenetic review of the genus *Hirudo*. *Molecular Phylogenetics and Evolution* 121: 52–60. <https://doi.org/10.1016/j.ympev.2017.12.024>
- Folmer O, Black M, Hoeh W, Lutz R, Vrijenhoek R (1994) DNA primers for amplification of mitochondrial cytochrome c oxidase subunit I from diverse metazoan invertebrates. *Molecular Marine Biology and Biotechnology* 3(5): 294–299. [Retrieved from] <https://www.ncbi.nlm.nih.gov/pubmed/7881515>
- Gee NG, Wu CF (1926) A list of some Chinese leeches. *The China Journal of Science and Arts* 4(1): 43–45.
- Herlin C, Bertheuil N, Bekara F, Boissiere F, Sinna R, Chaput B (2017) Leech therapy in flap salvage: Systematic review and practical recommendations. *Annales de Chirurgie Plastique et Esthétique* 62(2): e1–e13. <https://doi.org/10.1016/j.anplas.2016.06.004>
- Kumar S, Stecher G, Tamura K (2016) MEGA7: Molecular evolutionary genetics analysis version 7.0 for bigger datasets. *Molecular Biology and Evolution* 33(7): 1870–1874. <https://doi.org/10.1093/molbev/msw054>

- Kutschera U, Pfeiffer I, Ebermann E (2007) The European land leech: Biology and DNA-based taxonomy of a rare species that is threatened by climate warming. *Naturwissenschaften* 94(12): 967–974. <https://doi.org/10.1007/s00114-007-0278-3>
- Kvist S, Oceguera-Figueroa A, Siddall ME, Erseus C (2010) Barcoding, types and the *Hirudo* files: Using information content to critically evaluate the identity of DNA barcodes. *Mitochondrial DNA* 21(6): 198–205. <https://doi.org/10.3109/19401736.2010.529905>
- Kwak HJ, Park JS, Medina Jimenez BI, Park SC, Cho SJ (2019) Spatiotemporal expression of anticoagulation factor Antistasin in freshwater leeches. *International Journal of Molecular Sciences* 20(16): e3994. <https://doi.org/10.3390/ijms20163994>
- Lai YT, Chen JH (2010) *Leech fauna of Taiwan*. National Taiwan University Press, Taipei, 118 pp.
- Liu Z, Wang Y, Tong X, Su Y, Yang L, Wang D, Zhao Y (2018) De novo assembly and comparative transcriptome characterization of *Poecilobdella javanica* provide insight into blood feeding of medicinal leeches. *Molecular Omics* 14(5): 352–361. <https://doi.org/10.1039/C8MO00098K>
- Muller C, Lukas P, Bohmert M, Hildebrandt JP (2020) Hirudin or hirudin-like factor - that is the question: Insights from the analyses of natural and synthetic HLF variants. *FEBS Letters* 594(5): 841–850. <https://doi.org/10.1002/1873-3468.13683>
- Nikitina A, Babenko V, Akopian T, Shirokov D, Manuvera V, Kurdyumov A, Kostryukova E, Lazarev V (2016) Draft mitochondrial genomes of *Hirudo medicinalis* and *Hirudo verbana* (Annelida, Hirudinea). *Mitochondrial DNA. Part B, Resources* 1(1): 254–256. <https://doi.org/10.1080/23802359.2016.1157774>
- Phillips AJ, Siddall ME (2009) Poly-paraphyly of Hirudinidae: Many lineages of medicinal leeches. *BMC Evolutionary Biology* 9(1): e246. <https://doi.org/10.1186/1471-2148-9-246>
- Ronquist F, Teslenko M, van der Mark P, Ayres DL, Darling A, Höhna S, Larget B, Liu L, Suchard MA, Huelsenbeck JP (2012) MrBayes 3.2: Efficient Bayesian phylogenetic inference and model choice across a large model space. *Systematic Biology* 61(3): 539–542. <https://doi.org/10.1093/sysbio/sys029>
- Saglam N (2019) Internal and external morphological characteristics of the medicinal leech species *Hirudo sulukii* and *Hirudo verbana*. *Turkiye Parazitoloji Dergisi* 43(4): 204–209. <https://doi.org/10.4274/tpd.galenos.2019.6422>
- Saglam N, Saunders R, Lang SA, Shain DH (2016) A new species of *Hirudo* (Annelida: Hirudinidae): historical biogeography of Eurasian medicinal leeches. *BMC Zoology* 1(5): 1–12. <https://doi.org/10.1186/s40850-016-0002-x>
- Sawyer RT (1986) *Leech biology and behaviour*. Clarendon press, Oxford, 1065 pp.
- Siddall ME, Trontelj P, Utevsky SY, Nkamany M, Macdonald III KS (2007) Diverse molecular data demonstrate that commercially available medicinal leeches are not *Hirudo medicinalis*. *Proceedings. Biological Sciences* 274(1617): 1481–1487. <https://doi.org/10.1098/rspb.2007.0248>
- Sig AK, Guney M, Guclu AU, Ozmen E (2017) Medicinal leech therapy-an overall perspective. *Integrative Medicine Research* 6(4): 337–343. <https://doi.org/10.1016/j.imr.2017.08.001>
- Sket B, Trontelj P (2008) Global diversity of leeches (Hirudinea) in freshwater. *Hydrobiologia* 595(1): 129–137. <https://doi.org/10.1007/s10750-007-9010-8>

- Trontelj P, Utevsky SY (2005) Celebrity with a neglected taxonomy: Molecular systematics of the medicinal leech (genus *Hirudo*). *Molecular Phylogenetics and Evolution* 34(3): 616–624. <https://doi.org/10.1016/j.ympev.2004.10.012>
- Trontelj P, Utevsky SY (2012) Phylogeny and phylogeography of medicinal leeches (genus *Hirudo*): Fast dispersal and shallow genetic structure. *Molecular Phylogenetics and Evolution* 63(2): 475–485. <https://doi.org/10.1016/j.ympev.2012.01.022>
- Utevsky SY, Trontelj P (2005) A new species of the medicinal leech (Oligochaeta, Hirudinida, *Hirudo*) from Transcaucasia and an identification key for the genus *Hirudo*. *Parasitology Research* 98(1): 61–66. <https://doi.org/10.1007/s00436-005-0017-7>
- Utevsky SY, Schiaparelli S, Trontelj P (2007) Molecular phylogeny of pontobdelline leeches and their place in the descent of fish leeches (Hirudinea, Piscicolidae). *Zoologica Scripta* 36(3): 271–280. <https://doi.org/10.1111/j.1463-6409.2007.00279.x>
- Wang H, Zhang J, Chen L (2018) The efficacy and safety of medical leech therapy for osteoarthritis of the knee: A meta-analysis of randomized controlled trials. *International Journal of Surgery* 54: 53–61. <https://doi.org/10.1016/j.ijso.2018.04.035>
- Whitman CO (1886) The leeches of Japan. *The Quarterly Journal of Microscopical Science* 26: 317–416. [New Series] <https://doi.org/10.1242/jcs.s2-26.103.317>
- Yang T (1996) *Fauna Sinica, Annelida: Hirudinea*. Science Press, Beijing, 259 pp.
- Ye F, Liu T, Zhu WB, You P (2015) Complete mitochondrial genome of *Whitmania laevis* (Annelida, Hirudinea) and comparative analyses within *Whitmania* mitochondrial genomes. *Belgian Journal of Zoology* 145(2): 114–128. <https://doi.org/10.26496/bjz.2015.52>

Descriptions of two new Idiocerini leafhoppers of the genus *Idioscopus* (Hemiptera, Cicadellidae) from China

Xian-Yi Wang¹, Jia-Jia Wang¹, Ren-Huai Dai¹, Mick D. Webb²

1 Institute of Entomology, Guizhou University; The Provincial Key Laboratory for Agricultural Pest Management Mountainous Region, Guiyang, Guizhou 550025, China **2** Department of Life Sciences (Entomology), The Natural History Museum, Cromwell Road, SW7 5BD, London, UK

Corresponding authors: Ren-Huai Dai (dmolbio@126.com), Mick D. Webb (mdwebb04@gmail.com)

Academic editor: C. H. Dietrich | Received 19 October 2021 | Accepted 25 March 2022 | Published 13 April 2022

<http://zoobank.org/1FA86EE8-B0E4-4797-9AB2-662BE6336D15>

Citation: Wang X-Y, Wang J-J, Dai R-H, Webb MD (2022) Descriptions of two new Idiocerini leafhoppers of the genus *Idioscopus* (Hemiptera, Cicadellidae) from China. ZooKeys 1095: 97–110. <https://doi.org/10.3897/zookeys.1095.76731>

Abstract

Two new species of the leafhopper genus *Idioscopus* Baker are described from China: *Idioscopus bihamulus* **sp. nov.** and *I. ventrispinus* **sp. nov.**, the latter recorded on a species of *Myrica* L. (Myricaceae) as its host plant. A key and checklist to species of the genus from China are provided and *Idioscopus taiwanus* Huang & Maldonado-Capriles, 1992 is placed as a junior synonym of *Idioscopus clypealis* (Lethierry, 1889), **syn. nov.**

Keywords

Checklist, *Myrica*, taxonomy

Introduction

The leafhopper genus *Idioscopus* was described by Baker, 1915, with *I. clypealis* (Lethierry, 1889) as its type species. Subsequently, many new species of the genus were described by Pruthi (1936), Maldonado-Capriles (1964, 1974), Viraktamath (1976, 1979a, 1979b), Kuoh and Fang (1985), Huang and Maldonado Capriles (1992), and Wang and Dai (2018). Xue et al. (2017) and Wang and Dai (2018) provided keys as

well as checklists to Chinese Idiocerinae, including the genus *Idioscopus*. Many species of *Idioscopus* are important agricultural and forest pests; their known hosts are mainly *Mangifera* spp. (Anacardiaceae), *Dimocarpus* sp. (Sapindaceae), *Prunus* sp. (Rosaceae), and *Myrica* sp. (Viraktamath 1989; Khatri and Webb 2014; Wang and Dai 2018). At present, *Idioscopus* comprises more than 30 species of which 10 species are recorded from China (see Checklist). Another species recorded from China by Zhang and Li (2012: 208, pl. 7), i.e., *Idioscopus bimaculatus* (Pruthi, 1936) is misidentified (C. Viraktamath pers. comm.). In this paper, we describe and illustrate two new species of *Idioscopus* from Yunnan Province, China, and provide a revised key and checklist to species from China. In addition, *Idioscopus taiwanus* Huang & Maldonado-Capriles, 1992 is placed as a junior synonym of *Idioscopus clypealis* (Lethierry, 1889), syn. nov., and the identities of two other Idiocerinae from Taiwan, i.e., *Idiocerus apicalis* Matsumura and *I. formosanus* Matsumura are discussed and photographs of the habitus of their types taken by Masami Hayashi in 1995 are provided.

Materials and methods

The specimens examined were collected from Yunnan Province, China, using a sweep net. Techniques for the preparation of the genital structures follow Oman (1949) and morphological terminology mainly follows Dietrich (2005). All specimens examined are deposited in the Institute of Entomology, Guizhou University, Guiyang, China (GUGC) and The Natural History Museum, Department of Life Sciences (Entomology), Cromwell Road, SW7 5BD, London, UK.

Taxonomy

Genus *Idioscopus* Baker, 1915

Type species. *Idiocerus clypealis* Lethierry, 1889 by original designation.

Diagnosis. The genus *Idioscopus* can be distinguished from other genera of Idiocerini by the combination of the following features: style with slender setae on dorsal margin, subapex wide and flat on later on lateral view, aedeagal shaft with one or two pairs of processes.

Description. Body small (♂ 3.10–5.50 mm; ♀ 3.30–5.50 mm). Head wider than pronotum. Head and thorax shagreen or crown and frontoclypeus dorsad of ocelli finely transversely rugose. Face as long as wide to slightly longer than wide; frontoclypeus with lateral margins extending to just above antennae; anteclypeus broad distally, longer than wide, sometimes exceeding apex of gena; rostrum in some species variably expanded apically; ocelli placed closer to midline than to the corresponding eye. Length of visible mesonotum nearly as long or longer than pronotum and crown together. Forewing with four apical and usually two (open or closed) subapical cells. Hind femur with 2 + 1 apical setae.

Male genitalia. Male pygofer in lateral view triangular its height more than its width; dorsoposterior lobe differentiated by dorsoanterior vertical cleft; dorsal anal collar present joined to pygofer; anal tube comprising a single segment, short or long; with or without a basiventral process. Subgenital plate elongate, curved dorsad, with long hair-like marginal setae. Connective Y- or T-shaped, short. Style elongate, apophysis curved dorsally, inner margin crenulate or dentate, outer margin distally with a row of hair-like setae or with a tuft of stout setae. Aedeagus with shaft elongate, either slightly curved dorsally or sinuate, laterally compressed, with one or two pairs of apical processes, gonopore apical on ventral surface; dorsal apodeme well developed, apically expanded laterally.

Distribution. African, Oriental, and Palearctic regions.

Checklist of *Idioscopus* species from China

(See Xue et al. 2017 for complete synonymy)

I. bihamulus sp. nov.

I. clypealis (Lethierry, 1889: 252, *Idiocerus*)

I. taiwanus Huang & Maldonado-Capriles, 1992: 5–6, syn. nov.

I. furcaprocessus Wang, Wang, Zhou & Dai, 2021: 376, fig. 1

I. longiprocessus Wang, Wang, Zhou & Dai, 2021: 378, fig. 2

I. myrica Wang & Dai, 2018: 12–13, figs 1–10

I. nitellicus Kuoh & Fang, 1985: 190, figs 8–16

I. nitidulus (Walker, 1869: 322, *Iassus*)

Idiocerus niveosparsus Lethierry, 1889: 160; Matsumura, 1912: 322 (Taiwan)

I. recurvatus Kuoh & Fang, 1985: 189, figs 1–7

I. serratastylus Wang, Wang, Zhou & Dai, 2021: 378, fig. 3

I. ventrispinus sp. nov.

Key to the species of *Idioscopus* from China

- | | | |
|---|---|---------------------------------|
| 1 | Forewing with yellow patch on clavus (Fig. 2A) | 2 |
| – | Forewing without yellow patch on clavus..... | 4 |
| 2 | Aedeagus with a pair of subapical processes and a single ventral process (Fig. 2H) | <i>I. ventrispinus</i> sp. nov. |
| – | Aedeagus with a pair of subapical processes, without a single ventral process | 3 |
| 3 | Aedeagus with processes directed laterally | <i>I. furcaprocessa</i> |
| – | Aedeagus with processes directed ventrally | <i>I. serratastylus</i> |
| 4 | Clypellus dark brown..... | <i>I. clypealis</i> |
| – | Clypellus not dark brown | 5 |
| 5 | Aedeagus with a single pair of apical processes and a single dorsal subapical process | <i>I. myrica</i> |
| – | Aedeagus with one or two pair of subapical processes, without a single dorsal process | 6 |

6	Aedeagus with one pair of distal processes.....	7
–	Aedeagus with two pair of distal processes.....	8
7	Aedeagus with processes strongly curved (Fig. 1H, I).....	
	<i>I. biamulus</i> sp. nov.
–	Aedeagus with processes weakly curved.....	<i>I. longiprocessus</i>
8	Aedeagus with shaft evenly curved in lateral view.....	<i>I. nitidulus</i>
–	Aedeagus with shaft sinuate in lateral view.....	9
9	Aedeagus with one very long and one short subapical processes	
	<i>I. nitellicus</i>
–	Aedeagus with two pair of moderately long subapical processes	
	<i>I. recurvatus</i>

***Idioscopus biamulus* sp. nov.**

<http://zoobank.org/8049B242-A15D-408D-8E57-C3F95F0856D8>

Figs 1, 3 A–D

Type material. *Holotype*: ♂, Baoshan City, Mt Gaoligongshan, Yunnan Province, China (98°47'42"E, 25°18'20"N; 1745 m elev.), 4 August 2018, coll. Zhou Yu (GUGC).

Paratypes: 1♂, 6♀♀, same data as holotype.

Diagnosis. The new species can be distinguished from other *Idioscopus* species by the combination of the following features: anal tube short; style apophysis with a row of three or four subapical teeth along inner margin; aedeagal shaft with long, recurved, hook-like apical processes.

Description. *Coloration.* Ground coloration translucent brown. Vertex pale brown with two round spots close to the adjacent eyes (Fig. 1A). Eyes and ocelli brown (Fig. 1A–C). Face (Fig. 1B, C) yellowish white, narrow area along inner margin of eye, area surrounding bases of antennae, and inner margins of gena along frontal suture black, upper area with dark brown semicircular marking. Pronotum (Fig. 1A) yellowish brown along anterior margin, posterior two-thirds brown, with a brown U-shaped band medially. Mesosternum (Fig. 1A) black, mesepimeron with black spot. Mesonotum (Fig. 1A) yellow with pair of triangular, laterobasal, black maculae. Forewing with veins brown (Fig. 1A).

External features as in generic description with face and pronotum shagreen and crown finely transversely rugose. Male antennae without apical disc. Forewing (Fig. 1D) with two subapical cells; inner subapical open.

Male genitalia. Male pygofer (Fig. 1E, F) without ventral process; anal collar thin with apex upturned; anterodorsal apodemes well developed. Anal tube (Fig. 1E) short. Subgenital plates (Fig. 1E) of uniform width, with reduced hair-like marginal setae. Connective (Fig. 1G) T-shaped, with stem narrow. Style apophysis (Fig. 1G) with a row of three or four tooth-like projections along inner margin subapically, outer margin with macrosetae in distal one-third. Aedeagus (Fig. 1H, I) with shaft laterally compressed, with pair of long, recurved, hook-like processes subapically from ventral margin, acute apically; basal apodeme pillar-like in lateral view, distally and laterally expanded in ventral view.

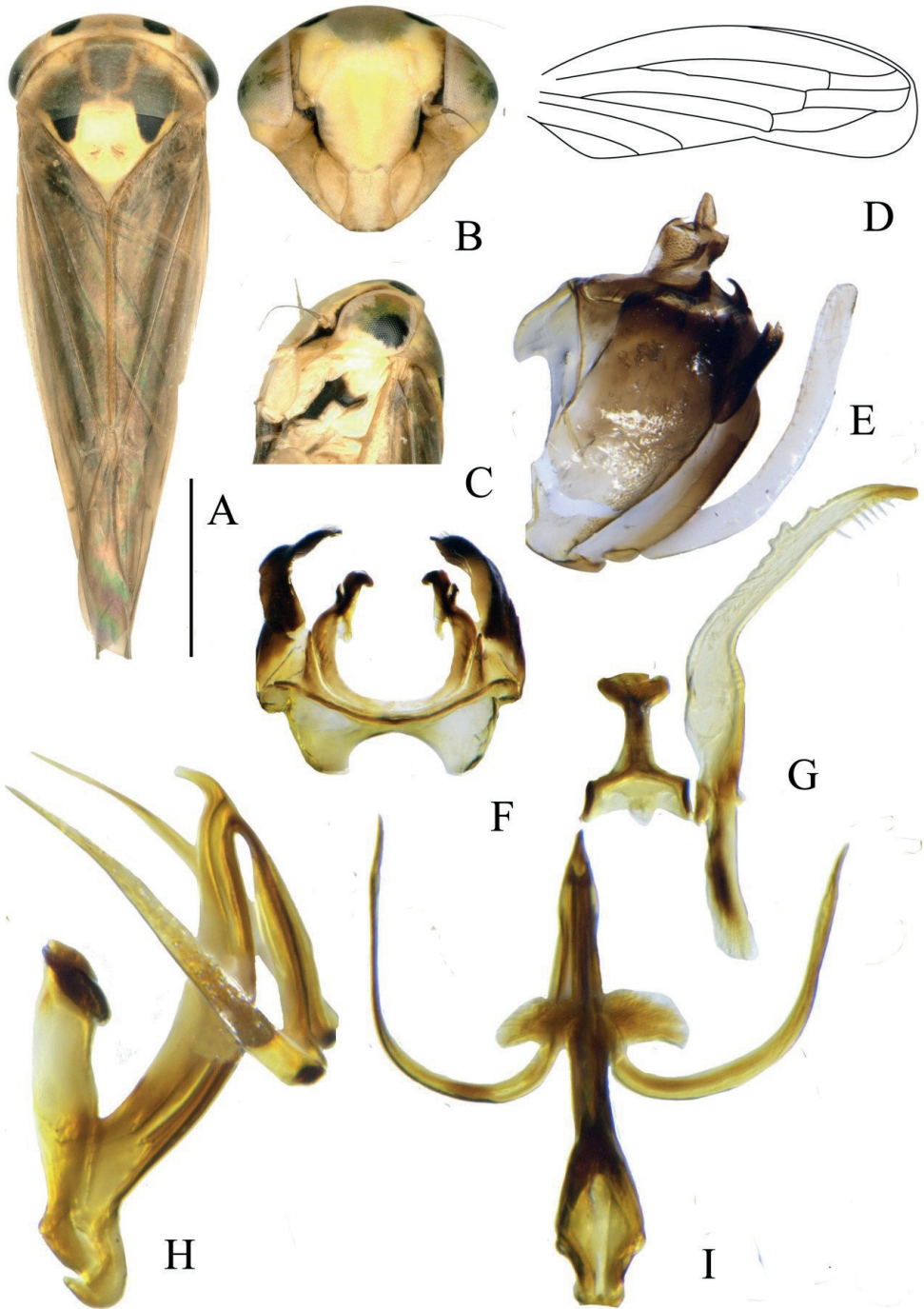


Figure 1. *Idioscopus bihamulus* sp. nov. male **A** habitus, dorsal view **B** face **C** head and thorax, lateral view **D** forewing **E** genital capsule, lateral view **F** pygofer dorsal view **G** connective and style, dorsal view **H** aedeagus, lateral view **I** aedeagus ventral view. Scale bar: 1.0 mm.

Female genitalia. Posterior margin of sternite VII (Fig. 3A) slightly produced medially. Valvulae as in Figure 3B–E.

Measurements (mm). Male: body length including tegmina 3.70–3.80. Medial length of crown 0.13–0.16, width 1.25–1.30. Distance from ocellus to eyes 0.15–0.20. Medial length of pronotum 0.40–0.45, width 1.10–1.20; scutellum length 0.50–0.55, width 0.95–1.05. Female: body length including tegmina 3.70–3.90.

Etymology. The specific epithet refers to the two hamulus-like (hook-like) aedeagal processes.

Host plant. Unknown.

Distribution. China (Yunnan).

***Idioscopus ventrispinus* sp. nov.**

<http://zoobank.org/F0FFE31A-7C3B-48FD-93F8-F6E3DCB62537>

Figs 2, 3E–H

Type material. Holotype: ♂, Xiping County, Mt Ailaoshan, Yunnan Province, China (101°57'57"E, 24°07'39"N; 1956 m elev.), 22 July 2018, coll. Xianyi Wang & Jiajia Wang. **Paratypes:** 58♂♂ 2♀♀, same as holotype. 4♂♂, Lvchun County, Mt Hoanglianshan, Yunnan Province, China (102°17'27"E, 22°56'03"N; 1815 m elev.), 7 June 2019, coll. Jiajia Wang & Chao Zhang. 1♂, Baoshan City, Mt Gaoligongshan, Yunnan Province, China (98°48'03"E, 25°18'15"N; 1581 m elev.), 22 May 2019, coll. Jiajia Wang & Chao Zhang.

Diagnosis. This new species resembles *Idioscopus furcaprocessus* in general appearance, including having a yellow patch on the forewing clavus. The sinuate shaft of the aedeagus in lateral view is similar to *I. confuscous* (Pruthi) (see Viraktamath, 1980: fig. 15), *I. bihamulus*, *I. recurvatus*, and *I. nitellicus*, but it differs from these and other species in having an unpaired, ventral, spine-like process proximad of the midlength of the shaft.

Description. Coloration. General color reddish brown. Crown yellowish with darker reddish-brown markings; eyes yellowish (Fig. 2A–C). Pronotum and mesonotum (Fig. 2A) reddish brown, mesonotum paler with yellowish hue. Face (Fig. 2B) greenish yellow with frontoclypeus and anteclypeus pale reddish brown; male antennae with apical disc, black. Mesepimeron (Fig. 2C) with black patch. Forewing clavus (Fig. 2A) with large, lemon-yellow patch bordered with dark reddish brown.

External features as in generic description with head and thorax shagreen; male antennae with apical disc (Fig. 2A–C); forewing (Fig. 2D) with two subapical cells, inner subapical open.

Male genitalia. Male pygofer (Fig. 2E, F) conically rounded apically, without ventral process; anal collar thin, upturned apically; dorsoanterior apodemes well developed. Anal tube (Fig. 2E) long. Subgenital plates (Fig. 2E) broader in distal one-third in lateral view, longer than pygofer, sharply upturned in basal third, with long hair-like

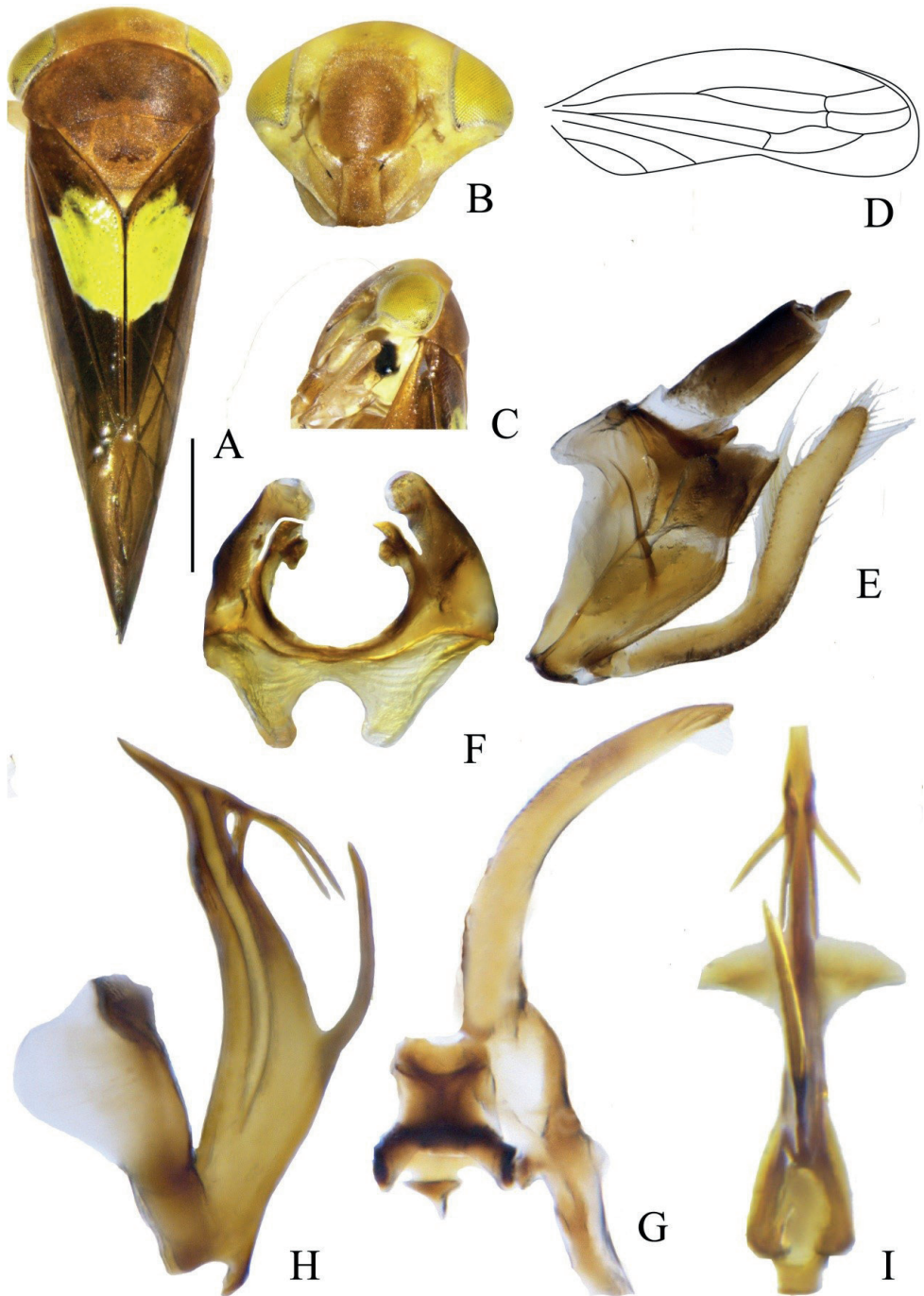


Figure 2. *Idioscopus ventrispinus* sp. nov. male **A** habitus, dorsal view **B** face **C** head and thorax, lateral view **D** forewing **E** genital capsule, lateral view **F** pygofer dorsal view **G** connective and style, dorsal view **H** aedeagus, lateral view **I** aedeagus ventral view. Scale bar: 1.0 mm.

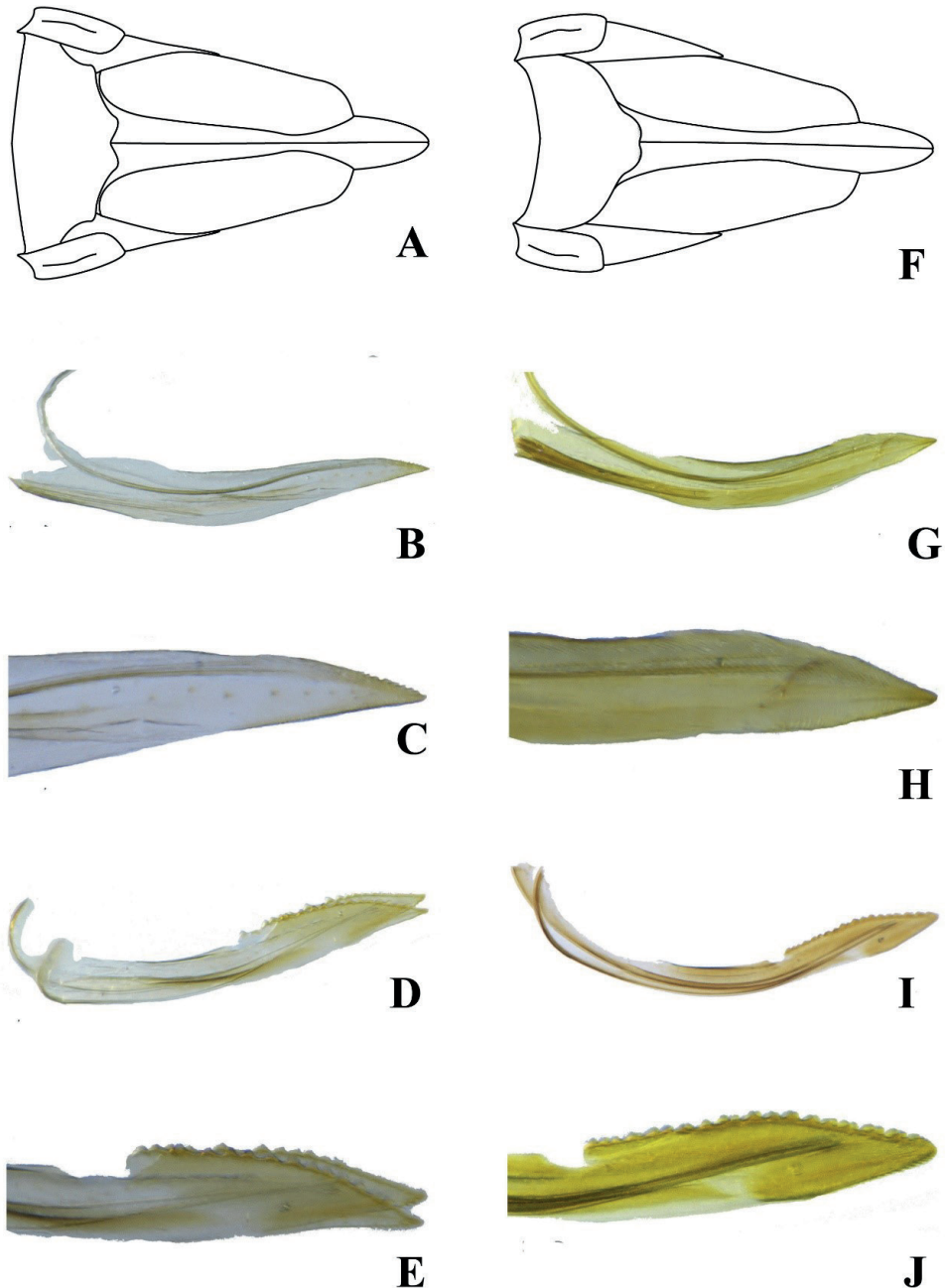


Figure 3. Ovipositor. Female. **A–E** *Idioscopus bihamulus* sp. nov. **F–J** *Idioscopus ventrispinus* sp. nov. **A, F** sternite VII **B, G** first valvula **C, H** apex of first valvula **D, I** second valvula **E, J** apex of second valvula.

marginal setae distally. Connective (Fig. 2G) Y-shaped, broad, with short stem. Style apophysis (Fig. 2G) narrowed to apex with weakly serrated inner margin. Aedeagus (Fig. 2H, I) with shaft laterally compressed, broad in basal half then narrowed and

slightly sinuate distally to acute apex in lateral view, with one pair of subapical bifid processes, each fork unequal, an unpaired ventral spine-like process proximad of midlength; dorsal apodeme laterally compressed, distally expanded in lateral view and laterally expanded distally in ventral view.

Female genitalia. Posterior margin of sternite VII (Fig. 3F) slightly produced medially. Valvulae as in Figure 3G–J.

Measurements (mm). Male: body length including tegmina 4.50–4.95. Medial length of crown 0.18–0.22, width 1.55–1.60. Distance from ocellus to eyes 0.15–0.20. Medial length of pronotum 0.45–0.48, width 1.35–1.45; scutellum length 0.50–0.55, width 0.65–0.70. Female: body length 4.60–5.20 including tegmina.

Etymology. The new species name is derived from the words *ventri-* and *spinus*, referring to the ventral spine-like process of the aedeagal shaft.

Host plant. *Myrica* sp.

Distribution. China (Yunnan).

Idioscopus clypealis (Lethierry)

Fig. 4

Idiocerus clypealis Lethierry, 1889: 252—Matsumura 1912: 322 (Taiwan).

Idioscopus clypealis—Maldonado Capriles 1964: 92–93, figs 6–9; Khatri and Webb 2014: 282–284, table 1, fig. 5.

Idioscopus taiwanus Huang & Maldonado-Capriles, 1992: 7, fig. 3, syn. nov.

Remarks. The above synonymy of *I. taiwanus* with *I. clypealis* is based on the similarity of the published figures of both species and examination of some paratypes of *I. taiwanus* (see below). It is surprising that *I. taiwanus* was described as a new species and not recognized as the widespread *I. clypealis*, as the latter species was well-known to Maldonado-Capriles and had been earlier figured by him (Maldonado-Capriles 1964). Also, the described colour of *I. taiwanus* more or less matches the “typical” colour form of *I. clypealis* figured by the same author and latter figured by Khatri and Webb (2014) from mainland Asia. A variation of this colour is seen in some specimens collected from mainland China which have more extensive brown marking medially on the face (Fig. 4A–C), matching some Pacific material figured by Khatri and Webb (2014).

Idioscopus taiwanus was described from the holotype and 80 paratypes with the following data: “Taiwan, Taichung, 16/1/1987, C. T. Yang collector. Paratypes: 40 males and 40 females, same collection data as holotype. Host plant: *Mangifera indica*” (Huang & Maldonado-Capriles 1992). In the introduction to their paper, Huang & Maldonado-Capriles stated that the type material was in the “Department of Entomology, National Chung-Hsing University (NCHU), Taichung; Division of Collection and Research, National Museum of Natural Science (NMNS), Taichung; and in the Department of Applied Zoology, Taiwan Agriculture Research Institute (TARI), Wufeng, Taichung.” They added that “Some paratypes deposited in the junior author’s collection”. For other new species described in the same paper the holotype depository is given as NMNS,

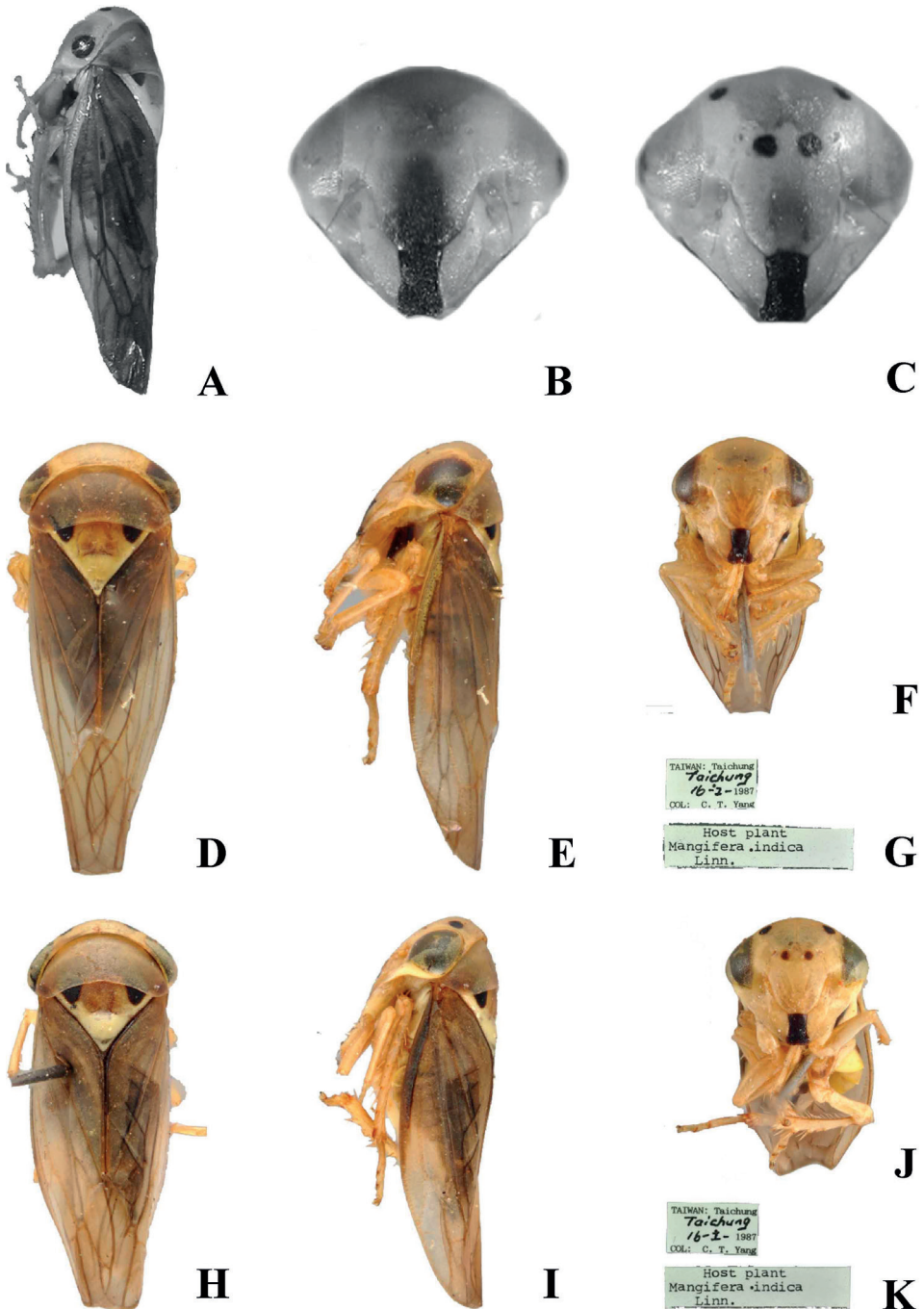


Figure 4. *Idioscopus chypealis* **A–C** female (China) **A** lateral habitus female **B, C** face (male and female respectively) showing atypical marking of clypeus; photographs by Xue Qingquan **D–G** paratype male of *I. taiwanus* **D** dorsal habitus **E** lateral habitus **F** ventral habitus **G** labels **H–K** paratype female of *I. taiwanus* **H** dorsal habitus **I** lateral habitus **J** ventral habitus **K** labels; photographs by David Redei.

but no depository is given for *I. taiwanus*; however, the male genitalia dissection of the holotype is present in NMNS (Jing-Fu Tsai pers. comm.) and paratypes are present in both NCHU (see Fig. 4D–K) and NMNS but not in TARI or Maldonado-Capriles's collection (National Museum of Natural History, Washington, DC, USA).

***Idiocerus apicalis* Matsumura**

Fig. 5A, B

Idiocerus apicalis Matsumura, 1912: 323—Huang and Maldonado-Capriles 1992: 4 (listed); Xue et al. 2016: 407 (listed).

Remarks. This species was described from a single female specimen (holotype) from Taiwan. Both Andy Hamilton and Masami Hayashi (pers. comm.) examined the type (Entomological Institute, Hokkaido University, Sapporo, Japan) and the latter's photographs of the type are reproduced here (Fig. 5A, B). The holotype bears a determination label by Andy Hamilton indicating the species belongs to *Balocerus* but this needs to be confirmed, particularly as the specimen is female. The label information on the specimen is as follows (hw = handwritten, pr = printed):

1. *I. apicalis* sp. nov. (hw), det. Matsumura (pr)
2. Formosa, Matsumura (printed), (underside) Toroen, 19/4 '07 (hw)
3. Holotype (red label, printed), *Idiocerus apicalis* Matsumura (hw)
4. *Balocerus apicalis* (Matsum.), Det. KGAH '76 (hw; label with red frame)

***Idiocerus formosanus* Matsumura**

Fig. 5C, D

Idiocerus taiwanus Matsumura—Huang and Maldonado-Capriles 1992: 4 (listed); Xue et al. 2016: 407 (listed).

Remarks. This species was described from an unknown number of specimens (syntypic) from Koshun (= Hengchun), southern Taiwan. Both Andy Hamilton and Masami Hayashi (pers. comm.) examined the type series in Entomological Institute, Hokkaido University, Sapporo, Japan (9 ♂♂ and 4 ♀♀) and the latter's photographs of a syntype are reproduced here (Fig. 5C, D). One of the male syntypes had been dissected and bears a determination label by Andy Hamilton indicating the species belongs to *Amritodus*, which needs to be confirmed, together with an unpublished lectotype label. The label information on the specimens is as follows (hw = handwritten, pr = printed), double quotation marks show each label, a single oblique line (except between day and month) is used for changing to new line, and the description on underside is indicated after double oblique lines:

- 1 male [dissected], “Formosa / Matsumura [printed] // Koshun / 7/7-02 [hw]”, “*I. formosanus* n.sp. [hw] / det. Matsumura [pr]”, “Type Matsumura” (red printed label), “Lectotype [red printed label] / *Idiocerus formosanus* Mm. [hw by K.G.A. Hamilton, not published]”, “*Amritodus formosanus* (Matsum.) / Det. KGAH '76” [in double red frame, hw]. 2 male, same data as previous, “PARATYPES [yellow printed label] / *Idiocerus formosanus* Mm. [hw]”
- 4 male, 3 female, [upper right male dissected], “Formosa / Matsumura [pr] // 7/VII 1906 | Koshun [hw]”, “Paratypes (yellow printed label) / *Idiocerus formosanus* Mm.” [hw];
- 1 female, “Formosa / Matsumura [pr] // 29/VI 1906 / Koshun (hw)”
- 1 male, “Formosa / Matsumura [pr] // 7/VII 1906 / Koshun [hw]”
- 1 male, “Formosa / Matsumura [pr] // 10/VIII 1906 / Koshun [hw]”

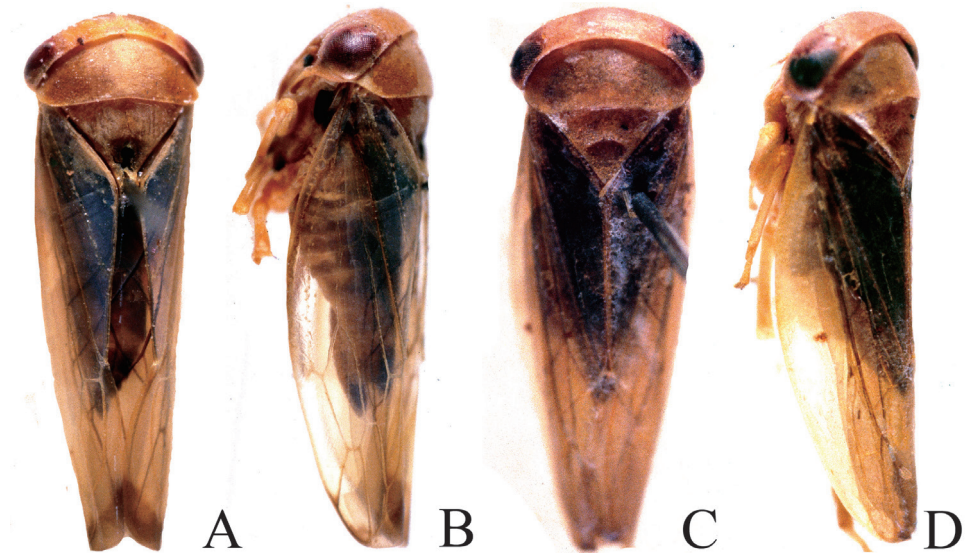


Figure 5. Matsumura Taiwan Idiocerine species **A, B** *Idiocerus apicalis*, dorsal and lateral, habitus respectively (holotype) **C, D** *I. formosanus*, dorsal and lateral, habitus respectively (syntype). Photographs by Masami Hayashi.

Acknowledgements

We wish to thank the following people for their help in preparing this manuscript: Chandra Viraktamath for reviewing the manuscript, David Rédei (currently working in Taiwan) for paratype images of *Idioscerus taiwanus*, Jing-Fu Tsai for information on the type series of *I. taiwanus*, Masami Hayashi and Andy Hamilton for information on the types of *I. apicalis* Matsumura and *I. formosanus* Matsumura and the former for making available photographs of the types, and Chao Zhang and Zhou Yu (GUGC) for providing material for this study. We would also like to express our sincere gratitude to the staff

of Yunnan Mt Gaoligongshan National Nature Reserve and Mt Huanglianshan National Nature Reserve for assistance in collecting the specimens. This study was supported by the National Natural Science Foundation of China (no. 31672342), the Program of Excellent Innovation Talents, Guizhou Province, China [grant number 20206003], and the Guizhou Province Graduate Research Fund [no.YJSCXJH (2020)073].

References

- Baker CF (1915) Studies in Philippine Jassoidea. IV. The Idiocerini of the Philippines. *Philippine Journal of Crop Science* 10: 317–343.
- Dietrich CH (2005) Keys to the families of Cicadomorpha and subfamilies and tribes of Cicadellidae (Hemiptera: Auchenorrhyncha). *The Florida Entomologist* 88(4): 502–517. [https://doi.org/10.1653/0015-4040\(2005\)88\[502:KTTFOC\]2.0.CO;2](https://doi.org/10.1653/0015-4040(2005)88[502:KTTFOC]2.0.CO;2)
- Huang KW, Maldonado-Capriles J (1992) Idiocerinae of Taiwan (Homoptera: Cicadellidae). *Journal of Taiwan Museum* 45(1): 1–14.
- Khatri I, Webb MD (2014) Review of the idiocerine leafhoppers of Pakistan (Hemiptera, Cicadellidae) with a description of a new species. *Zootaxa* 3860(3): e280. <https://doi.org/10.11646/zootaxa.3860.3.6>
- Kouh ZL, Fang QQ (1985) Two new species of *Idioscopus* from China (Hemiptera: Cicadellidae: Idiocerinae). *Dong Wu Fen Lei Xue Bao* 10(2): 189–192.
- Lethierry LF (1889) Definitions of three new Homoptera. *Journal of the Asiatic Society of Bengal* 58: 252–253.
- Maldonado-Capriles J (1964) Studies on Idiocerinae leafhoppers: II. The Indian and Philippine species of *Idiocerus* and the genus *Idioscopus* (Homoptera: Cicadellidae). *Proceedings of the Entomological Society of Washington* 66: 89–100.
- Maldonado-Capriles J (1974) Studies on Idiocerinae leafhoppers XII. *Idioscopus clavosignatus* spec. nov. (Homoptera, Cicadellidae). *Zoölogische Mededeelingen* 48(15): 163–167.
- Oman PW (1949) The Nearctic leafhoppers (Homoptera: Cicadellidae) a generic classification and check list. *Memoirs of the Entomological Society of Washington* 3: 1–253.
- Pruthi HS (1936) Studies on Indian Jassidae (Homoptera). Part III. Description of some new genera and species, with first records of some known species from India. *Memoirs of the Indian Museum* 11: 101–131.
- Viraktamath CA (1976) Four new species of Idiocerine leafhoppers from India with a note on male *Balocha astute* (Melichar) (Homoptera: Cicadellidae: Idiocerinae). *Mysore Journal of Agricultural Sciences* 10: 234–244. <https://doi.org/10.1080/00305316.1976.10432323>
- Viraktamath CA (1979a) *Jogocerus* gen. nov. and new species of idiocerine leafhoppers from southern India (Homoptera: Cicadellidae). *Entomon* 4(1): 17–26.
- Viraktamath CA (1979b) Four new species of *Idioscopus* (Homoptera: Cicadellidae) from Southern India. *Entomon* 4(2): 173–181.
- Viraktamath CA (1980) Notes on *Idioscopus* species (Homoptera: Cicadellidae) described by Dr. H.S. Pruthi, with description of a new species from Meghalaya, India. *Entomon* 5(3): 227–231.

- Viraktamath CA (1989) Auchenorrhyncha (Homoptera) associated with mango, *Mangifera indica* L. Tropical Pest Management 35(4): 431–434. <https://doi.org/10.1080/09670878909371423>
- Walker F (1869) Catalogue of the Homopterous insects collected in the Indian Archipelago by Mr. A.R. Wallace, with descriptions of new species. Zoological Journal of the Linnean Society 10(45): 276–330. <https://doi.org/10.1111/j.1096-3642.1869.tb00663.x>
- Wang XY, Dai RH (2018) A new species of *Idioscopus* harming *Myrica rubra* (Hemiptera: Cicadellidae: Idiocerinae). Journal of Mountain Agriculture and Biology 37(6): 10–13. [in Chinese]
- Wang XY, Wang JJ, Zhou XL, Dai RH (2021) Description of three new species of the leafhopper genus *Idioscopus* Baker, (Hemiptera: Cicadellidae: Eurytelinae) from Yunnan, China. Zootaxa 4995(2): 375–381. <https://doi.org/10.11646/zootaxa.4995.2.10>
- Xue QQ, Viraktamath CA, Zhang YL (2017) Checklist to Chinese Idiocerine leafhoppers, key to genera and description of a new species of *Anidiocerus* (Hemiptera: Auchenorrhyncha: Cicadellidae). Entomologica Americana 122(3): 405–417. <https://doi.org/10.1664/1947-5144-122.3.405>
- Zhang B, Li Z (2012) Idiocerinae. In: Dai L, Li Z, Jin D (Eds) Insects from Kuankuoshui Landscape. Guizhou Science and Technology Press, Guiyang, 202–209.

Four new species of *Diglyphomorphomyia* Girault (Hymenoptera, Eulophidae) from China, with a key to Chinese species

Jun-Jie Fan¹, Cheng-De Li¹

¹ School of Forestry, Northeast Forestry University, Harbin, 150040, China

Corresponding author: Cheng-De Li (lichengde0608@sina.com)

Academic editor: Miles Zhang | Received 17 January 2022 | Accepted 28 March 2022 | Published 13 April 2022

<http://zoobank.org/FC57A27D-3546-44A0-B6CD-E82C5E3BCA32>

Citation: Fan J-J, Li C-D (2022) Four new species of *Diglyphomorphomyia* Girault (Hymenoptera, Eulophidae) from China, with a key to Chinese species. ZooKeys 1095: 111–121. <https://doi.org/10.3897/zookeys.1095.80671>

Abstract

Four new species of *Diglyphomorphomyia* Girault, *D. depressa* **sp. nov.**, *D. fossa* **sp. nov.**, *D. hainana* **sp. nov.**, and *D. octoseta* **sp. nov.**, are described from China. A key to the eight species of the genus *Diglyphomorphomyia* occurring in China is provided.

Keywords

Chalcidoidea, Eulophinae, parasitoid, taxonomy

Introduction

The genus *Diglyphomorphomyia* (Hymenoptera: Eulophidae) is one of several small genera of the Eulophidae, erected by Girault (1913) with *Diglyphomorphomyia nigriscutellum* Girault as type species. Girault (1913, 1915) also described *Sympiesomorphelleus albiclava* Girault and *S. specimenipennis* Girault from Australia, which were later transferred by Bouček (1988) to *Diglyphomorphomyia*, together with *Chiloneurus rufescens* Motschulsky. Zhu and Huang (2003) described four species from China; Ubaidillah (2003) described one species from Indonesia; Yefremova (2007)

described one species from Yemen; Narendran (2004, 2011) and Narendran et al. (2005a, b) described eight species from India. Currently the genus contains 18 valid species (Noyes 2021).

This study describes four new species of the genus *Diglyphomorphomyia* and provides a key to all species of the genus distributed in China.

Materials and methods

All specimens were collected by sweeping or yellow-pan trapping, and were dissected and mounted in Canada balsam on slides following the method of Noyes (1982), or mounted on a card. Photographs were taken with a digital CCD camera attached to an Olympus BX51 compound microscope or Aosvi AO-HK830-5870T digital microscope. Measurements were made using an eyepiece reticle, or using the ruler tool in Adobe Photoshop 2020.

Terminology follows the Hymenoptera Anatomy Consortium (2021), and the following abbreviations are used:

- F1–6** flagellomeres 1–6;
- MV** marginal vein;
- OOL** minimum distance between a posterior ocellus and corresponding eye margin;
- PMV** postmarginal vein;
- POL** minimum distance between posterior ocelli;
- SMV** submarginal vein;
- STV** stigmal vein.

All type material is deposited in the insect collections at Northeast Forestry University (NEFU), Harbin, China.

Results

Diglyphomorphomyia Girault

Diagnosis. *Diglyphomorphomyia* can be recognized by the following combination of characteristics: funicle 4 or 5 segmented; midlobe of mesoscutum or scutellum with deep punctures or pits; midlobe of mesoscutum with two or three, rarely four, pairs of setae; scutellum with sublateral grooves very distinct, punctate on bottom; propodeum with anterior margin raised into a perpendicular lamina, median carina and plicae distinct; transverse carina lateral to plicae distinct behind propodeal spiracle; gaster subsessile or short-petiolate.

Description. Head in frontal view a little wider than its height; Antenna with six flagellomeres, including a 2-segmented clava; antenna inserted above level of lower eye mar-

gin, scape not reaching level of anterior ocellus. Eyes with short setae. Malar sulcus present. Pronotum without transverse carina, weakly reticulate, posterior margin with numerous setae and six long setae. Scutellum punctate. Dorsellum with engraved reticulation, meshes isodiametric. Propodeum smooth, with median carina and plicae, a transverse carina running from posterior part of each plica to outer margins of propodeum. Gaster subsessile.

Key to Chinese species of *Diglyphomorphomyia* based on females

- 1 Notauli strongly divergent posteriorly meeting inner angle of axillae; dorsellum smooth (Fig. 11 page 447 of Zhu and Huang 2003).....***D. metanotalia* Zhu & Huang**
- Notauli straight, converging posteriorly and meeting scuto-scutellar suture laterad to inner angle of axillae; dorsellum reticulate (e.g., Figs 1, 5).....**2**
- 2 Propodeum with median carina bifurcate anteriorly; midlobe of mesoscutum with 4 pairs of long setae (Fig. 17)***D. octoseta* sp. nov.**
- Propodeum with median carina not bifurcate anteriorly (e.g., Figs 1, 5); midlobe of mesoscutum with 2 or 3 pairs of long setae**3**
- 3 Scutellum with a median groove or a fovea anteriorly (e.g., Figs 1, 5)**4**
- Scutellum without median groove or fovea (e.g., Fig. 15)**5**
- 4 Antenna with scape, pedicel and F1 yellow and remainder of flagellomeres dark brown (Figs 6, 10)***D. fossa* sp. nov.**
- Antenna yellowish with F3 and F4 brownish, club brownish except yellowish apex (Fig. 2).....***D. depressa* sp. nov.**
- 5 Body dark brown to black.....***D. nigra* Zhu & Huang**
- Body mostly yellow.....**6**
- 6 Metasoma yellow without a brown patch; MV 1.7× SMV (Zhu and Huang 2003: 447, fig. 17).....***D. platys* Zhu & Huang**
- Metasoma yellow with a brown median patch; MV at most 1.2× SMV (e.g., Figs 12, 14, 15).....**7**
- 7 Antenna with scape, pedicel and F1 yellow, F2–F6 brown (Zhu and Huang 2003: 447, fig. 8); POL 2.8× OOL.....***D. aequus* Zhu & Huang**
- Antenna with scape yellow, pedicel and flagellum yellowish-brown (Fig. 13); POL 2.4× OOL.....***D. hainana* sp. nov.**

***Diglyphomorphomyia depressa* sp. nov.**

<http://zoobank.org/DEFBC4FD-0A88-494A-B029-34E61DD671EC>

Figs 1–4

Type material. *Holotype*, ♀ [NEFU; on card], CHINA, Sichuan Province, Guangyuan City, Qingchuan County, 21 VIII 2015, leg. Ye Chen and Chao Zhang, by sweeping.

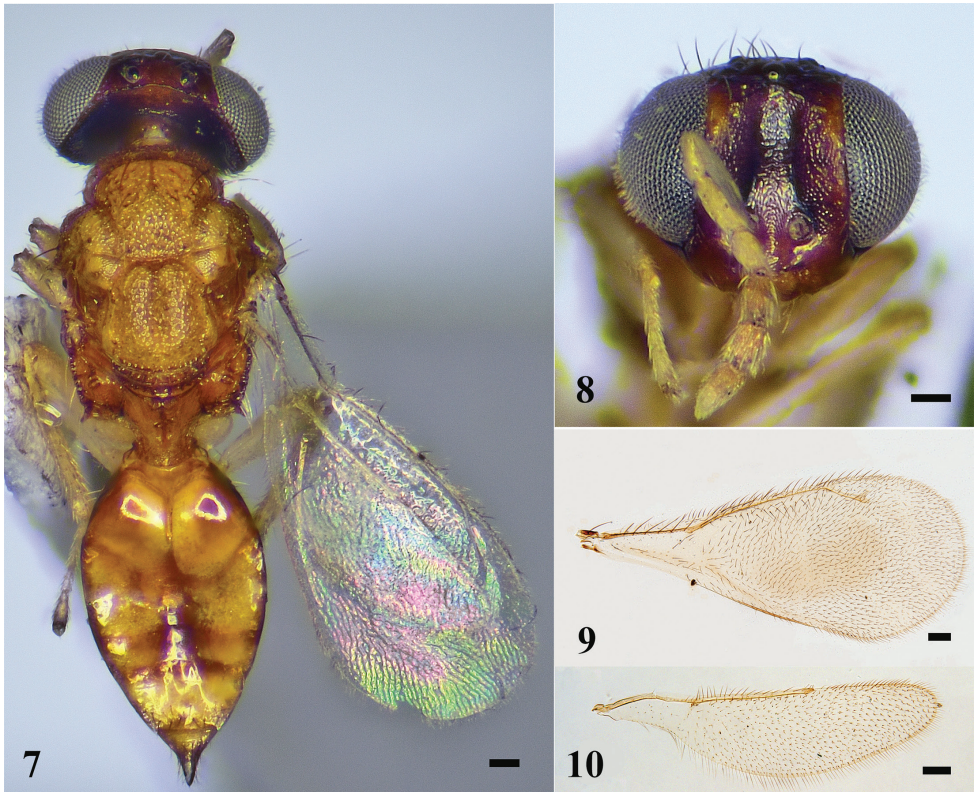
Paratypes: 2♀ [on slides], CHINA, Liaoning Province, Anshan City, Tiedong District, Gudaoguan, 19–21 VI 2015, leg. Yan Gao and Hui Geng, by yellow pan trapping.

Diagnosis. Head dark brown. Antennae yellowish except F3, F4 brownish, club brownish except yellowish apex. Mesosoma yellow except propodeum brown. Midlobe of mesoscutum with two pairs of long setae. Scutellum with a longitudinal depression in anterior 2/3.

Description. Female. Body length 2.4 mm, fore wing length 1.7 mm. Head dark brown. Antennae yellowish with F3 and F4 brownish, club brownish except yellowish apex. Mesoscutum, axillae and scutellum yellow. Propodeum brown. Legs yellowish. Gaster mostly yellow with two brown transverse bands posteriorly and margins brown. Ovipositor black.

Head (Fig. 2) 1.2× as wide as high in frontal view and ~ 2.2× as wide as long in dorsal view. Lower face smooth, frons weakly reticulate. Vertex with engraved reticulation, meshes isodiametric, and scattered setae. POL 1.8× OOL. Malar space 0.4× eye height. Occiput weakly reticulate. Relative measurements (length: width): scape = 28: 5; pedicel = 10: 5; F1 = 16: 5; F2 = 11: 5; F3 = 12: 7; F4 = 10: 7; clava = 16: 7.

Mesosoma (Fig. 1). Midlobe of mesoscutum punctate with two pairs of long setae, lateral lobe of mesoscutum reticulate. Notauli ending laterad to inner angles of axilla. Axillae weakly reticulate and separated from each other. Scutellum with a longitudinal



Figures 1–4. *D. depressa* sp. nov., female, holotype 1 habitus in dorsal view 2 head in frontal view 3 fore wing 4 hind wing. Scale bars: 100 μ m.

depression in anterior 2/3 and two pairs of long setae, sublateral grooves meet posteriorly. Spiracle with a transverse carina anteriorly, separated from metanotum by a distance shorter than a diameter of spiracle; each propodeal callus with seven long setae.

Wings. Fore wing (Fig. 3) 2.3× as long as wide. Speculum narrow. Relative measurements (length): SMV = 43; MV = 40; PMV = 22; STV = 16. Hind wing (Fig. 4) ~ 4.0× as long as wide.

Metasoma (Fig. 1). Gaster ovate, 1.8× as long as wide, and 1.1× as long as mesosoma. Ovipositor exerted beyond apex of gaster.

Male. Unknown.

Host. Unknown.

Distribution. China (Sichuan, Liaoning).

Etymology. Latin: *depressum* = depression, sink; and refers to the longitudinal depression in anterior 2/3 of scutellum.

Remarks. This new species differs from all other known members of the genus in having a scutellum with a longitudinal depression on its anterior 2/3.

***Diglyphomorphomyia fossa* sp. nov.**

<http://zoobank.org/808A2C5F-15CC-4BB4-BB58-1237002F6954>

Figs 5–10

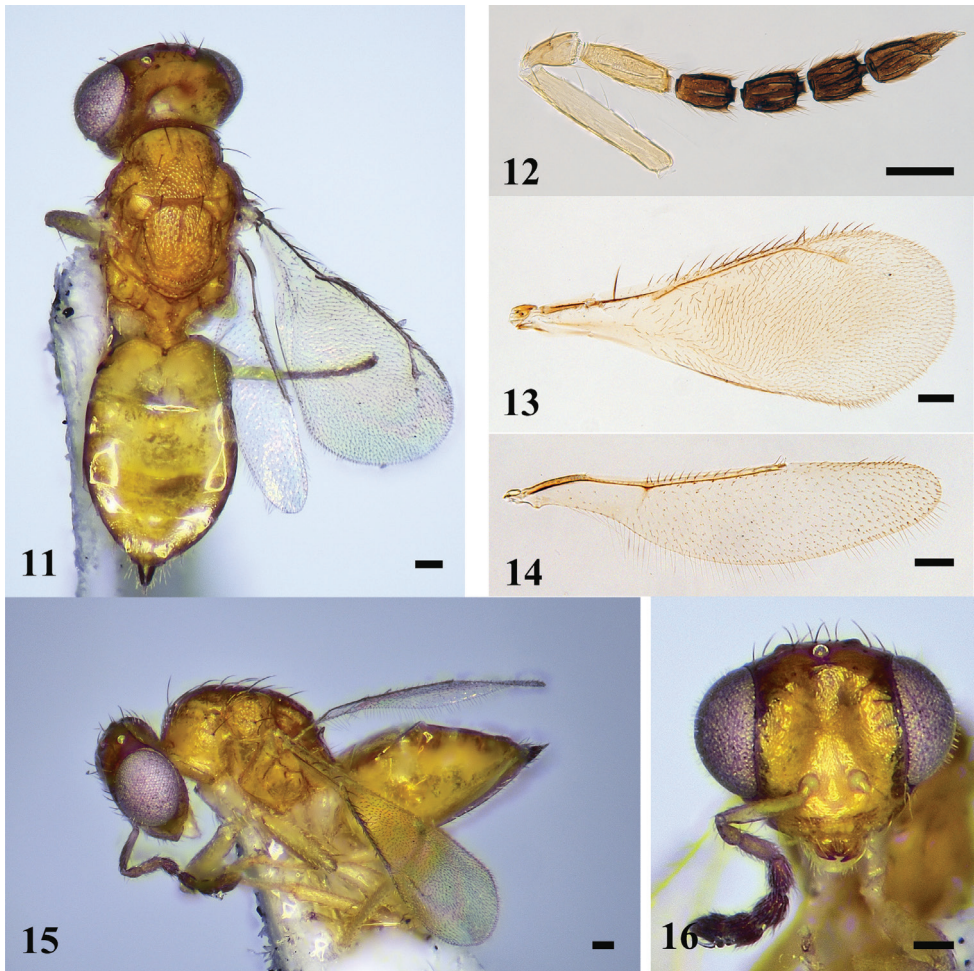
Type material. *Holotype*, ♀ [NEFU; on card], CHINA, Shandong Province, Qingdao City, Huangdao District, Dazhu Mountain, 22–24 V 2014, leg. Guo-Hao Zu, Xiang-Xiang Jing and Si-Zhu Liu, by yellow pan trapping. *Paratypes*: 1♀ [on slide], same data as holotype; 1♀ [on slide], CHINA, Shandong Province, Qingdao City, Huangdao District, Xiaozhu Mountain, 18–20 V 2014, leg. Guo-Hao Zu, Xiang-Xiang Jing and Si-Zhu Liu, by yellow pan trapping; 4♀ [on card], CHINA, Shandong Province, Qingdao City, Laoshan District, Beijiushui, 1–3 VIII 2014, leg. Guo-Hao Zu and Ye Chen, by yellow pan trapping; 1♀ [on card], CHINA, Shandong Province, Qingdao City, Laoshan District, Dahedong, 8–10 VII 2014, leg. Chao Zhang, Si-Zhu Liu and Ye Chen, by yellow pan trapping.

Diagnosis. Antenna with scape, pedicel and F1 yellow and rest of flagellomeres dark brown. Scutellum with median groove in approximately anterior 1/2. Legs mostly yellowish with fore and hind coxae yellowish white. Gaster yellowish except margins brown.

Description. Female. Body length 1.9 mm, fore wing length 1.3 mm. Body yellow. Mandibles yellow with teeth brown. Antenna with scape, pedicel, and F1 yellow and remainder of flagellomeres dark brown. Legs mostly yellowish except fore and hind coxae yellowish white. Gaster yellowish except margins brown. Ovipositor black.

Head (Fig. 10) 1.3× as wide as high in frontal view and ~ 2.3× as wide as long in dorsal view. Lower face and vertex transversely reticulate, frons weakly sculptured. POL 2.4× OOL. Malar space 0.4× eye height. Occiput weakly reticulate. Relative measurements (length: width): scape = 35:6; pedicel = 11:6; F1 = 19:6; F2 = 12:7; F3 = 13:8; F4 = 12:8; clava = 20:8.

Mesosoma (Fig. 5). Midlobe of mesoscutum punctate with three pairs of long setae, lateral lobe of mesoscutum reticulate. Notauli ending laterad to inner angles of axilla.



Figures 5–10. *D. fossa* sp. nov., female, holotype **5** habitus in dorsal view **6** antenna **7** fore wing **8** hind wing **9** habitus in lateral view **10** head in frontal view. Scale bars: 100 μ m.

Axillae weakly reticulate and separated from each other. Scutellum with median groove in approximately anterior 1/2 and two pairs of long setae, sublateral grooves meet posteriorly. Spiracle with a transverse carina anteriorly, separated from metanotum by a distance almost as long as a diameter of spiracle; each propodeal callus with six setae.

Wings. Fore wing (Figs 5, 7) 2.6 \times as long as wide. Relative measurements (length): SMV = 33; MV = 45; PMV = 17; STV = 12. Hind wing (Figs 5, 8) ~ 4.5 \times as long as wide.

Metasoma (Fig. 5). Gaster ovate, 1.7 \times as long as wide, and 1.2 \times as long as mesosoma. Ovipositor exerted beyond apex of gaster.

Male. Unknown.

Host. Unknown.

Distribution. China (Shandong).

Etymology. Latin: *fossa* = ditch, trench; and refers to the median groove in the approximate anterior 1/2 of scutellum.

Remarks. *Diglyphomorphomyia fossa* is similar to *D. aequus* Zhu & Huang, 2003 in sharing the antenna with a yellow scape, pedicel, and F1, while the remaining segments are brown; and the notauli straight and converging posteriorly to meet laterad to inner angles of axillae, but the new species can be separated from *D. aequus* by the following combination of characters: legs yellowish with fore and hind coxae yellowish white (legs yellow in *D. aequus*); gaster yellowish except margins brown (gaster yellow with a brown patch in *D. aequus*); gaster 1.7× as long as wide (gaster 1.4× as long as wide in *D. aequus*).

***Diglyphomorphomyia hainana* sp. nov.**

<http://zoobank.org/B3718EA6-954C-48D6-8741-A608907D1F9C>

Figs 11–16

Type material. *Holotype*, ♀ [NEFU; on card], CHINA, Hainan Province, Wenchang City, Dongjiao Town, 22–24 IV 2019, leg. Yu-Ting Jiang, by yellow pan trapping.

Paratypes: 2♀ [on slides], same data as holotype.

Diagnosis. Antennae yellowish brown with scape yellow. Midlobe of mesoscutum with two pairs of long setae. Legs mostly yellowish white with fore and hind coxae white, mid coxae yellow.

Description. Female. Body length 1.8 mm, fore wing length 1.5 mm. Body yellow. Antennae yellowish brown with scape yellow. Legs mostly yellowish white except fore and hind coxae white, mid coxae yellow. Gaster dorsally mostly yellow with a brown patch and lateral margins brown, ventrally mostly whitish.

Head (Figs 11, 13) 1.4× as wide as high in frontal view and 2.4× as wide as long in dorsal view. Frons weakly sculptured. Vertex with engraved reticulation, meshes isodiametric. POL 2.4× OOL. Malar space 0.3× eye height. Occiput weakly reticulate. Relative measurements (length: width): scape = 29: 5; pedicel = 11: 5; F1 = 13: 5; F2 = 10: 5; F3 = 10: 6; F4 = 9: 6; clava = 15: 5.

Mesosoma (Fig. 15). Notauli straight, ending laterad to inner angle of axilla. Midlobe of mesoscutum punctate with two pairs of long setae, lateral lobe of mesoscutum reticulate. Axillae weakly reticulate and separated from each other. Scutellum longer than mesoscutum with two pairs of long setae, sublateral grooves meet posteriorly. Spiracle with a transverse carina anteriorly, slightly separated from metanotum by a distance shorter than a diameter of spiracle; each propodeal callus with seven or eight setae.

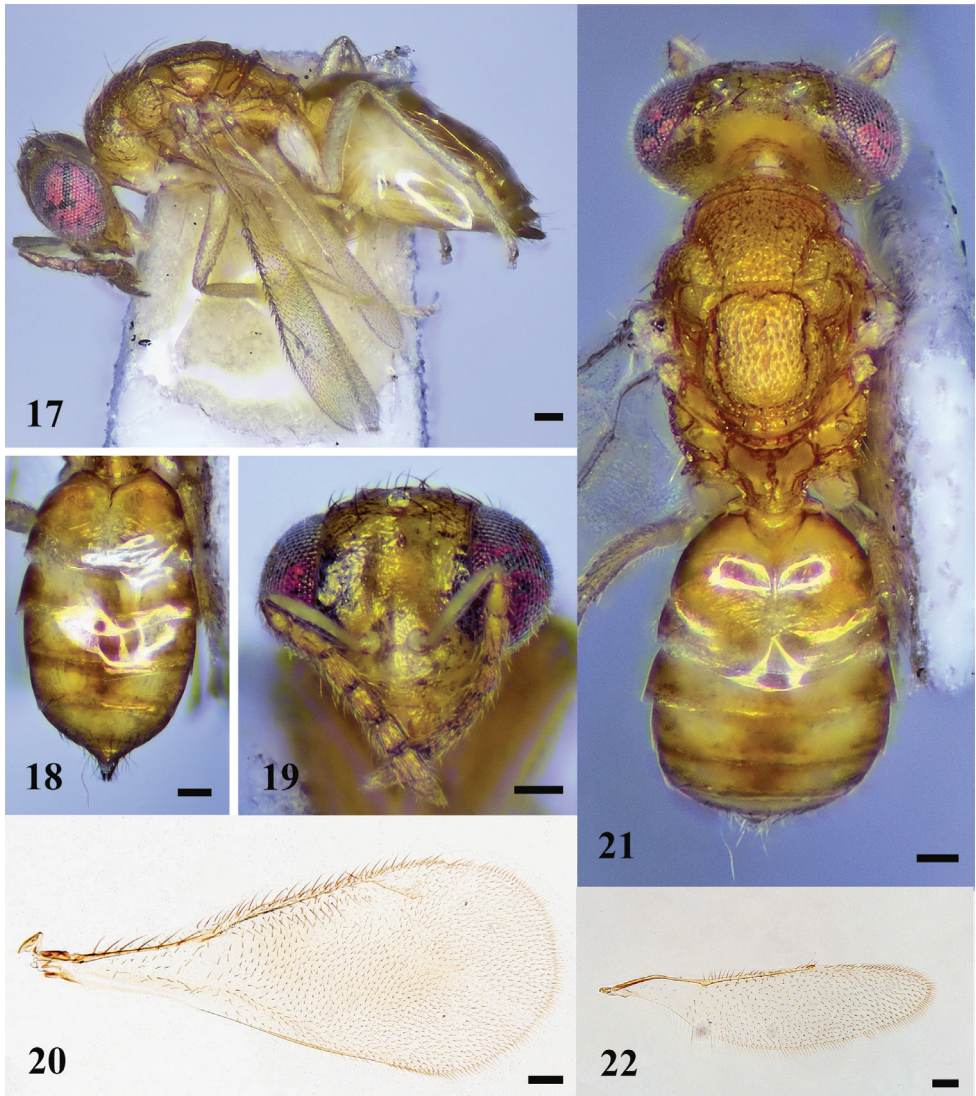
Wings. Fore wing (Fig. 14) 2.3× as long as wide. Speculum narrow. Relative measurements (length): SMV = 35; MV = 36; PMV = 16; STV = 12. Hind wing (Fig. 16) ~ 4.0× as long as wide.

Metasoma (Fig. 12). Gaster ovate; 1.8× as long as wide and 1.3× as long as mesosoma. Ovipositor exerted beyond apex of gaster.

Male. Unknown.

Host. Unknown.

Distribution. China (Hainan).



Figures 11–16. *D. hainana* sp. nov., female, holotype **11** habitus in lateral view **12** gaster in dorsal view **13** head in frontal view **14** fore wing **15** habitus in dorsal view **16** hind wing. Scale bars: 100 μ m.

Etymology. The specific name is derived from the type locality.

Remarks. *Diglyphomorphyomyia hainana* is similar to *D. aequus* Zhu & Huang, 2003 in sharing a body that is mostly yellow, and a gaster bearing a brown patch, but can be separated from *D. aequus* by the following combination of characters: antennae yellowish brown with scape yellow (antenna brown with scape, pedicel, and F1 yellow in *D. aequus*); POL 2.4 \times OOL (POL 2.8 \times OOL in *D. aequus*); legs mostly yellowish white with fore and hind coxae white, mid coxae yellow (legs yellow in *D. aequus*).

***Diglyphomorphomyia octoseta* sp. nov.**

<http://zoobank.org/66B78964-DF2B-469D-AA6E-FDC23D26B523>

Figs 17–22

Type material. *Holotype*, ♀ [NEFU; on card], CHINA, Jiangxi Province, Yichun City, Guanshan National Nature Reserve, 29 VIII 2017, leg. Guang-Xin Wang and Wen-Jian Li, by yellow pan trapping. *Paratype*: 1 ♀ [on slide], same data as holotype.

Diagnosis. The new species is easily distinguished from the other known members of the genus by the following combination of characters: Antenna with scape white, pedicel, F1–F3 pale yellow, clava brown except apex yellowish. Midlobe of mesoscutum punctate with four pairs of long setae. Propodeum with median carina bifurcate anteriorly and meeting a perpendicular lamina, anteromedially with two dorsal pits. Legs mostly white.

Description. Female. Body length 2.2 mm, fore wing length 1.6 mm. Body pale yellow. Head yellowish-white. Antenna with scape white, pedicel, F1–F3 pale yellow, F4 and clava brown except apex yellowish. Mandibles yellow with teeth brown. Legs mostly white. Gaster mostly yellowish white, with a median stripe and lateral margins brown.

Head (Fig. 18) 1.4× as wide as high in frontal view and 2.3× as wide as long in dorsal view. Frons smooth to alutaceous with a row of setae along eye margin. Vertex smooth. POL 1.8× OOL. Malar space 0.4× eye height. Occiput weakly reticulate. Relative measurements (length: width): scape = 28: 5; pedicel = 9: 5; F1 = 14: 5; F2 = 11: 6; F3 = 11: 7; F4 = 11: 7; clava = 19: 7.

Mesosoma (Fig. 17). Midlobe of mesoscutum punctate with 4 pairs of long setae, lateral lobe of mesoscutum reticulate. Notauli ending laterad to inner angles of axilla. Axillae weakly reticulated and separated from each other. Scutellum longer than mesoscutum with 2 pairs of long setae, sublateral grooves meet posteriorly. Propodeum smooth, with a median carina bifurcating anteriorly and meeting a perpendicular lamina, anteromedially with two dorsal pits; plicae distinct with a transverse carina joining outer margins; another transverse carina present anterior to spiracle; separated from metanotum by a distance as long as a diameter of spiracle; each propodeal callus with seven long setae.

Wings. Fore wing (Fig. 19) 2.4× as long as wide. Relative measurements (length): SMV = 63; MV = 57; PMV = 25; STV = 22. Hind wing (Fig. 20) 3.9× as long as wide.

Metasoma (Fig. 17). Gaster ovate, 1.5× as long as wide and as long as mesosoma. Ovipositor exerted beyond apex of gaster.

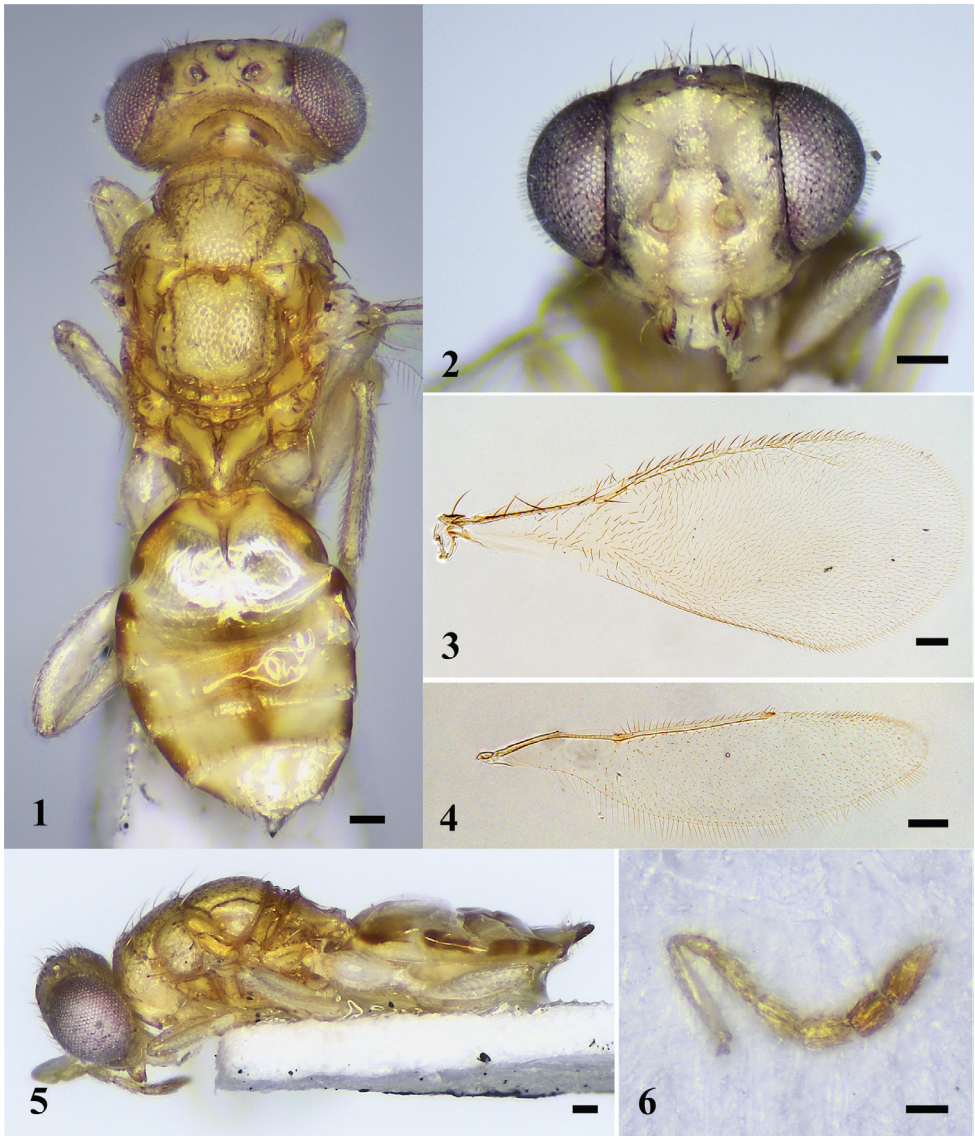
Male. Unknown.

Host. Unknown.

Distribution. China (Jiangxi).

Etymology. Latin: *octo* = eight; and refers to the midlobe of mesoscutum with four pairs of long setae.

Remarks. *Diglyphomorphomyia octoseta* is similar to *D. kairali* Narendran & Girish Kumar in sharing a propodeum with a median carina bifurcating anteriorly and meeting a perpendicular lamina, but can be separated from the latter by the



Figures 17–22. *D. octoseta* sp. nov., female, holotype **17** habitus in dorsal view **18** head in frontal view **19** fore wing **20** hind wing **21** habitus in lateral view **22** antenna. Scale bars: 100 µm.

following combination of characters: fore wing hyaline without infuscation (fore wing with brown infuscation a short distance below STV in *D. kairali*); antenna with scape white, pedicel and F1–F3 pale yellow, clava brown except apex yellowish (antenna brownish black with scape and pedicel pale brownish yellow in *D. kairali*); midlobe of mesoscutum with four pairs of long setae (three pairs of long setae in *D. kairali*).

Acknowledgements

We would like to thank reviewers Dr Christer Hansson, Dr Ryan Perry, and the subject editor for providing valuable comments on earlier drafts of this manuscript. We are also grateful to Dr Hui Geng, Dr Xiang-Xiang Jin, Dr Guo-Hao Zu, Dr Si-Zhu Liu, Mr Guang-Xin Wang, Dr Wen-Jian Li, Dr Ye Chen, Mr Chao Zhang, Miss Yan Gao, and Miss Yu-Ting Jiang for specimen collection.

References

- Bouček Z (1988) Australasian Chalcidoidea (Hymenoptera). A Biosystematic Revision of genera of fourteen families, with a reclassification of species. CAB International, Wallingford, Oxon/Cambrian News Ltd, Aberystwyth, Wales, 832 pp.
- Girault AA (1913) Australian Hymenoptera Chalcidoidea – IV. *Memoirs of the Queensland Museum* 2: 140–296. <https://www.biodiversitylibrary.org/page/39666066>
- Girault AA (1915) Australian Hymenoptera Chalcidoidea – IV Supplement. *Memoirs of the Queensland Museum* 3: 180–299.
- Hymenoptera Anatomy Consortium (2021) Hymenoptera Anatomy Ontology Portal. <http://glossary.hymao.org> [accessed 1 December 2021]
- Narendran TC (2004) Descriptions of a new subgenus and two new species of Eulophidae (Hymenoptera: Chalcidoidea) from India. *Records of the Zoological Survey of India* 103(3–4): 129–135.
- Narendran TC (2011) Fauna of India, Eulophinae (Hymenoptera: Eulophidae). *Zoological Survey of India, Kolkata*, [iii +] 442 pp.
- Narendran TC, Girish Kumar P, Santhosh S (2005a) Record of three new species of Eulophidae (Hymenoptera: Chalcidoidea) along with a new report of genus *Necremnoides* Girault from Indian subcontinent. *Journal of Entomological Research* 29(2): 149–153.
- Narendran TC, Girish Kumar P, Santhosh S, Sinu PA (2005b) A study on the taxonomy of *Diglyphomorphomyia* Girault (Hymenoptera: Eulophidae) of India. *Journal of Advanced Zoology* 26(1): 29–34.
- Noyes JS (1982) Collecting and preserving chalcid wasps (Hymenoptera: Chalcidoidea). *Journal of Natural History* 16(3): 315–334. <https://doi.org/10.1080/00222938200770261>
- Noyes JS (2021) Universal Chalcidoidea Database. World Wide Web electronic publication. <http://www.nhm.ac.uk/chalcidoids> [accessed 1 December 2021]
- Ubaidillah R (2003) Parasitoid wasps of Eulophinae (Hymenoptera: Eulophidae) in Nusa Tenggara Timur, Indonesia. *Treubia* 33(1): 43–70.
- Yefremova ZA (2007) The subfamilies Eulophinae, Euderinae and Entedoninae (Hymenoptera: Eulophidae) in Yemen. *Fauna of Arabia* 23: 335–368.
- Zhu CD, Huang DW (2003) Chinese species of *Diglyphomorphomyia* Girault (Hymenoptera: Eulophidae). *Zoological Studies (Taipei, Taiwan)* 42(3): 444–449.

Description of two new species of the genus *Tillicera* Spinola (Coleoptera, Cleridae, Clerinae), with new synonyms, new distributional records, and an updated key

Hiroyuki Murakami¹, Roland Gerstmeier², Kaoru Sakai³

1 Entomological Laboratory, Faculty of Agriculture, Ehime University, 3-5-7 Tarumi, Matsuyama, 790-8566 Japan **2** Zoologische Staatssammlung München, Münchhausenstraße 21, 81247 München, Germany **3** Ōta-ku, Tokyo, Japan

Corresponding author: Hiroyuki Murakami (hiroyuki068@gmail.com)

Academic editor: C. Majka | Received 10 January 2022 | Accepted 23 March 2022 | Published 13 April 2022

<http://zoobank.org/FF352C24-8477-4820-808E-324A32847888>

Citation: Murakami H, Gerstmeier R, Sakai K (2022) Description of two new species of the genus *Tillicera* Spinola (Coleoptera, Cleridae, Clerinae), with new synonyms, new distributional records, and an updated key. ZooKeys 1095: 123–142. <https://doi.org/10.3897/zookeys.1095.80097>

Abstract

Two species, *Tillicera fortis* **sp. nov.** and *Tillicera spinosa* **sp. nov.**, are newly described. New distributional records are presented for *Tillicera callosa* Gerstmeier & Bernhard, 2010, *Tillicera javana* Spinola, 1844, *Tillicera pseudocleroides* Gerstmeier & Bernhard, 2010, *Tillicera soror* Schenkling, 1902, and *Tillicera tonkinensis* Gerstmeier & Bernhard, 2010. *Clerus postmaculatus* Nakane, 1963 **syn. nov.** is synonymized with *Tillicera ihlei* Corporaal, 1949. The presence of sensory organs (sensilla) on the ventral surface of the antennae is discovered in *Tillicera* and *Hemitrachys* for the first time. A key to the valid species of *Tillicera* is provided.

Keywords

Antennal sensilla, checkered beetles, Oriental Region, taxonomy

Introduction

The genus *Tillicera* Spinola (Coleoptera, Cleridae) belongs to the subtribe Clerina Latreille, 1802 of the tribe Clerini Latreille, 1802 (Bartlett 2021). This genus forms part of the *Tillicera* genus group with *Apopemopsis* Schenkling, 1903, *Cardiostichus*

Quedenfeldt, 1885, *Hemitrachys* Gorham, 1876, *Placocerus* Klug, 1837, and *Plathanocera* Schenkling, 1902 (Gerstmeier and Stapel 2016). Until now, 17 species of the genus have been known from the Oriental region (Gerstmeier and Bernhard 2010; Yang et al. 2011). Many species are known for their mimicry of the wasp family Mutillidae (Shelford 1902; Opitz 2010).

In this paper, we describe two new species and synonymize one species, *Clerus postmaculatus* Nakane, 1963a with *Tillicera ihlei* Corporaal, 1949. We provide an updated key to the valid species of the genus, plus photographs illustrating the antennal sensory organs previously discussed by Yang et al. (2011).

Materials and methods

The dissection method of terminal parts and genitalia follows Murakami (2016). The terminology of male genitalia follows Bartlett (2021). The material in this study is deposited in following institutions and private collections:

- EUMJ** Ehime University Museum, Matsuyama, Japan;
KSCJ private collection of Kaoru Sakai, Tokyo, Japan;
MMCJ private collection of Masafumi Matsumura, Okinawa, Japan;
MTCJ private collection of Minoru Tanaka, Japan;
NHMB Natural History Museum Basel, Switzerland;
NHMI Natural History Museum and Institute, Chiba, Japan;
NMPC National Museum Prague, Czech Republic;
OLML Oberösterreichisches Landesmuseum Linz, Austria;
QSBG Queen Sirikit Botanic Garden, Entomology Section, Chiang Mai Prov., Thailand;
RGCM Roland Gerstmeier Collection, Munich (deposited in ZSM, Zoological State Collection Munich), Germany;
SEHU Systematic Entomology, Hokkaido University, Sapporo, Japan.

The original spelling of label data is indicated by double quotation marks (“ ”); line brakes are indicated by a slash (/).

The abbreviations for measurements are as follows:

- BL** body length (from tip of head to elytral apex);
EL elytral length (from basal margin to apex along suture);
EW maximum conjoined width of elytra;
EyD distance between eyes in dorsal view;
EyW maximum width of a single eye in dorsal view;
PL maximum length of pronotum;
PW maximum width of pronotum.

Taxonomic account

Genus *Tillicera* Spinola, 1841

Tillicera Spinola, 1841: 73; Gerstmeier and Bernhard 2010: 3; Gerstmeier and Stapel 2016: 539.

Diagnosis. The genus *Tillicera* is closely related to *Hemitrachys* Gorham but differs from it by the following characteristics (Yang and Yang 2013; Gerstmeier and Stapel 2016): antennomeres V–XI not clubbed; elytral length to width ratio 2.01–2.37; pulvillar formula 4–4–2, 4–4–3 or 4–4–4 (*Hemitrachys*: antennomeres V–XI clubbed; elytral length to width ratio 1.58–1.80; pulvillar formula 4–2–2).

Remarks. In male and female adults of *Thanasimus substriatus*, sensilla basiconica were distributed in clusters that formed a line along the posterior border from the fifth to the eighth antennomere (Zhang et al. 2021). The area of the apical margin of antennae in ventral view, which is vested with sensilla basiconica, was discovered in *Tillicera callosa*, *Tillicera fortis* sp. nov., *Tillicera spinosa* sp. nov., and *Hemitrachys tubericollis* Yang & Yang, 2013 for the first time (Figs 29–31, 34, 35). The genus *Tillicera* is included in the *Tillicera* genus group with *Apopemopsis*, *Cardiostichus*, *Hemitrachys*, *Placocerus*, and *Plathanocera* (Gerstmeier and Stapel 2016); the monophyly of the genus group, however, is questioned by Bartlett (2021).

In the first author's observations, this remarkable antennal structure is also seen in two other genera, *Clerus* Geoffroy, 1762 and *Omadius* Laporte, 1838, which are included into the subtribe Clerina Latreille, 1802 (see Bartlett 2021). Further investigation is required to clarify the intergeneric relationships.

Tillicera callosa Gerstmeier & Bernhard, 2010

Figs 4, 31, 36–40

Tillicera callosa Gerstmeier & Bernhard, 2010: 14, figs 4, 25. Type locality India, Darjeeling District.

Specimens examined. Vietnam: Mt. Tam Dao, Vinh Phuc Prov., 10.V.1996 (KSCJ, 2 males).

Additional description. Male. Antennomeres V–X with an area vested with sensilla basiconica at apical margin in ventral view; XI without pit-like sensillum. Elytra with two large callous areas at base. Tarsal pulvillar formula 4–4–2; protarsomeres I and II with large lobed pulvilli; III and IV with large bilobed pulvilli; mesotarsomeres I with vestigial minute pulvillus; II with small lobed pulvillus; III and IV with small bilobed pulvilli; metatarsomeres I and II without pulvilli; III and IV with small bilobed pulvilli.

Abdominal sternite V almost transverse. Pygidium weakly emarginated at apical margin (Fig. 36); apical margin of ventrite VI (Fig. 37) emarginated at middle; spicular forked, long (Fig. 38).

Tegmen (Fig. 39a–c) with dorsal and ventral sinuses at apical 1/6 of total length; tegminal arms long, extending 1/3–2/3 of total length. Median lobe (Fig. 40a–c) longer than tegmen; plate simple, without denticles.

Remarks. This species was originally described based on a single female specimen from India. In this paper, we describe the male in detail. This species is also related to *Hemitrachys bizonatus* Gorham, 1876 based on the structure of the male genitalia.

Distribution. India. New record: Vietnam.

Tillicera ihlei Corporaal, 1949

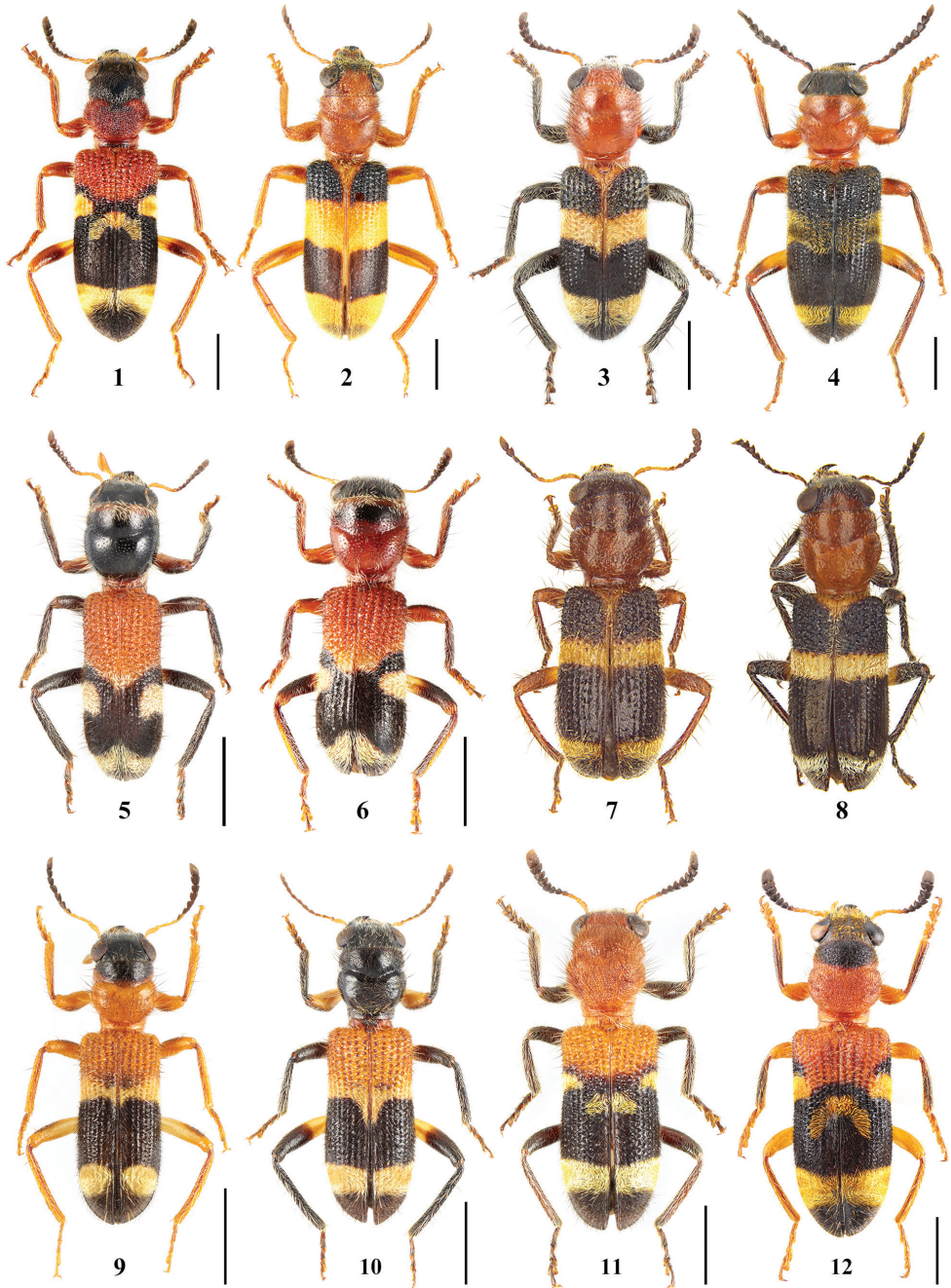
Figs 9, 10

Tillicera ihlei Corporaal, 1949: 99 (type locality Indonesia, Java); Gerstmeier and Bernhard 2010: 19, figs 9, 30–31

Clerus postmaculatus Nakane, 1963a: 46 (type locality Japan, Nakanoshima Is.); 1963b: 183; Miyatake 1985: 156. syn. nov.

Type specimen examined. Holotype of *Clerus postmaculatus*. **Japan:** “NAKANOSHIMA/ Is. Tokara/ 7.vii.1960/ M. Sato leg.” (SEHU, 1 male).

Other specimens examined. Japan: [Kagoshima] Kankake-dake, alt. 220 m, Yakushima, 19.VII.–22.VII.2006, T. Yamauchi leg. (EUMJ, 3 exs); same locality and collector, 8.VI.–28.VI.2007, (EUMJ, 2 exs); same locality and collector, 28.VI.–30.VII.2007, (EUMJ, 5 exs); Hanyama, alt. 250 m, Yakushima, 22.VI.–22.VIII.2006, T. Yamauchi leg. (EUMJ, 3 exs, Malaise Trap); same locality and collector, 28.VI.–30.VII.2007, (EUMJ, 3 exs); same locality and collector, 27.VII.–30.VII.2007 (EUMJ, 3 exs); Aiko-dake, alt. 150 m, 28.VI.–29.VII.2007, Y. Takeo leg. (EUMJ, 1 ex., Malaise Trap); Miyanoura, Yaku-shima, 10.VII.1961, K. Ueda leg. (EUMJ, 1 female); Ikari, Amami-Oshima, 19.VI.1961, T. Shibata leg. (EUMJ, 1 male); same locality and collector, but 3.VII.1961. (EUMJ, 1 male); Mt. Otake, Toshima-mura, Nakano-shima, 23.VI.2004, J. Yamasako leg. (EUMJ, 1 female); Toshima, Nakano-shima, 1–7.VII.2009, M. Matsumura leg. (MMCJ, 1 ex.). [Okinawa] Iji, Kunigami-son, Okinawa-jima, 2.V.1993, M. Matsumura leg. (MMCJ, 1 male); Okuni-rindo, Kunigami-son, Okinawa-jima, 13.VI.1997, K. Inada leg. (KSCJ, 1 male); Aha, Kunigami-son, Okinawa-jima, 24.V.2012, M. Matsumura leg. (MMCJ, 1 female). **Taiwan:** [Miaoli] Xuejian Recreation Area, Tainan Township, 10. VI. 2015, S. Shih leg. (EUMJ, 8 males & 18 exs) [Taitung] 9.VI.1971, Y. Maeda leg. (EUMJ, 1 female); Jinping-forestroa, Chihshang Township, 19.VI.2011, J. Yamasako leg. (EUMJ, 1 male). [Kaohsiung] Liukei Dist., 29.IV–8.V.1982, H. Takizawa leg. (KSCJ, 1 ex.); Tengjhih, Taoyuan Dist., 14.V.1991, W. L. Chen leg. (NHMI, 1 female). [Nantou] Nanzankei, Puli Township, 8.V.1965, T. Shirozu leg. (EUMJ, 1 male); same locality, 6.V.1971, Y. Hayashi leg. (EUMJ, 1 female); same locality, 17.IV.1977, W. Suzuki leg. (KSCJ, 1 ex.); Sung Kang,



Figures 1–12. Habitus of *Tillicera* species 1 *Tillicera auratofasciata* 2 *T. aurivillosa* 3 *T. bibalteata* 4 *T. callosa* 5, 6 *T. cleroides* 7, 8 *T. hirsuta* 9, 10 *T. ihlei* 11, 12 *T. javana*. Scale bars 2 mm.

Renai Township, 8.VIII.1983, K. Ra leg. (KSCJ, 1 ex.); Gaofeng, alt. c. 1700 m, Musha, Renai Township, 24–28.VIII.2016, M. Tanaka leg. (MTCJ, 1 male); Mt. Rozan, alt. c. 1200 m, Renai Township, 29–30.VII.1976, H. Kan leg. (EUMJ, 1 female); Napankanshan, Renai Township, alt. 2050–2800 m, 20.V.1991, A. Saito leg. (NHMI, 1 male, 1 female). **Laos:** Mt. Phu Pan, Ban Saleui, Xam Neua, Houa Pan Prov., 9.V.2007, T. Mizusawa leg. (KSCJ, 1 male); Mt. Phou Pan, Ban Saleui, Hua Phan Prov., 20°13'30"N, 103°59'26"E, 1350–1900 m, 22.V.2011, C. Holzschuh & Native leg. (OLML, 1 ex.). **Thailand:** Doi Pui, Chiang Mai Prov., 28.IV.1983, H. Kan leg. (EUMJ, 1 ex.); Meo Village, Chiang Mai Prov., 1.V.1987, S. Saito leg. (KSCJ, 1 ex.); Chang Dao, Pa kia, Chiang Mai Prov., 4–5.V.2000, K. Okajima leg. (KSCJ, 1 ex.); Wiang Pa Pao, Chiang Rai Prov., 17–21.V.2015, K. Takahashi leg. (KSCJ, 1 ex.); same locality, 20–29.V.2017, K. Takahashi leg. (KSCJ, 3 exs); Chiang Rai, Wiang Pa Pao, Mae Chedi, alt. 1200 m, 9–12.V.2018, S. Imada & S. Inoue leg. (EUMJ, 2 exs); Mae Hong Son, Ban Huai Po, 1600–2000 m, 9.–16.V.1991, J. Horah leg. (NMPC, 1 male). **Myanmar:** Maymyo (Pin Oo Lwin), alt. c. 1000 m, Mandalay Div., 6.VII.2001, Y. Kusakabe leg. (KSCJ, 1 ex.).

Description. For more details see Gerstmeier and Bernhard (2010). The color variation is recognized as follows (Figs 9, 10): pronotum black at apical 1/3 and reddish at basal 2/3; black at apical 1/2 and reddish on remainder, wholly black and partly reddish at base; elytra sometimes partly black between basal reddish area and basal whitish fascia; femora yellow at base and black at apex; however, that color area is variable. Antennomeres V–X with a smooth area at apical margins in ventral view; XI without pit-like sensillum.

Remarks. *Clerus postmaculatus* was described from Nakano-shima Is., Okinawa Pref., Japan, by Nakane (1963a). After close examination of the type specimen, we conclude its synonymy with *Tillicera ihlei*.

Distribution. Indonesia. New records: Japan, Laos, Myanmar, Taiwan, Thailand.

Tillicera javana Spinola, 1844

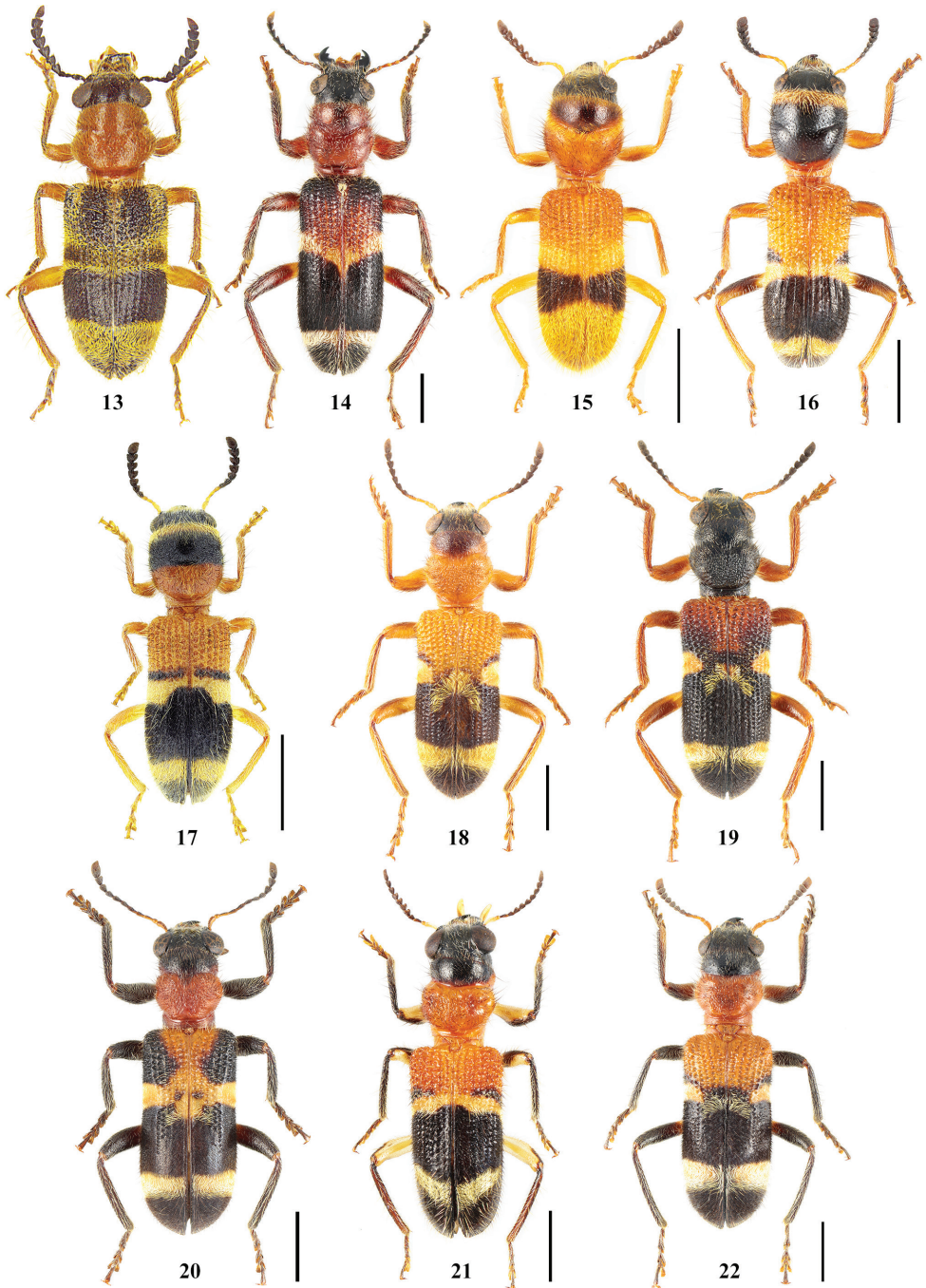
Figs 11, 12

Tillicera javana Spinola, 1844: 160, pl 12, fig. 2 (type locality Indonesia, Java); Schenckling 1906: 262; Gerstmeier and Bernhard 2010: 21.

Tillicera javanica: Desmarest 1860: 241, fig. 169; Gorham 1893: 567.

Tillicera javana ab. *luchti* Corporaal, 1949: 100 (type locality Indonesia, Sumatra); Gerstmeier and Bernhard 2010: 23.

Specimens examined. **Laos:** Phou Samsoum, Xiang Khouang Prov., 2.VI.2007, J. Yamasako leg. (EUMJ, 1 ex.); Souy Dist., West of Phonsavan 40–50 km, Xiang Khouang Prov., 17–18.VI.2008, J. Yamasako leg. (EUMJ, 1 female); Mt. Phu Pan, Ban Saleui, Xam Neua, Houa Pan Prov., alt. 1500–1700 m, 4.V.2002, N. Ohbayashi leg. (EUMJ, 1 ex.); same locality, alt. 1600–1900 m, 2–10.IV.2005, unknown collector (EUMJ, 1 ex.); same locality, alt. 1700–1800 m, 17–20.VI.2003, N. Ohbayashi leg.



Figures 13–22. Habitus of *Tillicera* species 13 *Tillicera michaeli* 14 *T. obscura* 15 *T. paula* 16, 17 *T. pseudocleroides* 18, 19 *T. sensibilis* 20 *T. soror* 21 *T. tonkinensis* 22 *T. wenii*. Scale bars 2 mm.

(EUMJ, 2 exs); same locality, alt. 1750 m, 16–20.V.2004, M. Sato leg. (EUMJ, 1 ex.); same locality, alt. 1400–1500 m, 20–24.VI.2003, N. Ohbayashi leg. (EUMJ, 1 ex.). **Thailand:** Khao Yai, 10. VI.1992. (EUMJ, 9 exs); Doi Pui, Chiang Mai Prov., 8.V.1983, H. Kan leg. (EUMJ, 1 ex.). **Vietnam:** Mt. Tam Dao, alt. 930 m, Vinh Phuc Prov., 1–7.V.1996, Y. Arita leg. (EUMJ, 4 exs); Mt. Lang Biang, alt. c. 1800 m, Lac Duong Dist., Lam Dong Prov., 31.V.2016, M. Matsumura leg. (EUMJ, 1 female).

Additional description. This species is variable in its pronotal color (Gerstmeier and Bernhard 2010). Additional variation is recognized as follows: head and pronotum completely reddish (Fig. 11); legs yellowish (Fig. 12). Antennomeres V–X vestigial with an area vested with sensilla basiconica at apical margin in ventral view; male XI of dorsal surface with pit-like sensillum.

Remarks. Opitz's (2010, fig. 217) photograph labelled *T. javana*, used to illustrate a likeness to mutilid wasps, appears to be a misidentified specimen of *Tillicera tonkinensis* Gerstmeier & Bernhard, 2010

Distribution. Indonesia (Java, Sumatra), Malaysia (Borneo, Sabah). New records: Laos, Thailand, Vietnam.

Tillicera pseudocleroides Gerstmeier & Bernhard, 2010

Figs 16, 17

Tillicera pseudocleroides Gerstmeier & Bernhard, 2010: 27, figs 15, 39–40. Type locality Indonesia (Java, Sumatra), Malaysia (Pahang).

Specimens examined. Laos: Attapeu Prov., Thong Kai Ohk, Ban Kachung (Mai) env., 1200–1450 m, 15°01.02'N, 107°26.27'E, 10.-24.VI.2011, M. Brancucci, M. Geiser, D. Hauck, Z. Kraus, A. Phantala & E. Vongphachan (NHMB, 1 female); Souy Dist., West Phonsavan 40–50 km, Xieng Khouang Prov., 17–18.VI.2008, J. Yamasako leg. (EUMJ, 1 female).

Additional description. The colour of the pronotum, elytra, and legs are variable in this species (Figs 16, 17). Antennomeres V–X with an area vested with sensilla basiconica at the apical margin in ventral view.

Distribution. Indonesia (Java, Sumatra), Malaysia. New record: Laos.

Tillicera soror Schenkling, 1902

Fig. 20

Tillicera soror Schenkling, 1902: 127 (type locality Bhutan); Schenkling 1903: 121, pl. 1, fig. 10; Corporaal 1939: 26; Gerstmeier and Bernhard 2010: 29, figs 16, 41, 42. *Rhytidoclerus soror*: Pic 1934: 133.

Specimens examined. Vietnam: Mt. Phang Xi Pang, N. rdg., alt. 1950–1970 m, Hoang Lien Son Mts., Lai Chau Prov., 11.V.1995, A. Saito leg. (KSCJ, 1 male); Mt.

Pia Oac, Deo Kolea, alt. 1250–1300 m, Cao Bang Prov., N. Vietnam, 23–24.V.1999, A. Saito leg (KSCJ, 1 female).

Additional description. Antennomeres V–X with an area vested with sensilla basiconica at apical margin in ventral view; male antennomere XI with pit-like sensillum. Tarsal pulvillar formula 4–4–2, but in one male from Vietnam 4–4–4.

Distribution. Bhutan, India, Nepal. New record: Vietnam.

***Tillicera tonkinensis* Gerstmeier & Bernhard, 2010**

Fig. 21

Tillicera tonkinensis Gerstmeier & Bernhard, 2010: 32, figs 17, 43–44. Type locality Vietnam, Tam dao.

Specimens examined. Laos: Salavan Prov., 16°08'N, 106°42.43'E, Xe Xap NPA, c. 15 km NE of Ta-oy, BAN DOUB env., 600–900 m, 26.–30.v.2012. NHMB Basel, Expedition Laos 2012: M. Brancucci, M. Geiser, V. Phanthavong, S. Xayalath (NHMB, 1 ex.).

Additional description. Antennomeres V–X with an area vested with sensilla basiconica at the apical margin in ventral view.

Distribution. Vietnam. New record: Laos.

***Tillicera fortis* sp. nov.**

<http://zoobank.org/E1E56C85-8AC4-4A6A-AA70-9A4AA6D0C692>

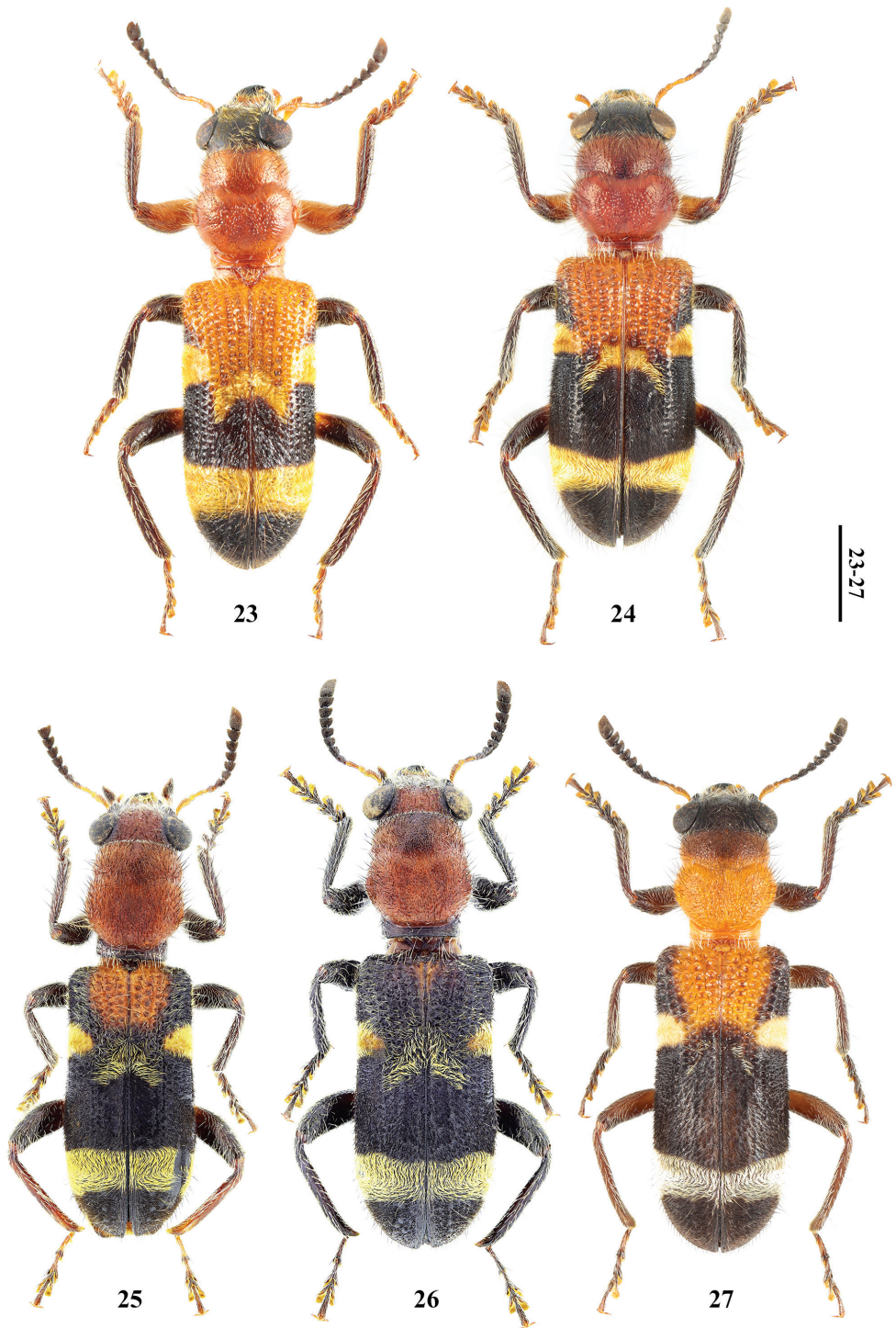
Figs 23, 24, 41–45

Types. Holotype. Laos: “E. Phonsavan, 25 km, / Xiang Khouang/ 19.VI.2005/ J. Yamasako leg.”, (EUMJ, 1 male) **Paratype. Thailand:** “Doi Pui/ Chiang Mai Prov./ N. Thailand/ 13–14. VI. 1979/ W. Suzuki leg”, (EUMJ, 1 female).

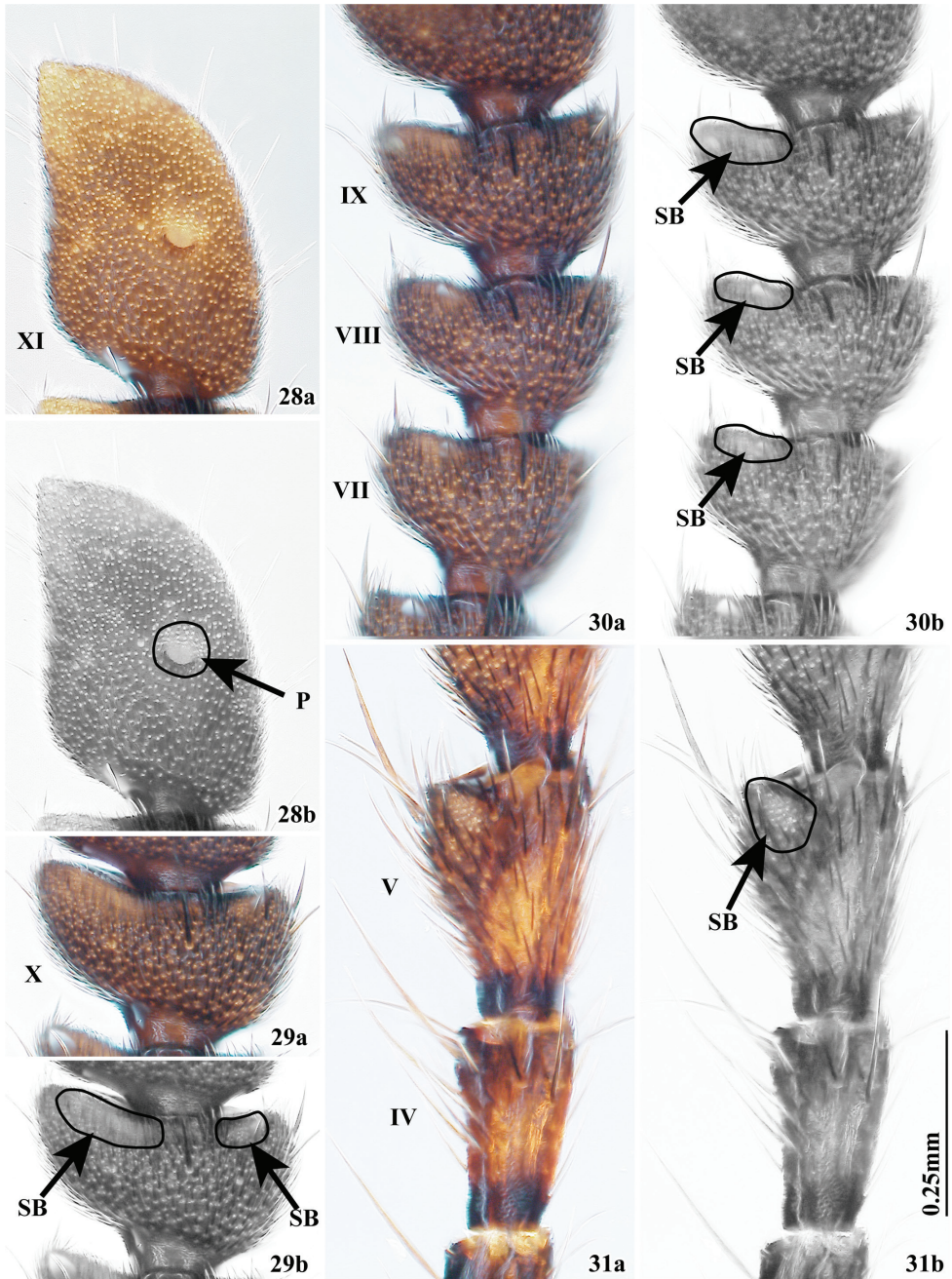
Diagnosis. This species is similar to *T. auratofasciata*, but can be distinguished by the following characteristics: male antennomere X as wide as long; punctuation of pronotum sparse; tegmen with deep sinus at apical 1/4; denticles of phallic plates extending to apex (vs. *T. auratofasciata*: male antennomere X wider than long; punctuation of pronotum dense; tegmen with sinus at apical 1/6; denticles of phallus not extending to apex).

Description. Male. Head black; antennomeres V–XI, apex of profemora, meso- and metafemora except for base, tibiae, and tarsi brownish black; pronotum and profemora except for apex and base of meso- and metafemora reddish; elytra reddish at basal 1/3, remainder black, with three yellow maculations extending from lateral margin of basal 1/4 interrupted before suture, outwardly curved from suture of basal 1/3, and transversely at apical 1/4, confluent with suture.

Head including eyes slightly narrower than pronotum; labrum incised medially; maxillary terminal palpomeres digitiform; labial terminal palpomeres widely triangu-



Figures 23–27. Habitus of *Tillicera* **23** *Tillicera fortis* sp. nov., Holotype, male **24** ditto, paratype, female **25** *T. spinosa* sp. nov., Holotype, male **26** ditto, paratype, male **27** ditto, paratype, female. Scale bars 2 mm.



Figures 28–31. Antennae of *Tillicera* spp. (28 dorsal view 29–31 ventral view) 28 male antennomere XI of *T. spinosa* sp. nov. 29 female antennomere X of *T. spinosa* sp. nov. 30 female antennomeres VII–IX of *T. spinosa* sp. nov. 31 male antennomeres IV and V of *T. callosa*. Abbreviations: P pit-like sensillum SB an area of sensilla basiconica.

lar; postgular plate narrow. Antennomere I claviform; II compact; III twice as long as II; IV–X triangular, becoming gradually widened; IX as long as wide; X slightly wider than long; V–X with an area vested with sensilla basiconica at apical margin in ventral view; XI with a pit-like sensillum.

Pronotum slightly longer than wide, widest at middle, with fine dense punctures. Mesoventrite with short anterior process.

Elytra oblong, parallel sided, covered with ten striae; striae I–III absent before basal oblique yellow fascia; IV–VI extending after middle; VII and VIII weakly punctured after base of lateral yellow fascia; IX and X obscure.

Tibiae stout, with longitudinal carina; tibial spur formula 1–2–2; tarsal pulvillar formula 4–4–4; pro- and mesotarsomeres I and II with large lobed pulvilli; III and IV with large bilobed pulvilli; metatarsomeres I with vestigial minute pulvillus; II with small lobed pulvillus; III and IV with large bilobed pulvilli; claws with basal denticles.

Abdominal sternite V deeply, marginated at apical margin. Pygidium (Fig. 41) almost transverse at apical margin; ventrite VI (Fig. 42) broadly emarginated at apical margin; spicular fork (Fig. 43) long, without intraspicular plate.

Tegmen (Fig. 44a–c) with dorsal and ventral sinus at apical 1/4; parameroid lobes tapered posteriorly at apex in lateral view, flattened at apex; tegminal arms short, extending middle to basal 1/4 of total length. Median lobe (Fig. 45a–c) slightly shorter than tegmen; plates with rows of denticles on apex of dorsal and ventral sides, on left side in ventral view these are positioned at apical 1/5, on right side in ventral view they are very short.

Female. Similar to male but distinguished by the following characteristics: antennomere XI without pit-like sensillum; sternite V with shallower emargination at apical margin. Elytral striae VI to VIII weakly punctured posterior to base of lateral yellow fascia.

Measurements and ratios. Male ($N = 1$). BL 8.80 mm; PL 2.60 mm; PW 2.25 mm; EL 6.20 mm; EW 2.80 mm; EyW 0.50 mm; EyD 0.95 mm; PL/PW 1.16; EL/EW 2.21; EL/PL 2.38; EW/PW 1.24; EyD/EyW 1.90. **Female** ($N = 1$). BL 8.65 mm; PL 2.45 mm; PW 2.25 mm; EL 6.20 mm; EW 2.90 mm; EyW 0.55 mm; EyD 1.05 mm; PL/PW 1.09; EL/EW 2.14; EL/PL 2.53; EW/PW 1.29; EyD/EyW 1.91.

Etymology. This specific name is derived from the Latin *fortis* (sturdy), referring to the stout tibiae.

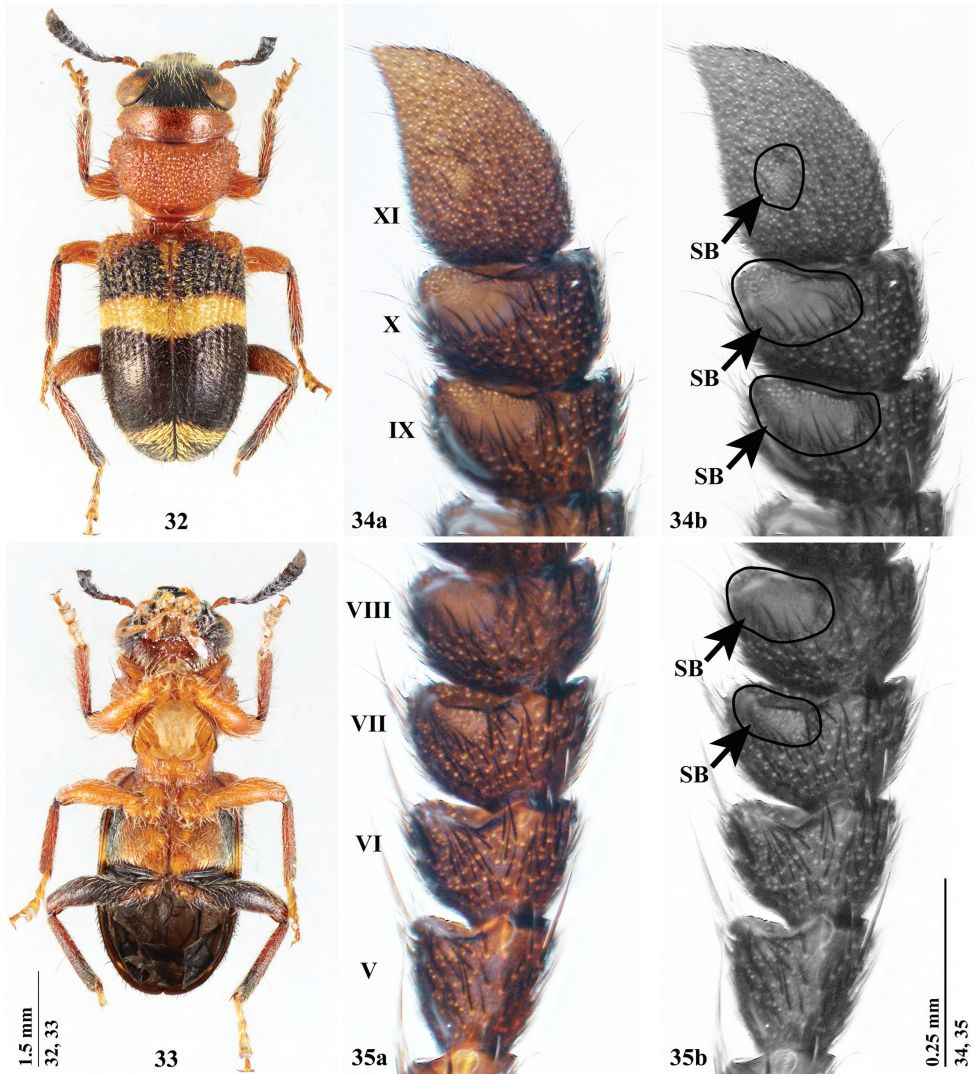
Distribution. Laos, Thailand.

***Tillicera spinosa* sp. nov.**

<http://zoobank.org/2E35F6F1-8F4A-4BB9-957F-82173B1EB70E>

Figs 25–30, 46–50

Types. Holotype. “Doi Pui, 1400–/ 1500 m, Chiang Mai, N. Thailand, 19-VI-1983, T. Shimomura leg”. (RGCM, 1 male, erroneously cited in Gerstmeier and Bernhard (2010) under *T. auratofasciata*). **Paratypes. Laos:** “NE LAOS/ Phu Pan, 1,750 m/ Ban Saleui, Xam Neua/ Houa Phan Prov./ 16–23.VI.2003/ Shinji Nagai



Figures 32–35. *Hemitrachys tubericollis* **32, 33** habitus in dorsal (**32**) and ventral (**33**) views **34** male antennomeres IX–XI in ventral view **35** male antennomeres V–VIII in ventral view. Abbreviations: **SB** an area of sensilla basiconica.

leg.” (KSCJ, 1 female). **Myanmar:** “near Kalaw/ 1,000–1,300 m in alt./ Shan Sta., Myanmar/ 10–25.V.2005/ Y. Kusakabe leg.” (EUMJ, 1 male & 1 female; KSCJ, 1 male & 2 females); “Mt. Victoria/ (Natmataung N. P.)/ alt. 1500–2750m/ Kanpelet side”, “Chin Sta., Myanmar/ 21–24. V. 2002/ Y. Kusakabe leg.” (EUMJ, 1 male; KSCJ, 1 male & 1 female); “Mt. Victoria/ alt. 1500–2000 m/ Mindat side”, “Chin Sta., Myanmar/ 13–14.VI.2002/ Y. Kusakabe leg.”, (KSCJ, 1 female). **Thailand:**

“Doi Pui Chieng Mai/ N – THAILAND/ 22.V.1986/ leg.” (KSCJ, 1 female); QSBG-2014-0160-0010, Amnat Charoen, Chanuman Dist., Doi Inthanon NP, 18°32'44.4"S, 98°30'53"E, 1376 m, 29.V.-1.VII.2014, Malaise trap, Wichai Srisuka et al. (RGCM, 1 ex.); Same with QSBG....-0008 (RGCM, 1 ex.); Same with QSBG....-0009 + 0011 (QSBG, 3 exs). **China:** S-Yunnan (Xishuangbanna), c. 30 km NW Jinghong, vic. Bameng, 1700–2000 m; Hua Zhuliangzi Mts., 22°08.01'N, 100°31.54'E, 1700–2000 m, 30.V.2008, leg. A. Weigel, sec. forest (RGCM, 1 male).

Diagnosis. This species is similar to *Tillicera soror* Schenkling, 1902, but distinguished by the following characteristics: antennomere VI–X gradually broadened; metatibiae apically extended to a broad spine; posterior margin of abdominal ventrite V, with broadly V-shaped emargination; phallobase notched at apical 1/5 of total length of tegmen (vs. *T. soror*: antennomere VIII–IX gradually broadened; hind tibiae not prominent at apex; posterior margin of abdominal sternite V broadly U-shaped and truncate; phallobase deeply notched at apical 1/3).

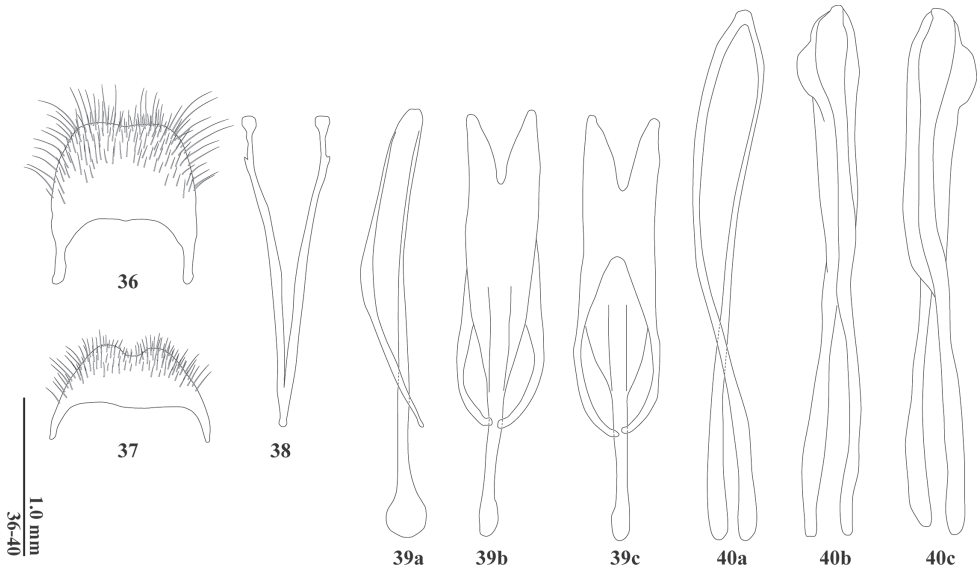
Description. Male. Head, antennomeres IV–XI, base of pronotum and legs brownish black; antennomeres I–III and pronotum reddish. Elytra black except for reddish area near basal suture and yellowish area at basal 1/4 near lateral margin. Head at apex and legs covered with white setae; basal 1/2 of head and pronotum with mingled white and black setae; elytra densely vested with yellowish setae obliquely at suture of basal 1/3 and transversally at lateral margin basal 1/4 and apical 1/4, the remainder vested with black setae (Fig. 10). This species has two color patterns: the first, antennomeres IV–XI, apex of pronotum, elytra except for area covered with yellowish setae, and legs black (Fig. 11); the second, head black; apical 1/4 of pronotum brownish black; elytral setae white and black (Fig. 12).

Head including eyes as wide as pronotum; labrum incised at middle; maxillary terminal palpomeres digitiform; labial terminal palpomeres widely triangular; postgular plate narrow. Antennomere I claviform; II compact; III twice as long as II; IV–X triangular, becoming gradually widened; V–IX (Fig. 30) with an area vested with sensilla basiconica; X (Fig. 29) with two areas vested with sensilla basiconica at apical margin in ventral view; XI (Fig. 28) with small pit-like sensillum in male.

Pronotum slightly longer than wide, widest at middle, with fine dense punctures. Mesoventrite with short anterior process.

Elytra oblong, parallel sided, covered with ten striae; striae I and II absent before basal oblique yellow fascia; III–V or VII extending after middle, sometimes absent before basal oblique yellow fascia; VI or VIII–X rudimentary.

Profemora stouter than meso- and metafemora; punctation of meso- and metafemora denser than that of profemora. Tibiae short prominent at apex, with distinct longitudinal carina on dorsal and ventral surfaces; tibial spur formula 1–2–0; tarsal pulvillar formula 4–4–2; pro- and mesotarsomeres I and II with large lobed pulvilli; III and IV with large bilobed pulvilli; metatarsomeres I and II without pulvilli; III and IV with large bilobed pulvilli; claws with basal denticles.



Figures 36–40. Male terminal parts and aedeagus of *Tillicera callosa* **36** pygidium **37** ventrite VI **38** spicular fork **39** tegmen in lateral (a), ventral (b) and dorsal (c) views **40** median lobe in lateral (a), ventral (b), and dorsal (c) views.

Abdominal ventrite V deeply emarginated at apical margin. Pygidium (Fig. 46) narrowly emarginated at apical margin; ventrite VI (Fig. 47) almost transverse at apical margin; spicular fork long (Fig. 48), without intraspicular plate.

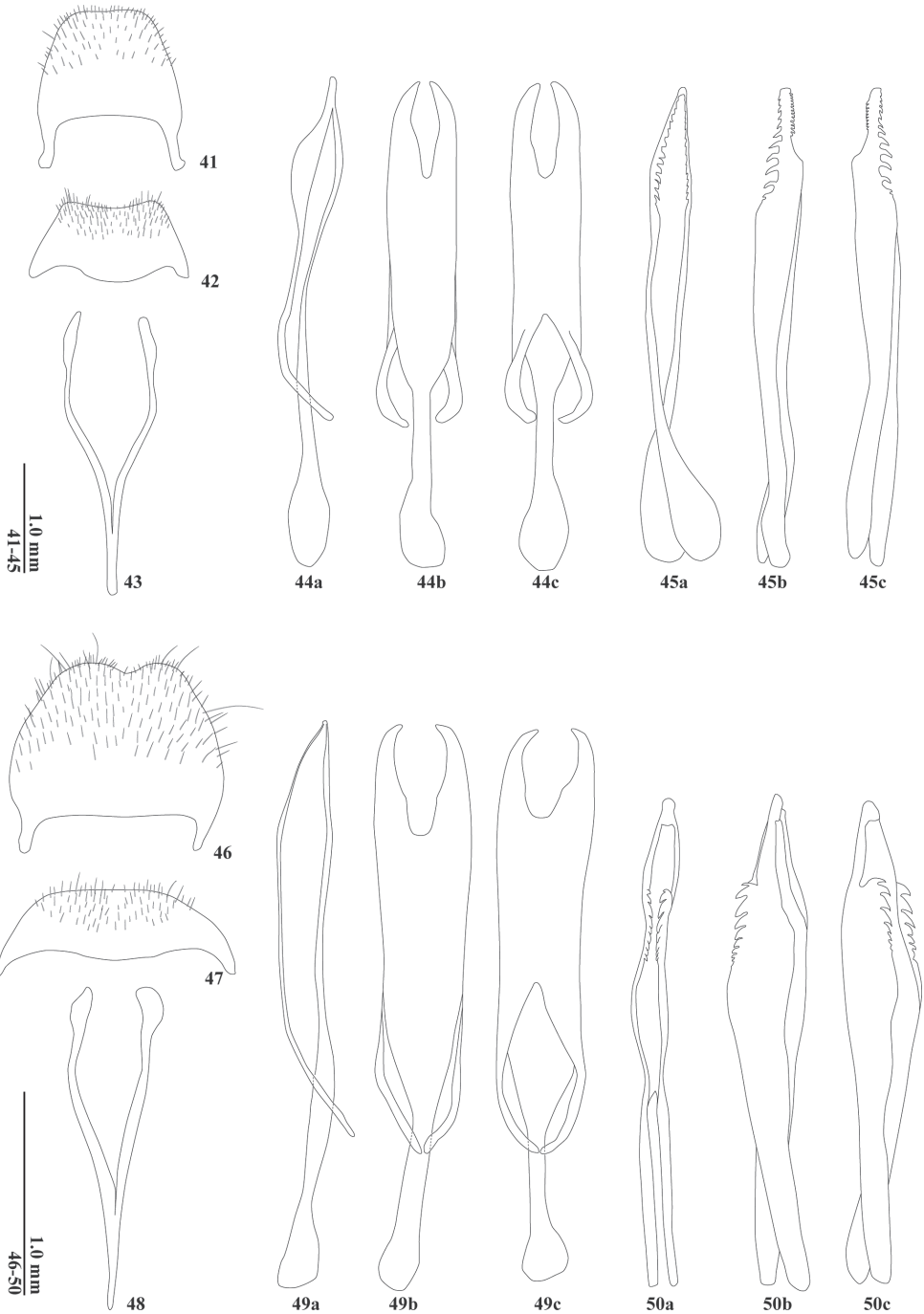
Tegmen (Fig. 49a–c) with dorsal and ventral sinus at apical 1/5; parameroid lobes tapered posteriorly at apex in lateral view; tegminal arms short, extending from middle to basal 1/4 of total length. Median lobe shorter than tegmen; plates with rows of denticles from apical 1/5 to 2/5 of total length on dorsal and ventral sides (Fig. 50a–c).

Female. Similar to male but distinguished by antennomere XI without pit-like sensillum, tibial spur formula 1–2–2 and apex of metatibiae not extended to a broad spine.

Measurements and ratios. Male ($N = 4$). BL 6.55–8.30 (7.14) mm; PL 1.75–2.30 (1.99) mm; PW 1.55–2.10 (1.78) mm; EL 4.60–6.00 (5.15) mm; EW 2.10–2.65 (2.29) mm; EyW 0.40–0.55 (0.49) mm; EyD 0.55–0.95 (0.76) mm; PL/PW 1.10–1.14 (1.12); EL/EW 2.09–2.36 (2.25); EL/PL 2.24–2.81 (2.60); EW/PW 1.22–1.35 (1.29); EyD/EyW 1.38–1.73 (1.56). **Female** ($N = 4$). BL 8.00–8.90 (8.49) mm; PL 2.20–2.50 (2.36) mm; PW 2.00–2.25 (2.10) mm; EL 5.80–6.50 (6.13) mm; EW 2.50–2.75 (2.65) mm; EyW 0.50–0.60 (0.54) mm; EyD 0.95–1.05 (1.00) mm; PL/PW 1.07–1.20 (1.13); EL/EW 2.23–2.36 (2.31); EL/PL 2.42–2.77 (2.59); EW/PW 1.22–1.31 (1.26); EyD/EyW 1.73–2.00 (1.87).

Etymology. This specific name is derived from the Latin *spinosa* (spine), referring to metatibiae apically extended to a broad spine.

Distribution. Laos, Myanmar, Thailand.



Figures 41–50. Male terminal parts and aedeagus **41–45** *Tillicera fortis* sp. nov. **46–50** *T. spinosa* sp. nov. **41, 46** pygidium **42, 47** ventrite VI **43, 48** spicular fork **44, 49** tegmen in lateral (a), ventral (b) and dorsal (c) views **45, 50** median lobe in lateral (a), ventral (b), and dorsal (c) views.

Key to the species of *Tillicera* Spinola, 1844

Based on Gerstmeier and Bernhard (2010) and Yang et al. (2011).

- 1 Elytra with sickle-like, posteriorly open, semicircle of silvery or golden setae 2
 – Elytra without such an arrangement of setae 8
- 2 Brown color of elytral base not reaching the lateral margin of elytra..... 3
 – Brown color of elytral base reaching the lateral margin of elytra..... 4
- 3 Only antennomere X wider than long or as wide as long; male metatibiae apically not extended to a broad spine (Bhutan, India, Laos, Nepal)
 *T. soror* Schenkling, 1902 (Fig. 20)
 – Antennomeres VIII–X wider than long; male metatibiae apically with a broad spine (Laos, Myanmar, Thailand) *T. spinosa* sp. nov. (Figs 25–27)
- 4 Tarsal pulvillar formula 4–4–3 (Taiwan)
 *T. wenii* Yang & Yang, 2011 (Fig. 22)
 – Tarsal pulvillar formula 4–4–2 or 4–4–4 5
- 5 Pronotum with sparse punctuation (Laos, Thailand)
 *T. fortis* sp. nov. (Figs 23, 24)
 – Pronotum with dense punctuation 6
- 6 Length to width ratio of terminal antennomere of both sexes > 1.5:1 (China, Laos, Myanmar, Thailand) ... *T. sensibilis* Yang & Yang, 2011 (Figs 18, 19)
 – Length to width ratio of terminal antennomere of both sexes < 1.5:1 7
- 7 Antennomeres IX and X about twice as wide as long (Indonesia, Laos, Malaysia, Thailand, Vietnam) *T. javana* Spinola, 1844 (Figs 11, 12)
 – Antennomeres IX and X less than twice wide as long (China, Laos, Myanmar, Thailand, Vietnam) *T. auratofasciata* (Pic, 1927) (Fig. 1)
- 8 Elytral base and humeri red-brown to brown 9
 – Elytral base and humeri black, sometimes with brown macula 13
- 9 Pronotum with yellowish fascia at apical margin 10
 – Pronotum without yellowish fascia at apical margin 12
- 10 Elytra with large yellowish fascia at apical 1/3, brown at apex (India)
 *T. paula* Schenkling, 1908 (Fig. 15)
 – Elytra with narrow yellowish fascia at apex, black at apex 11
- 11 Elytra largely yellowish red (China, Indonesia, Laos, Myanmar, Thailand) ...
 *T. cleroides* Gorham, 1892 (Figs 5, 6)
 – Elytra largely black or brownish black (Indonesia, Laos, Malaysia)
 *T. pseudocleroides* Gerstmeier & Bernhard, 2010 (Figs 16, 17)
- 12 Frons about 1.7 times wider than the width of a single eye (Indonesia, Japan, Laos, Myanmar, Taiwan, Thailand) *T. iblei* Corporaal, 1949 (Figs 9, 10)
 – Frons about as wide as a single eye (Vietnam)
 *T. tonkinensis* Gerstmeier & Bernhard, 2010 (Fig. 21)

- 13 Elytra with anterior pale fascia at least as broad as the black central part (India) *T. aurivillosa* Gorham, 1895 (Fig. 2)
- Elytra with anterior pale fascia of elytra conspicuously narrower than the black central part 14
- 14 Elytra with a sub-basal hump 15
- Elytra without a sub-basal hump 16
- 15 Transverse fasciae of pattern-forming bright golden setae (China, Laos, Vietnam) *T. michaeli* Gerstmeier & Bernhard, 2010 (Fig. 13)
- Transverse fasciae pale, pigmented; setae less brightly golden (India, Vietnam) *T. callosa* Gerstmeier & Bernhard, 2010 (Fig. 4)
- 16 Elytral punctation large at base; the space between each puncture within the same interval row narrower than diameter of a single puncture 17
- Elytral punctation small at base; the space between each puncture within the same interval row larger than or same as diameter of a single puncture (Malaysia) *T. obscura* Gerstmeier & Bernhard, 2010 (Fig. 14)
- 17 Head unicolored black; antennae gradually widening from antennomere V; elytra with longitudinal rows of tubercles on basal intervals (Indonesia, Malaysia, Vietnam) *T. hirsuta* (Pic, 1926) (Figs 7, 8)
- Head reddish brown posteriorly; antennae gradually widening from antennomere VI; elytra without longitudinal rows of tubercles on basal intervals (Cambodia, China, Laos, Myanmar, Thailand, Vietnam) *T. bibalteata* Gorham, 1892 (Fig. 3)

Acknowledgements

The first author would like to thank Kazuhiko Konishi and Hiroyuki Yoshitomi (both EUMJ) for their helpful support; Akiko Saito (NHMI), Shozo Osawa (Hiroshima, Japan), and Katsumi Akita (Mie, Japan) for the loan of the specimens preserved in NHMI; Masahiro Ohara and Juriya Okayasu (both SEHU) for examination of the type specimen; Masaki Endo (Hokkaido University, Japan), Shunsuke Imada (KUMJ), Masafumi Matsumura (Okinawa, Japan), Sinyan Shih (Changhua, Taiwan), Minoru Tanaka (Hyogo, Japan), and Takeo Yamauchi (Obihiro University) kindly made material available. The second author thanks Jiří Hájek (NMPC) and Fritz Gusenleitner (OLML) for loan of specimens.

References

- Bartlett JS (2021) A preliminary suprageneric classification for Clerinae (Coleoptera: Cleridae) based on molecular and morphological evidence, including a review of tegminal terminology. *Annales Zoologici (Warszawa)* 71(4): 737–766. <https://doi.org/10.3161/00034541ANZ2021.71.4.003>

- Corporaal JB (1939) Some Cleridae from India, Burma and Ceylon with descriptions of new species and notes on others. *Indian Forest Records, (New Series). Entomology* 6(2): 17–39.
- Corporaal JB (1949) Some new and rare Cleridae. *Bijdragen tot de Dierkunde* 28(1): 99–100. <https://doi.org/10.1163/26660644-02801014>
- Desmarest E (1860) Clériens. In: Chenu JC (Ed.) *Encyclopédie d'histoire naturelle ou traité de cette science d'après les travaux des naturalistes les plus éminents de tous les pays et de toutes les époques. Coléoptères. Deuxième partie.* Paris: Marescq et compagnie, 226–279.
- Gerstmeier R, Bernhard N (2010) Revision of the genus *Tillicera* Spinola, 1841 (Coleoptera: Cleridae, Clerinae). *Zootaxa* 2359(1): 1–34. <https://doi.org/10.11646/zootaxa.2359.1.1>
- Gerstmeier R, Stapel J (2016) A review of the *Tillicera* genus group with a revision of *Plathanocera* Schenkling (Coleoptera, Cleridae, Clerinae). *Zootaxa* 4193(3): 517–540. <https://doi.org/10.11646/zootaxa.4193.3.4>
- Gorham HS (1876) Notes on the Coleopterous family Cleridae, with description of New Genera and Species. *Cistula Entomologica* ii: 57–106.
- Gorham HS (1893) A list of the Coleoptera, of the family Cleridae, collected by Mr. Doherty in Burmah and Northern India, with descriptions of new species; and of some species from Borneo, Perak, &c., from the collection of Alexander Fry, Esq. *Proceedings of the Zoological Society of London* 39: 566–581.
- Miyatake M (1985) Cleridae. In: Kurosawa Y, Hisamatsu S, Sasaji H (Eds) *Colored illustrations of the Coleoptera of Japan. Vol. 3.* Osaka: Hoikusha publishing Co., 158–161. [x + 500 pp, 72 pls] [in Japanese]
- Murakami H (2016) A new species of the genus *Thaneroclerus* (Coleoptera, Cleridae, Thaneroclerinae) from Ishigaki-jima island, Japan. *Elytra, Tokyo. New Series* 6(2): 285–289.
- Nakane T (1963a) New or little-known Coleoptera from Japan and its adjacent regions XVI–XXII. *Fragmenta Coleopterologica* 11: 43–46.
- Nakane T (1963b) Cleridae. In: Nakane T, Ohbayashi K, Nomura S, Kurosawa Y (Eds) *Iconographia Insectorum Japonicum, Colore naturali edita, 2 (Coleoptera).* Hokuryūkan, Tokyō, 182–184[, pls 91, 92]. [445 pp, 192 pls] [In Japanese]
- Opitz W (2010) Classification, natural history, phylogeny, and subfamily composition of the Cleridae and generic content of the subfamilies (Coleoptera: Cleridae). *Entomologica Basiliensia et Collectionis Frey* 32: 31–128.
- Pic M (1927) Coléoptères de l'Indochine. *Mélanges exotico-entomologiques* 49: 1–36.
- Pic M (1934) Hors-Texte. *Exchange* 50(458): 125–136.
- Schenkling S (1902) Neue Cleriden des Museums zu Leyden. *Notes from the Leyden Museum* 23: 123–130.
- Schenkling S (1903) Coleoptera. Malacodermata. Fam. Cleridae. In: Wytzman P (Ed.) *Genera Insectorum* 13: 1–124.
- Schenkling S (1906) Die Cleriden des Deutschen Entomologischen National-Museums, nebst Beschreibungen neuer Arten. *Deutsche Entomologische Zeitschrift* 1906: 241–320.
- Shelford R (1902) Observations on some mimetic insects and spiders from Borneo and Singapore. *Proceedings of the Zoological Society of London* 2(2): 230–284.
- Spinola M (1841) *Monographie des Térédiles.* *Revue Zoologiques par la Société Cuvierienne*, 4: 70–76.

- Spinola M (1844) Essai Monographique sur les Clérites, Insectes Coléoptères. Gênes: Imprimerie des frères Ponthenier, vols 1 (I–IX, 1–386), 2 (1–119), Suppl. (121–216), 47 pls.
- Yang GY, Yang XK (2013) Revision of the genus *Hemitrachys* Gorham, with discovery of a second species (Coleoptera: Cleridae: Clerinae). *Zootaxa* 3710(1): 72–80. <https://doi.org/10.11646/zootaxa.3710.1.5>
- Yang GY, Montreuil O, Yang XK (2011) New species, new records and new morphological characters of the genus *Tillicera* Spinola from China (Coleoptera, Cleridae, Clerinae). *ZooKeys* 122: 19–38. <https://doi.org/10.3897/zookeys.122.1457>
- Zhang J, Cheng B, Fu L, Sun S (2021) Morphology and Distribution of Antennal Sensilla of the Predatory Clerid Beetle, *Thanasimus substriatus* (Coleoptera: Cleridae). *Journal of Entomological Science* 56(3): 441–455. <https://doi.org/10.18474/JES20-70>

Morphology and distribution of the Middle Asian centipede genus *Krateraspis* Lignau, 1929 (Chilopoda, Geophilomorpha, Mecistocephalidae)

Yurii V. Dyachkov¹, Lucio Bonato²

¹ Altai State University, Lenin Avenue 61, Barnaul 656049, Russia ² Dipartimento di Biologia, Università di Padova, via U. Bassi 58b, I-35131 Padova, Italy

Corresponding author: Yurii V. Dyachkov (dyachkov793@mail.ru)

Academic editor: Pavel Stoev | Received 19 January 2022 | Accepted 10 March 2022 | Published 14 April 2022

<http://zoobank.org/7078C72B-B894-4479-87DC-CA85B07054C7>

Citation: Dyachkov YuV, Bonato L (2022) Morphology and distribution of the Middle Asian centipede genus *Krateraspis* Lignau, 1929 (Chilopoda, Geophilomorpha, Mecistocephalidae). ZooKeys 1095: 143–164. <https://doi.org/10.3897/zookeys.1095.80806>

Abstract

A comprehensive redescription of the poorly known mecistocephalid genus *Krateraspis* Lignau, 1929 and its two species is provided, based on the examination of type material and new specimens, as well as the critical evaluation of all published information. *Krateraspis* is confirmed differing from all other Mecistocephalidae especially for a peculiar pattern of areolation and setation of the clypeus. Records from 24 localities indicate that *Krateraspis* is limited to a narrow area of Middle Asia, from the Western Tian-Shan to the western offshoots of Pamir Mountains. Two species are morphologically distinguishable: *K. meinerti* (Sselivanoff, 1881) and *K. sselivanovi* Titova, 1975. They differ mainly in details of the clypeus and maxillae, in the pattern of forcipular denticles, and in the number of legs. *Tygarrup asiaticus* Verhoeff, 1930 is confirmed as a junior synonym of *K. meinerti*, and a lectotype is designated for the former.

Keywords

Kazakhstan, *Krateraspis*, Kyrgyzstan, Tajikistan, taxonomy, Uzbekistan

Introduction

The genus *Krateraspis* Lignau, 1929 is one of the least known and least distinct genera of the centipede family Mecistocephalidae Bollman, 1893 (Bonato et al. 2003). All reliable records are from a narrow area in the Middle Asia (Titova 1975; Dyachkov 2019,

2020; Dyachkov and Nedoev 2021), and they are currently referred to two species, *K. meinerti* (Sselivanoff, 1881) and *K. sselivanovi* Titova, 1975 (Bonato et al. 2016). A satisfactory diagnosis of the genus is missing, the published accounts on its morphology are incomplete and contained ambiguous details, and the differential characters of the species have not been scrutinized carefully.

The first specimen of *Krateraspis* was reported by Sselivanoff (1881a, 1881b) from near Tashkent (Uzbekistan) and was originally described as a species of *Mecistocephalus* Newport, 1843, namely *M. meinerti*, with very incomplete morphological information and without illustrations. Other specimens collected later near the type locality allowed Lignau (1929a, 1929b) and Verhoeff (1930) to complement the morphological description of this species and to provide the first illustrations. However, while Lignau (1929a, 1929b) assigned his specimen to *M. meinerti* and separated the species in a distinct genus *Krateraspis*, Verhoeff (1930) described his specimens as a new species of *Tygarrup* Chamberlin, 1914, namely *T. asiaticus*. The latter name was recognized as a synonym of *Krateraspis meinerti* by Titova (1975). In the same paper, Titova described a second species of *Krateraspis*, namely *K. sselivanovi* Titova, 1975, from Sharak (Tajikistan), as well as a putative third species from the Russian Far East, namely *K. striganovae* Titova, 1975, which however has been later recognized in a distinct genus *Agnostrup* Foddai, Bonato, Pereira & Minelli, 2003. Other records of *Krateraspis meinerti*, additional information on its morphology and some first photographs were published by Dyachkov (2019, 2020) and Dyachkov and Nedoev (2021).

This paper contributes a comprehensive redescription of the morphology of the genus *Krateraspis* and its species, and an update of their distribution, based on the examination of the available type material and the critical evaluation of all published information.

Materials and methods

We examined the holotype of *K. meinerti* (at ZISP; for abbreviations see below), one of the syntypes of its junior synonym *Tygarrup asiaticus* (at NHRS), at least six paratypes and some other possible paratypes of *K. sselivanovi* (at ZMMU; see corresponding Remarks), a specimen originally assumed by Verhoeff (1930) to be a juvenile *T. asiaticus* (at ZMB), 67 specimens of *K. meinerti* (at ASU, ZMMU, and ZISP) already reported by Dyachkov (2019, 2020) and Dyachkov and Nedoev (2021), and 18 other specimens of *K. meinerti* and nine of *K. sselivanovi* (at ZMMU).

The specimens were examined with stereo microscopes: Olympus SZX16, Olympus BX51, Leica Z16 APO. Some non-typical specimens of *K. meinerti* and *K. sselivanovi* were dissected, and their cephalic capsule, forcipular segment, mandibles, maxillary complex, and remaining body were mounted in permanent slides using euparal. Photographs were taken using an Olympus DP74 or a Leica DFC490 digital cameras attached to the microscopes. Measurements were taken from the photos using the software FAST 1.0 (Vaganov et al. 2020).

We compiled a revised diagnosis of the genus *Krateraspis* by comparison with all currently recognized genera of Mecistocephalidae (Bonato et al. 2003; Uliana et al. 2007; Bonato et al. 2016). We also revised the differential diagnoses between the species of *Krateraspis* by direct comparison of specimens and critical reinterpretation of the published accounts. The terminology of morphology follows Bonato et al. (2010b).

Localities are indicated as in the original labels or publications. Modern English names and additional information are in square brackets. All localities were georeferenced unambiguously, with the single exception of “Fayzabad” because there are at least two homonymous villages with this name (Dyachkov 2020: 78). Localities were mapped with SimpleMappr (Shorthouse 2010).

Abbreviations

AF	A.A. Fomichev;	NHRS	Swedish Museum of Natural History, Stockholm;
AR	A. Ryvkin;	NZ	N.A. Zarudniy;
ASU	Altai State University (Barnaul, Russia);	Tj	Tajikistan;
D	Daniyarov;	V	Veltishev;
dors.	dorsal.;	ventr.	ventral;
juv.	juvenile/s;	VR	V. Russov;
LB	L. Berg;	YD	Yu.V. Dyachkov;
LBS	leg-bearing segment(s);	ZISP	Zoological Institute of the Russian Academy of Sciences, Saint Petersburg;
lg	legit;	ZMB	Museum für Naturkunde, Berlin;
MG	M.S. Ghilarov;	ZMMU	Zoological Museum of the Moscow State University;
NHMUK	Natural History Museum, London;	ZSM	Zoologische Staatssammlung, München.
NHMW	Natural History Museum, Vienna;		

Results

Krateraspis Lignau, 1929

Krateraspis: Lignau 1929a: 160 (available name), 165. Lignau 1929b: 207 (original description). Verhoeff 1930: 265. Titova 1975: 39, 46 (in key). Titova 1983: 148. Bonato et al. 2003: 544, 547, 549, 550, 552, 553. Foddai et al. 2003: 1255. Bonato et al. 2009: 195, 199, 207. Bonato et al. 2010a: 515. Bonato and Zapparoni 2011: 331. Bonato 2011: 434. Volkova 2016: 675. Dyachkov 2019: 368, 370, 372. Dyachkov 2020: 79; Dyachkov and Nedoev 2021: 44.

Type species. *Mecistocephalus meinerti* Sseliwanoff, 1881, by monotypy (Lignau 1929a, 1929b).

Remarks on nomenclatural issues. The genus name *Krateraspis* was first introduced by Lignau (1929a) without a description or diagnosis, but it was explicitly used for the species *Mecistocephalus meinerti* Sselivanoff, 1881 and therefore it is available since that publication (ICZN 1999: Art. 12.2.5). Instead, the first morphological description of *Krateraspis* was given in a different paper by the same author, published in the same year but in a later date (Lignau 1929b).

The type species of *Krateraspis* was determined by monotypy (see also Jeekel 2005: 86), not by original designation as erroneously reported by Bonato et al. (2016) and Dyachkov (2019).

Diagnosis. A genus of Mecistocephalidae with: anterior areolate part of the clypeus extending along the lateral margins of the clypeus to the labrum; two clypeal plagulae separated by a mid-longitudinal areolate strip; central part of the clypeus with distinct but fainter areolation in comparison with the markedly areolate anterior part and the mid-longitudinal strip; clypeal setae only three or four pairs, on the antero-central part of the clypeus; buccae without spiculum; labral anterior ala with the internal margin reduced to a point; labral posterior ala with the posterior margin entire, without bristles; coxosternite of first maxillae divided by a mid-longitudinal suture; coxosternite of second maxillae entire, without mid-longitudinal suture, with the grooves from the metameric pores reaching the lateral margins of the coxosternite at approximately their mid-length; telopodite of second maxillae bearing a small claw-like pretarsus; forcipular tergite slightly wider than long; sternites without pore fields; either 45 or 53 pairs of legs; ultimate legs without claw but with an apical small spine.

Krateraspis differs from other mecistocephalids (Table 1) mainly in the pattern of clypeal areolation and setation: a broad weakly areolate central part of the clypeus is distinguishable from the distinctly areolate anterior part as well as the non-areolate posterior plagulae, and a few setae are present on the medial part only. Of two other Middle Asian mecistocephalid genera, *Tygarrup* and *Arrup*, *Krateraspis* is more similar to the former. *Tygarrup* differs from *Krateraspis* for an entire non-areolate plagula lacking a mid-longitudinal areolate strip, and for the presence of setae on both the central and lateral parts of the clypeus. *Arrup* differs from *Krateraspis* not only in the clypeus (markedly areolate in both the central and anterior part, with setae on the both the lateral and central parts), but also in the maxillary complex (coxosternite of the first maxillae entire, without mid-longitudinal suture; coxosternite of the second maxillae with grooves from the metameric pores running backwards towards the posterior corners of the coxosternite), in the forcipular tergite (much wider than long), and the number of legs (41 pairs).

Included species. *Krateraspis meinerti* (Sselivanoff, 1881) and *K. sselivanovi* Titova, 1975.

Distribution. Recorded from 24 localities in Middle Asia so far, from Western Tian-Shan to the western offshoots of Pamir Mts (Fig. 1).

Remarks on published morphological accounts. The peculiar pattern of clypeal areolation is well recognizable only using a light microscope with slides, while it is very poorly visible using stereo (dissecting) microscope. Additionally, the semblance of the areolation is conditioned by the preparation of the specimen, the optical properties of

Table 1. Main differences between *Krateraspis* and the other genera of Mecistocephalidae.

Characters	<i>Krateraspis</i> Lignau, 1929	<i>Arrup</i> Chamberlin, 1912	<i>Partygarrupius</i> Verhoeff, 1939	<i>Agostrop</i> Foddai, Bonato, Pereira & Minelli, 2003	<i>Nannarrup</i> Foddai, Bonato, Pereira & Minelli, 2003	<i>Dicelophitus</i> Cook, 1896	<i>Anarrup</i> Chamberlin, 1920	<i>Proterotainanella</i> Bonato, Foddai & Minelli, 2002	<i>Fygarrip</i> Chamberlin, 1914	<i>Mecistocephalus</i> Newport, 1843	<i>Takabimnia</i> Miyosi, 1955
clypeus: central part: areolation	yes	yes	yes	yes	yes	no	no	yes	no	yes	no
clypeus: areolation of central part compared with anterior part	fainter	similar	similar	similar	similar	no	no	similar	no	similar or fainter; sometimes non-areolate insulae	no
clypeus: posterior mid-longitudinal areolate strip	yes	yes	no	yes	yes	no	no	yes	no	yes	no
clypeus: areolation extending all along the lateral margins	yes	yes	no	no	yes	no	no	yes	no	no	no
clypeus: setae on antero-lateral corners	no	yes	no	no	no	yes	yes	no	usually yes	yes or no	no
clypeus: setae on lateral parts	no	longitudinally elongate areas	narrow transverse band	longitudinally elongate areas	longitudinally elongate areas	longitudinally elongate areas	narrow transverse band	longitudinally elongate areas	narrow transverse band	narrow transverse band	no
bucca: spiculum	no	no	no	no	no	no	no	no	no	yes	yes
labrum: anterior ala: internal margin reduced to a point	yes	yes	yes	yes	yes	yes	yes	yes	yes	yes	yes
labrum: posterior ala: posterior margin: bristles	no	no	no	no	no	yes	no	no	no	usually no	no
first maxillae: coxosternite: mid-longitudinal suture	yes	no	yes	yes	yes	yes	yes	yes	yes	yes	yes
second maxillae: coxosternite: mid-longitudinal suture	no	no	no	no	no	no	yes	no	no	no	no
second maxillae: coxosternite: groove from metameric pore reaching lateral margin	yes	no	no	no	no	no	yes	yes	yes	yes	yes
second maxillary telopodite: distinctly surpassing the first maxillary telopodite	yes or no	no	no	no	no	yes	yes	no	yes	yes	yes
second maxillae: pretarsus	small claw	no or small claw	small claw	no	no	spinous tubercle	spinous tubercle	small claw	small claw	small claw	small claw
forcipular segment: tergite: width/length	~1.5	~2.0	~1.5	~2.0	~2.0	~1.5	~1.5	~1.5	~1.5	~1.5	~1.5
trunk: leg-bearing segments	45 or 53	41	41	41	41	41 or 43 or 45	41	45 or 49	43 or 45	45 or more	45
ultimate leg pair: pretarsus	no	no	no	no	no	spinous tubercle	spinous tubercle	spinous tubercle	no	no	no

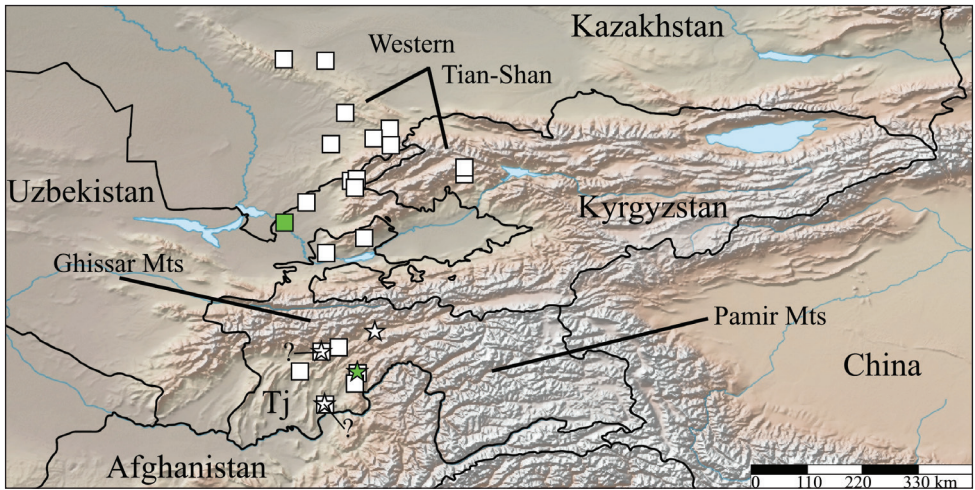


Figure 1. Distribution of *Krateraspis* Lignau, 1929: square, *K. meinerti* (Sselivanoff, 1881); star, *K. sselivanovi* Titova, 1975. Green symbols indicate type localities. Some very close localities are marked by a single symbol. The question marks indicate alternative positions of the uncertain locality “Fayzabad” (see Materials and methods).

the inclusion medium and the mode of illumination. This may explain why the pattern of areolation on the clypeus has been interpreted, described, and illustrated in inconsistent ways by different authors. Lignau (1929b) did not distinguish between a markedly areolate anterior part and a weakly areolate central part, neither in the textual description of *K. meinerti* (“Vorderclypeus fein gefeldert, nimmt etwas mehr als die Hälfte der gesamten Fläche ein” [anterior clypeus finely areolate, extending a little more than half of the total area]) nor in the associated illustration (his fig. 10). In the same way, Titova (1975) described *K. sselivanovi* without indicating any variation in the areolation between anterior and central parts of the clypeus, neither in the textual description (“Peredniy clypeus zanimaet bolee poloviny nalichnika, ego poverhnost sostoit iz polygonalnikh poley, po seredine uzkooy polosoy razdelyayuschikh zadniy clypeus na 2 poloviny” [anterior clypeus covers more than a half of the total clypeal area, its surface consists of polygonal cells that divide the posterior clypeus in the middle into 2 parts by a narrow strip]), nor in the accompanying illustration (her fig. 2: 1A). On the other hand, Verhoeff (1930) described and illustrated *T. asiaticus* (synonym of *K. meinerti*, see below) ignoring the weak areolation in the central part of clypeus and assigning this part to the non-areolate plagulae. Dyachkov (2019) used term “insula” for the weakly areolate central part of the clypeus of *K. meinerti*, but the term was previously used for a non-areolate area inside the areolate anterior clypeus (Bonato et al. 2010b).

The pattern of clypeal setae and sensilla has also been reported inconsistently: the eight “Punkte” [points] described and illustrated by Lignau (1929b: fig. 10) in the central part of clypeus of his single specimen of *K. meinerti* are probably the sockets of broken setae, because these points (in his fig. 10) correspond in number and position

with the eight clypeal setae present in most specimens of this species. In the same way, Lignau (1929b) described the antennae as “kahl” [without setae] probably because the antennal setae were broken in his material.

The description of *K. meinerti* provided by Lignau (1929b) includes another obvious mistake: the sentence “2. Maxille mit getrennten Hüften” [second maxillae with divided coxosternite] should be read “1. Maxille mit getrennten Hüften” [first maxillae with divided coxosternite], because it is contradicted by a previous sentence in the same text (“ganz verwachsenen Hüften der 2. Maxille” [entirely coalescent coxosternite of the second maxillae]), as well as by an associated illustration (his fig. 9).

***Krateraspis meinerti* (Sseliwanoff, 1881)**

Figures 2–28

Mecistocephalus meinerti: Sseliwanoff 1881a: 9 (nomen nudum). Sseliwanoff 1881b: 232 (original description). Sseliwanoff 1884: 73 (description). Attems 1903: 168, 210. Attems 1904: 115. Attems 1914: 21. Attems 1929: 156. Izotova 1960: 150 (misidentification).

Krateraspis meinerti: Lignau 1929a: 160, 165 (new record). Lignau 1929b: 207 (redescription); figs 7–11. Verhoeff 1930: 264. Titova 1965: 871 (new record). Titova 1969: 165. Titova 1975: 39, 45 (new records), 46 (in key); fig. 2: 2–4B. Bonato et al. 2003: 543, 545, 546, 550, 551, 577. Ilie et al. 2009: 14. Bonato 2011: 434. Volkova 2016: 675. Dyachkov 2019: 368, 371 (new records; description), 373 (in key); figs 6–10. Dyachkov 2020: 79 (new records), 85. Dyachkov and Nedoev 2021: 44 (new records), 47.

Tygarrup asiaticus: Verhoeff 1930: 260 (original description); figs 20–21. Verhoeff 1934: 31. Verhoeff 1937: 235 (in key). Verhoeff 1939: 88 (in key). Takakuwa 1940: 84. Verhoeff 1940: 31. Verhoeff 1942: 49 (in key). Shinohara 1965: 303 (in key), 304. Titova 1965: 871, 874 (in key). Titova 1983: 147, 148.

Type locality. “Chinas, bl. Tashkenta” (Sseliwanoff 1881a), also indicated as “Chinad [*sic*] bliz Tashkenta” (Sseliwanoff 1881b) and “Mestechko Chinas, bliz Tashkenta” (Sseliwanoff 1884) [UZBEKISTAN, Tashkent region, Chinaz town, ca. 40°56'N, 68°45'E].

Synonyms. *Tygarrup asiaticus* Verhoeff, 1930 (synonymization since Titova 1975; see below, under Remarks).

Examined specimens. **Holotype** of *Mecistocephalus meinerti* Sseliwanoff, 1881: ♀, from Chinas bl. Tashkenta [UZBEKISTAN, Tashkent region, Chinaz near Tashkent], 1878, VR lg (ZISP). **Lectotype** of *Tygarrup asiaticus* Verhoeff, 1930 (see below, under Remarks): ♂, from Tashkent (NHRS-JONI 714). **Other material:** 1 ♀, from Tashkent, 13.III [year unknown], NZ lg (ZISP chilo-52); 1 ♀, from Ugam Mts, Sidzhak, nut [*Juglans*] forest, soil samples, 28.IV.[19]74, MG lg (ZMMU Rc 7408); 1 ♀, from Chimgan, nut forest, 07.V.[19]74, MG lg (ZMMU Rc 7413); 1 ♀, from Chimgan, Tashkent

ravine, VII.[19]06, LB lg (ZISP chilo-1); 1 ♀, from Vrevskaya Station [now Almazar, ca. 40°57'N, 68°50'E], 26.IV.1932, V lg (ZISP chilo-5); 1 ♂ and 1 ♀, from Kamsay, near Khumsan, *Juglandetum*, 03.V.[19]74, MG lg (ZMMU Rc 7407); 1 ♂ and 5 ♀♀, from Khumsan, right bank of Ugam river, nut forest, 1.V.[19]74, MG lg (ZMMU Rc 7406); 1 ♀, from [TAJIKISTAN, Districts of Republican Subordination, Roghun district] left side of Obikandak river valley (left stream tributary of Obigarm river), stony meadow with rocks, 38°43.275'N, 69°43.863'E, 1250–1540 m, 23.IV.2019, AF lg (ASU No. 261); 2 ♂♂, from [Khatlon region, Mu'minobod district], Muminabad [Mu'minobod, now Leningradsky, ca. 38°06'N, 70°01'E], 0–10 [cm deep], 19.V.[19]62 (ZMMU Rc 8158) and 11.V.[19]65 (ZMMU Rc 8159); 2 ♂♂, 3 ♀♀ and 1 body fragment from Sharak [village, ca. 38°16'N, 70°04'E], 10–20 [cm deep], 15.VIII.[19]65 (ZMMU Rc 8136), 10–20 [cm deep], 27.V.[19]65 (ZMMU Rc 8185), 20–30 [cm deep], 19.X.[19]64 (ZMMU Rc 8148), 10–20 [cm deep], 31.V.[19]65 (ZMMU Rc 8155), grass, 0–10 [cm deep], 3.VI.[19]63 (ZMMU Rc 8139); 1 ♂ and 6 ♀♀, from [Yovon district], Yavan [Yovon, ca. 38°18'N, 69°03'E]: *Triticum*, 20–40 cm deep, 25.VII.[19]67 (ZMMU Rc 8151), *Triticum*, 20–60 [cm deep], 20.X.[19]67 (ZMMU Rc 8186), *Triticum*, 0–30 [cm deep], 19.X.[19]68 (ZMMU Rc 8170), *Triticum*, 10–20 [cm deep], 21.V.[19]68 (ZMMU Rc 8183), *Hordeum*, 0–10 [cm deep], 13.V.[19]67 (ZMMU Rc 8169), *Avena*, 0–10 [cm deep], 26.V.[19]68 (ZMMU Rc 8172); 2 ♂♂ and 4 body fragments, from [Sughd region], Matcha district [ca. 40°32'N, 69°25'E]: 10–20 [cm deep], [date unknown], D lg (ZMMU Rc 8157), 15.V.[19]65 (ZMMU Rc 8149), and 0–10 [cm deep], D lg (ZMMU Rc 8190); 1 ♀, from Mogol-Tau Mts [ca. 40°23'N, 69°31'E], under stones, [19]74 (ZMMU Rc 7409); 1 ♀, from F-bad [unknown region, Fayzobod], *Triticum*, 10–20 [cm deep], 6.V.[19]66 (ZMMU Rc 8174); 1 ♂, from [KYRGYZSTAN, Jalal-Abad region], Sary-Chelek Nature Reserve, near Arkit Village [ca. 41°47'N, 71°57'E], forest with *Juglans* and *Acer*, 03.VII.[19]83, AR lg (ZMMU Rc 7670); 1 ♂, from near Kyttsay stream, forest with *Juglans*, 04.VII.[19]83, AR lg (ZMMU Rc 7667); 5 ♂♂, 3 ♀♀ and 3 juv., from KAZAKHSTAN, Turkistan region, 10 km SW Abay Village, Karatau Mt. Range, Karatau State Nature Reserve, cereals and tulip steppe, under stones, 43°47'04.2"N, 68°46'42.0"E, 1020 m, 06–07.V.2017, YD lg (ASU No. 214); 1 ♀, from 50 km NW Achisay Village, Kyzylkol Lake coast, in clay stones, 43°46'34.0"N, 69°30'36.4"E, 328 m, 08–09.V.2017, YD lg (ASU No. 215); 5 ♂♂, 10 ♀♀ and 5 juv., from Karatau Mt Range, Syrdarya-Turkestan Natural Park, near Terekty Village, Boralday River coast, *Morus* and cereals, under stones, 42°51'48.2"N, 69°51'55.0"E, 529 m, 14–15.V.2017, YD lg (ASU No. 216); 9 ♂♂, 6 ♀♀ and 3 juv., from Ugam Mt Range, Sayram-Ugam National Park, 10 km NE Tylkubas Village, Iirsu River Valley, meadow, under stones, 42°24'58.0"N, 70°21'30.08"E, 1296 m, 16–18.V.2017, YD lg (ASU No. 217).

Remarks on nomenclatural issues. The species name *Mecistocephalus meinerti* was first introduced by Sseliwanoff (1881a) without description, definition, or indication, and therefore it is not available from that publication (ICZN 1999: Art. 12.1 and 12.2). The name became available since another paper published later (Sseliwanoff 1881b), which provided a morphological description of the species, based on a specimen.

Verhoeff (1930) described *Tygarrup asiaticus* based on nine specimens from two localities (seven from Vreskaja, ca. 50 km SW of Tashkent, and two from Tashkent) and

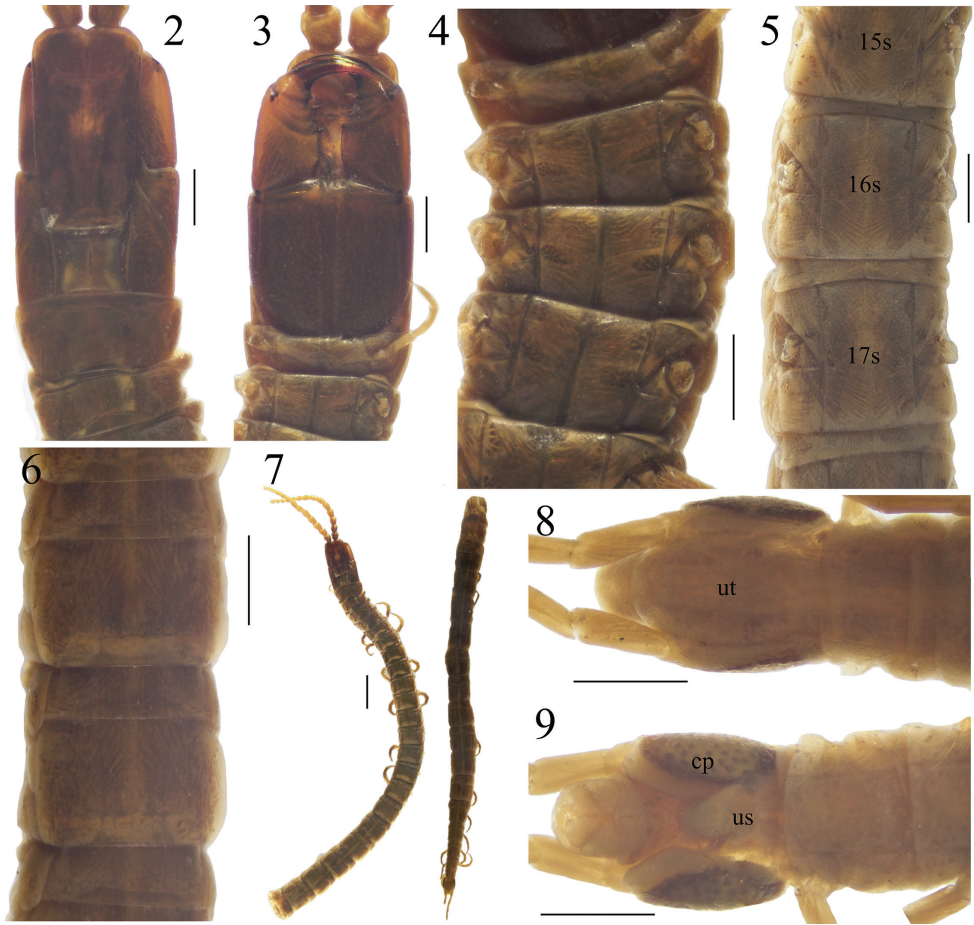
all these specimens should be considered as syntypes (ICZN 1999: Recommendation 73F). They are preserved in different museums: at least four in ZSM (SysTax 2021), one in ZMB (Moritz and Fischer 1979; pers. obs.), one in NHMUK (Natural History Museum 2021), one in NHRS (pers. obs.), and one in NHMW (Ilie et al. 2009). The descriptions and illustrations provided by Verhoeff and our direct examination of two syntypes (NHRS-JONI 714 and ZMB 3610) revealed that Verhoeff described *T. asiaticus* mainly on some syntypes that are fully consistent with *Krateraspis meinerti*. Other syntypes actually belonging to another species were misinterpreted by Verhoeff as juveniles of *Tygarrup asiaticus*. To stabilize the usage of the name, we herewith designate NHRS-JONI 714 as lectotype of *T. asiaticus* (ICZN 1999: Art. 74.1.1). This specimen (Fig. 18) is fully consistent with the original description and illustrations published by Verhoeff (1930) for the adult morphology of *T. asiaticus* and *Krateraspis meinerti*. It is an adult male 31 mm long, labeled “*Tygarrup asiaticus* Verh. Turkestan”, acquired by NHRS in 1931 and indicated explicitly as type in the catalogue of NHRS. This specimen has been now labeled “lectotype”, whereas other previous syntypes has been now labeled “paralectotype” (ICZN 1999: Recommendation 74C).

ZMB 3610 (labeled as a syntype of *T. asiaticus*, from Tashkent, with 43 pairs of legs; Figs 29–32) actually belongs to a species of *Arrup* Chamberlin, 1912, as indicated by the following characters: clypeus with many setae on the lateral parts and very short paired plagulae (Fig. 30), first maxillae with relatively small telopodites (Fig. 30), forcipular tarsungulum with a relatively long denticle (Fig. 32), and 41 pairs of legs (erroneously reported 43 on the label on the microscopic slide; Fig. 29). More precisely, ZMB 3610 probably belongs to the species *A. asiaticus* (Titova, 1975), which is already known from Middle Asia and differs from all other known species of *Arrup* in the variable presence of coxal organs and pores (apparently absent in some specimens, including well grown specimens) and the branching structure of the channels of the anal organs and their broad openings (Fig. 31; Titova 1975; Dyachkov 2019).

Diagnosis. A species of *Krateraspis* with: clypeus showing the transition between marked and weak areolation very close to the clypeal anterior margin (at ca. 0.1 of the medial length of the clypeus), so that all clypeal setae are inside the weakly areolate central part of the clypeus; some small spine-like sensilla on the lateral parts of the clypeus; second maxillary telopodites distinctly surpassing the tips of the telopodites of the first maxillae; first article of the second maxillary telopodites without a distinct distal bulge on the external side; all forcipular articles with a distinct denticle; invariably 45 pairs of legs. See also Table 2.

Table 2. Main differences between *Krateraspis meinerti* (Sselivanoff, 1881) and *K. sselivanovi* Titova, 1975.

Morphological characters	<i>K. meinerti</i>	<i>K. sselivanovi</i>
Clypeus: transition between marked and weak areolation: longitudinal position	very close to the anterior margin of the clypeus	at ca. 0.3–0.4 of the total length of the clypeus
First maxillae: telopodite: first article: distal bulge on external side	absent	present
Second maxillae: telopodite: elongation	distinctly surpassing the tip of first maxillary telopodite	approximately reaching the tip of first maxillary telopodite
Forciple: femur: denticle	yes	no
Leg-bearing segments: number	45	53

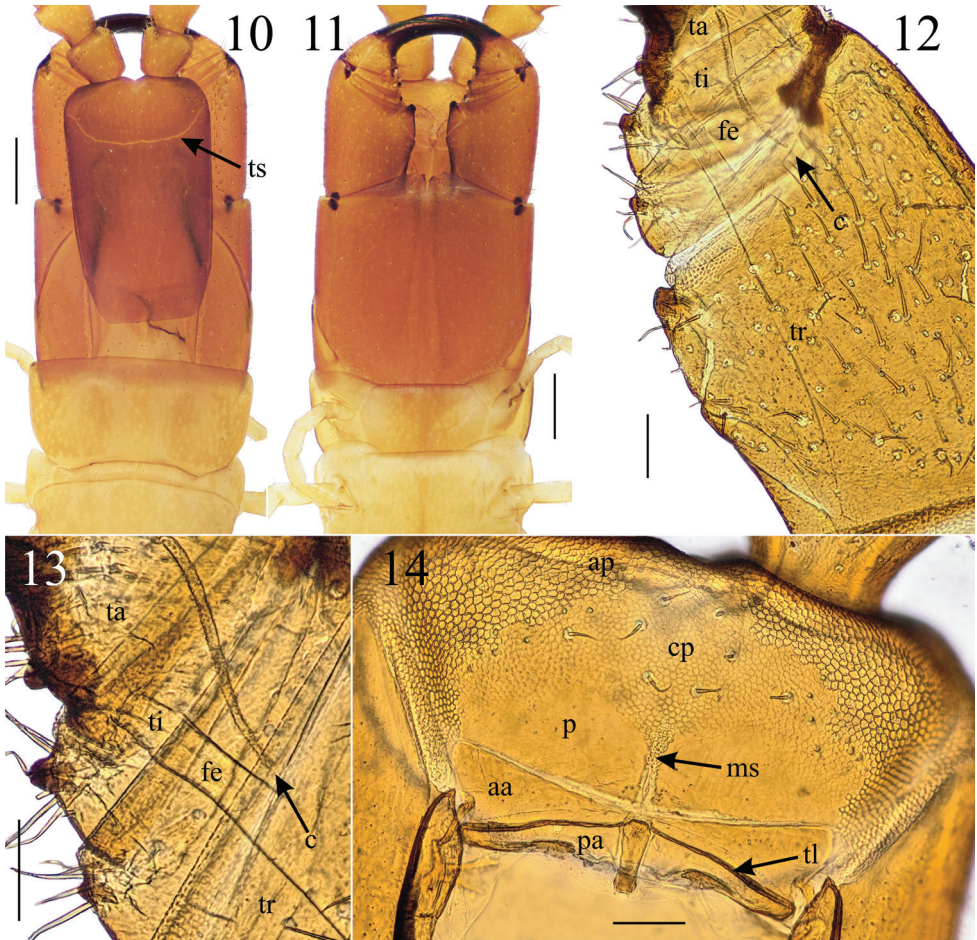


Figures 2–9. Holotype of *Krateraspis meinerti* (Sseliwanoff, 1881), from Chinaz near Tashkent (ZISP): **2, 3** head, forcipular and LBS 1 (dors., ventr.) **4** anterior LBS (ventr.) **5, 6** intermediate LBS (ventr., dors.) **7** anterior and posterior parts of the body (dors.) **8, 9** terminal part of the body (dors., ventr.). Abbreviations: 15s, 16s, 17s – metasternites 15–17, cp – coxopleural pores, us – metasternite of the ultimate LBS, ut – metatergite of the ultimate LBS. Scale bars: 0.5 mm (**2–6, 8–9**); 2 mm (**7**).

Redescription of holotype. Body stiffened, divided in two parts (Fig. 7); many legs missing. Total length ca. 48 mm; maximal width 1.4 mm (at ca. LBS 21–22). Color (in 70% ethanol) brown.

Head (Fig. 2). Cephalic plate $1.7 \times$ as long as wide, sub-rectangular but slightly widening anteriorly, its posterior margin straight. Transverse suture distinct, with a medial forward angle. Antennae ca. 5 mm, ca. $4.5 \times$ as long as the head maximum width.

Forcipular segment (Figs 2, 3). Tergite sub-trapezoid, ca. $1.5 \times$ as wide as long, with a mid-longitudinal distinct furrow inside an oval depression. Coxosternite as long as wide, with a pair of small anterior denticles. Trochanteroprefemur $1.4 \times$ as long as wide; tarsungulum $2.9 \times$ as long as wide. All forcipular articles with denticles: a large

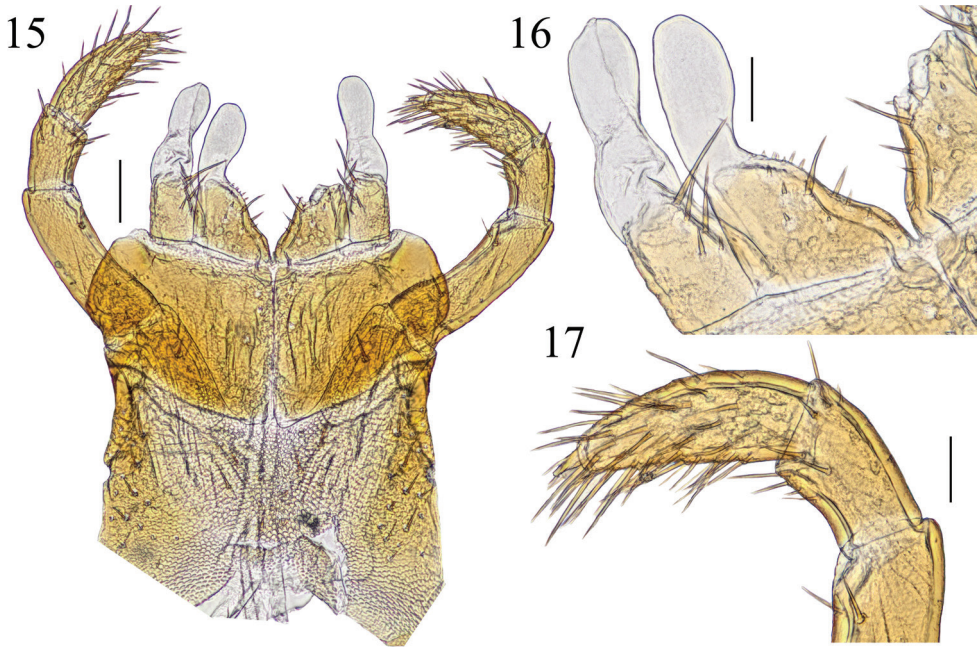


Figures 10–14. *Krateraspis meinerti* (Sselivanoff, 1881): **10, 11** head, forcipular and LBS 1 (dors., ventr.) **12, 13** left forcipule (ventr.) **14** clypeus and labrum (ventr.). Specimens: ♀ (**10, 11, 13, 14**) and ♂ (**12**), from Syrdarya-Turkestan Natural Park (ASU No. 216). Abbreviations: aa – anterior ala, ap – markedly areolate anterior part of clypeus, c – calyx of poison gland; cp – central part of clypeus with distinct but fainter areolation, fe – femur, ms – mid-longitudinal areolate strip, p – plagula, pa – posterior ala, ta – tarsungulum, ti – tibia, tl – transverse thickened line, tr – trochanteroprefemur, ts – transverse suture. Scale bars: 0.5 mm (**10, 11**); 0.1 mm (**12–14**).

distal denticle on the trochanteroprefemur, femur and tibia each with a small denticle, tarsungulum with a basal small denticle. Inner edge of tarsungulum slightly serrated.

Leg-bearing segments (Figs 4–6). Tergites 2–43 with a pair of paramedian sulci. Metasternites 2–44 with a median longitudinal sulcus. 45 LBS. Legs 1 slightly smaller than following legs; pretarsi with two accessory spines.

Ultimate leg-bearing segment (Figs 8, 9). Metatergite shield-shaped, $1.7 \times$ as long as wide, and $1.2 \times$ as wide as the pretergite. Metasternite subtriangular, $1.1 \times$ as wide as long, its anterior margin ca. $3 \times$ as wide as the posterior one. Ca. 50 pores on each



Figures 15–17. *Krateraspis meinerti* (Sseliwanoff, 1881), ventr.: **15** maxillary complex **16** right telopodite and coxal projection of first maxillae **17** left telopodite of second maxillae. Specimen: ♀ from Syrdarya-Turkestan Natural Park (ASU No. 216). Scale bars: 0.1 mm (**15**); 0.05 mm (**16**, **17**).

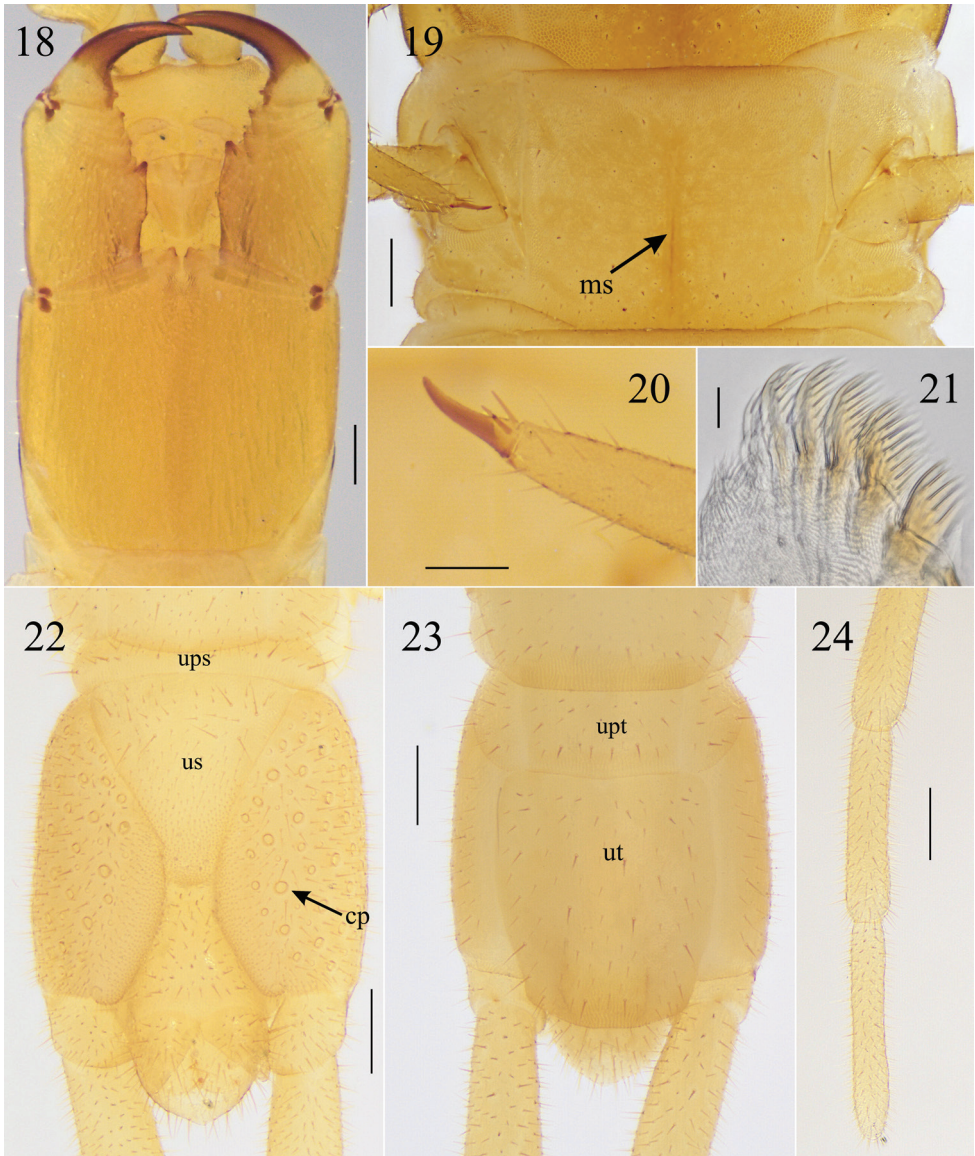
coxopleuron, scattered on ventral and lateral sides. Legs slender, but incomplete (missing tarsus 2 of right leg, tibia and both tarsi of left leg).

Postpedal segments (Figs 8, 9). Intermediate sternite and first genital sternite well-developed. Gonopods bi-articulate, triangular, and touching each other at their bases. Anal pores present.

Intraspecific variation. Maximum body length: 71 mm in ♀♀ ($n = 44$; the largest specimen in the sample ZMMU Rc 7406), 58 mm in ♂♂ ($n = 31$). Color (in 70% ethanol) usually yellow, with cephalic plate, forcipular segment, and antennae light brown (Figs 10, 11).

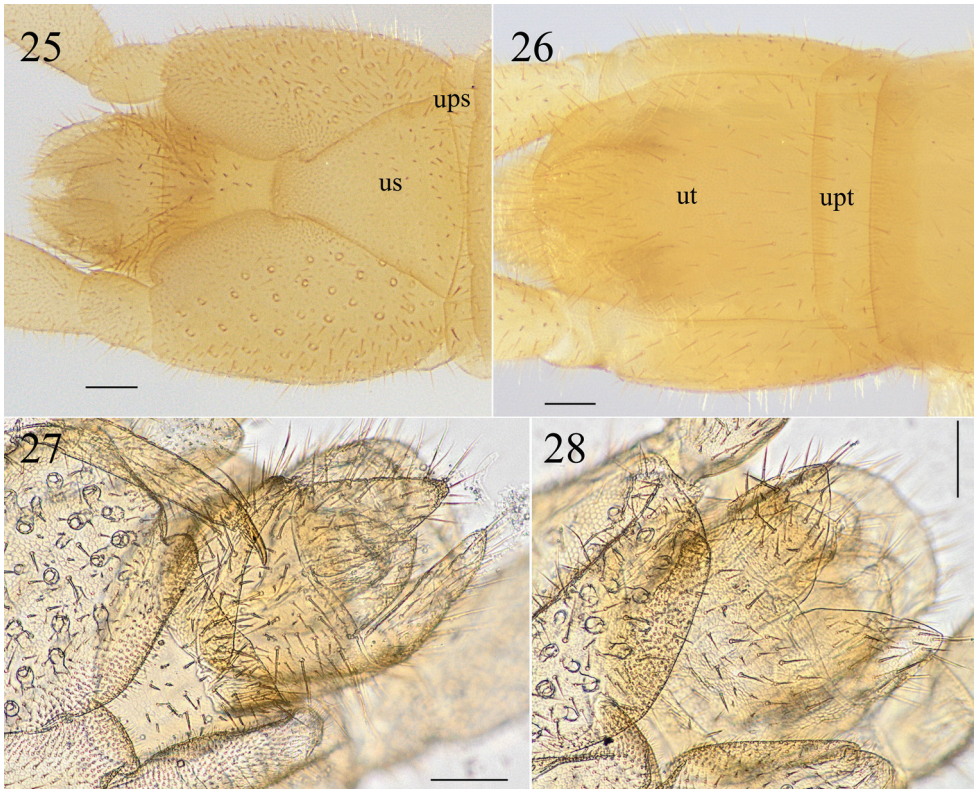
Head. Anterior markedly areolate part of the clypeus extending medially for 10–17% of the total clypeal length (Fig. 14). Clypeal setae usually 8, rarely 6. Labral mid-piece usually pointed and projecting backwards beyond the posterior margins of the labral lateral ones. Each mandible (Fig. 21) usually with six lamellae, with 5–9 teeth in each lamella. Second maxillae (Figs 15–17): 1st article invariably without a distinct distal bulge on the external side; distal parts of 2nd and 3rd articles usually with numerous setae.

Forcipular segment. Tergite usually partially covered by tergite 1 (Fig. 10) and forcipules usually surpassing the anterior margin of the cephalic plate (Figs 11, 18). All forcipular articles with denticles (Figs 11–13), with the single exception of a specimen missing the denticle on the right femur (collected together with other specimens with usual morphology, in the sample ASU No. 216). Worth noting is that an analogous case of asymmetry has been detected in a specimen of *K. sselivanovi*, where a denti-



Figures 18–24. *Krateraspis meinerti* (Sseliwanoff, 1881): **18** head and forcipular segment (ventr.). **19** LBS 2 (ventr.) **20** distal end of tarsus of leg 12 (lateral view) **21** left mandible (ventr.) **22, 23** ultimate LBS and postpedal segments (ventr., dors.) **24** terminal articles of ultimate leg (ventr.). Specimens: **18** lectotype of *Tygarrup asiaticus* Verhoeff, 1930 from Tashkent (NHRS-JONI 714) **19–24** ♀ from Syrdarya-Turkestan Natural Park (ASU No. 216). Abbreviations: cp – coxopleural pores, ms – median longitudinal sulcus, ups – presternite of ultimate LBS, upt – pretergite of ultimate LBS, us – metasternite of ultimate LBS, ut – tergite of ultimate LBS. Scale bars: 0.2 mm (**18, 19, 22–24**); 0.1 mm (**20**); 0.02 mm (**21**).

cle has been recognized on one femur but not in the other femur (see below). Distal denticle on the trochanteroprefemur usually larger than all other denticles (Fig. 12). Denticle on the tibia slightly larger than the denticle on the femur and the basal den-



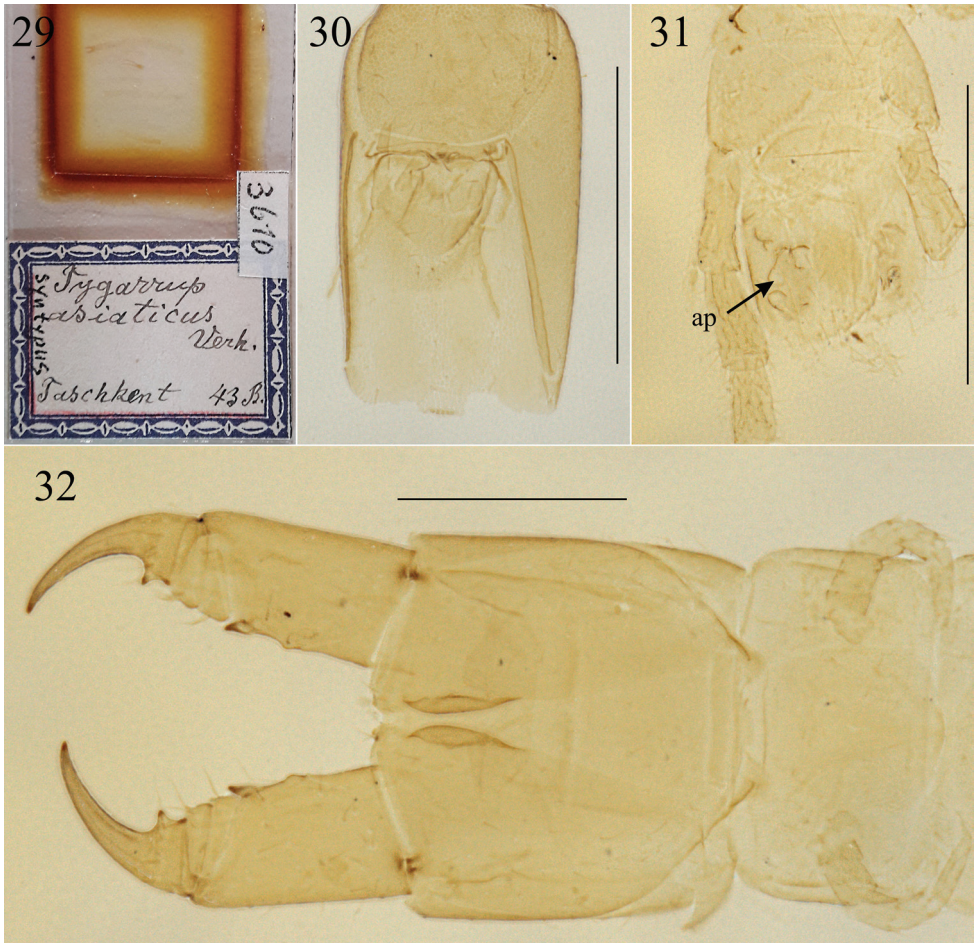
Figures 25–28. *Krateraspis meinerti* (Sselivanoff, 1881): **25, 26** ultimate LBS and postpedal segments (ventr., dors.) **27, 28** postpedal segments (♂ and ♀; ventr.). Specimens: ♂ (**25, 26**), from Sayram-Ugam National Park (ASU No. 217); ♂ (**27**) and ♀ (**28**), from Syrdarya-Turkestan Natural Park (ASU No. 216). Abbreviations: ups – presternite of ultimate LBS, upt – pretergite of ultimate LBS, us – metasternite of ultimate LBS, ut – tergite of ultimate LBS. Scale bars: 0.1 mm.

ticle on the tarsungulum (Figs 12, 13). Calyx of poison gland usually reaching the trochanteroprefemur in both sexes (Figs 12, 13).

Leg-bearing segments. Invariably 45 pairs of legs. Worth noting is that *K. sselivanovi* has invariably 53 pairs of legs and the difference of eight pairs between the two species corresponds to a putative evolutionary change that have repeatedly occurred in the Mecistocephalidae (Bonato et al. 2003).

Ultimate leg-bearing segment. Almost similar in both sexes, slightly thickened in male (Figs 22, 23, 25, 26). Metasternite subtriangular, its length to width ratio varying between 0.8 and 1.1, and the anterior margin 3–5 wider than the posterior one; up to ca. 50 pores on each coxopleuron in both sexes; legs densely setose, without pretarsus in both sexes.

Postpedal segments. Densely setose in both sexes (Figs 22, 23, 25–28). Male gonopods bi-articulate, narrower and separated by a conic projection in between (Figs 25, 27). Female gonopods bi-articulate, subtriangular, and touching each other at their bases (Figs 22, 28).



Figures 29–32. Specimen of *Arrup* misidentified by Verhoeff (1930) as juvenile *Tygarrup asiaticus* Verhoeff, 1930 (ZMB 3610), ventr.: **29** microscopic slide **30** head **31** ultimate LBS and postpedal segments; **32** forcipular segment and LBS 1. Abbreviation: ap – anal pore. Scale bars: 0.5 mm (**30–32**).

Distribution. Recorded from 24 localities, from Western Tian-Shan to the western offshoots of Pamir Mts (Fig. 1), in the following countries and administrative units: Kazakhstan (Turkistan and Jambyl regions), Uzbekistan (Tashkent region), Kyrgyzstan (Jalal-Abad region), and Tajikistan (Region of Republican Subordination, Khatlon, and Sughd regions) (Sselivanoff 1881a, 1881b, 1884; Lignau 1929a, 1929b; Titova 1965, 1975; Dyachkov 2019, 2020; Dyachkov and Nedoev 2021; present records).

A specimen from Tatarstan (European Russia) was assigned by Izotova (1960) to *K. meinerti* with doubt (see also Volkova 2016; Dyachkov 2019). The relative size of the forcipular tergite (Izotova 1960: fig. 6) shows that this specimen does not belong to Mecistocephalidae, and the shape of the forcipular segment suggests instead a species of the geophilid genus *Arctogeophilus* Attems, 1909. The latter is known from European Russia and resembles *Krateraspis* in the elongation of the head, the shape

of the forcipular coxosternite, the pattern of forcipular denticles, the number and arrangement of coxal pores, and the absence of ultimate pretarsi (see, e.g., Folkmanová and Dobroruka 1960).

Remarks on published morphological accounts. Verhoeff (1930) indicated that *Tygarrup asiaticus* differs from *Krateraspis meinerti* in the clypeal areolation (a single long non-areolate plagula, with a short mid-longitudinal areolate strip, instead of two paired short plagulae), the shape of labrum (mid-piece not projecting backwards beyond the posterior margins of the labral lateral pieces), and the second maxillary pretarsi (absent). However, Verhoeff ignored the weak areolation on the central part of the clypeus and described an entire non-areolate plagula, even though recognizing a mid-longitudinal areolate strip. The putative difference in the labrum may be explained by artefacts. As for the second maxillary pretarsus, it was described and illustrated as missing in *T. asiaticus* by Verhoeff (1930), but this character was ignored in keys published later by the same author (Verhoeff 1937, 1939, 1942). Moreover, a pretarsus is recognizable in the second maxillae of the lectotype (NHRS-JONI 714; Fig. 18), while it is absent in ZMB No. 3610, which is an *Arrup* specimen originally misinterpreted by Verhoeff (1930) as a juvenile *T. asiaticus* (see above, under Remarks on nomenclatural issues).

Krateraspis sselivanovi Titova, 1975

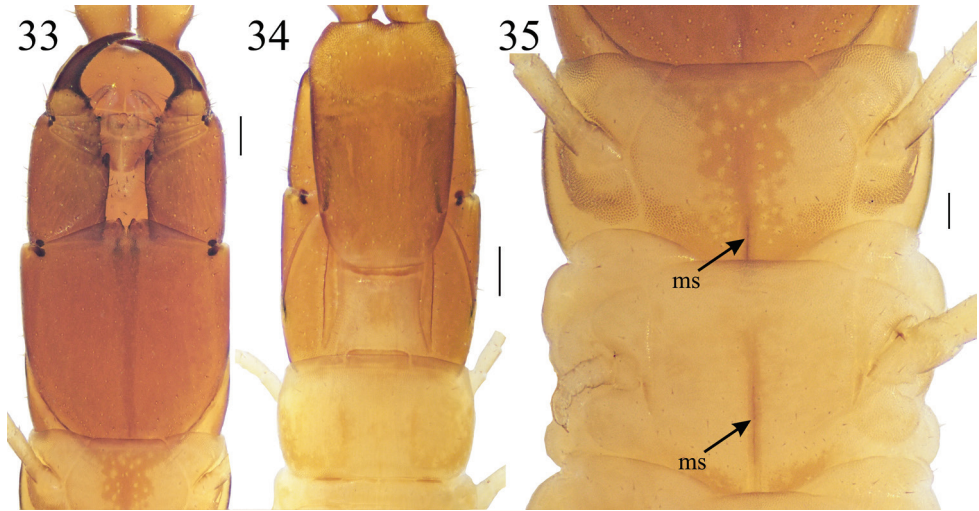
Figures 33–43

Krateraspis sselivanovi: Titova 1975: 41 (original description), 45, 46 (in key); fig. 2: 1–5A. Bonato et al. 2003: 543, 545, 546, 550, 551, 552, 577. Dyachkov 2019: 368, 373 (in key). Dyachkov 2020: 84.

Type locality. “Tajikistan, Sharak” (Titova 1975) [TAJIKISTAN, Khatlon region, Sharak village, ca. 38°16'N, 70°04'E].

Examined specimens. Paratypes: 1 ♂, from [TAJIKISTAN, Khatlon region, Mu'minobod district], Sharak, 10–20 [cm deep], 31.V.[19]65 (ZMMU Rc 8154); 2 ♂♂ and 2 ♀♀, from Sharak, 0–10 [cm deep], 29.V.[19]65 (ZMMU Rc 8167); 1 ♂, from Sharak, 10–20 [cm deep], 4.VI.[19]64 (ZMMU Rc 8175). **Other material:** 3 ♀♀, from Sharak, 10–20, 20–30, 40–50 [cm deep], 15.X.[19]64 (ZMMU Rc 8153); 1 ♂ and 2 ♀♀, from Sharak, 0–10 [cm deep], 4.VI.[19]69 (ZMMU Rc 8163); 1 ♂, from Sharak, 20–40 [cm deep], 8.X.[19]65 (ZMMU Rc 8165); 1 ♂, from [unknown region] F-bad [Fayzobod village], *Hordeum*, 70–80 [cm deep], 30.VII.[19]66 (ZMMU Rc 8173); 1 ♂, from [Districts of Republican Subordination], Garm [village, ca. 39°1'N, 70°22'E], 21.VI.[19]69 (ZMMU Rc 8187).

Remarks on nomenclatural issues. The type series of *K. sselivanovi* comprises 21 specimens: the holotype and 19 paratypes from Sharak, and another paratype from Faizobod (Titova 1975). These specimens are expected to be at the ZMMU, but we did not find the holotype, and the paratypes are not marked as such. Nevertheless, we



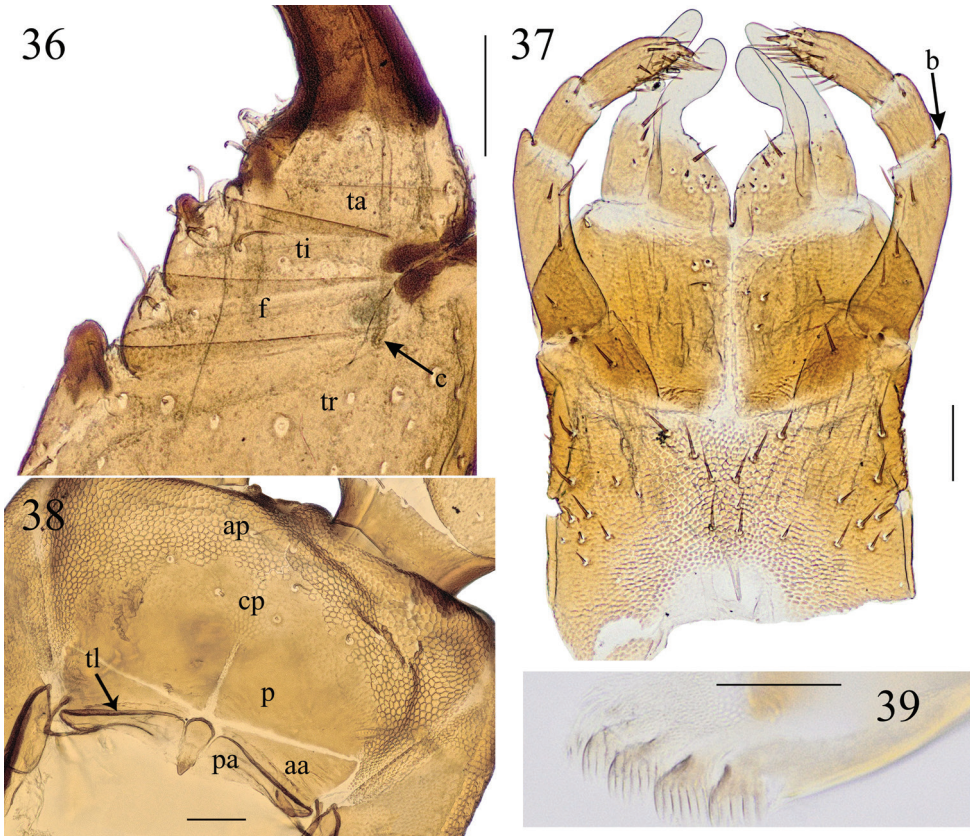
Figures 33–35. *Krateraspis sselivanovi* Titova, 1975: **33, 34** head, forcipular and LBS 1 (ventr., dors.) **35** LBS 1 and 2 (ventr.). Specimen: ♂ from Sharak (ZMMU Rc 8154). Abbreviations: ms – median longitudinal sulcus. Scale bars: 0.2 mm (**33, 34**); 0.1 mm (**35**).

detected six specimens that can be recognized as paratypes according to the locality and date reported on labels (ZMMU Rc 8154, ZMMU Rc 8167, ZMMU Rc 8175), while one specimen (ZMMU Rc 8187) can be recognized as not belonging to the type series, because it is from a locality not mentioned by Titova (1975). Instead, the date on the labels of the other eight specimens (ZMMU Rc 8153, ZMMU Rc 8163, ZMMU Rc 8165, ZMMU Rc 8173) do not fully correspond to the dates reported by Titova (1975), so it is uncertain whether they are paratypes or not.

Diagnosis. A species of *Krateraspis* with: clypeus showing the transition between marked and weak areolation at ca. 0.3–0.4 of the clypeal medial length, so that some clypeal setae are surrounded by marked areolation while other setae are surrounded by weak areolation; no spine-like sensilla on the lateral parts of the clypeus; second maxillary telopodites not distinctly surpassing the tips of the telopodites of the first maxillae; first article of the second maxillary telopodites with a distinct distal bulge on the external side; all forcipular articles with a distinct denticle with the exception of the femur; invariably 53 pairs of legs. See also Table 2.

Intraspecific variation. Maximum body length: 62 mm in ♀♀ ($n = 7$) and 67 mm in ♂♂ ($n = 8$) but the largest specimens of both sexes are slightly macerated and stretched. Color (in ethanol 70%) usually yellow, with head, forcipular segment (except forcipular tergite), and antennae light brown (Figs 33, 34).

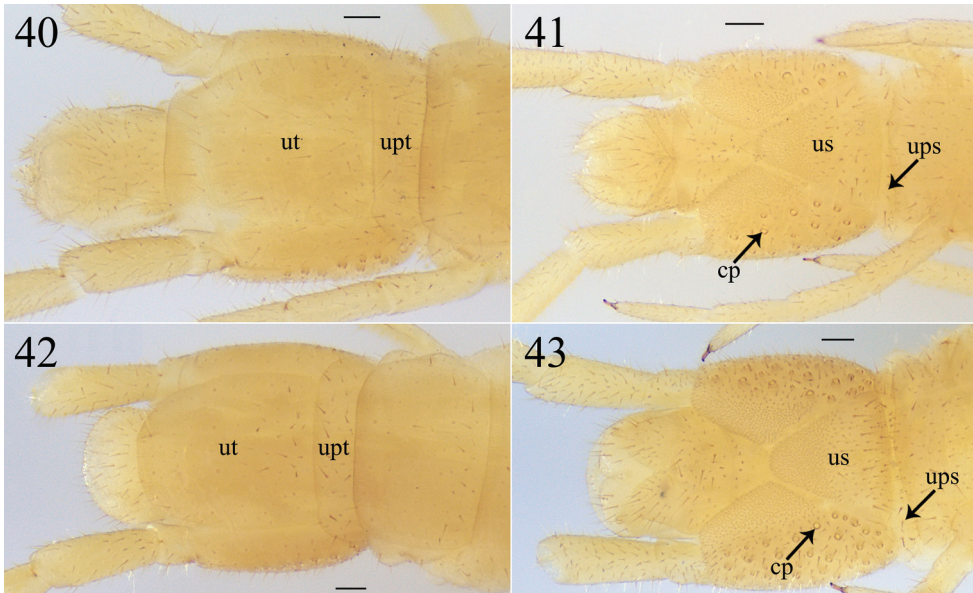
Head. Anterior markedly areolate part of the clypeus extending medially for 30–40% of the total length of the clypeus (Fig. 38). Invariably eight clypeal setae: 2–4 setae on the markedly areolate part, 2–4 setae located on the border between the markedly areolate part and the weakly areolate part, and two setae on the weakly areolate one; spine-like sensilla on the clypeal lateral parts always absent. Each mandible (Fig. 39)



Figures 36–39. *Krateraspis sselivanovi* Titova, 1975: **36** left forcipule (ventr.) **37** maxillary complex (ventr.) **38** clypeus and labrum (ventr.) **39** left mandible (lateral view). Specimens: **36, 39** ♂ from Fayzobod (ZMMU Rc 8173) **37, 38** ♂ from Sharak (ZMMU Rc 8165). Abbreviations: aa – anterior ala, ap – markedly areolate anterior part of clypeus, b – bulge, c – calyx of poison gland, cp – central part of clypeus with distinct but fainter areolation, f – femur, p – plagula, pa – posterior ala, ta – tarsungulum, ti – tibia, tl – transverse thickened line, tr – trochanteroprefemur. Scale bars: 0.1 mm (**36–38**); 0.05 mm (**39**).

usually with six lamellae, with 5–7 teeth in each lamella. Second maxillae (Fig. 37): 1st article invariably with a distinct distal bulge on the external side; distal part of 2nd article usually with two or three setae, distal part of 3rd article with numerous setae.

Forcipular segment. Tergite usually partially covered by the tergite 1. Forcípules, when closed, usually reaching the anterior margin of the cephalic plate (Figs 33, 34). Trochanteroprefemur, tibia and tarsungulum with denticles, while femur without denticle (Figs 33, 36), with the single exception of a specimen with a denticle on the right femur (however collected together with specimens with usual morphology in the sample ZMMU Rc 8163). Worth noting is that an analogous case of asymmetry has been detected in a specimen of *K. meinerti*, where a denticle has been recognized on one femur but not in the other femur (see above). The distal denticle of trochanteroprefemur usually larger than both denticles on the tibia and tarsungulum (Fig. 36). Calyx of poison gland usually reaching the trochanteroprefemur in both sexes.



Figures 40–43. *Krateraspis sselivanovi* Titova, 1975: **40, 41** ultimate LBS and postpedal segments of ♂ (dors., ventr.) **42, 43** ultimate LBS and postpedal segments of ♀ (dors., ventr.). Specimens from Sharak: **40, 41** ♂ (ZMMU Rc 8154) **42, 43** ♀ (ZMMU Rc 8153). Abbreviations: cp – coxopleural pores, ups – presternite of ultimate LBS, upt – pretergite of ultimate LBS, us – metasternite of ultimate LBS, ut – tergite of ultimate LBS. Scale bars: 0.1 mm.

Leg-bearing segments. Invariably 53 pairs of legs in all examined specimens. Worth noting is that *K. meinerti* has invariably 45 pairs of legs and the difference of eight pairs between the two species corresponds to a putative evolutionary change that have repeatedly occurred in the Mecistocephalidae (Bonato et al. 2003).

Ultimate leg-bearing segment. Almost similar in both sexes (Figs 40–43): metasternite subtriangular, its length to width ratio varying between 0.9 and 1.0, and the anterior margin 4–5 × wider than the posterior one; up to 20 pores on each coxopleuron in ♂♂, and up to 50 pores in ♀♀; legs slender and densely setose, without pretarsus.

Postpedal segments. Densely setose in both sexes (Figs 40–43). Male gonopods bi-articulate, narrow, and separated by a conic projection in between (Fig. 41). Female gonopods bi-articulate, subtriangular, and touching each other at their bases (Fig. 43).

Distribution. Recorded from three localities in the western offshoots of Pamir Mts (Fig. 1), all in Tajikistan (Khatlon region and Districts of Republican Subordination) (Titova 1975; present records).

Acknowledgements

We are grateful to J.A. Dunlop and F. Tillack (ZMB), J. Stigenberg (NHRS), A.A. Schilyko (ZMMU), and V.A. Krivokhatsky (ZISP) for the loan of material and for their

logistic help. We are grateful also to A.A. Fomichev (Barnaul, Russia) who loaned other specimens, C. Martínez-Muñoz (Turku, Finland) who provided useful information on the type material repositories, and J.S. Volkova (Ulyanovsk, Russia) who provided literature. The first author wishes to thank R.V. Yakovlev who organized field trips to Kazakhstan, M.M. Silantieva and N.J. Speranskaya for their logistic help, O.V. Fast, L.A. Khvorova, and A.V. Vaganov (Barnaul) who kindly provided the FAST software. We also thank A.A. Schilevko and A. Minelli for their careful review of the manuscript.

References

- Attems C (1903) Synopsis der Geophiliden. Zoologische Jahrbücher. Abteilung für Systematik 18: 155–302.
- Attems C (1904) Central- und hoch-asiatische Myriopoden. Zoologische Jahrbücher. Abteilung für Systematik, Geographie und Biologie der Tiere 20: 113–130. <https://doi.org/10.5962/bhl.part.18578>
- Attems C (1914) Die indo-australischen Myriopoden. Archiv für Naturgeschichte 80A: 1–398.
- Attems C (1929) Myriapoda. 1. Geophilomorpha. Das Tierreich. De Gruyter 52: 1–388. <https://doi.org/10.1515/9783111430638>
- Bonato L (2011) Geophilomorpha. In: Minelli A (Ed.) Treatise on zoology – anatomy, taxonomy, biology. The Myriapoda. Volume 1. Brill, Leiden-Boston, 407–445.
- Bonato L, Zapparoli M (2011) Chilopoda–Geographical distribution. In: Minelli A (Ed.) Treatise on zoology – anatomy, taxonomy, biology. The Myriapoda. Volume 1. Brill, Leiden-Boston, 327–337. https://doi.org/10.1163/9789004188266_017
- Bonato L, Bevilacqua S, Minelli A (2009) An outline of the geographical distribution of world Chilopoda. Contributions to Natural History, Bern 12: 183–209.
- Bonato L, Chagas Jr A, Edgecombe GD, Lewis JGE, Minelli A, Pereira LA, Shelley RM, Stoev P, Zapparoli M (2016) ChiloBase 2.0 – A World Catalogue of Centipedes (Chilopoda). <https://chilobase.biologia.unipd.it>
- Bonato L, Dányi L, Minelli A (2010a) Morphology and phylogeny of *Dicellyphilus*, a centipede genus with a highly disjunct distribution (Chilopoda: Mecistocephalidae). Zoological Journal of the Linnean Society 158(3): 501–532. <https://doi.org/10.1111/j.1096-3642.2009.00557.x>
- Bonato L, Edgecombe GD, Lewis JG, Minelli A, Pereira LA, Shelley RM, Zapparoli M (2010b) A common terminology for the external anatomy of centipedes (Chilopoda). ZooKeys 69: 17–51. <https://doi.org/10.3897/zookeys.69.737>
- Bonato L, Foddai D, Minelli A (2003) Evolutionary trends and patterns in centipede segment number based on a cladistic analysis of Mecistocephalidae (Chilopoda: Geophilomorpha). Systematic Entomology 28(4): 539–579. <https://doi.org/10.1046/j.1365-3113.2003.00217.x>
- Dyachkov YuV (2019) New data on the family Mecistocephalidae Bollman, 1893 (Chilopoda: Geophilomorpha) from Middle Asia. Arthropoda Selecta 28(3): 368–373. <https://doi.org/10.15298/arthscl.28.3.02>

- Dyachkov YuV (2020) New data on the centipede (Chilopoda) fauna from Tajikistan. *Ecologica Montenegrina* 36: 78–86. <https://doi.org/10.37828/em.2020.36.6>
- Dyachkov YuV, Nedojev KK (2021) A contribution to the centipede (Chilopoda: Geophilomorpha, Scolopendromorpha) fauna of Uzbekistan and Turkmenistan. *Ecologica Montenegrina* 41: 41–50. <https://doi.org/10.37828/em.2021.41.6>
- Foddai D, Bonato L, Pereira LA, Minelli A (2003) Phylogeny and systematics of the Arrupinae (Chilopoda Geophilomorpha Mecistocephalidae) with the description of a new dwarfed species. *Journal of Natural History* 37(10): 1247–1267. <https://doi.org/10.1080/00222930210121672>
- Folkmanová B, Dobroruka LJ (1960) Contribution to knowledge of centipedes (Chilopoda) of USSR. [Зоологический журнал] *Zoologicheskii Jurnal* 39(12): 1811–1818. [In Russian with German summary]
- Ilie V, Schiller E, Stagl V (2009) Type specimens of the Geophilomorpha (Chilopoda) in the Natural History Museum in Vienna. *Kataloge der wissenschaftlichen Sammlungen des Naturhistorischen Museum in Wien*. Verlag des Naturhistorischen Museum in Vienna 22(4): 1–75.
- ICZN [International Commission on Zoological Nomenclature] (1999) The International Code of Zoological Nomenclature. The International Trust for Zoological Nomenclature.
- Izotova TE (1960) On myriapods (Myriapoda) of Tatar SSR. *Trudy obschestva estestvoispytately* 120(6): 139–154. [In Russian]
- Jeekel CAW (2005) *Nomenclator generum et familiarum Chilopodorum: A list of the genus and family-group names in the class Chilopoda from the 10th edition of Linnaeus, 1758, to the end of 1957*. Myriapod Memoranda, Supplement I, Ulvenhout, 130 pp.
- Lignau NG (1929a) Zur Kenntnis der zentralasiatischen Myriopoden. *Zoologischer Anzeiger* 85(5/8): 159–175.
- Lignau NG (1929b) Neue Myriopoden aus Zentralasien. *Zoologischer Anzeiger* 85(9/10): 205–217.
- Moritz M, Fischer SC (1979) Die Typen der Myriapoden-Sammlung des zoologischen Museums Berlin. II. Chilopoda. *Mitteilungen aus dem Zoologischen Museum in Berlin* 55: 297–352. <https://doi.org/10.1002/mmnz.4830550215>
- Natural History Museum (2021) Natural History Museum (London) Collection Specimens. Occurrence dataset <https://doi.org/10.5519/0002965> accessed via GBIF.org on 2021-12-14. <https://www.gbif.org/occurrence/1057349793>
- Shinohara K (1965) A new species of Chilopoda from Himalaya. *Journal of the College of Arts and Science, Chiba University, Natural Science Series* 4: 303–306.
- Shorthouse DP (2010) SimpleMappr, an online tool to produce publication-quality point maps. <http://www.simplemappr.net>
- Sselivanoff AV (1881a) Geophilidae from the Museum of Imperial Academy of Sciences. *Zapiski Imperatorskoi Akademii Nauk* 40: 1–27. [in Russian]
- Sselivanoff AV (1881b) Turkestanskia stonochki (Geophilidae Leach). *Izvēstiya Imperatorskago Obshchestva Lyubitelei Estestvoznaniya, Antropologii i Etnogografii pri Imperatorskom Moskvovskom Universitate* 37: 229–232 [In Russian].
- Sselivanoff AV (1884) Materials towards the study of Russian myriapods. *Trudy Russkago Entomologicheskago obshchestva*. St. Petersburg 18: 69–121. [in Russian]

- SysTax (2021) SysTax – Zoological Collections. Occurrence dataset <https://doi.org/10.15468/zyqkbl> accessed via GBIF.org on 2021-12-14. <https://www.gbif.org/occurrence/1038216360>
- Takakuwa Y (1940) Geophilomorpha. In: Okada Y et al. (Eds) Fauna Nipponica, 9, fasc. 8(1), Sanseido, Tokyo, 1–156.
- Titova LP (1965) A new centipede (*Tygarrup muminabadicus* Titova sp. n.; Mecistocephalidae, Chilopoda) from southern Tajikistan. Zoologicheskij Zhurnal 44(6): 871–876. [in Russian]
- Titova LP (1969) Geophilids of the USSR fauna and news in the distribution of the fam. Mecistocephalidae. In: Aleinikova MM (Ed.) Problemy pochvennoi zoologii. Materialy Tretiego Vsesoyuznogo soveshchaniya. Kazan, 1969. Nauka Publ., Moscow, 165–166. [in Russian]
- Titova LP (1975) Geophilids of the family Mecistocephalidae in the USSR fauna (Chilopoda). [Зоологический журнал] Zoologicheskii Jurnal 54(1): 39–48. [in Russian]
- Titova LP (1983) Two new *Tygarrup* Chamb. (Chilopoda, Geophilida, Mecistocephalidae) from Indochina. Annalen des Naturhistorischen Museums in Wien 85B: 147–156.
- Uliana M, Bonato L, Minelli A (2007) The Mecistocephalidae of the Japanese and Taiwanese islands (Chilopoda: Geophilomorpha). Zootaxa 1396(1): 1–84. <https://doi.org/10.11646/zootaxa.1396.1.1>
- Vaganov AV, Fast OV, Khvorova LA (2020) Development of a software module for analysis of images of biological micro- and macro-objects. MAK: Matematiki – Altaiskomu Krayu 2: 154–156 [in Russian].
- Verhoeff KW (1930) Über Myriapoden aus Turkestan. Zoologischer Anzeiger 91: 243–266.
- Verhoeff KW (1934) Beiträge zur Systematik und Geographie der Chilopoden. Zoologische Jahrbucher. Abteilung für Systematik, Ökologie und Geographie der Tiere 66: 1–112.
- Verhoeff KW (1937) Chilopoden aus Malacca nach den Objecten des Raffles Museum in Singapore. Bulletin of the Raffles Museum 13: 198–270.
- Verhoeff KW (1939) Chilopoden der Insel Mauritius. Zoologische Jahrbücher. Abteilung für Systematik 72: 71–98.
- Verhoeff KW (1940) Chilopoden von Kärnten und Tauern, ihre Beziehungen zu europäischen und mediterranen Ländern und über allgemeine geographische Verhältnisse Abhandlungen der Preussischen Akademie der Wissenschaften, mathematisch-naturwissenschaftliche Klasse, 1940 5: 1–39.
- Verhoeff KW (1942) Chilopoden aus innerasiatischen Hochgebirgen. Zoologischer Anzeiger 137: 35–52.
- Volkova YuS (2016) An annotated catalogue of geophilomorph centipedes (Myriapoda, Geophilomorpha) from the European part of Russia. [Зоологический журнал] Zoologicheskii Jurnal 95(6): 669–678. <https://doi.org/10.7868/S0044513416060179>

A new species of *Pseudophanerotoma* (Hymenoptera, Braconidae) from Nayarit, Mexico

Armando Falcón-Brindis^{1,2}, Jorge L. León-Cortés¹, Rubén F. Mancilla-Brindis³,
Mario Orlando Estrada-Virgen³, Octavio J. Cambero-Campos³

1 Departamento de Conservación de La Biodiversidad, El Colegio de La Frontera Sur, María Carretera Panamericana y Periférico Sur, CP 29290, San Cristóbal de Las Casas, Chiapas, Mexico **2** Department of Entomology, University of Kentucky Research and Education Center, 348 University Drive, Princeton, KY 42445, USA **3** Posgrado en Ciencias Biológico Agropecuarias, Unidad Académica de Agricultura, Universidad Autónoma de Nayarit, Carretera Tepic-Compostela Km 9, CP 63155, Xalisco, Nayarit, Mexico

Corresponding authors: Jorge L. León-Cortés (jleon@ecosur.mx),
Armando Falcón-Brindis (armandofalcon123@gmail.com)

Academic editor: Andreas Köhler | Received 11 September 2021 | Accepted 28 March 2022 | Published 14 April 2022

<http://zoobank.org/5277C150-DFFF-4CB4-9B7A-CCB8006DDCAC>

Citation: Falcón-Brindis A, León-Cortés JL, Mancilla-Brindis RF, Estrada-Virgen MO, Cambero-Campos OJ (2022) A new species of *Pseudophanerotoma* (Hymenoptera, Braconidae) from Nayarit, Mexico. ZooKeys 1095: 165–177. <https://doi.org/10.3897/zookeys.1095.74308>

Abstract

Parasitoid wasps are known to be among the most abundant and species-rich on Earth and thus considered an ecologically important group of arthropods. Braconid wasps play a key role in regulating the populations of Lepidoptera, Coleoptera, and Diptera. However, the biology and taxonomy of numerous parasitoid species remain poorly known. In Mexico, only 17 species of the subfamily Cheloninae have been described. A new species of *Pseudophanerotoma* Zettel, 1990 (Hymenoptera, Braconidae), *P. huichol* **sp. nov.**, is described from Nayarit, Mexico. The tortricid moth *Cryptaspasma perseana* Gilligan & Brown, 2011 is reported as the host of this parasitoid wasp. Detailed taxonomic and barcoding information are provided.

Keywords

Cheloninae, COI barcode, integrative taxonomy, Mexican biodiversity, Neotropical region, parasitoid wasp, Tortricidae

Introduction

The family Braconidae comprises 21,221 species worldwide (Yu et al. 2016), and the description of new species is exponentially increasing in the Neotropical region (Fernandez-Triana and Boudreault 2018; Sharkey et al. 2021). Braconid wasps are primarily specialized parasitoids of Lepidoptera, Coleoptera, and Diptera, thus playing an important role in regulating their populations. Usually, braconid wasp does not oviposit in the host egg (Wharton et al. 1997). However, members of the subfamily Cheloninae oviposit in the eggs of Lepidoptera and emerge from later larval instars or the pupa (Quicke 2015).

Cheloninae are mostly solitary endoparasitoid wasps of several Microlepidoptera, i.e., Pyraloidea and Tortricoidea (Shaw 1997). Within this subfamily, the genus *Pseudophanerotoma* Zettel, 1990 is highly specialized in parasitizing tortricid moths (Costa Lima 1956; Hoddle and Hoddle 2008; Pentead-Dias et al. 2008). Members of this genus are restricted to the Americas, occurring from southern Texas to Peru and Brazil (Zettel 1990; Kittel 2018; Sharkey et al. 2021).

One of the main limitations of studying parasitoid wasps is the large number of species and high variability in life histories (Shaw 1995; Hanson and Gauld 2006). The taxonomy of Braconidae has been poorly documented, especially in the tropics (LaSalle and Gauld 1991). Since the classical description of species started undergoing the so-called taxonomy crisis almost two decades ago (Godfray 2002), the integrative taxonomy framework (Dayrat 2005) has brought complementary approaches to tackle challenging groups. As in most parasitoid wasps, the taxonomy of Cheloninae has been changing and the use of molecular tools allowed advances for the systematics of the group. For instance, *Pseudophanerotoma* and *Furcidentia* Zettel, 1990 are now two separate genera based on molecular and morphological characters (Zettel 1990; Kittel et al. 2016). Kittel (2018) essentially cleared up the taxonomy of both genera and added new species, but a recent work also provided additional species names (Sharkey et al. 2021).

In Mexico, *Pseudophanerotoma* members correspond to a poorly documented taxon with a few records from the States of Oaxaca, Quintana Roo, Tamaulipas, Veracruz, and Yucatán (Sánchez-García and López-Martínez 2000; Coronado-Blanco 2011). However, none of these specimens have been determined to species level, limiting our knowledge upon such specialized genus but most importantly, reducing our ability to identifying priority biodiversity areas in the face of human disturbance (Ceballos et al. 2015). In this work, we describe a new species, *Pseudophanerotoma huichol* sp. nov., which attacks the tortricid moth *Cryptaspasma perseana* Gilligan & Brown, 2011 occurring in Nayarit, Mexico (Mancilla-Brindis et al. 2019). We provide detailed taxonomic diagnoses for both sexes and support our findings with DNA barcoding. In addition, we present an updated checklist of *Pseudophanerotoma* species, their potential phylogenetic relationship, and discuss elements of their biology and distribution.

Methods

As part of a survey to evaluate the prevalence of *Cryptaspasma perseana* among avocado orchards in Nayarit, Mexico, several fruits and seeds were collected from December 2019 to October 2020 (Mancilla-Brindis et al. 2021). The rearing process was conducted at the Universidad Autónoma de Nayarit. The emerged wasps were preserved in 96% ethanol and shipped to the Collection of Entomology (**ECO-SC-E**) of El Colegio de la Frontera Sur (**ECOSUR**), San Cristóbal de las Casas, Chiapas, Mexico, for taxonomic identification.

DNA extraction was conducted at the Barcoding Laboratory of Life of ECOSUR, Chetumal, Quintana Roo, Mexico, using standard protocols (Hebert et al. 2003; Ivanova et al. 2006). Extracted DNA was amplified for a 650-bp region near the 5' terminus of the cytochrome c oxidase subunit I (COI) gene using the primers ZplankF1 (TCT ASW AAT CAT AAR GAT ATT GG) and ZplankR1 (TTC AGG RTG RCC RAA RAA TCA) (Posser et al. 2013). Amplified PCR product was then shipped to Eurofins Scientific, Louisville, KY, USA, for purification and sequencing using Sanger technology. Sequence was cleaned and aligned using BioEdit (Hall 1999). We performed a phylogenetic analysis using the neighbor-joining method (Saitou and Nei 1987), based on a bootstrap consensus tree inferred from 10,000 replicates (Felsenstein 1985) to evaluate the relationship of 10 *Pseudophanerotoma* species. In addition, a genetic distance matrix between pairs of sequences was calculated through maximum composite likelihood to estimate the evolutionary divergence between species (Tamura et al. 2004). *Pseudophanerotoma alvarengai* Zettel, 1990, *P. longicornia* Zettel, 1990, *P. maculosa* Zettel, 1990, *P. peruana* Zettel, 1990, and *P. zeteki* (Cushman) 1922 were not included since there is no barcoding information for them. The analysis involved 10 nucleotide sequences, eliminating positions with missing data. Bootstrap analysis, genetic distance matrix, and phylogenetic tree were conducted in MEGA11 (Tamura et al. 2021).

Morphological determination of *Pseudophanerotoma* followed Sharkey et al. (2021). Taxonomic features provided in this study followed van Achterberg (1988) and Wharton et al. (1997). Images were taken with a Leica MC 170 HD camera, adapted to a Leica M205C stereoscopic microscope. Morphometric data and image aligning was performed with the Leica Application Suite software. Holotype and paratype specimens are deposited in ECO-SC-E.

We used the following abbreviations to describe key ocellar measurements (Kittel 2018):

- LOL** lateral ocellar line (distance between lateral and anterior ocelli);
- OOL** ocular ocellar line (distance between lateral ocellus and compound eye);
- POL** posterior ocellar line (distance between lateral ocelli).

Results

Pseudophanerotoma huichol Falcón-Brindis, sp. nov.

<http://zoobank.org/DB6DDDDA-E2C6-4DD6-9BCB-438870114206>

Diagnosis. *Pseudophanerotoma huichol* sp. nov. can be distinguished from the other species by the unicolorous head, meso, and metasoma, except for the dark brownish integument on the apical half of hind femora and a small spot on the mesopleuron (sometimes absent in males); antenna with 52 antennomeres in females and 46 antennomeres in males, occipital carina complete.

Description (female). Body length 5.5 mm; ratio of length of fore wing to body 0.8; ratio of metasoma to mesosoma 1.2 (Fig. 1A–C).

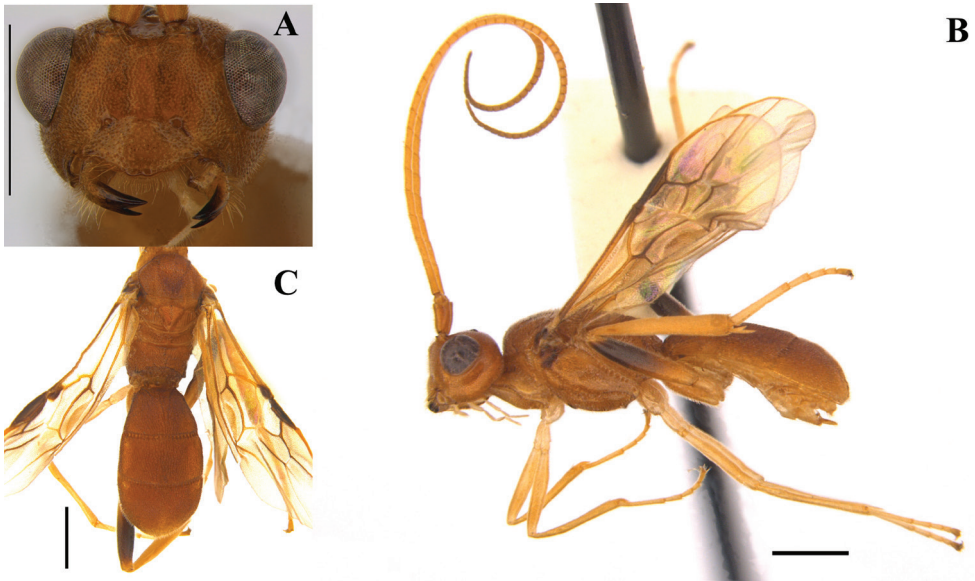


Figure 1. *Pseudophanerotoma huichol* sp. nov., female **A** head frontal **B** lateral habitus **C** dorsal view of meso and metasoma. Scale bars: 1.0 mm.

Head. Antenna with 52 antennomeres; ratio of width of face to its height in frontal view 1.4; ratio of width of clypeus to its height 1.8; ratio of length of third antennomere to width 3.7; ratio of length of fourth antennomere to width 3.0; ratio of length of penultimate antennomere to width 1.3; malar space to base of mandible 0.3 mm. Clypeus convex and sparsely punctate with two teeth; face straight in lateral view, punctate; frons and vertex densely punctate; ratio of LOL:POL:OOL 0.1:0.1:0.1:0.4.

Mesosoma. Mesoscutum shiny and densely punctate, mid mesoscutal area coarsely sculptured; notauli present; mesopleuron punctures shallow and less dense; scutellar sulcus present, with coarse pits; mesoscutellum convex and punctate; propodeum

areolate; propodeal tubercles absent; ratio of mesosoma height to its length 0.6; ratio of hind tibia to hind tarsus 2.1; ratio of length to width of hind coxa 2.0; ratio of length to width of hind femur 5.2; ratio of length to width of hind tibia 7.5; ratio of length to width of hind tarsus 6.2; ratio of length of fore wing to body 0.8; fore wing length 4.2 mm; 1RS present; M curved; RS+M spectral (Fig. 2).



Figure 2. *Pseudophanerotoma huichol* sp. nov., fore wing. Scale bar: 1.0 mm.

Metasoma. Oval in dorsal view; sculpture striate throughout; ratio of metasomal width to length 0.6; ratio of length of the three metasomal tergites 0.7:0.7:0.8.

Color. Scape, head, meso and metasoma ferruginous; antennomeres and legs pale orange to yellowish; dark brown integument on tegula, a small spot on the top of mesopleuron (below the tegula) and apical half of hind femora. Wings hyaline with greenish-purplish reflections, wing venation brown to dark brown; parastigma and pterostigma dark brown.

Type material. Holotype and paratypes specimens are pinned and deposited in ECO-SC-E. **Holotype:** MEXICO: ♀, Lo de Lamedo, Tepic, Nayarit 21.54222, -104.92833; 880 m elev., 10 Oct. 2020; 21.53388, -104.93722; 860 m elev., 04 Sep. 2020; R.F. Mancilla-Brindis leg. Holotype voucher code 69271. **Paratypes:** 6 ♀: 69272, 69273, 69274, 69275, 69276, 69277; 5 ♂: 69278, 69279, 69280, 69281, 69282.

Description (male). Antenna with 46 antennomeres. Body length 5.2 mm; ratio of length of fore wing to body 0.8; ratio of length of metasoma to mesosoma 1.2 (Fig. 3A–C).

Head. Antenna with 46 antennomeres; ratio of width of face to its height in frontal view 1.2; ratio of width of clypeus to its height 2.0; ratio of length of third antennomere to width 4.5; ratio of length of fourth antennomere to width 3.6; ratio of length of penultimate antennomere to width 1.9; malar space to base of mandible 0.3 mm.

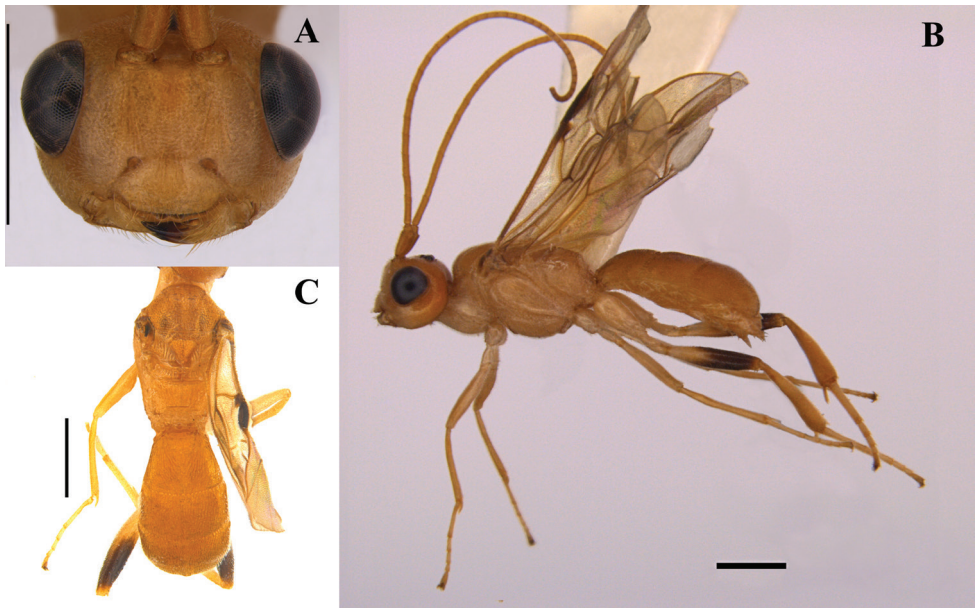


Figure 3. *Pseudophanerotoma huichol* sp. nov., male **A** head frontal **B** lateral habitus **C** dorsal view of meso and metasoma. Scale bars: 1.0 mm.

Clypeus convex and sparsely punctate with two teeth; face straight in lateral view, punctate; frons and vertex densely punctate; ratio of LOL:POL:OOL 0.1:0.1:0.1:0.3.

Mesosoma. Same sculpture patterns as in female; ratio of mesosoma height to its length 0.7; ratio of hind tibia to hind tarsus 1.9; ratio of length to width of hind coxa 2.1; ratio of length to width of hind femur 4.4; ratio of length to width of hind tibia 5.3; ratio of length to width of hind tarsus 5.8; ratio of length of fore wing to body 0.8; fore wing length 4.1 mm.

Metasoma. Oval in dorsal view; sculpture striate throughout; ratio of metasomal width to length 0.6; ratio of length of the three metasomal tergites 0.6:0.6:0.8.

Color. In general, male is paler than female; scape, head, meso and metasoma light orange; antennomeres and legs pale yellow to beige; dark brown integument on tegula and apical half of hind femora. Wings the same color pattern as in female.

Remarks. This species differs from all the other congeners by having a large number of antennomeres in both sexes: 52 and 46 antennomeres in females and males respectively.

Biology. Parasitoid of *Cryptaspasma perseana*, a tortricid pest of avocado documented in Hidalgo, Michoacán, and Nayarit, Mexico (Mancilla-Brindis et al. 2019).

Sequence data. GenBank accession number for this species is COI MZ501206.

Etymology. The species is named in honor to the Huichol culture from Nayarit, Mexico.

According to the phylogenetic analysis for the barcoded *Pseudophanerotoma* species (Fig. 4), the closest species to *P. huichol* sp. nov. was *P. alexandromarini* Sharkey, 2021 (90%), both being sister species of *P. paranaensis* Costa Lima, 1956 (100%). The results from the evolutionary distance analysis showed that *P. alexsmithi* and *P. austini*

are the closest species (0.0051), followed by *P. huichol* sp. nov. – *P. alejandromarini* (0.0133), *P. alejandromarini* – *P. paranaensis* (0.0261). In contrast, the pairwise comparison between *P. austini* – *P. allisonbrownae* and *P. alexsmithi* – *P. allisonbrownae* revealed the largest evolutionary divergence (0.2167) (Table 1).

Table 1. Estimates of evolutionary divergence between sequences. The number of base substitutions per site from between sequences are shown.

	<i>P. alanflemingi</i>	<i>P. albanjimenezi</i>	<i>P. alejandromarini</i>	<i>P. alexsmithi</i>	<i>P. allisonbrownae</i>	<i>P. bobrobbinsi</i>	<i>P. paranaensis</i>	<i>P. austini</i>	<i>P. thapsina</i>
<i>P. albanjimenezi</i>	0.1250								
<i>P. alejandromarini</i>	0.1188	0.1277							
<i>P. alexsmithi</i>	0.1186	0.1335	0.1120						
<i>P. allisonbrownae</i>	0.1843	0.1943	0.2052	0.2167					
<i>P. bobrobbinsi</i>	0.1442	0.1534	0.1412	0.1467	0.1663				
<i>P. paranaensis</i>	0.1248	0.1402	0.0261	0.1243	0.2085	0.1506			
<i>P. austini</i>	0.1124	0.1366	0.1088	0.0051	0.2167	0.1401	0.1210		
<i>P. thapsina</i>	0.0450	0.1371	0.1308	0.1278	0.2086	0.1634	0.1400	0.1214	
<i>P. huichol</i>	0.1220	0.1340	0.0103	0.1119	0.2089	0.1477	0.0314	0.1119	0.1341

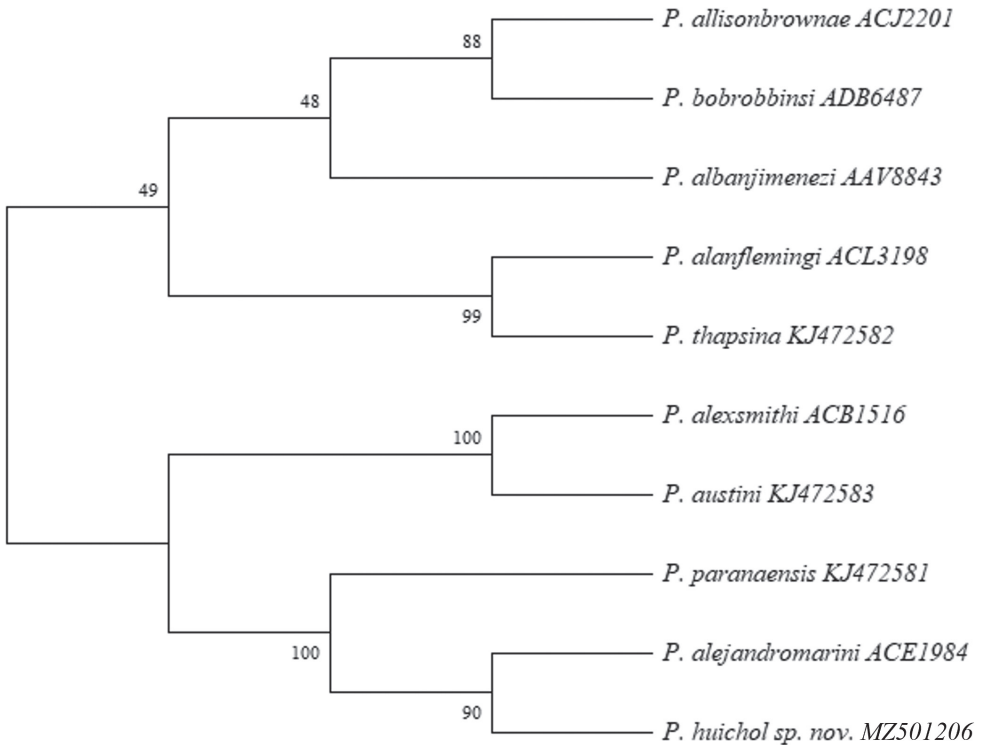


Figure 4. Bootstrap consensus tree of *Pseudophanerotoma* species. Five species are missing due to the lack of sequence information. The percentage of replicate trees in which the associated taxa clustered together in the bootstrap test are shown next to the branches. The lower clade has a weak bootstrap support.

Discussion

This is the first work describing a new species of the genus *Pseudophanerotoma* in Mexico. Previous reports documented individuals at the generic level (Sánchez-García and López-Martínez 2000; Coronado-Blanco 2011). It is likely that *P. thapsina* (recorded in the United States and French Guiana) and *P. austini* (Guatemala) also occur in Mexico (Kittel 2018). However, further revisions are required to confirm their presence. Moreover, it is certain that other species of the genus occurring in Neotropical Mexico are deposited in museum collections (Sánchez-García and López-Martínez 2000; Coronado-Blanco 2011).

According to the most recent key for species of *Pseudophanerotoma* (Kittel 2018), *P. huichol* sp. nov., can be separated in couplet four, where the difference with *P. thapsina* is the dark brownish integument on the apical half of hind femora and the dark spot present on top of the mesopleuron. Despite the close phylogenetic relationship between *P. huichol* sp. nov. and *P. alejandromarini*, the latter species lacks dark integument on the hind femora. In summary, *P. huichol* sp. nov. has the largest number of antennomeres known from the species presented by Kittel (2018) and is undoubtedly different from those recently added by Sharkey et al. (2021).

Members of the subfamily Cheloninae have been used in the biocontrol of exotic pests (Narendran 2001). In Mexico, 704 species of Braconidae have been listed from 34 subfamilies (Coronado-Blanco et al. 2012), of which, only 17 species of Cheloninae have been identified (Coronado-Blanco and Zaldívar-Riverón 2014). However, most of these species belong to the genus *Chelonus* Panzer, 1806 (Coronado-Blanco et al. 2004), which is well known to control the populations of the fall armyworm *Spodoptera frugiperda* (J.E. Smith, 1797) feeding on forage maize in north and central Mexico (Rios-Velasco et al. 2011; Estrada-Virgen et al. 2013; García-González et al. 2020). Nonetheless, the biology of most chelonines occurring in Mexico remains unknown.

Likewise, the biology of the 15 known *Pseudophanerotoma* species has been poorly documented (Table 2). In most cases (66%), there is no information about host preferences and the same proportion is known from a single sex. The described *P. huichol* sp. nov. corresponds to the *Pseudophanerotoma* sp. reported parasitizing *C. perseana* in two localities from Nayarit, Mexico (Mancilla-Brindis et al. 2019, 2021). Therefore, this study has helped to identify an important interaction between *P. huichol* sp. nov. and a serious pest of avocado. However, further research is needed to provide details of, for example, the life history, distribution, and management of *P. huichol* sp. nov., potentially regulating the populations of *C. perseana*.

Our preliminary phylogenetic analysis indicates that there is strong evidence for *P. huichol* sp. nov., *P. alejandromarini*, and *P. paranaensis* being sister species, albeit the cluster classification showed poor resolution (weak bootstrap support). In addition, the weak evolutionary divergence between *P. alexsmithi* and *P. austini* (0.0051) reveals the closest relationship among the genus *Pseudophanerotoma*. Such clades are naturally affected by the missing barcoded species, but the explanations could be attributed to

Table 2. A checklist of *Pseudophanerotoma* species according to Zettel (1990), Pentead-Dias et al. (2008), Kittel (2018), Sharkey et al. (2021), and this work. Only accepted scientific names are included. Types refer to the known sexes on each species.

Species	Occurrence	Host data	Types	Sequence accession number
<i>P. alanflemingi</i> Sharkey, 2021	Guanacaste, Costa Rica	Unknown	♀	BOLD:ACL3198
<i>P. albanjimenezi</i> Sharkey, 2021	Alajuela, Costa Rica	<i>Episimus ortygia</i> (Tortricidae) feeding on <i>Vismia baccifera</i> (Hypericaceae)	♂	BOLD:AAV8843
<i>P. alejandromarini</i> Sharkey, 2021	Guanacaste, Costa Rica	Unknown	♀	BOLD:ACE1984
<i>P. alexsmithi</i> Sharkey, 2021	Alajuela, Costa Rica	Cosmorrhyncha albistrigulana (Tortricidae) feeding on <i>Dialium guianense</i> (Fabaceae)	♀	BOLD:ACB1516
<i>P. allisonbrownae</i> Sharkey, 2021	Guanacaste, Costa Rica	Unknown	♂	BOLD:ACJ2201
<i>P. alvarengai</i> Zettel, 1990	Bahía, São Paulo, Brazil	<i>Cydia tonosticha</i> (Tortricidae) feeding on <i>Stryphnodendron adstringens</i> (Fabaceae)	♀♂	NA
<i>P. austini</i> Kittel, 2018	Petén, Guatemala	Unknown	♂	GenBank KJ472583
<i>P. bobrobbinsi</i> Sharkey, 2021	Guanacaste, Costa Rica	Unknown	♀	BOLD:ADB6487
<i>P. huichol</i> Falcón-Brindis, sp. nov.	Nayarit, Mexico	<i>C. perseana</i> (Tortricidae) feeding on <i>Persea americana</i> var. <i>Drymifolia</i> (Lauraceae)	♀♂	MZ501206
<i>P. longicornia</i> Zettel, 1990	Paraguay; Ecuador	Unknown	♀♂	NA
<i>P. maculosa</i> Zettel, 1990	Barro Colorado, Panama	Unknown	♂	NA
<i>P. paranaensis</i> Costa Lima, 1956	Paraná, Brazil; Saül, French Guiana	<i>Olethreutes anthracana</i> (Tortricidae)	♂	GenBank KJ472581
<i>P. peruana</i> Zettel, 1990	Alto-Samboroi, Peru	Unknown	♂	NA
<i>P. thapsina</i> Walley, 1951	Texas, California, Arizona, Florida, USA; Mt. Chevoux, French Guiana	Unknown	♀♂	GenBank KJ472582
<i>P. zeteki</i> (Cushman, 1922)	St. Bernardino, Panama	Unknown	♀♂	NA

several factors (e.g., lack of alternative barcoded regions, different gene history, or early diverging lineages) (Doyle 1992). Thus, our phylogenetic analysis should be interpreted with caution, as it only attempted to compare the position of the new species within the sequenced congeners.

Even though divergent opinions, molecular methods are now an important part of taxonomy, allowing integrative approaches (Padial et al. 2010). In this regard, many braconid species have been described using DNA barcoding (Smith et al. 2007, 2008; Sharkey et al. 2021). Sharkey et al. (2021) recently added more than 400 species to the list of Braconidae, including six new species of *Pseudophanerotoma*, with descriptions based on the COI barcoded region. This approach can certainly be helpful when describing large numbers of species, but morphological descriptions are handy when molecular tools are not available. In this sense, whereas the last taxonomic key to *Pseudophanerotoma* species did not thoroughly include molecular data (Kittel 2018), the six new species lack of morphological description (Sharkey et al. 2021) and thus further research is required to strengthen their presumed relationships.

Acknowledgements

We thank Dr Manuel Elías Gutierrez for his guidance with the molecular work. Dr Alma Estrella García Morales for her gentle support with the DNA extraction and amplification. Collect permissions were granted by the Comité Estatal de Sanidad Vegetal del Estado de Nayarit (CESAVENAY). AF-B received a post-doctoral scholarship (grant number 30223), through a grant from the National Council for Science and Technology in Mexico (CONACYT) to JLL-C (258792: CB-2015-01).

Funding from the Universidad Autónoma de Nayarit (UAN) supported the project: “*Cryptaspasma* sp. (Lepidoptera, Tortricidae): its distribution and natural enemies in avocado orchards from Nayarit, Mexico” and provided the necessary resources through the UAN Special Taxes.

References

- Ceballos G, Ehrlich PR, Barnosky AD, García A, Pringle RM, Palmer TM (2015) Accelerated modern human-induced species losses: Entering the sixth mass extinction. *Science Advances* 1(5): e1400253. <https://doi.org/10.1126/sciadv.1400253>
- Coronado-Blanco JM (2011) Serie avispa parasíticas de plagas y otros insectos. Braconidae (Hymenoptera) de Tamaulipas, México. Editorial Planea, Victoria, Tamaulipas, Mexico, 203 pp.
- Coronado-Blanco JM, Zaldívar-Riverón A (2014) Biodiversity of Braconidae (Hymenoptera: Ichneumonoidea) in México. *Revista Mexicana de Biodiversidad* 85(Supplement 1): S372–S378. <https://doi.org/10.7550/rmb.32000>
- Coronado-Blanco JM, Ruíz-Cancino E, Valera-Fuentes SE (2004) Adenda a Braconidae (Hymenoptera) In: Llorente J, Morrone JJ, Yáñez O, Vargas I (Eds) Biodiversidad, taxonomía y biogeografía de artrópodos de México: hacia una síntesis de su conocimiento. UNAM, México, 713–720.
- Coronado-Blanco JM, Ruíz-Cancino E, Ivanovich KA, Mireles-Cepeda S, Rodríguez-Mota AJ, Castillo-Flores PM (2012) Revisión de la clasificación de Braconidae (1990–2012): Subfamilias en México. *CienciaUAT* 7(1): 14–21. <https://doi.org/10.29059/cienciauat.v7i1.45>
- Costa Lima A (1956) Tortricideo de semillas de “imbuia” e respectivo parasito (Hymenoptera, Braconidae). *Revista Brasileira de Entomologia* 5: 291–244.
- Dayrat B (2005) Towards integrative taxonomy. *Biological Journal of the Linnean Society. Linnean Society of London* 85(3): 407–417. <https://doi.org/10.1111/j.1095-8312.2005.00503.x>
- Doyle JJ (1992) Gene trees and species trees: Molecular systematics as one-character taxonomy. *Systematic Botany* 17(1): 144–163. <https://doi.org/10.2307/2419070>
- Estrada-Virgen O, Cambero-Campos J, Robles-Bermudez A, Rios-Velasco C, Carvajal-Cazola C, Isordia-Aquino N, Ruíz-Cancino E (2013) Parasitoids and entomopathogens of the fall armyworm *Spodoptera frugiperda* (Lepidoptera: Noctuidae) in Nayarit, Mexico. *Southwestern Entomologist* 38(2): 339–344. <https://doi.org/10.3958/059.038.0216>
- Felsenstein J (1985) Confidence limits on phylogenies: Sn approach using the bootstrap. *Evolution; International Journal of Organic Evolution* 39(4): 783–791. <https://doi.org/10.1111/j.1558-5646.1985.tb00420.x>

- Fernandez-Triana J, Boudreault C (2018) Seventeen new genera of microgastrine parasitoid wasps (Hymenoptera, Braconidae) from tropical areas of the world. *Journal of Hymenoptera Research* 64: 25–140. <https://doi.org/10.3897/jhr.64.25453>
- García-González F, Rios-Velasco C, Iglesias-Pérez D (2020) *Chelonus* and *Campoletis* species as main parasitoids of *Spodoptera frugiperda* (J.E. Smith) in forage maize of lagunera region, Mexico. *Southwestern Entomologist* 45(3): 639–642. <https://doi.org/10.3958/059.045.0306>
- Godfray HCJ (2002) Challenges for taxonomy. *Nature* 417(6884): 17–19. <https://doi.org/10.1038/417017a>
- Hall TA (1999) BioEdit: A user-friendly biological sequence alignment editor and analysis program for Windows 95/98/NT. *Nucleic Acids Symposium Series* 41: 95–98.
- Hanson P, Gauld I (2006) Hymenoptera de la región tropical. *Memoirs of the American Entomological Institute* 77: 1–994.
- Hebert PDN, Cywinska A, Ball SL, deWaard JR (2003) Biological identifications through DNA barcodes. *Proceedings. Biological Sciences* 270(1512): 313–321. <https://doi.org/10.1098/rspb.2002.2218>
- Hoddle MS, Hoddle CD (2008) Lepidoptera and associated parasitoids attacking Hass and non-Hass avocados in Guatemala. *Journal of Economic Entomology* 101(4): 1310–1316. <https://doi.org/10.1093/jee/101.4.1310>
- Ivanova NV, Dewaard JR, Hebert PD (2006) An inexpensive, automation-friendly protocol for recovering high-quality DNA. *Molecular Ecology Notes* 6(4): 998–1002. <https://doi.org/10.1111/j.1471-8286.2006.01428.x>
- Kittel RN (2018) A taxonomic review of the parasitoid wasp genera *Furcidentia* Zettel and *Pseudophanerotoma* Zettel (Hymenoptera: Braconidae: Cheloninae) from the Neotropics with the description of four new species. *Zootaxa* 4486(2): 146–160. <https://doi.org/10.11646/zootaxa.4486.2.4>
- Kittel RN, Austin AD, Klopstein S (2016) Molecular and morphological phylogenetics of chelonine parasitoid wasps (Hymenoptera: Braconidae), with a critical assessment of divergence time estimations. *Molecular Phylogenetics and Evolution* 101: 224–241. <https://doi.org/10.1016/j.ympev.2016.05.016>
- LaSalle J, Gauld ID (1991) Parasitic Hymenoptera and the biodiversity crisis. *Insect Parasitoids* 74(3): 315–334.
- Mancilla-Brindis RF, De Dios-Ávila N, Cambero-Campos OJ, Rios VC, Luna-Esquivel G, Isordia-Aquino N, Estrada-Virgen O (2019) Primer registro de *Cryptasasma perseana* en Nayarit, México. *Southwestern Entomologist* 44(3): 799–802. <https://doi.org/10.3958/059.044.0328>
- Mancilla-Brindis RF, Cambero-Campos OJ, Estrada-Virgen O, Rios VC, Luna-Esquivel G, Ruiz-Cancino E, Isordia-Aquino N (2021) Distribution, abundance and parasitoids associated with *Cryptasasma perseana* (Tortricidae) in Mexican creole avocado (*Persea americana* var. *drymifolia*) cultivars from Nayarit, Mexico. *Journal of the Lepidopterists Society* 75(4): 291–296. <https://doi.org/10.18473/lepi.75i4.a7>
- Narendran TC (2001) Parasitic Hymenoptera and biological control. In: Upadhyay RK, Mukerji KG, Chamola BP (Eds) *Biocontrol Potential and its Exploitation in Sustainable Agriculture*. Springer, Boston, MA, 1–12. https://doi.org/10.1007/978-1-4615-1377-3_1
- Padial JM, Miralles A, De la Riva I, Vences M (2010) The integrative future of taxonomy. *Frontiers in Zoology* 7(1): e16. <https://doi.org/10.1186/1742-9994-7-16>

- Penteado-Dias AM, Nascimento AR, Dias MM (2008) The description of the male and the first host data of *Pseudophanerotoma* (*Pseudophanerotoma*) *alvarengai* Zettel, 1990 (Hymenoptera: Braconidae: Cheloninae). *Zoologische Mededeelingen* 82: 401–405.
- Posser S, Martínez-Arce A, Elías-Gutiérrez M (2013) A new set of primers for COI amplification from freshwater microcrustaceans. *Molecular Ecology Resources* 13: 1151–1155. <https://doi.org/10.1111/1755-0998.12132>
- Quicke DLJ (2015) *The Braconid and Ichneumonid Parasitoid Wasps: Biology, Systematics, Evolution and Ecology*. Wiley Blackwell, Chichester, 704 pp. <https://doi.org/10.1002/9781118907085>
- Rios-Velasco C, Gallegos-Morales G, Cambero-Campos J, Cerna-Chávez E, del Rincón-Castro MC, Valenzuela-García R (2011) Natural enemies of the fall armyworm *Spodoptera frugiperda* (Lepidoptera: Noctuidae) in Coahuila, México. *The Florida Entomologist* 94(3): 723–726. <https://doi.org/10.1653/024.094.0349>
- Saitou N, Nei M (1987) The neighbor-joining method: A new method for reconstructing phylogenetic trees. *Molecular Biology and Evolution* 4: 406–425.
- Sánchez-García JA, López-Martínez V (2000) Géneros de Braconidae (Insecta: Hymenoptera) depositados en la colección entomológica del Instituto de Fitosanidad del Colegio de Postgraduados. *Acta Zoológica Mexicana* 79: 257–276.
- Sharkey MJ, Janzen DH, Hallwachs W, Chapman EG, Smith MA, Dapkey T, Brown A, Ratnasingham S, Naik S, Manjunath R, Perez K, Milton M, Hebert P, Shaw SR, Kittel RN, Solis MA, Metz MA, Goldstein PZ, Brown JW, Quicke DLJ, van Achterberg C, Brown BV, Burns JM (2021) Minimalist revision and description of 403 new species in 11 subfamilies of Costa Rican braconid parasitoid wasps, including host records for 219 species. *ZooKeys* 1013: 1–665. <https://doi.org/10.3897/zookeys.1013.55600>
- Shaw SR (1995) The Braconidae. In: Hanson P, Gauld I (Eds) *The Hymenoptera of Costa Rica*. Oxford University Press, Oxford, 431–464.
- Shaw SR (1997) Family Cheloninae. In: Wharton RA, Marsh PM, Sharkey MJ (Eds) *Manual of the New World Genera of Braconidae (Hymenoptera)*. Special Publication of the International Society of Hymenopterists 1. The International Society of Hymenopterists, Washington, DC, 193–202.
- Smith MA, Wood DM, Janzen DH, Hallwachs W, Hebert PND (2007) DNA barcodes affirm that 16 species of apparently generalist tropical parasitoid flies (Diptera, Tachinidae) are not all generalists. *Proceedings of the National Academy of Sciences of the United States of America* 104(12): 4967–4972. <https://doi.org/10.1073/pnas.0700050104>
- Smith MA, Rodriguez JJ, Whitfield JM, Deans AR, Janzen DH, Hallwachs W, Hebert PND (2008) Extreme diversity of tropical parasitoid wasps exposed by iterative integration of natural history, DNA barcoding, morphology, and collections. *Proceedings of the National Academy of Sciences of the United States of America* 105(34): 12359–12364. <https://doi.org/10.1073/pnas.0805319105>
- Tamura K, Nei M, Kumar S (2004) Prospects for inferring very large phylogenies by using the neighbor-joining method. *Proceedings of the National Academy of Sciences of the United States of America* 101(30): 11030–11035. <https://doi.org/10.1073/pnas.0404206101>

- Tamura K, Stecher G, Kumar S (2021) MEGA 11: Molecular Evolutionary Genetics Analysis version 11. *Molecular Biology and Evolution* 38(7): 3022–3027. <https://doi.org/10.1093/molbev/msab120>
- van Achterberg C (1988) Revision of the subfamily Blacinae Foerster (Hymenoptera: Braconidae). *Zoologische Verhandelingen* 249: 1–324.
- Wharton RA, Marsh PM, Sharkey MJ (1997) *Manual of the New World Genera of Braconidae* (Hymenoptera). Special Publication of the International Society of Hymenopterists 1. The International Society of Hymenopterists, Washington, DC, 439 pp.
- Yu DSK, van Achterberg C, Horstmann K (2016) *Taxapad 2016, Ichneumonoidea 2015*. Database on flash-drive. Nepean, Ontario. <http://www.taxapad.com>
- Zettel H (1990) Eine Revision der Gattungen der Cheloninae (Hymenoptera, Braconidae) mit Beschreibungen neuer Gattungen und Arten. *Annalen des Naturhistorischen Museums in Wien* 91(B): 147–196.

